Effects of land-based climate change mitigation on ecosystem carbon cycling and beyond

Zur Erlangung des akademischen Grades eines

DOKTORS DER NATURWISSENSCHAFTEN

von der Fakultät für

Bauingenieur-, Geo- und Umweltwissenschaften

des Karlsruher Instituts für Technologie (KIT)

genehmigte

DISSERTATION

von

Dipl.-Geogr. Andreas T. Krause

aus Schweinfurt

Tag der mündlichen

Prüfung: 08.02.2018

Referentin: Prof. Dr. Almut Arneth

Korreferent: Prof. Dr. Mark Rounsevell

Korreferentin: Prof. Dr. Anja Rammig

Karlsruhe 2018

Abstract

Land-use and land-cover changes (LULCC) have large impacts on climate. Cumulative LULCC emissions between 1750 and today were responsible for about one third of total anthropogenic CO_2 emissions during this time, thereby making a large contribution to the increase in global mean surface temperature of around 1°C relative to the pre-industrial era. However, the land as a whole currently represents a net carbon sink, with the capacity to store additional carbon if managed properly. In fact, the removal of carbon from the atmosphere ("negative emissions") via land-based climate change mitigation technologies is increasingly regarded as a necessary option to limit global warming below 2°C. However, the potential carbon removal under the consideration of limited land availability and associated impacts on the environment are highly uncertain. In this thesis I make use of recent progress with respect to the representation of LULCC in dynamic global vegetation models (DGVMs), in particular the LPJ-GUESS model, to explore long-term effects of land-use change on the recovery of ecosystems, carbon removal potential from land-based mitigation, and associated side effects on a range of other ecosystem service indicators beyond carbon storage.

Idealised land-use scenarios are used to study the effects of land-use history (in terms of agricultural type and duration) on the recovery of carbon in ecosystems following agricultural abandonment. Simulations with LPJ-GUESS show that nearly all global ecosystems require decades or centuries to regenerate to the pre-disturbed state. The type and duration of former land use is particularly important for the recovery of soil carbon, with recovery times often differing by centuries across scenarios, but is also significant for vegetation carbon and composition recovery which typically show differences of several decades. Spatially, the greatest sensitivity to prior land use is found in boreal forests and subtropical grasslands. The simulations show that land-use history is an important consideration when assessing LULCC as an option to remove carbon from the atmosphere.

Land-based carbon removal options are then explored further based on land-use projections of future mitigation strategies (forest maintenance and expansion, bioenergy combined with carbon capture and storage, or a combination of both approaches) from two land-use models, with the aim to study the likely efficacy and the environmental risks of land management for carbon storage. The land-use scenarios are used as input to four DGVMs to simulate carbon removal from the atmosphere via land-based mitigation in an RCP2.6 climate. The carbon removal achieved in the DGVMs by the end of the century is typically lower (19-130 GtC) than originally implemented in the land-use models (86-141 GtC). Differences in carbon removal between the models are mainly due to model assumptions regarding bioenergy crop yields, and how the soil carbon response to LULCC is simulated, with smaller contributions from differences in forest biomass and the rate of forest regrowth. With respect to impacts on other ecosystem service indicators, avoided deforestation and afforestation generally induces larger changes than bioenergy cultivation, which is related to the different land demand of both approaches. Afforestation results in an increase, compared to a baseline scenario, in evapotranspiration

of 1.3-2.1%, and of 15.7-24.1% for emissions of biogenic volatile organic compounds, the ranges resulting from simulations based on the two different land-use models. In contrast, decreases of 0.8-1.3% in albedo, 0.7-2.2% in runoff, 3.5-35.1% in crop production, and 6.7-13.2% in nitrogen loss occur. In the bioenergy simulations, there is a decrease in crop production of 6.6-9.7%, in N loss of 7.6-10.3%, and of 2.2-8.2% for emissions of biogenic organic compounds, but only minor changes in albedo, evapotranspiration, and runoff.

In conclusion, an adequate representation of LULCC in vegetation models in combination with a detailed analysis of direct and indirect effects is critical to draw more robust conclusions about the impacts of land-based mitigation on the carbon cycle and the impacts (both from a co-benefit and trade-off perspective) it has on ecosystem functioning underlying other ecosystem services. Nevertheless, the results of this thesis suggest that the amount of carbon removal typically assumed to be achievable in ambitious climate mitigation scenarios might well be overoptimistic. Furthermore, when associated impacts on other ecosystem services and technological challenges are also considered, relying on an ever increasing amount of negative emissions to achieve the 2°C target appears a very high-risk strategy.

Zusammenfassung (German)

Landnutzungs- und Bodenbedeckungsänderungen haben große Auswirkungen auf das Klima. Die kumulativen Landnutzungsemissionen zwischen 1750 und heute entsprechen etwa einem Drittel der gesamten menschlichen CO_2-Emissionen in diesem Zeitraum und trugen somit erheblich zum Anstieg der globalen Durchschnittstemperatur um etwa 1°C im Vergleich zum vorindustriellen Zeitalter bei. Das Land stellt insgesamt jedoch momentan eine Netto-Kohlenstoffsenke dar und besitzt die Möglichkeit zusätzlichen Kohlenstoff zu speichern, falls eine entsprechende Nutzung erfolgt. Tatsächlich wird die Kohlenstoffentnahme aus der Atmosphäre („negative Emissionen“) durch landbasierte Klimaschutztechnologien mehr und mehr als notwendig erachtet, um die globale Erwärmung auf unter 2°C zu begrenzen. Jedoch ist die potentielle Kohlenstoffentnahme unter Berücksichtigung der begrenzten Landverfügbarkeit und der damit verbundenen Auswirkungen auf die Umwelt sehr unsicher. In dieser Doktorarbeit nutze ich jüngste Fortschritte bezüglich der Darstellung von Landnutzungs- und Bodenbedeckungsänderungen in dynamischen globalen Vegetationsmodellen (insbesondere mit Hilfe des Models LPJ-GUESS), um die längerfristigen Auswirkungen von Landnutzungswandel auf die Regeneration von Ökosystemen zu erforschen. Außerdem untersuche ich das Kohlenstoffentnahmepotential durch landbasierte Klimawandelminderungsstrategien, sowie die damit verbundenen Nebeneffekte auf eine Reihe weiterer Indikatoren von Ökosystemdienstleistungen über die Kohlenstoffspeicherung hinaus.

Idealisierte Landnutzungsszenarien werden benutzt, um den Einfluss der Landnutzungsgeschichte (bezüglich der landwirtschaftlichen Nutzungsart und Zeitdauer) auf die Regeneration von Kohlenstoff in Ökosystemen nach Beendigung der landwirtschaftlichen Nutzung zu erforschen. Simulationen mit dem LPJ-GUESS Modell zeigen, dass nahezu alle globalen Ökosysteme Jahrzehnte oder Jahrhunderte benötigen, um zu ihrem ursprünglichen Zustand zurückzukehren. Die Art und Zeitdauer der früheren Landnutzung ist besonders wichtig für die Regeneration des Bodenkohlenstoffs, für den sich die Regenerationszeiten oftmals um Jahrhunderte innerhalb der Szenarien unterscheiden. Die Landnutzungsgeschichte ist jedoch auch für die Regeneration des Vegetationskohlenstoffs und der Vegetationszusammensetzung von Bedeutung, für die sich Unterschiede von mehreren Jahrzehnten innerhalb der Szenarien ergeben. Räumlich betrachtet findet man den größten Einfluss der früheren Landnutzung in borealen Wäldern und subtropischen Grasländern. Die Simulationen zeigen, dass die Landnutzungsgeschichte bei der Bewertung von Landnutzungs- und Bodenbedeckungsänderungen als Möglichkeit zur Kohlenstoffentnahme aus der Atmosphäre berücksichtigt werden sollte.

Landbasierte Kohlenstoffentnahmeoptionen werden dann auf der Grundlage von Landnutzungsprojektionen zukünftiger Klimawandelminderungsstrategien (der Erhalt und die Ausweitung von Wäldern, Bioenergie kombiniert mit Kohlenstoffabscheidung und Speicherung oder eine Kombination beider Ansätze) zweier Landnutzungsmodelle weiter erforscht, um die voraussichtliche Wirksamkeit und die Umweltrisiken von Landbewirtschaftung zur Kohlenstoffspeicherung zu ermitteln. Die Landnutzungs-

szenarien dienen als Eingabedaten für vier dynamische globale Vegetationsmodelle, um die Kohlenstoffentnahme aus der Atmosphäre durch landbasierte Klimawandelminderungsstrategien in einem RCP2.6 Klima zu simulieren. Die Kohlenstoffentnahme, die am Ende des Jahrhunderts in den dynamischen Vegetationsmodellen erreicht wird, ist normalerweise geringer (19-130 GtC) als die Kohlenstoffentnahme, die ursprünglich in den Landnutzungsmodellen realisiert wurde (86-141 GtC). Die Unterschiede in der Kohlenstoffentnahme zwischen den Modellen sind vermutlich vor allem den Modellannahmen über die Erträge von Bioenergiepflanzen zuzuschreiben und wie Änderungen im Bodenkohlenstoff durch Landnutzungsänderungen simuliert werden. Ein geringer Anteil wird auch durch Unterschiede in der Waldbiomasse und der Waldwachstumsrate erklärt. Bezüglich der Auswirkungen auf weitere Indikatoren von Ökosystemdienstleistungen zeigt sich, dass der Schutz und die Ausweitung der Wälder allgemein größere Effekte als der Anbau von Bioenergiepflanzen hervorrufen. Dies hängt mit dem unterschiedlichen Flächenbedarf beider Ansätze zusammen. Aufforstung führt im Vergleich zu einem Referenzszenario zu einer 1.3-2.1% höheren Verdunstung und Transpiration und zu 15.7-24.1% höheren Emissionen von flüchtigen organischen Verbindungen, wobei sich die Spannweite aus den Simulationen ergibt die auf den beiden unterschiedlichen Landnutzungsmodellen basieren. Außerdem kommt es zu einer um 0.8-1.3% verringerten Albedo, einem um 0.7-2.2% verringerten Abfluss, einer um 3.5-35.1% verringerten landwirtschaftlichen Produktion und einer Verringerung der Stickstoffverluste um 6.7-13.2%. In den Bioenergiesimulationen kommt es zu einer Abnahme der landwirtschaftlichen Produktion um 6.6-9.7%, der Stickstoffverluste um 7.6-10.3% und der Emissionen flüchtiger organischer Verbindungen um 2.2-8.2%, während die Albedo, die Verdunstung und Transpiration, sowie der Abfluss kaum beeinflusst werden.

Zusammengefasst sind eine angemessene Darstellung von Landnutzungs- und Bodenbedeckungsänderungen in Vegetationsmodellen, sowie eine detaillierte Auswertung der direkten und indirekten Effekte entscheidend, um robustere Aussagen darüber treffen zu können, wie sich landbasierte Klimawandelminderungsstrategien auf den Kohlenstoffkreislauf auswirken. Außerdem können so die Folgen für Ökosystemfunktionen, die weiteren Ökosystemdienstleistungen unterliegen, besser abgeschätzt werden, sowohl hinsichtlich von Zusatznutzen als auch von Einbußen. Die Ergebnisse der vorliegenden Doktorarbeit weisen darauf hin, dass die Kohlenstoffentnahme, die üblicherweise in ambitionierten Klimaschutzszenarien als realisierbar erachtet wird, deutlich zu hoch angesetzt sein könnte. Wenn zusätzlich die damit verbundenen Auswirkungen auf weitere Ökosystemdienstleistungen, sowie die technologischen Herausforderungen berücksichtigt werden, so erscheint die stetig wachsende Abhängigkeit von negativen Emissionen, um das 2°C Ziel zu erreichen, als eine höchst riskante Strategie.

For my mother

Eidesstattliche Versicherung gemäß § 6 Abs. 1 Ziff. 4 der Promotionsordnung des Karlsruher Instituts für Technologie für die Fakultät für Bauingenieur-, Geo- und Umweltwissenschaften.

1. Bei der eingereichten Dissertation zu dem Thema “Effects of land-based climate change mitigation on ecosystem carbon cycling and beyond” handelt es sich um meine eigenständig erbrachte Leistung.

2. Ich habe nur die angegebenen Quellen und Hilfsmittel benutzt und mich keiner unzulässigen Hilfe Dritter bedient. Insbesondere habe ich wörtlich oder sinngemäß aus anderen Werken übernommene Inhalte als solche kenntlich gemacht.

3. Die Arbeit oder Teile davon habe ich bislang nicht an einer Hochschule des In- oder Auslands als Bestandteil einer Prüfungs- oder Qualifikationsleistung vorgelegt.

4. Die Richtigkeit der vorstehenden Erklärungen bestätige ich.

5. Die Bedeutung der eidesstattlichen Versicherung und die strafrechtlichen Folgen einer unrichtigen oder unvollständigen eidesstattlichen Versicherung sind mir bekannt.

Ich versichere an Eides statt, dass ich nach bestem Wissen die reine Wahrheit erklärt und nichts verschwiegen habe.

Ort und Datum Unterschrift

This thesis is submitted as a monograph and consists of three main sections (Sections 3-5). Slightly modified versions of these sections have also been published in peer-reviewed journals. The sections are as follows:

3. Impacts of land-use history on the recovery of ecosystems after agricultural abandonment
This section is based on the paper Krause, A., Pugh, T. A. M., Bayer, A. D., Lindeskog, M., and Arneth, A. (2016). Impacts of land-use history on the recovery of ecosystems after agricultural abandonment, *Earth System Dynamics*, **7**, 745-766, doi:10.5194/esd-7-745-2016.

4. Large uncertainty in carbon uptake potential of land-based climate-change mitigation efforts
This section is based on the paper Krause, A., Pugh, T. A. M., Bayer, A. D., Li, W., Leung, F., Bondeau, A., Doelman, J. C., Humpenöder, F., Anthoni, P., Bodirsky, B. L., Ciais, P., Müller, C., Murray-Tortarolo, G., Olin, S., Popp, A., Sitch, S., Stehfest, E., and Arneth, A. (2018). Large uncertainty in carbon uptake potential of land-based climate-change mitigation efforts, *Global Change Biology*, doi:10.1111/gcb.14144.

5. Global consequences of afforestation and bioenergy cultivation on ecosystem service indicators
This section is based on the paper Krause, A., Pugh, T. A. M., Bayer, A. D., Doelman, J. C., Humpenöder, F., Anthoni, P., Olin, S., Bodirsky, B. L., Popp, A., Stehfest, E., and Arneth, A. (2017). Global consequences of afforestation and bioenergy cultivation on ecosystem service indicators, *Biogeosciences*, **14**, 4829-4850, doi:10.5194/bg-14-4829-2017.

Due to the papers being published, and therefore involving the work of co-authors, I detail my contribution to the Sections 3-5 as follows:

3. I contributed to the experiment design, performed the simulations and analysis, and led the writing of the paper.

4. I contributed to the experiment design and the implementation of the land-use patterns into LPJ-GUESS, performed the LPJ-GUESS simulations, analysed the output from all participating models, and led the writing of the paper.

5. I contributed to the experiment design, performed the LPJ-GUESS simulations (which are the same as in Section 4 apart from the sensitivity simulations) and analysis, and led the writing of the paper.

Contents

Abbreviations and units

ADAFF	Avoided deforestation and afforestation/reforestation
AR5	Fifth Assessment Report
BASE	Baseline scenario without land-based mitigation
BECCS	Bioenergy combined with carbon capture and storage
BECCS&ADAFF	A scenarios that combined BECCS and ADAFF
BVOC	Biogenic volatile organic compound
C20, C60, C100	Land-use scenarios in which a transition from natural vegetation to cropland was followed by a transition back to natural vegetation after 20, 60, or 100 years
C	Carbon
CDR	Carbon dioxide removal
CFT	Crop functional type
CH_4	Methane
CMIP5	Coupled Model Intercomparison Project, Phase 5
CO_2	Carbon dioxide
DGVM	Dynamic Global Vegetation Model
Ecal	Exa-calories (10^{18} cal)
EJ	Exa-joule (10^{18} J)
ES	Ecosystem service
ESM	Earth System Model
FAO	Food and Agriculture Organization of the United Nations
GFED	Global Fire Emissions Database
GHG	Greenhouse gas
GPP	Goss primary productivity
GtC	Giga-tons of carbon (1 GtC is equal to 1 peta-gram of carbon or 3.67 $GtCO_2$)
HYDE	History Database of the Global Environment
IAM	Integrated Assessment Model
IMAGE	Integrated Model to Assess the Global Environment
IPCC	Intergovernmental Panel on Climate Change
IPSL-CM5A-LR	Climate model of the Institut Pierre Simon Laplace (low resolution configuration)
ISI-MIP	Inter-Sectoral Impact Model Intercomparison Project
JULES	Joint UK Land Environment Simulator
LAI	Leaf area index
LPJ-GUESS	Lund-Potsdam-Jena General Ecosystem Simulator

LPJmL	Lund-Potsdam-Jena model with managed Land
LU	Land use
LUC	Land-use change
LUH2	Land-Use Harmonization 2
LULCC	Land-use and land-cover change
LUM	Land-use model
MAgPIE	Model of Agricultural Production and its Impact on the Environment
Mha	Million hectares (1 Mha is equal to 10^6 ha or 10 000 km^2)
N	Nitrogen
N_2O	Nitrous oxide
NBP	Net biome productivity
NH_3	Ammonia
NO_X	Nitrogen oxides
NPP	Net primary productivity
ORCHIDEE	ORganizing Carbon and Hydrology In Dynamic EcosystEms model
O_3	Ozone
P20, P60, P100	Land-use scenarios in which a transition from natural vegetation to pasture was followed by a transition back to natural vegetation after 20, 60, or 100 years
PFT	Plant functional type
PgC	Peta-grams of carbon (1 PgC is equal to 1 giga-ton of carbon or 3.67 $GtCO_2$)
PHU	Potential heat unit
ppmv	Parts per million by volume (1 ppmv CO_2 is equal to 2.12 GtC)
RCP	Representative Concentration Pathway
SSP	Shared Socioeconomic Pathway
TeBS	Temperate broadleaved summergreen tree

List of Figures

List of Tables

1 General introduction

Historic land-use and land-cover changes (LULCC, often simply referred to as land-use changes, LUC) have resulted in dramatic alterations of the Earth's surface. LUC are expected to continue in the future as a function of population growth, changing diets, and changing crop yields, but also because land management is increasingly considered as an option to mitigate climate change. However, the efficacy of this approach is highly uncertain and associated side effects on the environment are often not considered or unknown. In this thesis, I explore the implications of LUC on the recovery of ecosystems, future C uptake potential, and impacts on other ecosystem functions by applying and analysing results from process-based global vegetation models. The introduction of the thesis begins with an overview about human-induced climate change, followed by a closer examination of LUC impacts on the carbon cycle, and on climate and ecosystem functions in general. Afterwards, I provide some background information about the drivers and the land demand of historic and future LUC, including the necessity of land-based mitigation to stabilise climate. Lastly, I depict recent progress in global vegetation modelling with respect to LUC before describing the structure and research questions addressed in this thesis.

1.1 Human interferences with the climate system

Climate on Earth has always been changing. For example, temperatures were so warm during the Early Eocene Climatic Optimum (51-53 million years ago) that no ice existed on its surface (Zachos *et al.*, 2008). In contrast, the Earth has several times entered extremely cold phases in which ice sheets reached tropical latitudes (Rieu *et al.*, 2007). The key forcings and feedbacks responsible for these climate fluctuations are still not fully known (e.g. Anagnostou *et al.*, 2016, Foster *et al.*, 2017, Spiegl *et al.*, 2015, Zachos *et al.*, 2001).

Climate continued to change during human evolution. In fact, the steady global cooling over the last 10 million years or so was probably a crucial driving factor for the divergence of human species from chimpanzees (Lieberman, 2014). The last 2.5 million years, the Quaternary, were characterised by repeating cycles of long cold and dry periods (glacials) interrupted by short warm and humid periods (interglacials), triggered by cyclic changes of the Earth's orbital parameters (Ruddiman, 2006). Humans only started to settle down permanently at the beginning of the current interglacial, the Holocene (ca. 11 700 years ago until present), in which climate was not only relatively warm and wet but also remarkably stable. However, temperatures started to rise again at the start of the Industrial Revolution (around year 1850), particularly since the 1970s. Global surface temperatures today are ~1°C warmer than at the start of the industrial era (Hansen *et al.*, 2017a) and warmer than most if not all of the Holocene (Marcott *et al.*, 2013). A large body of evidence suggests that recent climate change was

largely caused by human activities, most importantly the emissions of carbon dioxide (CO_2) and other greenhouse gases (GHG) such as methane (CH_4) and nitrous oxide (N_2O) to the atmosphere (Bindoff *et al.*, 2013). Atmospheric CO_2 levels recently passed 400 ppmv (Dlugokencky and Tans, 2017),

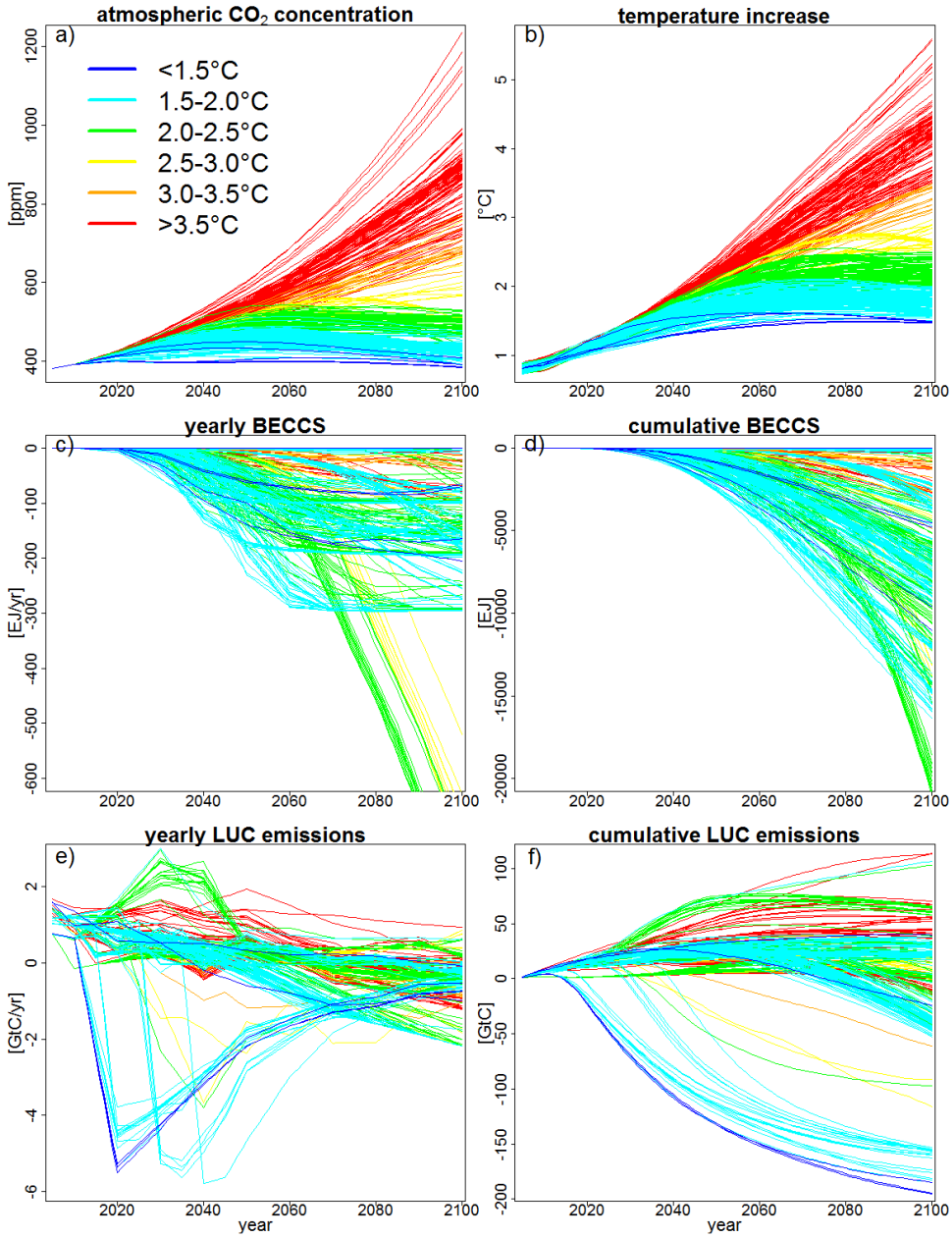

Figure 1.1: Time series (2000-2100) of atmospheric CO_2 concentration [ppm] (a), surface temperature increase [°C] relative to the pre-industrial era, calculated using the reduced complexity climate model MAGICC6 (b), yearly bioenergy with capture and storage [exa-joule, EJ] (c), cumulative bioenergy with capture and storage (d), yearly land-use change emissions [GtC] (e), and cumulative land-use change emissions (f) as calculated by Integrated Assessment Models (IAM) for the Fifth Assessment Report (AR5) of the Intergovernmental Panel on Climate Change. Each line shows the results from one IAM simulation extracted from the AR5 scenario database (https://secure.iiasa.ac.at/web-apps/ene/AR5DB/, last accessed September 2017). Subfields chosen are "Concentration|CO2|MAGICC6|MED", "Temperature|Global Mean|MAGICC6|MED", "Primary Energy|Biomass|w/ CCS", and "Emissions|CO2|Land Use". Missing values are linearly interpolated. Note that all scenarios with a bioenergy production of >400 EJ yr^{-1} are from the same IAM (GCAM 3.0). Since such bioenergy production rates seem highly unlikely (Creutzig et al., 2015) this suggests an error or miscalculation of some processes, or implausible assumptions for this model.

compared to typical values of 180-200 ppmv for glacials and 240-280 ppmv for interglacials, and thus exceed the range reconstructed for the last 800 000 years (Bereiter *et al.*, 2015, Luthi *et al.*, 2008). Climate projections suggest that for a "business-as-usual scenario" (i.e. extrapolating the historic trend in GHG emissions into the future), atmospheric CO_2 levels will continue to rise and likely exceed 800 ppmv by the end of the 21st century, resulting in an additional warming of several degrees Celsius (Fig. 1.1a-b; see also e.g. Friedlingstein *et al.*, 2014, Xu and Ramanathan, 2017). This would imply severe, long-term, and potentially irreversible impacts on ice sheets, sea level, ecosystems, and human well-being (e.g. Barnett *et al.*, 2005, Clark *et al.*, 2016, Doney *et al.*, 2009, Knutti *et al.*, 2016, Thomas *et al.*, 2004, Watts *et al.*, 2015). However, as set as an explicit goal in the UN Paris Agreement in 2015, rapid reductions in GHG emissions and the implementation of so-called "negative emissions" (the removal of CO_2 from the atmosphere) could possibly limit global warming below 2°C, or preferably even 1.5°C, relative to the pre-industrial era (Figueres *et al.*, 2017, Luderer *et al.*, 2016, Rockstrom *et al.*, 2017, Rogelj *et al.*, 2016a, Sanderson *et al.*, 2016, Schleussner *et al.*, 2016).

1.2 Perturbations of the terrestrial carbon cycle via land-use changes

The global carbon (C) cycle describes C exchanges between the atmosphere, hydrosphere, cryosphere, biosphere, pedosphere, and lithosphere, mainly in the form of CO_2 (Fig. 1.2; Ciais *et al.*, 2013). Most of the C on Earth is stored in the lithosphere in the form of sedimentary carbonates (>66 000 000 GtC) or in the oceans (~38 000 GtC), primary as inorganic C dissolved at great depths. A much smaller fraction exists in the vegetation (420-620 GtC), soils (1500-2400 GtC), or is stored in rock formations as fossil fuels (>4000 GtC, partly as accessible reserves; Ciais *et al.*, 2013). However, while these pools seem negligible compared to the lithospheric and oceanic reservoir, C fluxes occur much faster in the small pools, whereas the larger pools are not cycled on human-relevant time scales. The atmosphere currently contains around 850 GtC (~20 GtC more than in the 2013 report of the Intergovernmental Panel on Climate Change – IPCC; see Fig. 1.2). C exchanges between the biosphere and the atmosphere occur on different time scales. During day time, plants use energy from solar radiation to take up C from the air through their leaves, a process called photosynthesis. Each year, photosynthesis in the terrestrial biosphere removes around 120 GtC from the atmosphere (gross primary productivity, GPP; Beer *et al.*, 2010). However, at the same time plants also release C to the atmosphere. Around half of the GPP (60 GtC yr^{-1}) is directly re-emitted via autotrophic respiration, while the remainder (net primary productivity, NPP; Ito, 2011) is primary used for plant growth. When the plant, or part of the plant, dies, its dead biomass is transferred to the litter, where it is decomposed by microbes, and the C released back to the atmosphere (heterotrophic respiration). Under present-day conditions global GPP is slightly larger than the sum of autotrophic respiration, heterotrophic respiration, and other C losses (for example through fire), so that the land acts as a net C sink (see below). The decay of dead organic material is sometimes prevented by anaerobic conditions, which over time scales of millions

of years enables the formation of coal, oil, or natural gas. Over these very long time periods, the atmospheric C content is primarily determined by the balance between the weathering of rocks (removal) and volcanic eruptions (release).

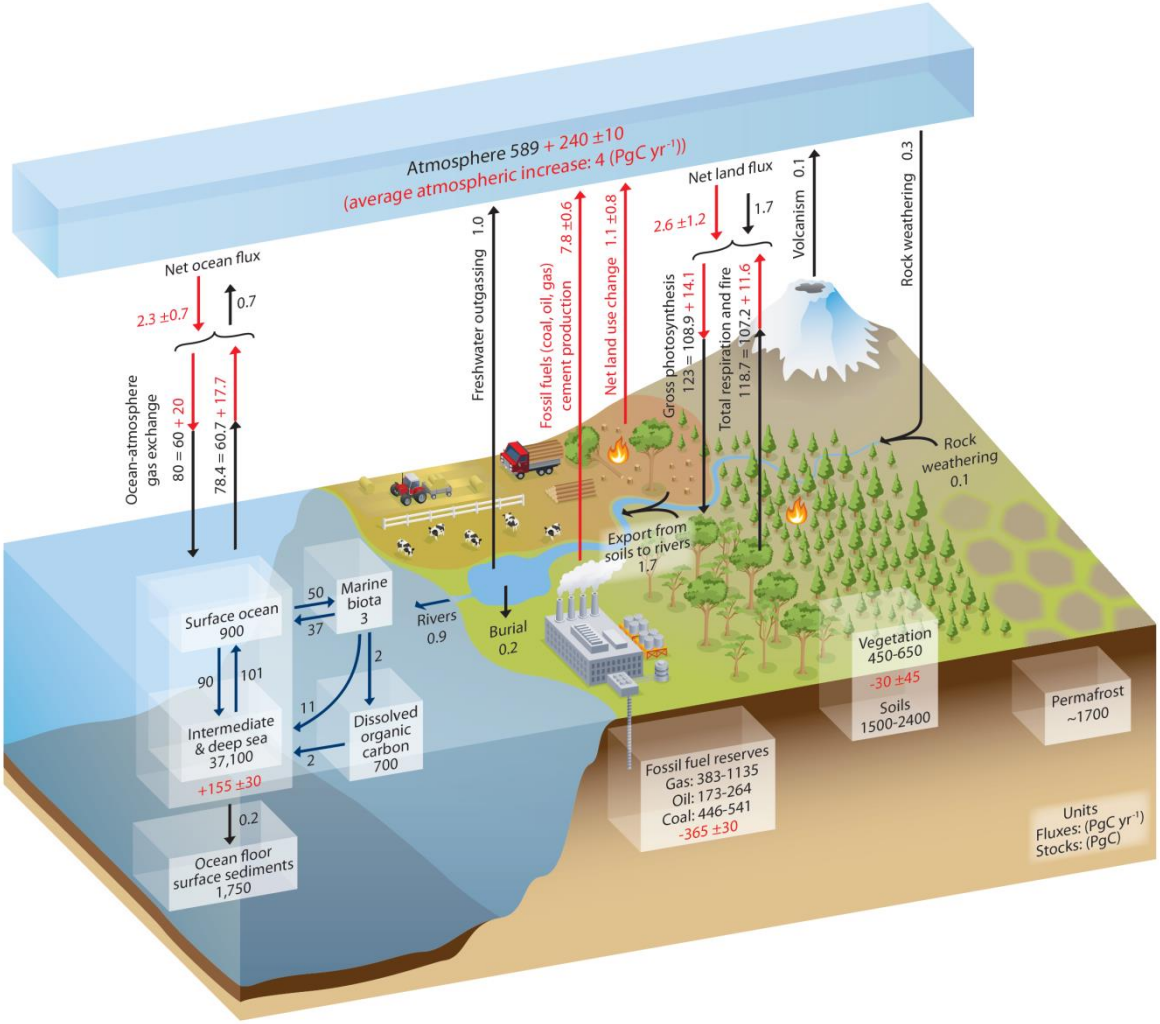

Figure 1.2: Simplified schematic of the global C cycle. Numbers represent C stocks [PgC] and annual C exchange fluxes [PgC yr^{-1}]. Black numbers and arrows indicate reservoir mass and exchange fluxes estimated for the time prior to the industrial era, about 1750. Red arrows and numbers indicate annual anthropogenic fluxes averaged over the 2000–2009 time period. The figure is from Ciais *et al.* (2013).

Past human activities have caused dramatic alterations of the C cycle, either via burning fossil fuels and cement production (a transfer of C from the Earth crust/lithosphere to the atmosphere), or via LUC (a transfer of C from the terrestrial biosphere and pedosphere to the atmosphere). As this thesis focuses on interactions between terrestrial ecosystems and the atmosphere, I provide an overview of LUC impacts on vegetation and soil C stocks in the following. Deforestation for agricultural land (croplands or pastures) releases large amounts of C stored in biomass to the atmosphere, either directly (if forests are burned) or subsequently (when the wood products are burned or decompose). Additionally, deforestation prevents continued C accumulation in old-growth forests (Luyssaert *et al.*, 2008), e.g. due to CO_2 fertilisation. Depending on prior vegetation cover, agricultural soils can also be a C

source, but emissions usually occur over longer time periods than for vegetation C. Croplands generally result in soil C losses compared to natural ecosystems because harvest reduces the C input to the soil and heterotrophic respiration and erosion rates are often high in croplands (Guo and Gifford, 2002, Smith *et al.*, 2016b). For pastures the picture is less clear, with the direction and magnitude of change depending on climate, soils, and management intensity (McSherry and Ritchie, 2013, Powers *et al.*, 2011). For example, a recent study estimated that agricultural soils represented a C source of around 133 GtC during the Holocene, with equal contributions from croplands and pastures (Sanderman *et al.*, 2017). In contrast, a review by Li *et al.* (submitted) found small soil C gains following forest conversions to grassland at most locations, but did not account for management intensity due to the lack of reported information. Conversely, once agricultural land abandonment occurs, regrowing secondary forests act as a long-term C sink (if not further disturbed) as vegetation and soil C pools recover (Chazdon, 2014, Chazdon *et al.*, 2016, Houghton and Nassikas, 2017).

Historic LUC emissions are typically calculated using bookkeeping approaches (Hansis *et al.*, 2015, Houghton, 2003a) or Dynamic Global Vegetation Models (DGVMs; Arneth *et al.*, 2017, Le Quere *et al.*, 2016). The cumulative net LUC emissions between 1750 and today have been estimated to be around 190 GtC, compared to 410 GtC from fossil fuel burning and industry (Le Quere *et al.*, 2016). However, the relative contribution of LUC emissions to total anthropogenic CO_2 emissions decreased over time, as fossil fuel emissions accelerated; net LUC emissions over the last decade are estimated to have been around 1.0 GtC yr^{-1}, compared to 9.3 GtC yr^{-1} from fossil fuel burning and cement production (Fig. 1.3). Currently, the land takes up around 30% of the total anthropogenic C emissions of ca. 10.3 GtC yr^{-1}, thereby reducing the growth rate of atmospheric CO_2 (Le Quere *et al.*, 2016). The land sink flux, F_{RES}, is typically derived as a remainder from the other terms of the global C cycle as:

$$F_{RES} = F_{FFC} + F_{LUC} - F_{OCEAN} - G_{ATM}$$

where F_{FFC} is fossil fuel and cement emissions, F_{LUC} the net LUC emissions, F_{OCEAN} the atmosphere-ocean flux, and G_{ATM} the growth rate of atmospheric CO_2. It is thus often termed the "residual sink". The net land flux (the sum of F_{RES} and F_{LUC}) is relatively well constrained by both CO_2 budgets and inversions. However, despite having been studied intensively for many years, the size of both LUC emissions and the residual sink are subject to very high uncertainties (Arneth *et al.*, 2017, Houghton *et al.*, 2012, Le Quere *et al.*, 2016, Peng *et al.*, 2017, Prestele *et al.*, 2017), and there is still no scientific census about the spatial distribution and nature of the sink (i.e. the relative contribution of climate change, CO_2, N deposition, recovery from past disturbances, and changing management) and its future persistence (Ahlstrom *et al.*, 2015, Bellassen and Luyssaert, 2014, Erb *et al.*, 2013, Houghton, 2003b, Houghton, 2007, Keenan *et al.*, 2016, Pan *et al.*, 2011, Poulter *et al.*, 2014, Schimel *et al.*, 2001, Sitch *et al.*, 2015, Zhu *et al.*, 2016).

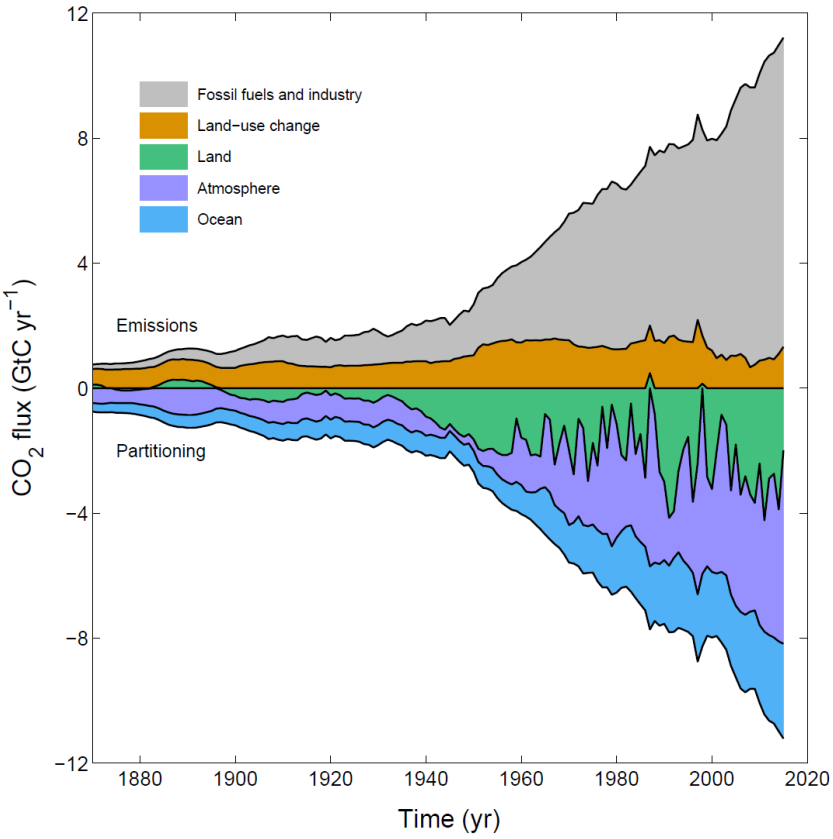

Figure 1.3: Combined components of the global C budget as a function of time, for emissions from fossil fuels and industry, and emissions from LUC, as well as their partitioning among the atmosphere, land, and oceans. The figure is from Le Quere *et al.* (2016).

1.3 Land-use impacts beyond CO_2

The effects of LUC on climate can generally be classified into two broad categories, alterations of atmospheric composition (biogeochemical effects, e.g. Arneth *et al.*, 2010) and changes in surface energy and water fluxes (biophysical effects, Foley *et al.*, 2003). Changes in atmospheric CO_2 levels belong to the former group, with other biogeochemical effects being emissions of CH_4 (primary from ruminants and rice cultivation) and N_2O (primary from fertilisers) (Tian *et al.*, 2016, Tubiello *et al.*, 2015, Zaehle *et al.*, 2011). Additionally, agriculture can alter the emissions of non-GHG reactive nitrogen (N) (Erisman *et al.*, 2011), mineral dust aerosols (Ginoux *et al.*, 2012), fire aerosols (Kloster *et al.*, 2010), or biogenic volatile organic compounds (BVOCs; Rosenkranz *et al.*, 2015, Unger, 2014), thereby influencing climate directly or indirectly via the formation of ozone (O_3, a GHG), secondary aerosols, or by changing the properties of clouds.

Despite this, biophysical LUC effects impact climate primarily on the local to regional scale. Surface albedo varies significantly between forests and open land, especially in regions under snow cover, thereby affecting the proportion of absorbed sunlight (Betts, 2000, Devaraju *et al.*, 2015, Jackson *et al.*, 2008). Forests are also known to evaporate more water (and to have a larger roughness length) than agricultural areas, resulting in regional surface cooling and potentially affecting cloud formation

(Bala *et al.*, 2007, Ban-Weiss *et al.*, 2011) and regional or remote precipitation patterns (Ellison *et al.*, 2012, Quesada *et al.*, 2017, Sampaio *et al.*, 2007, Swann *et al.*, 2012, Zemp *et al.*, 2014). Additionally, water vapour in the atmosphere acts as a GHG (Boucher *et al.*, 2004), and the absorbed energy will be released again once the vapour condenses, possibly at a very different location. While the albedo effect is particularly important in high latitudes, the evaporation effect dominates in the tropics (Bonan, 2008). Consequently, the question whether the net biophysical climate effect of deforestation is a regional warming or cooling depends on the specific location and time of the year (Alkama and Cescatti, 2016, Bright *et al.*, 2017, Li *et al.*, 2015, Perugini *et al.*, 2017).

Over the last years a number of modelling studies addressed the question of how important biophysical LUC effects on surface temperature are compared to biogeochemical effects (Perugini *et al.*, 2017). Some of these studies found biophysical and biogeochemical effects comparable in magnitude when applying idealised deforestation/afforestation scenarios (Bala *et al.*, 2007, Bathiany *et al.*, 2010, Devaraju *et al.*, 2015, Swann *et al.*, 2012). In contrast, most simulations driven by more realistic LUC suggest that biophysical impacts are relatively small on the global scale (Arora and Montenegro, 2011, Brovkin *et al.*, 2013, Pongratz *et al.*, 2011, Pongratz *et al.*, 2010), even though individual studies also reported large biophysical effects (Davies-Barnard *et al.*, 2014). On the local to regional scale, biophysical deforestation effects are often found to exceed the magnitude of the warming signal from increased GHG emissions (Arora and Montenegro, 2011, Betts *et al.*, 2007, de Noblet-Ducoudre *et al.*, 2012, He *et al.*, 2014). While most studies thus point towards negligible biophysical impacts on the global scale, this topic is still debated. Uncertainty mainly arises from the inadequate representation of landscape heterogeneity and LUC processes, and from different implementations of LUC into the climate/Earth system models (Brovkin *et al.*, 2013, de Noblet-Ducoudre *et al.*, 2012, Pitman *et al.*, 2009, Rounsevell *et al.*, 2014).

Furthermore, the impacts of LUC on the environment are not restricted to climate. Natural ecosystems provide a wide range of ecosystem services (ES), typically classified into provisioning, regulating, and cultural services (Haines-Yong and Potschin, 2013, Millennium Ecosystem Assessment, 2005). Historic human activities have caused dramatic alterations of a wide range of ecosystem functions and associated ES. For example, Rockström *et al.* (2009) proposed that three (biodiversity loss, interference with the N cycle, climate change) out of nine planetary boundaries have already been exceeded. Species extinction rates today are orders of magnitudes higher than natural background levels (Barnosky *et al.*, 2011, Pimm *et al.*, 2014), largely caused by LUC (Newbold *et al.*, 2014). Modern agriculture secures food provision for a growing population but enhances soil erosion, compaction, and salinisation, and the perturbation of biogeochemical cycles (Foley *et al.*, 2005, Stoate *et al.*, 2001). Impacts on aquatic systems are closely related to those on soils. Groundwater and rivers suffer from unprecedented amounts of toxicants and leached nutrients (Malmqvist and Rundle, 2002), and lakes as well as coastal regions are characterised by acidification and eutrophication (Galloway *et al.*, 2004).

An increasing amount of atmospheric pollutants such as tropospheric O_3 affect plant growth (Arneth *et al.*, 2010) and reduce human life expectancy (Kampa and Castanas, 2008). However, the multiplicity of such environmental side effects are often not considered when LUC and land management are being discussed, for example, as options to mitigate climate change (Williamson, 2016).

1.4 Agricultural land demand and the role of negative emissions

There is scientific agreement that humans started the domestication of wild plants and animals at the beginning of the Holocene in several regions of the world independently from each other (Ellis *et al.*, 2013, Lieberman, 2014). Agriculture quickly replaced hunting-and-gathering as the dominant lifestyle, and the substantial increase in the amount of calories available to people triggered a massive population growth and the establishment of permanent settlements (but also increased the risk of famine, malnutrition, disease, inequality, violence, and labor input; Harari, 2015). However, the extent of early agriculture and associated impacts on the environment are still controversial (Ellis *et al.*, 2013, Lewis and Maslin, 2015), and, despite agreement on the general picture, the available spatially-explicit global LUC reconstructions (Hurtt *et al.*, 2011, Kaplan *et al.*, 2011, Klein Goldewijk *et al.*, 2016, Klein Goldewijk *et al.*, 2011, Pongratz *et al.*, 2008, Ramankutty and Foley, 1999) differ substantially in terms of total cultivated area and spatial patterns over time. According to the Hurtt *et al.* (2011) reconstruction (which is based on the History Database of the Global Environment - HYDE - reconstruction by Klein Goldewijk *et al.*, 2011), by year 1850 around 564 Mha of the Earth's land surface was used for cropland and 774 Mha for pasture. LUC continues to take place until present and croplands and pastures in year 2005 covered around 1560 and 3340 Mha, respectively (Hurtt *et al.*, 2011; see also Fig. 1.4). Uncertainty in these numbers is particularly large for pastures partly due to terminological difficulties and a wide range of management intensities across regions (Alexander *et al.*, 2017b, Erb *et al.*, 2017). However, agricultural development since the early 20th century has not only been characterised by an expansion of agricultural land but also by rapidly changing management practices. The invention and application of synthetic fertilisers, pesticides, irrigation, and new crop varieties and machines ensured food provision for an accelerating population growth despite only moderately increasing production area (Pretty, 2008). Food availability, in combination with improved hygiene, freshwater access, and modern medicine triggered the rapid population increase from 2.5 to 7.5 billion people between 1950 and today (United Nations, 2015). At some places, increased agricultural productivity, production shifts, and societal changes also allowed for the abandonment of land previously used for cropping or grazing. Cramer *et al.* (2008) calculated an abandoned cropland area of around 210 Mha globally between 1700 and 1990 based on the LUC reconstruction by Ramankutty and Foley (1999). Using LUC reconstructions from the HYDE database, Campbell *et al.* (2008) estimated total abandoned agricultural area (cropland and pasture) in the year 2000 to be around 474-579 Mha (including areas converted to forest or urban), mainly in temperate regions. While these numbers

seem relatively small compared to present-day total agricultural area (~5000 Mha), there is potential for future cropland and pasture abandonment (see next paragraph).

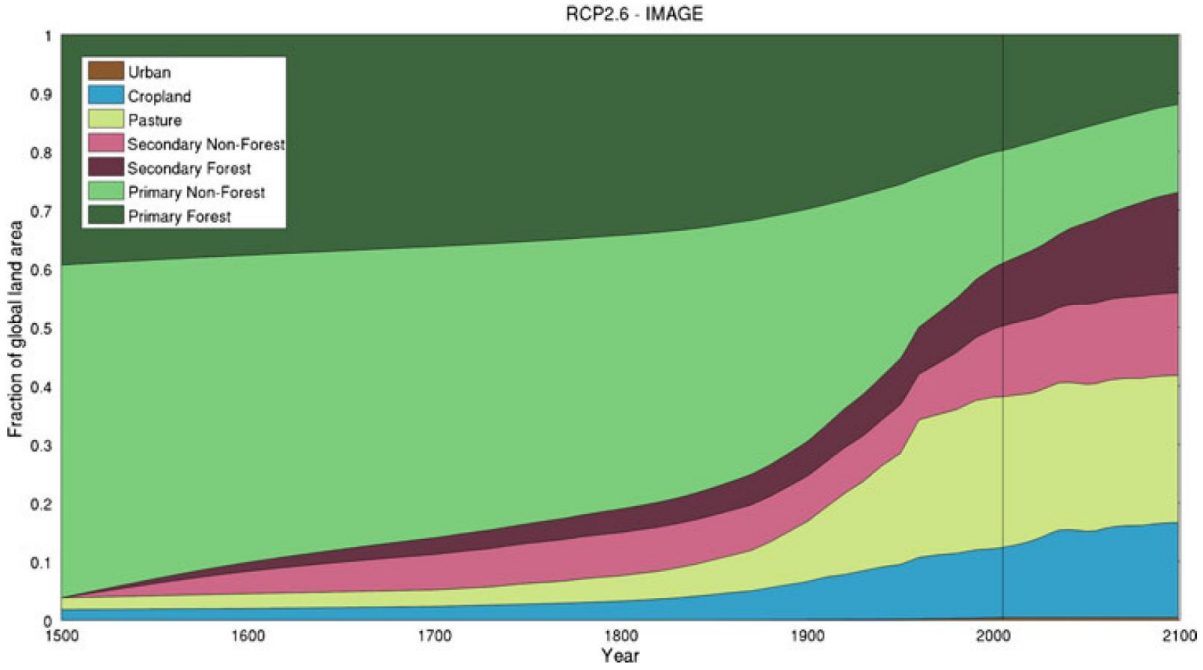

Figure 1.4: Time series of reconstructed/modelled fraction of global land surface area (excluding ice and open water) occupied by urban land, cropland, pasture, secondary non-forest, secondary forest, primary non-forest, primary forest for 1500–2100. The future period is based on RCP2.6-IMAGE. The total global ice-free land area is 12 900 Mha. The figure is from Hurtt *et al.* (2011).

LUC will continue to take place in the future, with large uncertainties in the projected trends and spatial patterns (Alexander *et al.*, 2017b, Eitelberg *et al.*, 2015, Popp *et al.*, 2017). According to five Shared Socioeconomic Pathways (SSPs), global population will continue to grow at least until mid-century and reach 6.9-12.6 billion people by the end of the century (Samir and Lutz, 2017). Increases in crop productivity and closing yield gaps might reduce the land demand to feed the growing population and potentially free up land for other usages (Erb *et al.*, 2016, Foley *et al.*, 2011, Godfray *et al.*, 2010, Mueller *et al.*, 2012). However, yields have been reported to stagnate or decline in several regions of the world (Alexandratos and Bruinsma, 2012, Ray *et al.*, 2012, Tilman *et al.*, 2002), and even retaining the rate of historic yield increases will likely prove insufficient to meet projected food demand (Laurance *et al.*, 2014, Ray *et al.*, 2013). Moreover, future yield increases might be hindered by climate change impacts on crop growth, at least in some regions (Pugh *et al.*, 2016, Rosenzweig *et al.*, 2014). Shifts in diets towards more meat and dairy consumption are expected to trigger additional pressure on natural ecosystems (Erb *et al.*, 2016, Valin *et al.*, 2014), although any shift towards vegetarian diets and the minimisation of food losses and overconsumption could reduce agricultural land demand (Alexander *et al.*, 2017a, Alexander *et al.*, 2016, Bajzelj *et al.*, 2014, Edmonds *et al.*, 2013, Godfray *et al.*, 2010). Taken together, a net expansion in food-producing agricultural area within the next decades seems more likely than large-scale agricultural abandonment.

Additionally, the necessity of negative emissions might trigger future LUC. From more than 1000 scenarios considered in the Fifth Assessment Report (AR5) of the IPCC, all scenarios limiting global end-of-century warming below 1.5°C, the majority of scenarios limiting warming below 2°C, and even many less ambitious scenarios needed to invoke substantial amounts of negative emissions, i.e. the removal of CO_2 from the atmosphere, in order to meet the targeted warming levels (Fuss *et al.*, 2014). Noteworthy, in all scenarios that remain below 2°C warming without negative emissions, global emissions peak around the year 2010, which, despite a recent slowdown in emissions growth (Peters *et al.*, 2017), is contrary to observations (Anderson, 2015). The amount of negative emissions necessary to achieve the 2°C target varies across studies and scenarios, depending on assumed GHG (and aerosol) emission trajectories, the desired likelihood to achieve the target (Rogelj *et al.*, 2015), and also on the time period chosen to define pre-industrial climate (Schurer *et al.*, 2017)[1]. The remaining cumulative emissions budget to stay below 2°C warming until 2100 has been estimated to be around 140-320 GtC (updated to the year 2017 based on Anderson, 2015, Anderson and Peters, 2016, Rockstrom *et al.*, 2017, Rogelj *et al.*, 2016b), with a recent study claiming that 180-220 GtC could still allow for the 1.5°C target (Millar *et al.*, 2017)[2]. Any exceedance of this would have to be compensated by negative emissions. To put the 140-320 GtC into perspective, total anthropogenic emissions today are around 11.2 GtC yr^{-1} (emissions in year 2015; Le Quere *et al.*, 2016), equivalent to 13-29 years of current CO_2 emission rates until the budget is reached. Using a simple coupled C-cycle climate model, Lenton (2010) found that, while negative emissions of 300 GtC (via afforestation, in addition to conventional mitigation in their baseline scenario which reached 2.5°C warming in 2100) proved insufficient to stay below the 2°C target, 1000 GtC (via biochar and biomass burial) resulted in an end-of-century warming of 1.34°C. Gasser *et al.* (2015) combined 11 state-of-the-art Earth System Models (ESMs) with stylised mitigation scenarios and estimated that, depending on timing and intensity of conventional mitigation efforts, between 25-100 (if fossil fuel CO_2 emission reductions start in 2015 at a rate of -5% per year) and 450-800 GtC (start in 2030 at -1% per year) will have to be removed from the atmosphere by year 2100 to reach the 2°C target. Cumulative negative emissions reported from Integrated Assessment Model (IAM) scenarios typically lie at the mid-to-lower end of this range[3], on average ~130-250 GtC (Boysen *et al.*, 2017b, Fuss *et al.*, 2016, Rogelj *et al.*, 2015, Smith *et al.*, 2016a, Tavoni and Socolow, 2013, Wiltshire and Davies-Barnard, 2015). The recent incorporation of negative emissions into IAMs increased the models' options to achieve ambitious mitigation targets. This resulted in

[1] This issue is further complicated by misinterpretations and inconsistencies across studies due to the confusion of gross *vs.* net negative emissions, the confusion of CO_2 *vs.* C, different definitions of negative emissions, e.g. bioenergy CCS *vs.* total CCS, or the inclusion/exclusion of other options than BECCS like afforestation, and different CCS efficiencies and conversion factors to translate between energy [J] and mass [kgC].

[2] Note that Millar *et al.* (2017) reported the "threshold exceedance budget", while the smaller "threshold avoidance budget" is probably a more appropriate measure; see e.g. https://www.cicero.uio.no/no/posts/klima/how-much-carbon-dioxide-can-we-emit (last accessed October 2017).

[3] Note that Gasser *et al.* (2015) claimed that their estimates of gross negative emissions fall in the lower end of the range reported by IAMs. The reason presumably is that Gasser *et al.* looked at total CCS (including fossil fuel CCS), while IAMs typically report BECCS.

the paradox that "despite little progress in international climate policy and increasing emissions, long-term climate stabilisation through the lens of IAM appears easier and less expensive" (Tavoni and Socolow, 2013). IAMs typically assume perfect foresight about socioeconomic and technological development, and thus tend to favour negative emissions over conventional mitigation if found to be economically beneficial. The production of bioenergy crops in combination with C capture and geologic storage upon combustion (BECCS) is currently regarded by the IAMs as the most promising option to achieve negative emissions (see also Fig. 1.1c-d). However, even though IAMs typically assume very high yields from second-generation bioenergy crops (Creutzig, 2016), this approach would require the allocation of a significant proportion of the land surface for bioenergy cultivation, thereby increasing pressure on remaining natural ecosystems and food-producing agriculture (Schueler *et al.*, 2016, Slade *et al.*, 2014). For example, Smith *et al.* (2016a) reported bioenergy land requirements of 380-700 Mha (assuming the cultivation of high-productive dedicated energy crops) by the end of the century for scenarios consistent with the 2°C target, and potentially a lot more if only forest or agricultural residues were used as bioenergy feedstocks[4]. Humpenöder *et al.* (2014) found a cumulative carbon dioxide removal (CDR) of 160 GtC on ~500 Mha bioenergy area by the end of the century, including the assumption of technological yield increases in their underlying vegetation model. Using an uncoupled version of the same vegetation model as Humpenöder *et al.*, Boysen *et al.* (2017a) estimated that in the absence of technological yield increases for bioenergy crops, at least 1300 Mha (~30% of current agricultural area) of low-productive land (which in their study is abandoned first) currently used for food production would have to be converted to bioenergy plantations by year 2020 to achieve >130 GtC in 2100. A smaller area would only be possible if more productive land was available for bioenergy cultivation (Boysen *et al.*, 2016).

An alternative or supplement to BECCS could be the protection and expansion of global forest area because forests are natural C sinks (Houghton *et al.*, 2015, Mackey *et al.*, 2013). In fact, some IAMs explicitly consider avoided deforestation and afforestation/reforestation (ADAFF) as an option to reduce atmospheric CO_2 (Fig. 1.1e-f). However, the associated land demand for a given CDR target would likely be even higher than for BECCS (Humpenöder *et al.*, 2014, Lenton, 2010, Smith *et al.*, 2016a). Some scientists proposed the irrigation of desert regions to allow for tree growth (Becker *et al.*, 2013, Keller *et al.*, 2014, Ornstein *et al.*, 2009), although there are doubts concerning costs and feasibility. Other options of less land requirements also have the potential to remove C from the atmosphere (or more generally speaking to stabilise climate, often termed geoengineering; Lenton and Vaughan, 2009), but so far are regarded as too costly, energy demanding, ineffective, technologically unproven, or bear serious environmental risks (Field and Mach, 2017, Keller *et al.*, 2014, Smith *et al.*, 2016a, Williamson, 2016).

[4] This is only for bioenergy cultivation in combination with CCS. However, many scenarios (including >2°C scenarios) also rely on substantial amounts of non-CCS bioenergy, thereby increasing total bioenergy land demand.

Finally, future LUC will in turn also be affected by climate change and atmospheric CO_2 levels which impact on vegetation composition (Holmgren *et al.*, 2013, Scholze *et al.*, 2006), forest mortality (Allen *et al.*, 2015, Choat *et al.*, 2012, Neumann *et al.*, 2017, Seidl *et al.*, 2014), forest regrowth (Anderson-Teixeira *et al.*, 2013), and crop yields (Brown *et al.*, 2000, Cai *et al.*, 2016, Challinor *et al.*, 2014, McGrath and Lobell, 2013, Pugh *et al.*, 2016, Rosenzweig *et al.*, 2014, Schauberger *et al.*, 2017), with direct implications on terrestrial C stocks and the area needed for food or bioenergy production. Reversely, if negative emissions result in a net removal of C from the atmosphere (i.e. gross negative emissions exceed fossil fuel emissions), natural C sink capacities might weaken and hinder the effectiveness of negative emissions (Fuss *et al.*, 2016, Jones *et al.*, 2016).

1.5 Representing land use in Dynamic Global Vegetation Models

DGVMs were originally designed to simulate water and C fluxes in potential natural vegetation and their response to environmental changes (Cramer *et al.*, 2001, Prentice *et al.*, 2007, Quillet *et al.*, 2010). They are usually run "offline" forced by prescribed climate and other forcing variables but sometimes are also run "online" as part of the land/vegetation component of IAMs or ESMs to study feedbacks between the terrestrial biosphere, socio-economy, and the physical climate system. Despite its importance for the C cycle and climate, until recently LUC was not, or only very rudimentarily, represented in DGVMs or similar models like land surface models (Pugh *et al.*, 2015). For example, most ESMs contributing to the fifth phase of the Coupled Model Intercomparison Project (CMIP5) treated cropland similar or equal to natural grassland, thereby not accounting for differences in phenology, physiology, and management (Brovkin *et al.*, 2013, Xu and Hoffman, 2015). Bioenergy plantations were treated as cropland or grassland, or were entirely ignored (Boysen *et al.*, 2017b).

Progress over the last decade with respect to LUC in DGVMs includes the parameterisation of specific crop functional types (CFTs; Bondeau *et al.*, 2007, Levis *et al.*, 2012, Lindeskog *et al.*, 2013), including dedicated bioenergy crops (Beringer *et al.*, 2011, Mayer, 2017), management techniques like tillage (Levis *et al.*, 2014, Pugh *et al.*, 2015, Stocker *et al.*, 2014) and irrigation (Jagermeyr *et al.*, 2015, Lindeskog *et al.*, 2013), flexible sowing and harvesting dates (Bondeau *et al.*, 2007, Lindeskog *et al.*, 2013), variable grassland management (Rolinski *et al.*, 2017), the implementation of the N cycle enabling crop fertilisation (Olin *et al.*, 2015b), and gross land-cover transitions, including shifting cultivation, wood harvest, and subsequent forest regrowth in different age classes (Arneth *et al.*, 2017, Bayer *et al.*, 2017, Shevliakova *et al.*, 2009, Stocker *et al.*, 2014, Wilkenskjeld *et al.*, 2014). The more detailed representation of anthropogenic activities tends to increase historic LUC emissions in the DGVMs, and consequently questions our current process understanding about ecosystem responses to environmental changes (Arneth *et al.*, 2017, Pugh *et al.*, 2015).

1.6 Thesis structure and objectives

The main research questions of this thesis are as follows:

- What are the impacts of land-use and land-cover changes on the terrestrial carbon cycle and to what degree are these impacts reversible?
- Can large-scale land-based mitigation efforts contribute to climate stabilisation by removing substantial amounts of carbon from the atmosphere?
- What would be the environmental side effects of land-based climate change mitigation?
- How do different representations of agricultural processes in vegetation models affect the results?

To answer these questions the results of this thesis are broken into three main sections (Sections 3-5), each with their own objectives. Section 2 summarises information about the common methodology used in all sections of this thesis (i.e., the applied DGVM LPJ-GUESS) as well as about the specific methodology used in Sections 3-5. Section 3 studies the long-term impacts of the LU history on the recovery of ecosystems in LPJ-GUESS. The research questions addressed are:

- How fast do ecosystems return to their pre-disturbed state (in terms of vegetation composition, carbon pools, and fluxes) following agricultural abandonment?
- Is there an impact of different land-use histories (in terms of agricultural duration and management type) on the recovery of ecosystems?
- Are there any regions where the ecosystem never returns to its pre-disturbed state?

Sections 4 and 5 directly address the potential, and environmental side effects, of land-based climate change mitigation projects. Both sections build upon output from DGVMs driven by LUC scenarios from two land-use models. In these scenarios, C removal is achieved via bioenergy production combined with C capture and storage and/or avoided deforestation and afforestation[5]. Section 4 focuses on potential C removal from land-based mitigation, not only in LPJ-GUESS, but also in three other DGVMs. The questions addressed are:

- What amounts of carbon removal from the atmosphere can be achieved in Dynamic Global Vegetation Models when driven by scenarios of future land management for climate change mitigation?
- How do these numbers compare to the carbon removal achieved in the land-use models used to create the scenarios?
- What are the main mechanisms responsible for the differences?

Section 5 focuses on potential environmental side effects of land-based mitigation in addition to C removal, as calculated using LPJ-GUESS simulations. For this, a number of ecosystem services indi-

[5] The term afforestation refers to both afforestation and reforestation in the following.

cators are considered, including surface albedo, evapotranspiration, runoff, crop production, N loss, and BVOC emissions. The research questions are:

- What are the impacts of land management for carbon uptake on other ecosystem services and ecosystem service indicators?
- Do the effects of land-based climate change mitigation on ecosystem service indicators differ based on the mitigation approach (BECCS, ADAFF, or a combination of both)?
- If so, can a mitigation approach be identified in which trade-offs between other ecosystem service indicators are less pronounced than in the other approaches?
- What are the spatial and temporal patterns of the impacts of land-based mitigation on ecosystem service indicators?

Sections 3-5 are based on results from three papers, with slightly edited results, discussion, and conclusions chapters in order to fit the thesis structure. Section 3 builds upon the paper "Impacts of land-use history on the recovery of ecosystems after agricultural abandonment" by Krause *et al.* (2016) published in *Earth System Dynamics*. Section 4 is based on the paper "Large uncertainty in carbon uptake potential of land-based climate-change mitigation efforts" by Krause *et al.* (2018) published in *Global Change Biology*. Section 5 builds upon the paper "Global consequences of afforestation and bioenergy cultivation on ecosystem service indicators" by Krause *et al.* (2017) published in *Biogeosciences.* The two open access papers (Krause et al. 2016; Krause et al. 2017) are attached in the Appendix of this thesis. A general conclusion and outlook section with respect to the overall research questions is presented in Section 6, providing a broader perspective on the findings of this thesis.

As much of the work presented in the following involved also some input from the co-authors of the published/prepared versions of the sections, I will generally use "we" instead of "I" throughout the Sections 2-5.

2 Methods

2.1 The LPJ-GUESS Dynamic Global Vegetation Model

The primary tool used in this thesis is the Lund-Potsdam-Jena General Ecosystem Simulator (LPJ-GUESS) DGVM. LPJ-GUESS is a process-based model designed to simulate vegetation dynamics and corresponding C, N, and water fluxes from regional to global scales (Smith *et al.*, 2001, Smith *et al.*, 2014). It is forced by daily temperature, precipitation, and shortwave radiation, typically at a spatial resolution of 0.5° x 0.5° for global studies. Global atmospheric CO_2 mixing ratio is prescribed at annual time steps, gridded reactive N deposition at decadal time steps, and gridded soil texture is set constant over time. LPJ-GUESS adopts many physiological and biophysical features from the LPJ DGVM (Sitch *et al.*, 2003), but explicitly represents tree size structure and demographics. Potential woody vegetation is simulated as age cohorts of different groups of plant species (Fig. 2.1), competing for light, space, nutrients, and water in a number of patches (typically between 5 and 50), each representing an area of 1000 m^2 (Smith *et al.*, 2001). This approach adopts features of forest gap models (Bugmann, 2001), enabling a more realistic and detailed representation of forest succession, competition, and interaction between plant individuals compared to most other DGVMs. Patches are simulated repeatedly to capture the stochastic implementation of mortality and establishment processes. Grasses are represented by a single individual at ground level. LPJ-GUESS typically represents around 12 plant functional types (PFTs; see Table 2.1) which differ in terms of their bioclimatic limits, growth form (trees or herbaceous plants), phenology (evergreen, summergreen or raingreen), life history strategy (shade-tolerant or intolerant), and photosynthetic pathway (C_3 or C_4), and cover all major high plant types. Model processes include photosynthesis, respiration, water uptake, evapotranspiration, phenology, C and N allocation, growth, and mortality, simulated on daily or annual time steps. Daily C assimilation is calculated based on a modified Farquhar photosynthesis scheme (Haxeltine and Prentice, 1996b) and allocated to leaves, stems, and fine roots at the end of each year according to a set of prescribed allometric relationships for each woody PFT (Sitch *et al.*, 2003). Wildfires destroy parts of the biomass as a function of litter moisture and load (Thonicke *et al.*, 2001), while patch-destroying disturbances are implemented as stochastic events with an expected return interval of 100 years. Following such disturbances, or if agricultural land is converted back to natural vegetation, there is a typical succession from grasses to light-demanding pioneer trees, eventually followed in many ecosystems by the establishment of shade-tolerant PFTs. Soil C and N dynamics are based on the CENTURY model (Parton *et al.*, 1993), representing 11 soil and litter pools that differ in their C:N ratios and decay rates (Smith *et al.*, 2014). Major model updates over the last years include the implementation of an improved hydrology scheme (Gerten *et al.*, 2004), BVOC emissions (Arneth *et al.*, 2007, Schurgers *et al.*, 2009), agricultural land (Lindeskog *et al.*, 2013, Olin *et al.*, 2015a, Olin *et al.*, 2015b), and a coupled C-N cycle (Smith *et al.*, 2014, Warlind *et al.*, 2014). The model has been extensively evaluated against a broad range of experimental and observational data, including large-scale

vegetation patterns (Hickler *et al.*, 2012), ecosystem-atmosphere C fluxes (Ahlstrom *et al.*, 2012, Fleischer *et al.*, 2015, Piao *et al.*, 2013), forest succession (Smith *et al.*, 2014), vegetation seasonality (Lindeskog *et al.*, 2013), and crop yields (Blanke *et al.*, 2017, Olin *et al.*, 2015a, Olin *et al.*, 2015b, Pugh *et al.*, 2015).

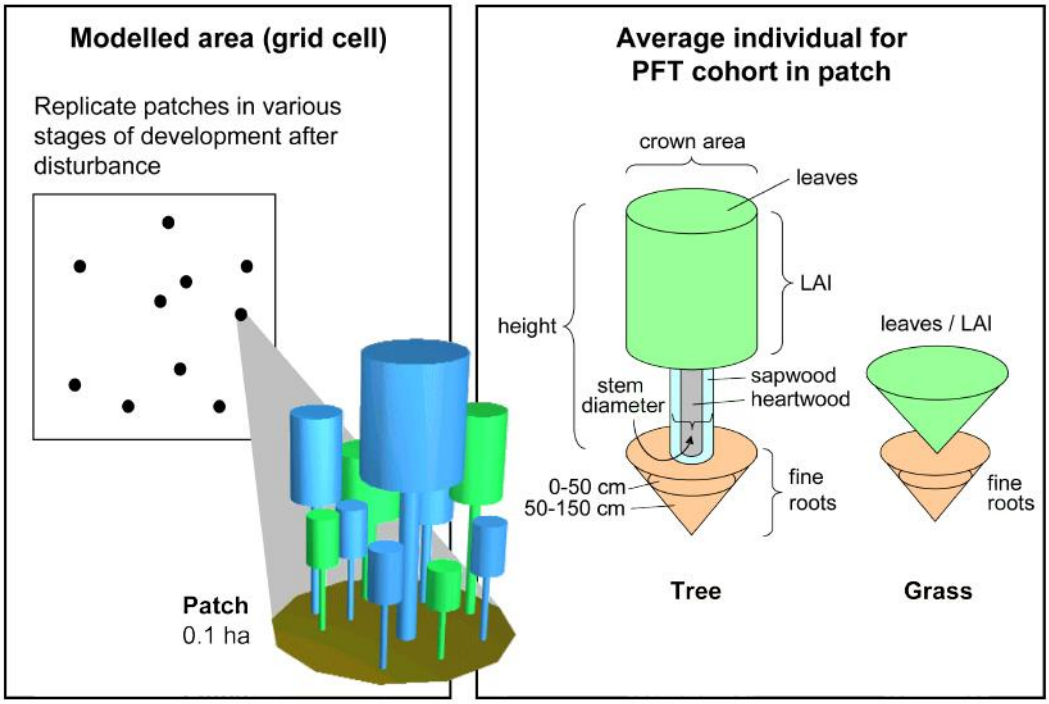

Figure 2.1: Vegetation representation in LPJ-GUESS with consideration of age cohorts. The figure is from Smith *et al.* (2014).

Agricultural processes have recently been introduced into LPJ-GUESS so that besides natural vegetation, the model now represents pasture and cropland land-cover classes (Lindeskog *et al.*, 2013). Land-cover transitions are prescribed at annual time steps. Pastures are populated by competing C_3 and C_4 grasses which are annually harvested (50% of above-ground biomass) to account for the effects of livestock grazing on C cycling. Croplands are represented by the globally most important crop species, grouped into four CFTs: wheat, maize, rice, and other temperate summer crops (Bondeau *et al.*, 2007, Lindeskog *et al.*, 2013). The C-only version of LPJ-GUESS represents additional CFTs but C-N cycling so far is only included for these four CFTs. CFT fractions are prescribed and CFTs thus do not compete with each other within a grid-cell. CFTs differ in their temperature limits, heat requirements, C allocation, and C:N ratios in different plant organs. The timing of sowing is modelled dynamically depending on temperature and precipitation variability in a grid-cell (Waha *et al.*, 2012), with temperature limits as in Bondeau *et al.* (2007). C allocation in crops is simulated on a daily time step. Harvesting (90% of the grain) occurs once a crop-specific potential heat unit (PHU) sum is fulfilled based on the mean temperature of the last 10 years (Lindeskog *et al.*, 2013). Farmers are assumed to adapt to climate shifts by adjusting the crop variety to climate, which is implemented in the model as an adaptation of the crops' PHU. Optional management techniques include irrigation (the irrigated/rain-fed

fraction of each CFT is prescribed for each grid-cell and year), cover crops, residue removal (Lindeskog *et al.*, 2013), tillage (Chatskikh *et al.*, 2009, Olin *et al.*, 2015a, Pugh *et al.*, 2015), and N fertilisation at specific stages of crop development (prescribed for each grid-cell and year; Olin *et al.*, 2015b). It is now also possible to simulate gross land-cover transitions within LPJ-GUESS (Bayer *et al.*, 2017).

Table 2.1: LPJ-GUESS plant functional types used in this thesis.

BNE	Boreal needleleaved evergreen tree
BINE	Boreal shade-intolerant needleleaved evergreen tree
BNS	Boreal needleleaved summergreen tree
TeNE	Temperate needleleaved evergreen tree (not used in Section 3)
TeBS	Shade-tolerant temperate broadleaved summergreen tree
IBS	Shade-intolerant broadleaved summergreen tree
TeBE	Temperate broadleaved evergreen tree
TrBE	Tropical broadleaved evergreen tree
TrIBE	Tropical shade-intolerant broadleaved evergreen tree
TrBR	Tropical broadleaved raingreen tree
C3G	Cool C_3 grass
C4G	Warm C_4 grass

2.2 Specific methodology Section 3

2.2.1 LPJ-GUESS model version

At the time the simulations for Section 3 were performed, the CFTs in LPJ-GUESS had not yet been updated to include a coupled C-N cycle (the simulations for the Sections 4 and 5 were performed with CFTs). We therefore represented croplands by C_3 and C_4 grass PFTs modified to mimic important aspects for the C and N cycles. Settings for croplands and pastures were as follows:

1. For transitions from natural vegetation to cropland, we transferred only 3% of the cleared woody biomass to the litter instead of 12% for natural vegetation-pasture transitions. This accounts for the practice that farmers would try to remove as many coarse roots as possible before planting of crops.
2. Harvest efficiency (in this study: fraction of above-ground biomass that is assumed to be returned to the atmosphere within one year) was 0.5 yr^{-1} for pasture, representing the net effect of grazing processes (Lindeskog *et al.*, 2013). For crop simulations we changed the harvest efficiency to 0.8 yr^{-1}, representing simplified crop harvest, as in Lindeskog *et al.* (2013).

3. While we removed 100% of harvested N biomass for croplands, we changed this value to 65% for pastures. That accounts for significant urine N regain from animals fed on pastures (Dean *et al.*, 1975, Lauenroth and Milchunas, 1992).
4. Root turnover rate was 0.7 yr^{-1} for pasture and was adapted to 1.0 yr^{-1} for croplands to represent the annual plant types used in most croplands.
5. We estimated tillage effects in croplands by increasing heterotrophic respiration in the surface humus and microbial pools, as well as in the microbial and slow turnover pools of the soil by a factor of 1.94 (Olin *et al.*, 2015a).
6. We simulated N fertilisation in croplands by applying 75 kgN ha^{-1} yr^{-1} equally throughout the year to sustain crop productivity with time. This value represents a compromise between higher values presently found in parts of Europe and lower values in most of Africa (e.g. Potter *et al.*, 2010). We therefore exclude spatial differences in N fertilisation of croplands from the simulation results.

We used 50 patches to minimise the inter-annual variability at the grid-cell level.

2.2.2 Land-use scenarios

In this study, we analysed the recovery of ecosystems following different agricultural LU histories, irrespective of whether the ecosystem recovers as a result of climate/environmental protection activities or as a by-product of other socio-economic forces. For this, we created idealised LU scenarios in which we made a transition from natural vegetation to either pasture or cropland directly after the model spin-up, followed by a transition back to natural vegetation after time periods of 20, 60, and 100 years. This resulted in three pasture (P20, P60, P100) and three cropland (C20, C60, C100) simulations. Additionally, we created a reference scenario in which natural vegetation was retained throughout the whole simulation period to simulate the ecosystem without any human interference.

2.2.3 Simulation setup

The simulations for Section 3 were performed under (approximately) present-day environmental conditions. During spin-up (500 years) and the simulation period (900 years), we forced LPJ-GUESS with temperature-detrended, repeated 1981-2000 climate from the University of East Anglia Climate Research Unit 3.21 dataset (CRU, 2013), 1990s mean N deposition (Lamarque *et al.*, 2013), and a fixed atmospheric CO_2 mixing ratio of 356 ppmv. Land-cover transitions were taken from the idealised scenarios described in Section 2.2.2. For all simulations (P20, P60, P100, C20, C60, C100, reference simulation) we used potential natural vegetation cover to spin up the model. We ran the model for Europe and Africa (33°E to 55°W), covering a wide range of environmental conditions and all major biomes (Smith *et al.*, 2014). We chose Africa and Europe for the simulation domain because the original LU version of the model was evaluated against observations in Africa (Lindeskog *et al.*, 2013) and to limit the computational expense of the simulations. We did not intend to realistically represent

typical crop and pasture management across the domain (i.e. the spatial variability in fertiliser use, multiple cropping systems, or irrigation).

2.2.4 Analysed grid-cells and biome classification

To facilitate the interpretation, we classified each grid-cell to one biome. We used the same classification rules as Smith *et al.* (2014), aggregated to eight biomes as in Bayer *et al.* (2015). Afterwards, we excluded grid-cells from the analyses which were classified as desert or tundra, had a mean NPP below 0.1 kgC m^{-2} yr^{-1} (in the reference simulation), or were located above 62.5°N, making the assumption that the relevance of these low-production areas for agriculture is negligible.

2.2.5 Analysed variables and definition of recovery

We studied the influence of LU history on ecosystems by analysing four key variables: dominant PFT, vegetation C, soil C (excluding litter), and net biome productivity (NBP). NBP is the net atmosphere-land C flux after C losses associated with respiratory fluxes, fire, harvest, land clearing, and decomposition of LUC product pools are subtracted from GPP. We investigated the legacy effects of LU history by calculating a recovery time for each variable, simulation, and grid-cell after the conversion back to natural vegetation. For vegetation C, soil C, and NBP, recovery time was defined as the year in which the 20-year running mean of the variable exceeded the threshold of one standard deviation (σ) below the mean of the reference simulation (full simulation period) for the first time after agricultural abandonment. σ was calculated on the 20-year running mean of the reference simulation. To avoid "false-positive" identifications of recovery in cases for which the variable of interest was initially within 1 σ, but then exhibited dynamics taking it outside this range (e.g. P20 soil C in Fig. 2.2), we

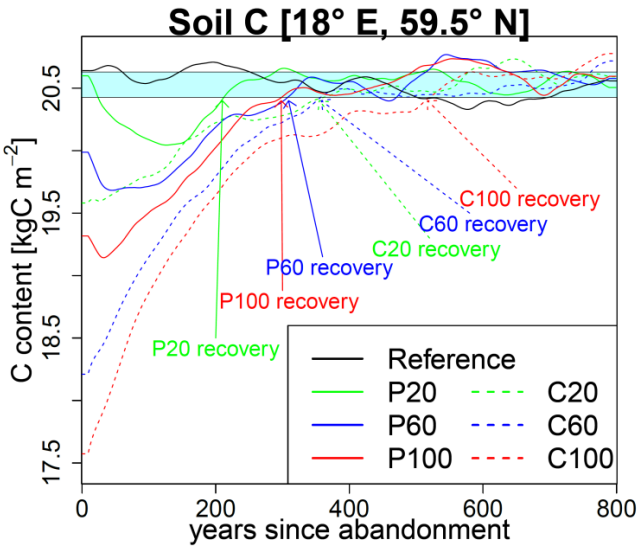

Figure 2.2: Soil C [kgC m^{-2}] for the six simulations after conversion to natural vegetation at one single example site to illustrate how recovery time was calculated according to our definition. The cyan-shaded area corresponds to reference simulation mean ± 1 σ. When soil C exceeds the mean - 1 σ threshold and the time of the minimum (which in this case is located in the first 200 years and below the mean - 1 σ threshold for all six simulations) is passed, recovery is achieved.

applied an additional criterion of whether the minimum after the transition to natural vegetation occurred in the first 200 years and if it was below the mean minus 1 σ threshold. If that was the case, the condition was expanded so that the variable could only be defined as recovered after the year in which the minimum occurred ("minimum rule"). We chose a 200-year window because the minimum occurred within the first 200 years for all biome averages of all variables and simulations. If the minimum was located after 200 years, we assumed the minimum to be a result of natural variability and recovery was achieved as soon as the variable in question exceeded the threshold of 1 σ below the reference mean. Figure 2.2 shows an example of how soil C recovery was calculated for one site.

For the dominant PFT recovery, we first identified which PFT dominates each grid-cell in the reference simulation based on the annual maximum leaf area index (LAI) amongst PFTs. We then checked for dominant PFT recovery in the same way as we did for vegetation C, soil C, and NBP (i.e., whether its LAI exceeded the threshold of 1 σ below the reference simulation mean; condition 1) but additionally checked whether its LAI was also larger than the LAI of any other PFT in the same simulation and year (i.e. the dominant PFT is the same as in the reference simulation, condition 2). Thus, dominant PFT recovery was only possible if both conditions were fulfilled. For example, if the temperate broadleaved evergreen (TeBS) tree was the dominant PFT in the reference simulation (with an average maximum LAI of, for example, 3.0 and standard deviation of ± 0.2), dominant PFT recovery in a specific LU simulation (e.g. P20) would occur once the LAI of TeBS in this simulation a) hits the threshold of 2.8 (3.0 - 0.2, condition 1) and b) is larger than the LAI of any other PFT in P20 in the specific year i.e., TeBS is the dominant PFT in the grid-cell (condition 2). For all variables, the recovery time was capped at 800 years after reconversion to natural vegetation, the point when simulations ended. Recovery times of 800 years thus represent a lower limit. However, the actual recovery time in these cases could theoretically lie between 801 years and infinity.

2.3 Specific methodology Section 4

2.3.1 The IMAGE and MAgPIE land-use models

Sections 4 and 5 both build upon DGVMs simulations driven by LUC scenarios from the IMAGE and MAgPIE models. The following paragraphs provide a short overview of the two models.

The Integrated Model to Assess the Global Environment (IMAGE) is an ecological-environmental model framework that includes several sub-models representing the energy system, agricultural economy, LU, natural vegetation, and climate system (Stehfest *et al.*, 2014). Socio-economic parameters are usually calculated for 26 world regions, and most environmental parameters are modelled on a 0.5° x 0.5° grid at annual time steps. LU dynamics are driven by demand for and supply of crops, animal products, and bioenergy. Bioenergy demand to achieve a specific CDR target is determined by the energy system sub-model which uses land availability from the LU sub-model following a set of

sustainability criteria (Hoogwijk *et al.*, 2003). For this study, bioenergy crops were included as fast-growing C_4 grasses (Doelman *et al.*, 2018) as these produce higher yields than woody plants in many locations. The level of agricultural intensification required to free up land for afforestation to achieve a specific CDR target is estimated using a stepwise approach of increasing yields and livestock efficiencies. This implies that reduced crop and pasture areas go with higher yields and livestock efficiencies, thereby allowing the same food production as in the baseline. Afforestation is assumed to occur first in grid-cells with high potential for forest growth. IMAGE also represents degraded forests which are assumed to be completely deforested and can be reforested as part of the afforestation activities (Doelman *et al.*, 2018). The degraded forest land-cover class was implemented in IMAGE due to larger deforestation rates reported by the Food and Agriculture Organization of the United Nations (FAO) 2015 Forest Resource Assessment (http://www.fao.org/3/a-i4793e.pdf, last accessed September 2017) than the historical expansions of cropland and pasture area reported by FAO. These differences are assumed to be caused by additional reasons (e.g. unsustainable forestry preventing regrowth of natural forests, mining, or illegal logging) and accounted for by a historically calibrated rate of forest degradation which is extrapolated into the future (Doelman *et al.*, 2018). Natural vegetation regrowth trajectories as well as crop yields, C, and water dynamics are modelled dynamically by the internally coupled DGVM Lund-Potsdam-Jena model with managed Land (LPJmL; Bondeau *et al.*, 2007, Stehfest *et al.*, 2014).

The Model of Agricultural Production and its Impact on the Environment (MAgPIE) is a global multi-regional partial equilibrium model of the agricultural sector (Lotze-Campen *et al.*, 2008, Popp *et al.*, 2014). MAgPIE aims to minimise the global costs for agricultural production throughout the 21st century at a 5-year time step (recursive dynamic optimisation) and is driven by demand for agricultural commodities and associated costs in 10 world regions. The cost minimisation is subject to various spatially explicit biophysical factors such as land and water availability as well as crop yields (provided by LPJmL). Major options to fulfil increasing demand are intensification (yield-increasing technologies), expansion (LUC), and international trade. Demand for CDR enters the model at the global scale, while the spatial distribution of bioenergy production or afforestation is derived endogenously in the model (involving economic and biophysical factors). Bioenergy demand is fulfilled chiefly through the growth and harvest of grassy energy crops; woody bioenergy in this study is grown only on less than 1% of the area used for bioenergy production. Actual bioenergy yields are derived from potential LPJmL yields (using information about observed LU intensity and agricultural area for initialisation), but can exceed LPJmL yields over time due to technological progress (Humpenöder *et al.*, 2014). Afforestation is assumed to occur as managed regrowth of natural vegetation according to parameterised s-shaped growth curves towards a maximum potential natural vegetation C density as provided by LPJmL, with soil C increasing linearly towards its potential maximum within 20 years (Humpenöder *et al.*, 2014). For simplicity, we refer to both IMAGE and MAgPIE as land-use models (LUMs) in the following.

2.3.2 Land-use scenarios

As input to the DGVMs we used the baseline projections (without land-based mitigation) from IMAGE and MAgPIE and three land-based mitigation scenarios, each calculated by both LUMs based on the assumption of a cumulative CDR target of 130 GtC by the year 2100. In the "BECCS" scenario this was achieved via bioenergy plant cultivation and subsequent CCS, the "ADAFF" scenario involved maintaining and expanding global forest area, and in "BECCS&ADAFF" the CDR demand was fulfilled in equal parts via both options. While in the LUMs the CDR target in ADAFF was achieved via terrestrial C uptake (CDR = Δ vegetation C + Δ soil C + Δ product pool C), in BECCS it was fulfilled solely via CCS (CDR = cumulative CCS; calculated by multiplying the harvested bioenergy C by a capture efficiency factor of 0.8; Klein *et al.*, 2014) and thus did not account for changes in vegetation and soil C. The baseline scenario ("BASE") involved no land-based mitigation but LUC took place in response to, among other factors, increasing food demand, dependent on population and GDP growth. Food production in the mitigation scenarios was maintained at the same levels as in BASE. LUC was provided by the LUMs as net land-cover transitions. Wood harvest was not accounted for in the data provided by the LUMs. Climate change and CO_2 fertilisation effects on plant growth were accounted for in the LUMs' crop growth and vegetation models. All scenarios were developed with the Representative Concentration Pathway (RCP) 2.6 climate produced by the climate model of the Institut Pierre Simon Laplace (IPSL-CM5A-LR). As it seems currently unlikely that RCP2.6 can be achieved without any land-based mitigation (Fuss *et al.*, 2014), the BASE scenario should rather be regarded as a diagnostic scenario to isolate the LU effects induced by the mitigation scenarios from other factors. Both LUMs harmonised their cropland and pasture LU patterns to the spatially explicit HYDE 3.1 dataset (Klein Goldewijk *et al.*, 2011) in the year 1995 (MAgPIE) or 2005 (IMAGE) to create a continuous historical-to-future time series, with small deviations in the area of the land-cover classes occurring due to different land masks and calibration routines. The simulation period was 1970-2100 in IMAGE and 1995-2100 in MAgPIE, with LU scenarios starting to diverge in year 2005. The spin-up in IMAGE was set to 700 years with natural vegetation cover followed by 300 years with year 1970 land-cover map, climate, and CO_2. In MAgPIE, potential C densities from LPJmL were used as initial (1995) values, with agricultural vegetation and litter C pools set to zero and soil C depleted based on IPCC recommendations to account for real land-cover at the start of the simulation period (Humpenöder *et al.*, 2014). Socioeconomic developments as input to the LUMs were based on SSP2 ("Middle of the Road"; O'Neill *et al.*, 2014, Popp *et al.*, 2017). Details about the conversion of IMAGE and MAgPIE-LU data to LPJ-GUESS input data can be found in Section 2.3.3.

In the two BASE scenarios, forest area decreases throughout the future for both IMAGE and MAgPIE (Fig. 2.3), but more so for IMAGE due to the representation of degraded forests (which are treated as grassland in IMAGE; see above). Even though MAgPIE and IMAGE derive crop yields and C densities from the same DGVM (LPJmL; dynamically coupled in IMAGE, and in MAGgPIE providing

potential C stocks, crop yields, irrigation water requirements, and blue water availability; Bondeau *et al.*, 2007), the land demand to meet the same CDR target is larger in IMAGE than in MAgPIE. This reflects different model approaches: in IMAGE, land allocation for bioenergy cultivation follows a rule-based approach according to sustainability criteria, implying that only marginal land not needed for food production is available for bioenergy. In MAgPIE, bioenergy and food production compete for fertile land based on a cost minimisation procedure. Concerning afforestation, managed regrowth (according to prescribed growth curves) is assumed in MAgPIE, while in IMAGE natural regrowth dynamically calculated within LPJmL is implemented. Consequently, bioenergy production in MAgPIE is located in regions with mostly higher yields compared to IMAGE, and forest regrowth

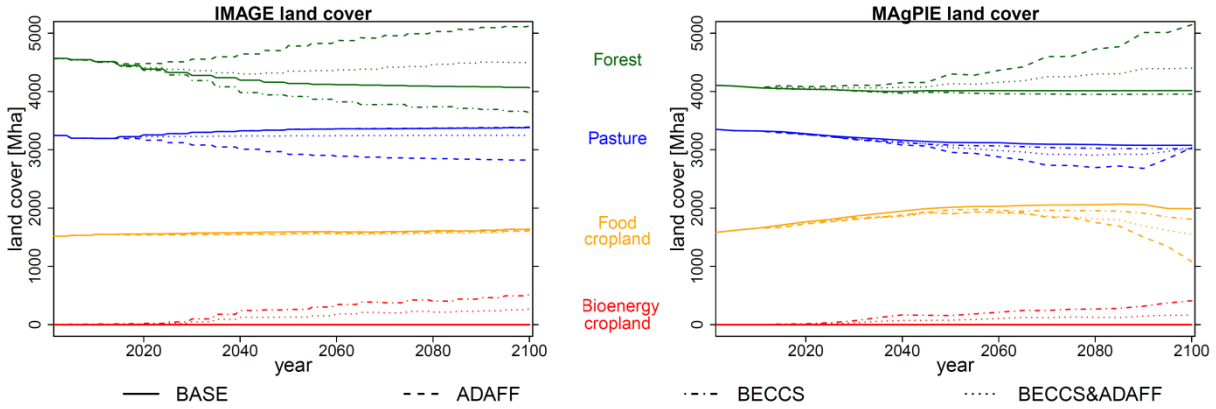

Figure 2.3: Time series (2000-2100) of forest area (including afforested area), pasture, food cropland, and bioenergy cropland [Mha] for the different LUC scenarios, for IMAGE (left) and MAgPIE (right). Other natural land and degraded forests (in IMAGE only) are not shown.

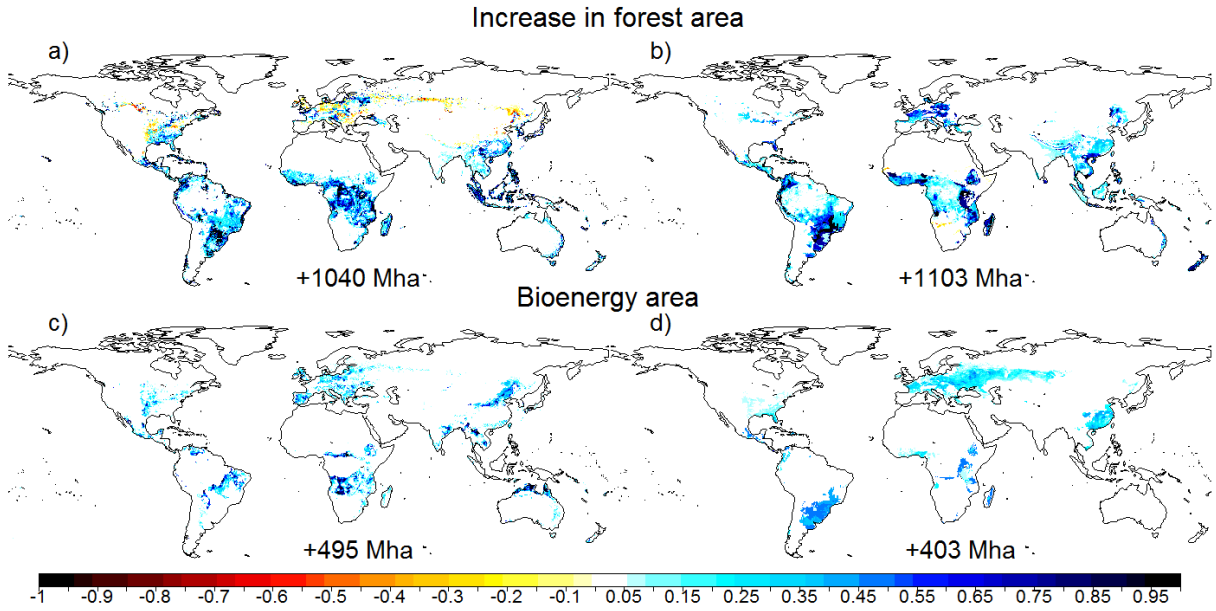

Figure 2.4: (top) Increase in forest cover (excluding other natural vegetation and degraded forest) in ADAFF by year 2099 (compared to BASE year 2099) for (a) IMAGE and (b) MAgPIE-LU patterns. (bottom) Bioenergy production area in BECCS by year 2099 for (c) IMAGE and (d) MAgPIE-LU patterns.

occurs at a faster rate, resulting in less LUC and mitigation actions starting later in the MAgPIE scenarios (Fig. 2.3). Land demand in the mitigation scenarios is generally greater for ADAFF than for BECCS (Fig. 2.4) because of different sequestration rates per unit area and because C uptake in forests diminishes when trees mature (Humpenöder *et al.*, 2014). Avoided deforestation and afforestation in the ADAFF scenarios is chiefly located in the tropics (Fig. 2.4). Forest area is 1040 Mha larger in ADAFF than in BASE for IMAGE by year 2099 and 1103 Mha larger for MAgPIE (Table 2.2). In IMAGE, ~42% of the difference in forest area between ADAFF and BASE can be attributed to avoided deforestation and 58% to afforestation (Fig. 2.3). In MAgPIE, avoided deforestation is responsible for only 4% of the difference in forest area between ADAFF and BASE, emphasizing the much larger role of afforestation compared to avoided deforestation in MAgPIE. The LUMs also differ in terms of land-cover classes affected by ADAFF activities. In IMAGE, forest maintenance and expansion usually takes place on future/former pastures or degraded forests (ADAFF compared to BASE), but in MAgPIE afforestation on abandoned croplands is also relevant (at least after year 2070; Fig. 2.3, Table 2.2; note that some of the abandoned cropland in MAgPIE ADAFF is not afforested but instead converted to pasture, while at other locations pastures are afforested, resulting in small net changes in pasture area by the end of the century). Bioenergy production area in BECCS is increased mainly at the expense of natural vegetation in IMAGE but taken also from existing agricultural land in MAgPIE. Total cropland area increases in the scenario combining both strategies (BECCS&ADAFF) compared to BASE for IMAGE but decreases for MAgPIE BECCS&ADAFF (Table 2.2).

Table 2.2: Land-cover changes [Mha] by year 2099 (parentheses: year 2050) in the mitigation scenarios (compared to BASE) as provided by the IMAGE and MAgPIE land-use models.

	ADAFF - BASE		BECCS - BASE		BECCS&ADAFF - BASE	
	IMAGE	MAgPIE	IMAGE	MAgPIE	IMAGE	MAgPIE
Forest	+1040 (+647)	+1103 (+288)	-410 (-223)	-60 (-30)	+427 (+212)	+383 (+122)
Other natural (excluding degraded forest)	+77 (+6)	-170 (-2)	-99 (-43)	-110 (-37)	+19 (+4)	-60 (-8)
Degraded forest	-535 (-196)	-	+0 (+0)	-	-535 (-196)	-
Cropland (food)	-28 (-29)	-855 (-115)	+6 (+2)	-174 (-44)	-36 (-38)	-428 (-103)
Cropland (bioenergy)	-	-	+495 (+262)	+403 (+157)	+255 (+130)	+164 (+77)
Pasture	-554 (-428)	-78 (-171)	+7 (+2)	-58 (-47)	-130 (-112)	-60 (-87)

2.3.3 Conversion of IMAGE and MAgPIE land-use data to LPJ-GUESS input data

For Section 4, which is based on simulations from four DGVMs driven by the LU projections from the two LUMs, the implementation of the LU patterns from the LUMs into the DGVMs was left to the

responsibility of the individual DGVM groups. An overview about the four DGVMs and their representation of land management processes is provided in Section 2.3.4. The following paragraphs describe the implementation of the LU patterns into LPJ-GUESS.

Land-cover and crop transitions provided by the LUMs were converted to a suitable format to be used as input data for LPJ-GUESS simulations. Both LUMs provided the fraction of cropland (land used for food and bioenergy production), pasture, forest, other natural land, and built-up area in a 0.5° x 0.5° raster from 1901 to 2100, summing to one. Cropland and pasture land covers for LPJ-GUESS were directly adopted from the LUMs. On natural land, LPJ-GUESS simulates the dynamics of trees and grasses simultaneously as a function of environmental conditions, so the "forest" and "other natural" land covers were merged. We converted the corresponding degraded forest fractions to pastures in LPJ-GUESS to ensure consistency with the representation of degraded forests in IMAGE. Built-up area was negligible for all scenarios and for simplicity was also attributed to natural vegetation. IMAGE used a slightly larger grid-list than MAgPIE and accounted for the water fraction of a grid-cell; but as the impacts on land-based mitigation in LPJ-GUESS turned out to be small (<2 GtC over the simulation period) we only included grid-cells in our simulations for which LU data were provided by both LUMs (assuming 100% land cover) to facilitate comparison of the results.

Table 2.3: Crop functional types (CFTs) used in LPJ-GUESS, how the land-use models' crop types were aggregated to these CFTs, and EarthStat major crops (Monfreda *et al.*, 2008) used to calculate circa year 2000 actual yields of these CFTs.

LPJ-GUESS CFT (photosynthetic pathway)	IMAGE and MAgPIE crop types aggregated to this CFT	EarthStat major crop types used to calculate circa year 2000 actual yields of LPJ-GUESS crops
temperate wheat (C_3), representing C_3 crops with winter or spring sowing depending on historical climate	temperate cereals, rapeseed	rye, barley, wheat, rapeseed
temperate other summer crops (C_3) representing C_3 crops with spring sowing only	potatoes, cassava, pulses, soybean, groundnuts, sunflower, palm oil, sugar beet, cotton, roots and tubers, oil crops, others	potato, cassava, groundnut, soybean, sunflower, oilpalm
rice (C_3)	(paddy) rice	rice
maize (C_4)	maize, tropical cereals, sugarcane, bioenergy crops	maize, millet, sorghum, sugarcane; bioenergy yields were not modified due to limited observational data
crop grass (C_3 or C_4)	fodder	unmodified as not used for crop production calculation

IMAGE used yearly (1970-2100) fractions of seven food crops (each separated into rain-fed and irrigated fractions) and rain-fed bioenergy grass in each grid-cell where cropland existed. MAgPIE provided yearly (1995-2100) fractions of 17 non-bioenergy crop types (separated into rain-fed and

irrigated) and two rain-fed bioenergy crop types (grassy and woody). The attribution between LPJ-GUESS CFTs and LUM crop types is shown in Table 2.3. For the years in which the LUMs did not provide CFT fractions (1901-1969 for IMAGE and 1901-1994 for MAgPIE) ratios were taken from the first provided year (e.g. if in IMAGE temperate wheat covered 70% of a grid-cell's cropland area in year 1970 and maize covered 30%, we assumed the same ratio throughout the entire spin-up and the 1901-1969 period). We made the attribution to C_3 or C_4 crop grass in croplands based on a preceding pasture-only simulation which was forced by the same environmental conditions as our actual simulations (RCP2.6). Dedicated bioenergy crops are currently not implemented in LPJ-GUESS and were represented by the CFT corresponding to maize, which is the highest yielding CFT in the model. Removed residues of bioenergy crops (90%) were included in the CCS calculation (see Section 2.4.3), while removed residues of food crops (75%) were emitted to the atmosphere. Residues left on-site (10 and 25%, respectively) were transferred to the litter.

Average annual N fertiliser rates per cropland area (synthetic and organic fertiliser, derived from yields) were provided by IMAGE (1970-2100) and MAgPIE (1995-2100) and had to be hindcasted to the year 1901. Historic N fertiliser rates (synthetic fertiliser on C_3 + C_4 annual and perennial crops) were available from the recently released Land-Use Harmonization 2 (LUH2) dataset (Hurtt et al, in preparation, http://luh.umd.edu/index.shtml, last accessed November 2017). However, as LUH2 only considers synthetic fertiliser (and ignores manure), the correlation between LUH2 and the LUMs in the first provided year (1970 and 1995, respectively) was poor in terms of spatial patterns and total amount of applied N, making a simple merging inapplicable. We thus decided to use IMAGE and MAgPIE N fertiliser rates and spatial patterns for the available time periods and computed a hindcast, starting with the initial spatial patterns and rates in IMAGE and MAgPIE multiplied by the relative year-to-year per-country change in the LUH2 dataset in the period prior to 1970 and 1995, respectively. This resulted in a smooth historical to future N fertiliser dataset reflecting the LUMs spatial patterns in terms of absolute values, with historic variations based on relative changes in LUH2 and late historic to future variations adopted unmodified from the LUMs. Fertiliser rates differed significantly between IMAGE and MAgPIE, with MAgPIE exceeding IMAGE fertiliser rates in most locations. As no fertilisation occurred before 1916 in LUH2 (before the Haber-Bosch process was found), we applied a minimum fertiliser rate of 6 kgN ha^{-1} yr^{-1} (in addition to atmospheric deposition) to all areas under crops throughout the entire simulation period to limit continued soil N depletion. As the LUMs only provided per-cropland fertiliser rates, we applied the same amount of fertiliser for all CFTs in a grid-cell, and distributed the annual amount over the year as a function of crop phenological state (Olin *et al.*, 2015b).

2.3.4 Description of the Dynamic Global Vegetation Models

The LU scenarios were used as input to four DGVMs: LPJ-GUESS (Olin *et al.*, 2015a, Smith *et al.*, 2014), ORCHIDEE (ORganizing Carbon and Hydrology In Dynamic EcosystEms; Krinner *et al.*,

2005), JULES (Joint UK Land Environment Simulator; Best *et al.*, 2011, Clark *et al.*, 2011), and LPJmL (Bondeau *et al.*, 2007, Sitch *et al.*, 2003). The models have different heritages; while ORCHIDEE and JULES were developed as land components of global climate models (IPSL and MetUM/HadGEM), LPJ-GUESS and LPJmL were originally designed as stand-alone offline models to simulate vegetation dynamics and associated C and water fluxes. LPJmL is also the vegetation sub-model of both IMAGE (where it is internally coupled) and MAgPIE (where potential C densities and actual yields - derived from modelled potential yields - are used), but the offline version used here differs from the versions used in the LUMs mainly by not considering technological yield increases in the future. All DGVMs represent vegetation using a number of PFTs, with LPJ-GUESS and LPJmL also representing dedicated CFTs. LPJ-GUESS distinguishes from the other DGVMs by its representation of different age classes amongst woody PFTs, allowing forest regrowth to be explicitly simulated, and by having N cycling as an additional constraint on ecosystem C processes (in addition to soil water availability which is accounted for in all DGVMs). All DGVMs represent LUC and land management explicitly even though the models differ in terms of implemented processes and level of detail. Table 2.4 provides an overview of model differences which are important for this study.

Table 2.4: Overview of major DGVM differences relevant to this study.

Variable or process	DGVM			
	LPJ-GUESS	ORCHIDEE	JULES	LPJmL
Major updates to the version used in Sitch *et al.* (in preparation) [a]	croplands are now represented by specific CFTs (including N fertilisation)	no	cropland and pasture harvest	no
Input variables	2m air temperature, precipitation, downwelling shortwave radiation, atm. N deposition and fertilisation, atm. CO_2, LU	2m air temperature, precipitation, downwelling shortwave radiation, near-surface wind speed, surface air pressure, specific humidity, atm. CO_2, LU		2m air temperature, precipitation, downwelling shortwave and longwave radiation, atm. CO_2, LU
Spatial resolution	0.5^o x 0.5^o	2° x 2°	0.5° x 0.5°	0.5^o x 0.5^o
Number of land grid-cells the DGVM simulated	59 098	4717 (76 836 when remapped to 0.5° resolution)	59 103	63 652
Fractional land mask (e.g. accounting for the urban or water fractions of a grid-cell, assumed to be constant over time)	no	yes (internal)		yes (post-processing; land mask taken from IMAGE for consistency)
Spin-up length	500 years	2000 years	1000 years	5390 years
Shortest time step for C and water fluxes	daily	30 min		daily

Fire	yes	no		yes
N cycle	yes	no		
Number of natural PFTs	12 (10 trees, C_3 + C_4 grass)	10 (8 trees, C_3 + C_4 grass)	5 (2 trees, 1 shrub, C_3 + C_4 grass)	9 (7 trees, C_3 + C_4 grass)
Implementation of LU patterns from the LUMs into the DGVM	absolute cropland, pasture, and natural area prescribed by LUMs, PFT distribution on natural land is simulated dynamically	changes in cropland, pasture, and forest *vs*. other natural area prescribed by LUMs, forest area and PFT distribution (static on natural land) in year 2005 according to internal map (from European Space Agency)	absolute cropland, pasture, and natural area prescribed by LUMs, PFT distribution on natural land is simulated dynamically	
Implementation of agricultural expansion	all natural PFTs are reduced proportionally		grasslands are reduced first, then shrubs, then forests	all natural PFTs are reduced proportionally
Historical LU	from IMAGE or MAgPIE	from IMAGE for all scenarios to reduce computation time		From IMAGE or MAgPIE
Representation of degraded forests (for IMAGE-LU patterns only)	as pasture	as natural grassland	as natural vegetation (forests or natural grassland)	as pasture
Fate of biomass upon deforestation	74% of woody biomass and 71% of leaves oxidised in same year, 20% of woody biomass to product pool (25-yr turnover time), remainder to litter	60% of aboveground heartwood and sapwood oxidised in the same year, remaining harvested biomass to two product pools (10-yr and 100-yr turnover time), remainder to litter	above-ground biomass moved to three product pools with 1, 10 and 100-yr turnover times (fractions PFT specific), belowground biomass to soil	67% of aboveground biomass oxidised in same year, 33% to product pool (25-yr turnover time), root biomass to litter
Forest (re)growth dynamics	cohort approach (competition between different age classes), natural regrowth	dilution approach (one average individual per PFT), natural regrowth		
Pasture management	harvest, woody vegetation is prevented from growing	no harvest, woody vegetation is prevented from growing	harvest [b], woody vegetation is prevented from growing	harvest with variable intensity, woody vegetation is prevented from growing
Representation of pasture harvest	50% of aboveground biomass oxidised each year, remainder	none	30% of litter flux oxidised	normally 75% of leaf biomass oxidised when leaf biomass

	to litter			reaches 0.1 kgC m^{-2}; in marginal areas 25% of leaf biomass is oxidised when maximum leaf biomass is reached
Cropland management	four CFTs (temperate wheat, maize, rice, temperate other), variable sowing and harvest date, tillage, irrigation, fertilisation, dynamic potential heat unit calculation, woody vegetation is prevented from growing	C_3 or C_4 crop grass (similar phenology as natural grass but adapted maximum LAI and slightly modified critical temperature and humidity parameters), harvest, woody vegetation is prevented from growing	C_3 or C_4 grass, harvest, woody vegetation is prevented from growing	12 CFTs, variable sowing and harvest date, irrigation, woody vegetation is prevented from growing
Representation of food crop harvest	annually, 90% of grain and 75% of other above-ground biomass oxidised, remainder to litter	45% of biomass oxidised after leaf senescence	30% of litter flux oxidised	annually, storage organs oxidised, 70% of remaining above-ground biomass oxidised, remainder to soil
Dedicated bioenergy CFTs	no (grown as maize)	no (grown as C_3 or C_4 crop grass)	no (grown as C_3 or C_4 grass)	yes (fast-growing C_4 grass, temperate and tropical short rotation coppice)
Representation of bioenergy crop harvest	annually, 90% of total above-ground biomass (which means residues are also used for CCS)	same as food crops		for grass, 85% of the leaf mass is harvested when above-ground biomass reaches 0.4 kgC m^{-2}; trees are cut every 8 years
Main model references	Smith *et al.* (2014)	Krinner *et al.* (2005)	Best *et al.* (2011), Clark *et al.* (2011)	Sitch *et al.* (2003), Schaphoff *et al.* (2013)
Main references for the model's agricultural component	Lindeskog *et al.* (2013), Olin *et al.* (2015a)	Piao *et al.* (2009)	Jones *et al.* (2011); crop harvest is a new feature	Bondeau *et al.* (2007), Beringer *et al.* (2011), Waha *et al.* (2012)

[a] This manuscript is based on simulations with the same DGVMs as used here that were driven by idealised LUC scenarios from IMAGE and MAgPIE.

[b] Pastures are treated as cropland in these JULES simulations. Normally pastures are not harvested in JULES.

2.3.5 Simulation setup

The DGVM simulation period was 1901-2099. The DGVMs were forced by daily meteorological variables, yearly CO_2 mixing ratio, and LU scenarios (see Table 2.4). Spin-up lengths in the DGVMs was set to 500, 2000, 1000, and 5390 years for LPJ-GUESS, ORCHIDEE, JULES, and LPJmL, respectively, sufficient to attain a stable equilibrium of C pools and fluxes in each model. The number of patches in LPJ-GUESS was set to 10 for primary vegetation (land that was never converted to agriculture) and 2 for secondary vegetation (agricultural land that was converted back to natural vegetation). All DGVMs used RCP2.6 IPSL-CM5A-LR climate data (1950-2099) from the first phase of the Inter-Sectoral Impact Model Intercomparison Project (ISI-MIP; Warszawski *et al.*, 2014), bias-corrected to the 1960-1999 historical period as in Hempel *et al.* (2013). The temperature increase is ~2°C by the end of the 21st century relative to the pre-industrial era. This value is in the middle of an ensemble of a wider range of climate models used in ISI-MIP (Warszawski *et al.*, 2014). Climate data for the DGVMs' spin-up and the 1901-1949 period were randomly taken from the 1950-1959 period. Historical (1901-2005) and future (RCP2.6, 2006-2099) atmospheric CO_2 mixing ratios were taken from Meinshausen *et al.* (2011). The year 1901 value (296 ppmv) was used for the spin-up. Future atmospheric CO_2 mixing ratio peaks at 443 ppmv in year 2052 and drops to 424 ppmv by the end of the century (Meinshausen *et al.*, 2011). Gridded N deposition rates (used by LPJ-GUESS only) were available as decadal monthly averages for the historical and future (RCP2.6) period (Lamarque *et al.*, 2010, Lamarque *et al.*, 2011). N deposition for the year 1901 was used for the spin-up. LUC was based on spatially explicit LU maps derived from the LUMs (for the historic period based on HYDE3.1; see Section 2.3.2 for more information about the LUC scenarios) and translated into the vegetation types of each DGVM (see Table 2.4). Year 1901 land cover was used for the spin-up. The DGVMs aimed to be as consistent as possible with the LUMs when implementing LU patterns from the LUM scenarios (e.g. for IMAGE scenarios all DGVMs apart from JULES followed the IMAGE assumption that no trees exist in degraded forests; see Table 2.4). Management information (crop types, irrigation, and N fertiliser) were also provided by the LUMs but were only used by some DGVMs which represented the relevant processes explicitly (Table 2.4). LPJ-GUESS was the only model being able to use N fertilisers as provided by the LUMs (see Section 2.3.3). The implementation of LU data into the DGVMs (e.g. mapping to DGVM vegetation types and defining rules by which managed land expands over natural vegetation), land masks, and additional required input variables (e.g. soil characteristics) were left to the responsibility of the individual DGVM groups. Different model structures and implementations of the LU patterns can result e.g. in differences in global forest area in the individual DGVMs (Fig. 2.5). The spatial resolution of the DGVMs was the same as the resolution of the input data (0.5° x 0.5°), except for ORCHIDEE (2° x 2°). In total, 32 combinations of DGVMs and LUC scenarios were simulated, including 24 combinations of DGVMs and mitigation LUC scenarios.

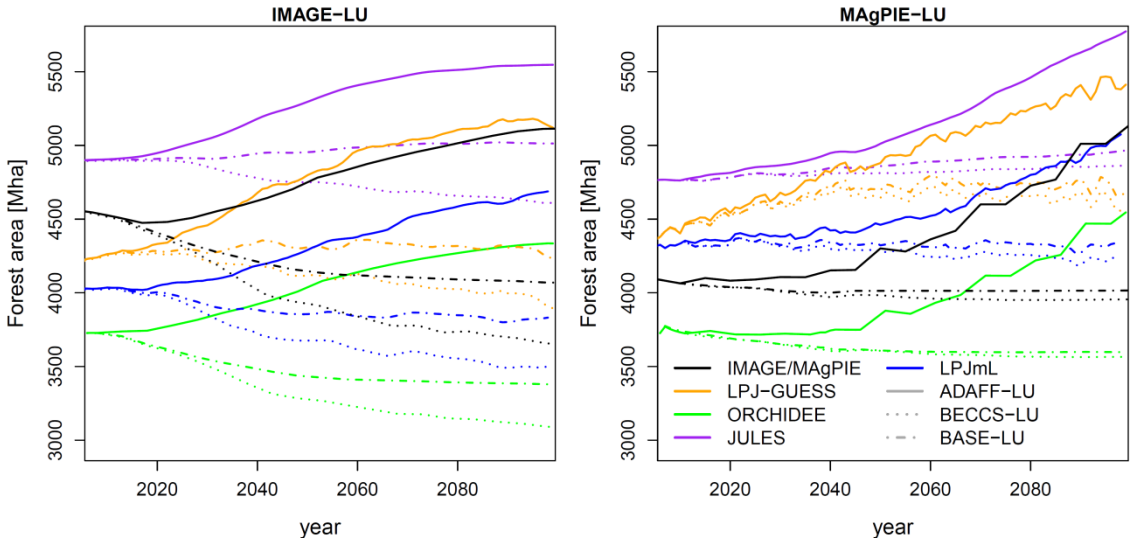

Figure 2.5: Time series of global forest area [Mha] in the individual models for the BASE, ADAFF, and BECCS scenarios, for the same input land-cover data from IMAGE (left, 5-year running means) and MAgPIE (right). Model differences arise from different land masks, different PFTs (e.g. in JULES there is a shrub PFT which was treated as forest here), and the response of natural vegetation to climate and CO_2 changes (static *vs.* dynamic vegetation).

2.4 Specific methodology Section 5

2.4.1 Land-use scenarios and simulation setup

The simulations analysed in Section 5 are the same as the LPJ-GUESS simulations that are also used in Section 4. Information about the LU scenarios, their implementation into LPJ-GUESS, and the simulation setup can thus be found in Section 2.3.

2.4.2 Analysed ecosystem service indicators

We analysed the implications of future LU patterns for the following ES indicators: C storage (as an indicator for global climate change mitigation), surface winter and summer albedo and evapotranspiration (indicators for regional climate effects in response to land-cover change), annual runoff (indicator for water availability), peak monthly runoff (indicator for flood protection), crop production (excluding production on areas where the LUMs grow cotton or forage crops, and excluding harvest of pastures; indicator for food production), N loss (in LPJ-GUESS currently not differentiated into dissolved N *vs.* N lost to the atmosphere; indicator for water or air quality, or GHG losses), and emissions of the most common BVOCs - isoprene and monoterpenes (indicator for air quality). We only used spatially explicit LU and land management (irrigation and synthetic plus organic N fertiliser) patterns from the LUMs as input to the LPJ-GUESS simulations; other variables also available from the LUMs (C storage and crop production) were calculated by LPJ-GUESS. Most variables were direct outputs from LPJ-GUESS simulations. Calculations for ES indicators not taken directly from model outputs (C storage via CCS, albedo, crop production scaled to EarthStat yields; Monfreda *et al.*, 2008) or different from the standard model setup (BVOCs) are provided in Section 2.4.3.

Table 2.5: Linking ecosystem functions to ecosystem services (ESs). An increase in an ecosystem function can be interpreted positive (+), negative (-), zero (0), or either positive or negative (+/-), depending on the background conditions or perspective. Effects can be small (+ or -) or large (++ or --). Regional effects are shown without brackets and global effects, where relevant, in brackets. Indirect effects that are more directly represented by another ecosystem function considered here are not shown. The table is based on evidence from the literature in cases where the link is not directly clear (see footnotes).

Ecosystem function / ES indicator	ES – climate change mitigation	ES – water availability	ES – flood protection	ES – water quality	ES – air quality	ES – food production
C storage ↑	++ (++)					
Surface albedo ↑	++ (+)[a]					
Evapotranspiration ↑	++ (+/-)[b]					
Annual runoff ↑		++	-	0/+[c]		
Peak monthly runoff ↑		0/+[d]	--	0/-[e]		0/-[f]
Crop production ↑						++ (++)
N loss ↑	+/- (+/-)[g]			--[g]	- (-)[g]	
BVOC emissions ↑	+/- (+/-)[h]				0/-- (0/-)[i]	

[a] The global effects of LU-driven albedo changes seem to be small (de Noblet-Ducoudre *et al.*, 2012).

[b] Local surface cooling as heat is needed to evaporate water. On larger scales, the effect could be either a warming due to increases in atmospheric water vapour (Boucher *et al.*, 2004) or a cooling due to increased planetary albedo resulting from more cloudiness (Bala *et al.*, 2007, Ban-Weiss *et al.*, 2011).

[c] High flows imply more volume for dilution, prevent algae growth, and maintain oxygen levels (Whitehead *et al.*, 2009).

[d] Effect of peak monthly runoff on water availability is dependent on seasonal rainfall distribution and regional water storage capacity. Annual runoff is the clearer indicator.

[e] Soil erosion and associated re-mobilisation of metals is enhanced during flood events (Whitehead *et al.*, 2009).

[f] Due to flood damage in croplands (Posthumus *et al.*, 2009).

[g] LPJ-GUESS at present calculates total N loss and does not differentiate between leaching and gaseous loss. Thus we indicate several effects that would arise from N emitted as N_2O (a GHG), as NO_X or NH_3 (affecting air quality and aerosol formation), or as dissolved N. The net effect of N loss on climate has been estimated to be a small cooling (Erisman *et al.*, 2011) but uncertainties are large.

[h] The net impact of BVOC emissions is very uncertain. On the global scale, increased BVOC emissions might result in a warming (Unger, 2014).

[i] BVOCs often increase O_3 and secondary organic aerosol formation, primarily locally (Rosenkranz *et al.*, 2015), with principally opposite warming and cooling effects (Unger, 2014).

The analysed ES indicators can serve as proxies for several ESs linked to human well-being. Table 2.5 gives a qualitative overview of how these ES indicators and corresponding ESs are interlinked. We did not aim to value and rank individual ES indicators and thus did not assess here how relative changes could be differently prioritised in decision-making for land management. While this is certainly too simple a generalisation for fully assessing the implications of such scenarios, ranking or prioritising

individual ES indicators is a substantial challenge, which was beyond the scope of the study. A given relative change can be more crucial for some indicators than for others and their importance can also vary across regions and parties concerned. ESs will be influenced by changes in climate, atmospheric chemistry, and LU even in the absence of land management for C mitigation. To separate these non-mitigation effects from those effects associated with a mitigation approach, we compared changes in ES indicators in the BASE simulations over the 21st century to the changes that occurred when a mitigation approach was implemented. Land-based mitigation may thus potentially enhance or degrade ESs to human societies.

2.4.3 Variables not directly available from LPJ-GUESS output

Bioenergy yields included removed harvestable organs and crop residues (90% of total above-ground biomass). We estimated the total amount of C sequestered via CCS in the bioenergy simulations by assuming an 80% capture rate upon oxidisation, which is the same value as in the LUMs (Klein *et al.*, 2014). We did not account for energy production via BECCS and focused on the more important climate benefit via C sequestration (Humpenöder *et al.*, 2014). The total C was then calculated as the sum of terrestrial C (vegetation C, soil and litter C, C stored in wood products), and cumulative C stored via CCS.

We calculated January and July surface albedo mainly based on mean winter (snow-free and snow-covered) and summer albedo values for different land-cover types derived from MODIS satellite observations by Boisier *et al.* (2013). For the Southern Hemisphere we switched snow-free winter and summer albedo values. The LPJ-GUESS PFTs' fractional plant cover determined the fraction of the grid-cell occupied by the land-cover groups (crops, grasses, evergreen trees, deciduous trees, bare soil). For tropical evergreen trees we assumed an albedo of 0.14 year-round based on Boisier *et al.* (2013). For woody bioenergy we assumed the same albedo as deciduous forests. The albedo of the non-vegetated fraction of the grid-cell under snow-free conditions was taken from Houldcroft *et al.* (2009) (average of white and black sky albedo), assuming a value of 0.15 at locations where no measurements were available. We estimated the grid-cell's monthly fraction under snow cover f_{snow} as

$$f_{\text{snow}} = \frac{z_{\text{sn}}}{0.01 + z_{\text{sn}}}$$

where z_{sn} was the average monthly snow depth [m] (Wang and Zeng, 2010, equation 17) which can be output from LPJ-GUESS. The albedo of the snow-covered fraction was calculated based on the values from Boisier *et al.* (2013) for snow-covered vegetation and bare soil and the grid-cell albedo was then the area-weighted average of snow-covered and snow-free albedos.

To account for spatial variations in crop management other than irrigation and fertilisation, which are not accounted for in LPJ-GUESS, we scaled our food crop yields to the actual yields from the

EarthStat dataset (Monfreda *et al.*, 2008), thereby only taking the absolute year-to-year changes from LPJ-GUESS. For this, we re-scaled yields of our four food CFTs (temperate wheat, temperate other summer crops, rice, maize) around the year 2000 (1997-2003) to match actual yields based on area-weighted yields of major food crops in the EarthStat dataset (aggregated to 0.5° x 0.5° resolution; see Table 2.3 for which EarthStat crop types were aggregated to which LPJ-GUESS CFT). We then used these actual yields over the full simulation crop yield time series, with year-to-year variations calculated based on the yield changes in LPJ-GUESS (area-weighted between rain-fed and irrigated yields). If crops were present in the LUMs but no adequate crop types were available in the EarthStat dataset for a grid-cell we took the yields unmodified from LPJ-GUESS. We first converted dry matter yields [kg m^{-2}] as given by LPJ-GUESS/EarthStat to fresh matter yields (by dividing rice yields by 0.87 and all other crop yields by 0.88) and finally to kcal m^{-2} (by multiplying wheat and temperate other summer crop fresh matter yields by 3283, rice fresh matter yields by 2800, and maize fresh matter yields by 3560; http://www.fao.org/docrep/003/X9892E/X9892e05.htm#P8217_125315, last accessed November 2017). Fodder and cotton were not used for the crop production calculation. Total crop production was then the sum of temperate wheat, temperate other summer crops, rice, and non-bioenergy maize production. Yields of bioenergy crops (grown as maize) were used unmodified to estimate CCS (see above) due to limited observational data of bioenergy crop yields.

Crop BVOC basal emission factors were taken from natural C_3 or C_4 grass, apart from woody bioenergy crops which we grew as maize but used isoprene basal emission factors of 45 μg[C] g^{-1}[leaf foliar mass] h^{-1} (Ashworth *et al.*, 2012). These values are much higher than the values for normal grasses (8 μg g^{-1} h^{-1} for C_4 grasses and 16 μg g^{-1} h^{-1} for C_3 grasses) and account for the fact that isoprene emissions from typical woody bioenergy species like oil palm or willow are very high.

3 Impacts of land-use history on the recovery of ecosystems after agricultural abandonment

This section analyses the long-term impacts of prior LU on vegetation regrowth and C sequestration following land abandonment. We use LPJ-GUESS simulations to explore the legacy effects of six different agricultural LU histories (in terms of LU type and duration; for information about the scenarios, the simulation setup, and the recovery definition see Section 2.2) on the recovery of ecosystems across a wide range of environments.

3.1 Results

3.1.1 Reference simulation

The reference simulation does not include any LUC activities and thus provides the distribution of potential C stocks as simulated by LPJ-GUESS under present-day (1981-2000) climate. Maps of simulated vegetation and soil C, as well as dominant PFT and biomes derived from PFT composition for the reference simulation are shown in Fig. 3.1. The salient features of biome and C storage distribution on the regional scale are captured (Haxeltine and Prentice, 1996a, Scharlemann *et al.*, 2014).

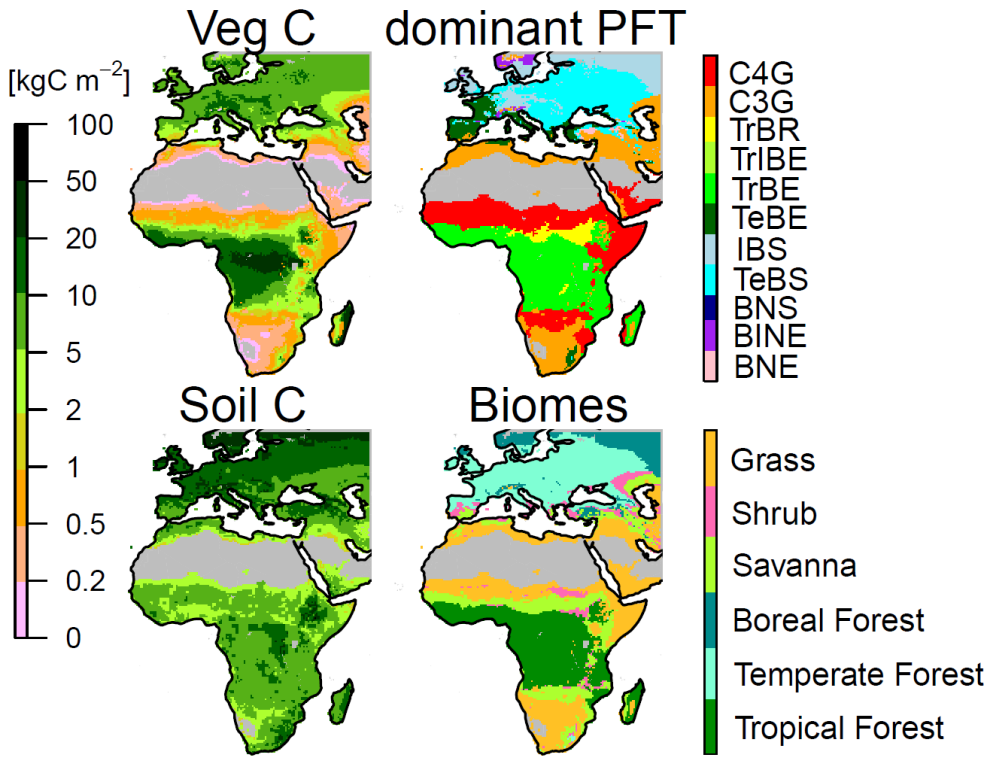

Figure 3.1: Vegetation C [kgC m^{-2}] for the reference simulation (present-day climate and no land-use change), averaged over the whole simulation period of 900 years (upper left), soil C [kgC m^{-2}] (lower left), dominant PFT (upper right), and corresponding biomes (lower right). Grid-cells with a NPP below 0.1 kgC m^{-2} yr^{-1}, deserts and tundra, and latitudes above 62.5°N are masked in grey. PFT abbreviations are given in Table 2.1.

Vegetation C reaches its highest values in tropical forests of central Africa and decreases towards the deserts of southern and northern Africa. Patterns are more homogeneous in Europe, where most areas store 5-10 kgC m^{-2}. Similar to vegetation C, soil C in the (sub-)tropics also decreases with drier conditions. However, the differences are small, with typical values of 5-10 kgC m^{-2}. Soils in the temperate and southern boreal ecosystems of Europe generally store more C (usually >10 kgC m^{-2}), especially in colder environments. While Europe is mostly dominated by woody PFTs (e.g. TeBS is the acronym for temperate broadleaved summergreen tree; see Table 2.1), in Africa there is a shift from C_3 and C_4 grasses in the dry regions to trees in the humid tropics. This gradient also appears in the corresponding biome map: in Africa and the Arabian Peninsula, LPJ-GUESS reproduces the transition from grasslands to savannas and tropical forests as the Equator is approached. Europe is mostly classified as temperate forests, with some boreal forests in the north and some shrublands/savannas in the south.

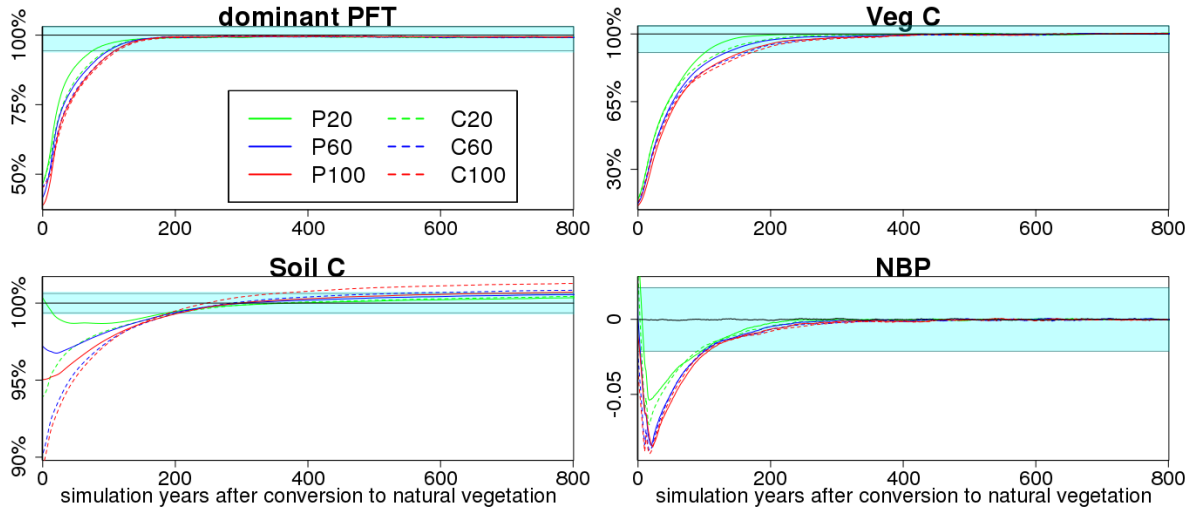

Figure 3.2: Time series (20-year running mean) of dominant PFT, vegetation C, soil C, and NBP for the different simulations, starting from the time of reconversion to natural vegetation and area-averaged over all grid-cells. Dominant PFT, vegetation C, and soil C are shown in relative values compared to reference simulation mean, while NBP is shown as absolute values [kgC m^{-2} yr^{-1}] because values cannot be presented relative to a zero background. The cyan-shaded area corresponds to the reference simulation (no land-use change) mean ± 1 σ. Note the different scales on the y-axes.

3.1.2 Recovery of the dominant plant functional type

The LAI of the dominant PFT recovers on average within around one century for all LU histories (Fig. 3.2). Maps of the recovery time (Fig. 3.3) show distinct geographical patterns which occur in all simulations. Most sub-tropical grasslands and savannas, and parts of the temperate and boreal forests recover within several decades, some grasslands even within 5 years. In contrast, recovery times are clearly longer (>100 years) in other parts of the temperate forests and in the tropical forests. Long recovery is associated with woody successional vegetation dynamics, as slow-recovering areas are usually dominated by temperate broadleaved summergreen and tropical broadleaved evergreen forests (compare PFT distribution in Fig. 3.1). These are shade-tolerant PFTs that establish only slowly after

disturbances. For 84% of all analysed grid-cells, condition 1 (LAI recovery) was the delaying condition for dominant PFT recovery (numbers exemplified for the P60 simulation), compared to only 3% for condition 2 (dominance recovery). For the remaining grid-cells, both conditions were fulfilled in the same year.

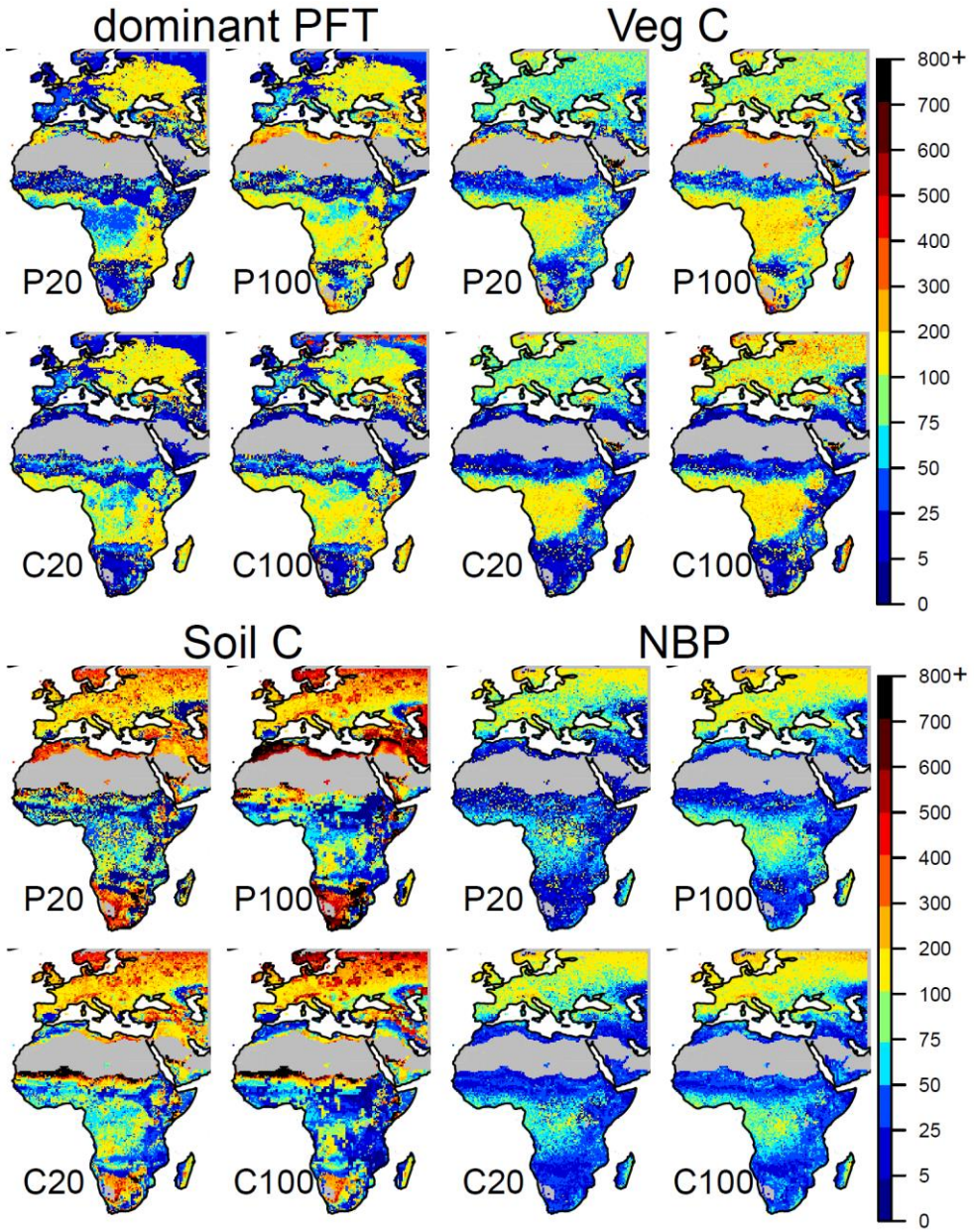

Figure 3.3: Maps of recovery times in years for the dominant PFT, vegetation C, soil C, and NBP for the P20, P100, C20, and C100 simulations.

Overall, differences across simulations of different LU histories are moderate, with generally only small differences in temperate forests, savannas, and shrublands (Fig. 3.3; see also biome averages in Table 3.1 and the histogram Fig. 3.4). Areas of major differences are central Africa, where P20 recovers faster than other simulations because post-agricultural net mineralisation rates are higher in this region for P20 than for the other simulations (Fig. 3.5), thereby relatively increasing post-agricultural

Table 3.1: Average recovery times and standard deviations per biome and for each simulation. Recovery times are depicted in Figure 3.3.

Biome	Simulation					
	P20	P60	P100	C20	C60	C100
	dominant PFT recovery time, averaged per biome					
Tropical forest	90 ± 55	112 ± 48	121 ± 50	113 ± 54	125 ± 52	126 ± 51
Temperate forest	102 ± 74	96 ± 63	93 ± 57	99 ± 71	89 ± 61	92 ± 69
Boreal forest	47 ± 89	52 ± 97	53 ± 90	47 ± 95	60 ± 111	145 ± 178
Savanna	47 ± 71	57 ± 74	62 ± 77	50 ± 65	57 ± 73	59 ± 76
Shrub	95 ± 93	104 ± 101	108 ± 100	103 ± 100	109 ± 112	109 ± 112
Grassland	76 ± 108	102 ± 109	115 ± 109	45 ± 77	55 ± 97	58 ± 100
Total	80 ± 85	93 ± 84	99 ± 84	77 ± 78	83 ± 85	90 ± 95
	Vegetation C recovery time, averaged per biome					
Tropical Forest	106 ± 50	137 ± 61	150 ± 65	121 ± 65	138 ± 73	139 ± 74
Temperate forest	84 ± 24	93 ± 31	108 ± 46	91 ± 29	124 ± 59	149 ± 79
Boreal Forest	102 ± 47	113 ± 57	127 ± 71	111 ± 55	144 ± 79	187 ± 107
Savanna	49 ± 37	61 ± 44	66 ± 46	35 ± 40	42 ± 43	43 ± 44
Shrub	73 ± 40	86 ± 48	96 ± 51	60 ± 38	69 ± 48	73 ± 54
Grassland	96 ± 136	119 ± 140	126 ± 138	40 ± 98	43 ± 102	45 ± 105
Total	88 ± 80	106 ± 87	117 ± 90	75 ± 74	92 ± 87	101 ± 98
	Soil C recovery time, averaged per biome					
Tropical forest	74 ± 60	69 ± 43	66 ± 45	80 ± 46	64 ± 46	49 ± 43
Temperate forest	207 ± 98	229 ± 105	241 ± 117	237 ± 108	261 ± 133	260 ± 144
Boreal forest	327 ± 107	381 ± 122	421 ± 140	362 ± 112	425 ± 132	454 ± 161
Savanna	84 ± 132	132 ± 191	162 ± 233	85 ± 112	83 ± 125	74 ± 126
Shrub	107 ± 140	129 ± 161	135 ± 168	137 ± 173	139 ± 183	125 ± 183
Grassland	286 ± 234	366 ± 262	422 ± 283	239 ± 227	219 ± 229	198 ± 228
Total	182 ± 176	220 ± 209	245 ± 236	182 ± 171	183 ± 186	174 ± 194
	NBP recovery time, averaged per biome					

Tropical forest	57 ± 37	65 ± 26	71 ± 27	56 ± 28	64 ± 24	65 ± 24
Temperate forest	97 ± 29	108 ± 29	113 ± 31	102 ± 30	112 ± 31	119 ± 36
Boreal forest	136 ± 55	146 ± 56	152 ± 58	139 ± 54	151 ± 59	169 ± 71
Savanna	31 ± 40	34 ± 30	36 ± 26	29 ± 18	32 ± 17	33 ± 17
Shrub	51 ± 37	58 ± 31	59 ± 29	52 ± 27	58 ± 26	59 ± 25
Grassland	25 ± 37	31 ± 31	35 ± 30	27 ± 15	34 ± 20	36 ± 22
Total	59 ± 51	66 ± 49	71 ± 49	60 ± 45	68 ± 47	72 ± 52

N availability compared to the other simulations (Fig. 3.6), and the African Mediterranean coast, where croplands recover much faster because the reduced C:N ratio in the soil (not shown) enhances N mineralisation and thus plant N availability compared to pastures. Furthermore, in parts of the boreal zone recovery takes several hundred years for C100 instead of a few decades for the other simulations because lower available N levels relatively reduce the growth of IBS (the dominant PFT in this region) compared to other woody PFTs. Figure 3.7 shows the maximum differences between recovery times across all simulations per biome (black dots), as well as across a subset of simulations (coloured squares and triangles). The differences were first calculated for each grid-cell and only then averaged over biomes, thereby providing an estimate of the relative importance of former LU duration versus former LU type on recovery times. While substantial differences occur across the pasture simulations (P20, P60, P100) in tropical forests, savannas, and grasslands, and across cropland simulations (C20, C60, C100) in boreal forests (emphasizing the importance of LU duration in these regions), major differences between P100 and C100 occur in boreal forests and grasslands (emphasizing the importance of LU type if agricultural duration was long). On the other hand, in our simulations, dominant PFT recovery in temperate forests is hardly influenced by the type of former LU or, conversely, pasture duration has negligible effects on boreal forest recovery. Interestingly, temperate forests recover faster for P100 and C100 than for P20 and C20. This pattern is generally restricted to areas where the TeBS PFT dominates. We interpret this behaviour as reduced soil N favouring TeBS in the competition with other tree PFTs, thereby reaching its background LAI levels earlier.

3.1.3 Recovery of vegetation carbon

Compared to dominant PFT, recovery occurs slightly later for vegetation C (Fig. 3.2, Table 3.1). Spatial patterns look more homogeneous than for the dominant PFT (Fig. 3.3). While most grasslands recover within a few decades for all simulations, in particular so for post-cropland recovery, recovery occurs only after several decades or centuries in forest ecosystems. Lower standard deviations for the mean differences in vegetation C recovery times compared to the standard deviations for the mean differences in dominant PFT recovery times for most biomes (Fig. 3.7a-b) reflect the spatially more uniform response of vegetation C recovery. Exceptions are tropical forests and grasslands, where the standard deviation is higher for vegetation C recovery compared to dominant PFT recovery.

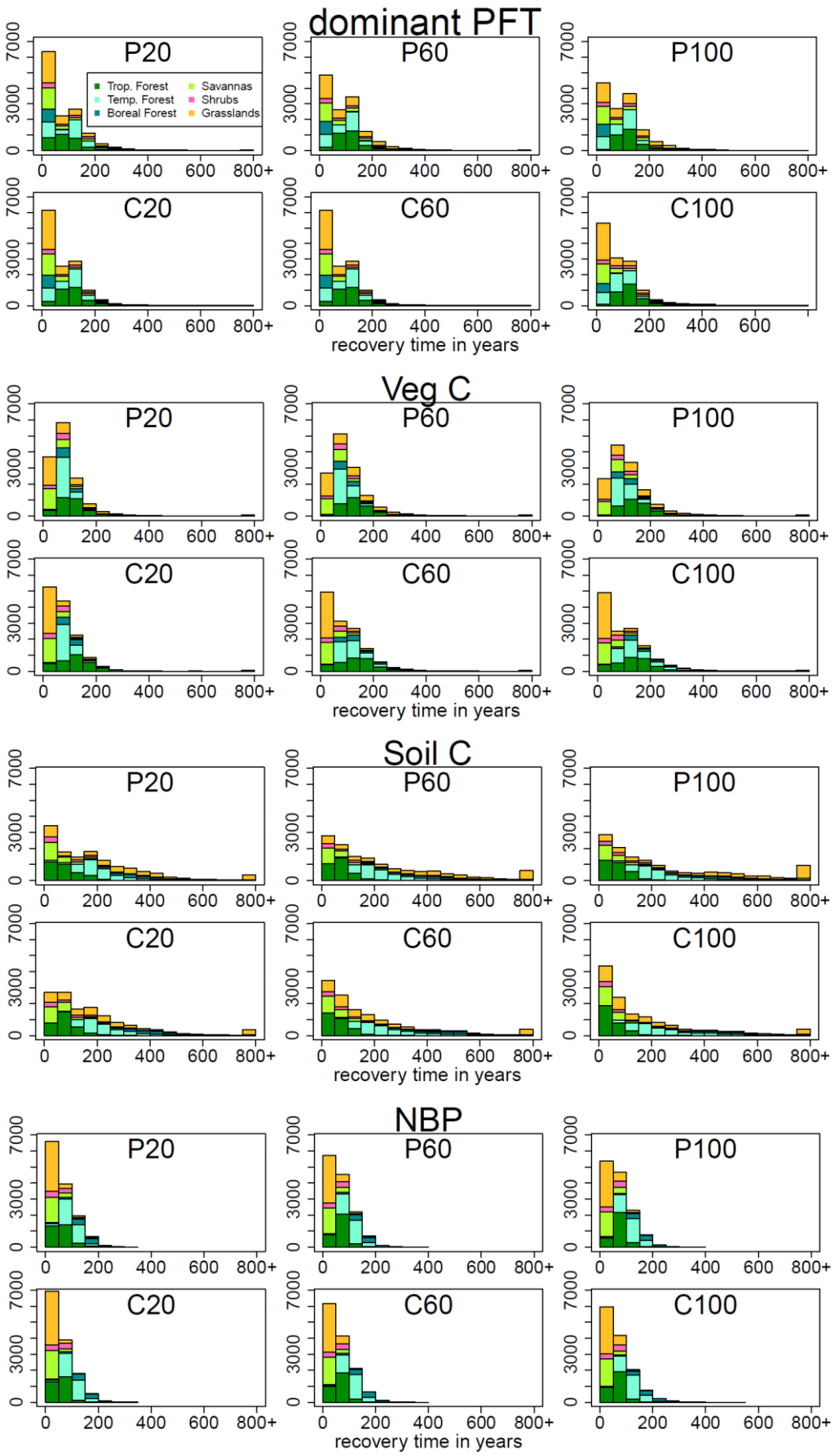

Fig. 3.4: Histograms of recovery times for the dominant PFT, vegetation C, soil C, and NBP for the six simulations. Colours indicate different biomes.

Significant differences in recovery times occur between simulations of different LU types that have the same duration, and between simulations of the same LU type but with different duration. For example, in the grasslands and savannas of southern, eastern and northern Africa, former croplands recover much faster than former pastures (see also Table 3.1) because post-agricultural N availability is enhanced in these regions (Fig. 3.6). In former croplands in these environments, the combined effect of fertilizing and harvesting is a net N flux to the ecosystem (not shown) and mineralisation rates are enhanced after cropland abandonment (Fig. 3.5). This net N flux can partially be explained by high levels of water stress in these savannas and grasslands, resulting in greater C and N allocation to roots relative to leaves and thereby decreased harvest removal in this region (see Fig. 3.8). Conversely, recovery in northern European forests is delayed for C60 and, to an even greater extent, C100 because in this region N removal by annual harvest exceeds N addition through fertilisation during the agricultural period (not shown) and post-agricultural N mineralisation rates in this region are substantially reduced compared to the other simulations many decades or even a few centuries after abandonment (Fig. 3.5). Differences in vegetation recovery times resulting from agricultural duration are mostly found in temperate and boreal forests for the cropland simulations (here longer durations result in longer recovery times due to reduced N availability, Fig. 3.6) and in tropical forests and shrublands for the pasture simulations, emphasizing the importance of agricultural duration in these regions (see also Fig. 3.7b).

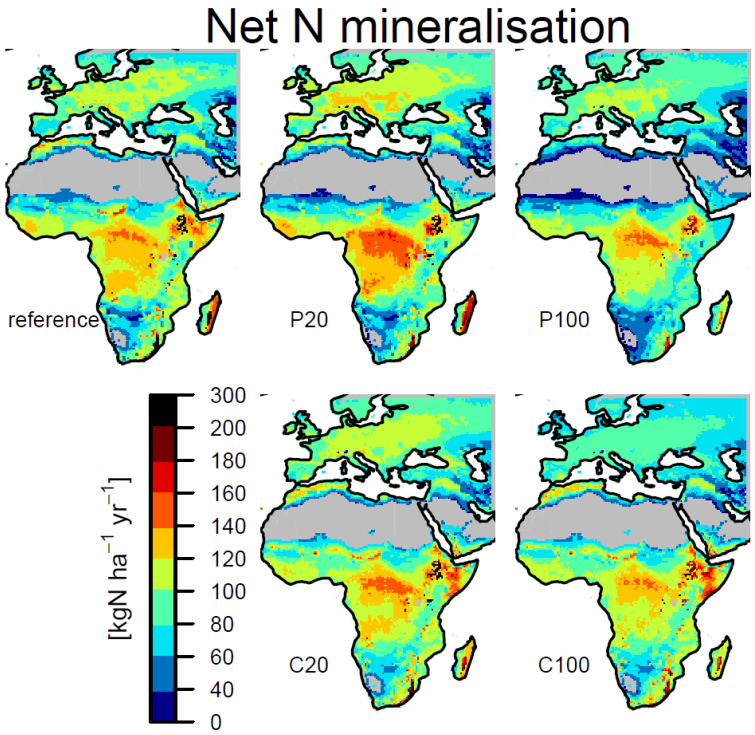

Figure 3.5: Average net N mineralisation rates [kgN ha^{-1} yr^{-1}] in the soil for the reference simulation (full simulation period) and averaged over the first 100 years of regrowth for the P20, P100, C20, and C100 simulations.

3.1.4 Recovery of soil carbon

Relative depletion of soil C content under crop and pasture LU is not as large (loss of 0-11% compared to the reference simulation) as for vegetation C (Fig. 3.2). However, regeneration proceeds over longer time scales due to slower C accumulation in soils than in vegetation. C depletion is generally more pronounced for former crops than for pastures due to the greater harvest efficiency, which leads to more biomass removed each year, and the effect of tillage enhancing soil respiration (Section 2.2.1). Upon re-conversion, soil C accumulation is delayed for the pasture simulations compared to the cropland simulations, especially for P20, where the residual roots and other litter left after the original deforestation event continue to decay and soil C decreases for some decades. The general delay for pastures is associated with larger heterotrophic respiration rates (not shown) compared to rates calculated in recovering croplands.

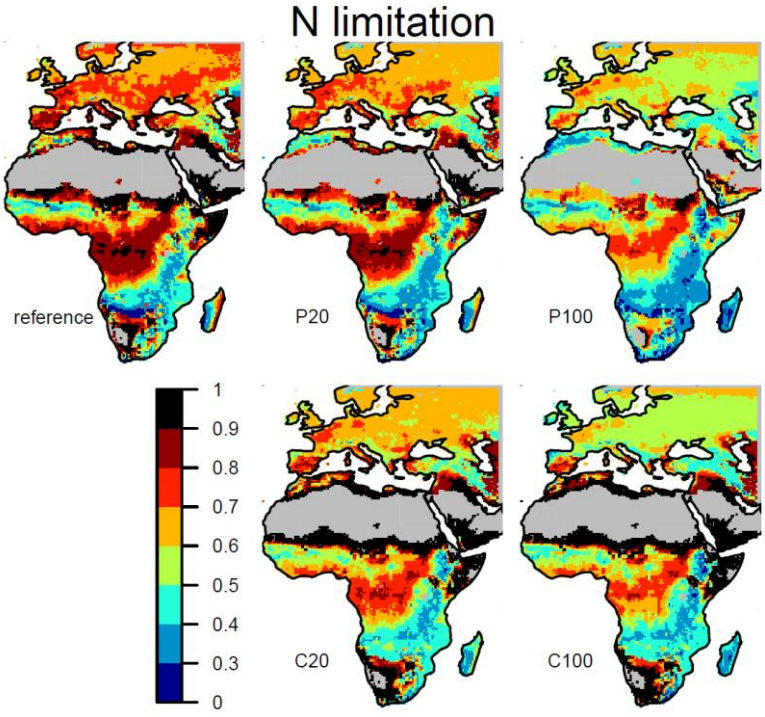

Figure 3.6: Average N limitation on vegetation RuBisCO capacity (and thus on gross primary production) for the reference simulation (full simulation period) and during the first 100 years of regrowth for the P20, P100, C20, and C100 simulations. N limitation is a number scaling from 0 (completely N-limited) to 1 (no N limitation; Smith *et al.*, 2014).

Soil C recovery rates are highly latitude-dependent (Fig. 3.3), being much slower in temperate (~250 years) and boreal forests (~400 years) than in the tropics (<100 years, sometimes even within 5 years). Initial soil C depletions are larger in higher latitudes, while these regions also suffer from low productivity, thereby reducing C input to the soil upon regrowth. Additionally, in the intensive LU simulations (P100, C60, C100), vegetation productivity in the boreal region is further reduced compared to the reference simulation in the first 200 years of regrowth (not shown) due to N limitation (Smith *et al.*, 2014), reducing litter input to the soil even further.

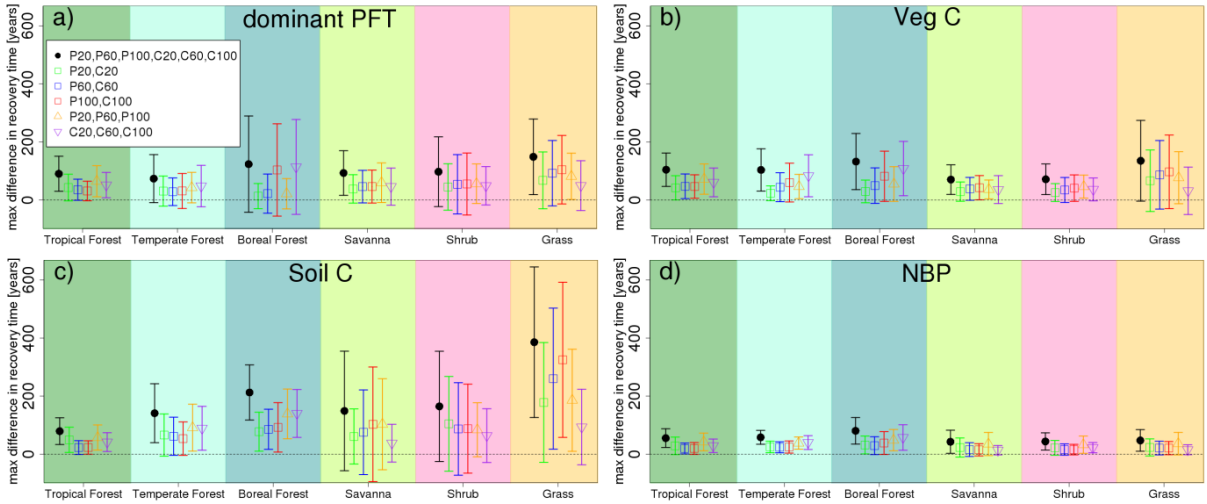

Figure 3.7: Maximum difference in recovery time (longest recovery time minus shortest recovery time of all selected simulations) for the dominant PFT, vegetation C, soil C, and NBP. Black dots show maximum differences across all six simulations (P20, P60, P100, C20, C60, C100), green squares differences across 20-year pasture and cropland simulations (P20, C20), blue squares differences across 60-year pasture and cropland simulations (P60, C60), red squares differences across 100-year pasture and cropland simulations (P100, C100), orange triangles differences across pasture simulations (P20, P60, P100), and purple triangles differences across cropland simulations (C20, C60, C100). Background colours indicate associated biomes, arrows one standard deviation, and the dashed line 0 years' difference. Thus, the black dots show the sensitivity of recovery times to LU history across all simulations for each biome. The red, blue, and green squares indicate the relative contribution of LU type for a specific LU duration to this sensitivity, and the orange and purple squares indicate the relative contributions of pasture and of cropland duration. For example, if recovery times for one variable in one grid-cell were to be 50, 60, 65, 90, 100, 110 years (for P20, P60, P100, C20, C60, C100), the maximum difference in recovery time across all simulations (black) would be 60 years, across the 20-year simulations (green) 40 years, across the 60-year simulations (blue) 40 years, across the 100-year simulations (red) 45 years, across the pasture simulations (orange) 15 years and across the cropland simulations (purple) 20 years.

Soil C recovery times differ substantially between simulations in many areas. LU type is particularly important in grasslands and non-tropical forests. While croplands tend to recover faster than pastures in grasslands of southern and northern Africa, the opposite occurs in most temperate and boreal forests but also the northern Sahel, where soil C after re-conversion from croplands does not recover at all. Post-agricultural N availability is enhanced in parts of the Sahel for the cropland simulations due to increased N mineralisation rates (Fig. 3.5 and Fig. 3.6), and trees benefit more than grasses, leading to a shift in the equilibrium vegetation state towards woody species (not shown), which results in an overall lower soil C pool size. It should be noted that even though some regions do not recover within 800 years, a large fraction of the original C loss is already replenished after a few centuries, thereby limiting implications for the C cycle. Counter to *a priori* expectations, for tropical and temperate forests and for shrublands, the difference between P20 and C20 is usually higher than between P60 and C60 or P100 and C100 (Fig. 3.7c). Pasture duration is relevant for speed of soil C recovery in most ecosystems and, apart from in the tropics, a longer duration usually delays recovery, mainly due to substantial initial depletions after long pasture durations (Fig. 3.2). For croplands, longer durations

tend to delay recovery in temperate and boreal forests but accelerate soil C recovery in the (sub-) tropics. This is somewhat unexpected for the tropical forest biome, where longer cropland durations usually do not increase N availability upon abandonment in our simulations (Fig. 3.6). However, while tropical soils lose large amounts of C during the first decades of cropland use, slow C accumulation takes place thereafter, resulting in higher soil C values at the end of the agricultural period for C100 than for C20 in large parts of eastern Africa. This occurs because tillage-driven C losses in more labile soil pools, which dominate the system's response during the first decades, are eventually supplanted as the dominant process by accumulation in more stable pools. This is different to temperate and boreal forest, where soil C decreases throughout the entire cropland period. Overall, the greatest sensitivity of soil C recovery times to different LU histories is found in boreal forests and grasslands, where maximum differences across simulations are often several centuries (Fig. 3.7c). The maximum differences across all simulations (P20/P60/P100/C20/C60/C100) in boreal forests are mainly due to differences across simulations of same LU type but different duration (e.g. P20/P60/P100), whereas the sensitivity of grasslands mainly reflects differences across simulations of different LU type but same duration (e.g. P100/C100), emphasizing the importance of duration and type of agriculture in a range of biomes.

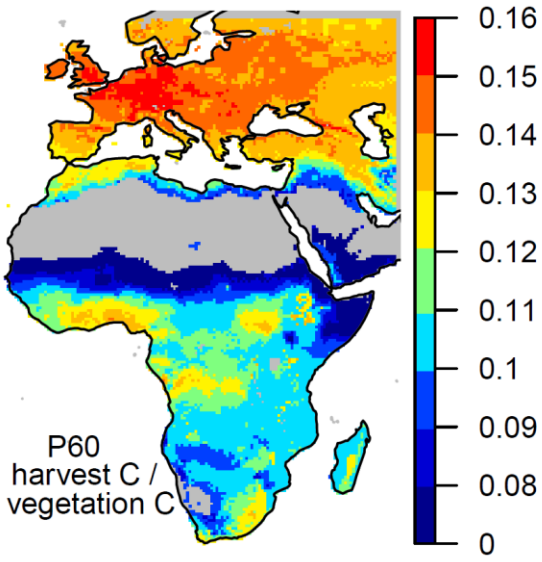

Figure 3.8: Annual ratio of C removed by harvest and C stored in vegetation, averaged over the whole agricultural period and for the P60 simulation. As only above-ground biomass is harvested, lower values indicate increased C allocation to roots compared to leaves due to limited water supply.

3.1.5 Recovery of Net Biome Productivity

NBP switches from being a C source to the atmosphere during the period of land management to a C sink after reconversion to natural vegetation (Fig. 3.2). The sink capacity of the recovering ecosystem is greatest during the first decades and then gradually returns to the NBP levels of the reference simulation. P20 and, to a lesser extent, C20 act as a smaller sink than the other simulations at least during the first 100 years of regrowth. Recovery generally occurs slower in temperate and boreal regions than

in the tropics for all simulations (Fig. 3.3). Apart from boreal forests, standard deviations of mean differences in recovery times are very small in all biomes compared to the other variables (Fig. 3.7d). Recovery times are often somewhat lower than those which would be expected from vegetation and soil C recovery times. This is because the greater standard deviation of NBP in our reference simulation (Fig. 3.2) reduces the threshold value in our recovery definition, thereby making it easier to reach recovery levels for NBP. We discuss the implications of this further in Section 3.2.2.

Differences in NBP recovery times between simulations are relatively small (typically a few years to decades; see Table 3.1). The largest differences in recovery times are found in the boreal forests between the cropland simulations, and, as for soil C, the differences are often greater between P20 and C20 than between P100 and C100 (Fig. 3.7d).

3.2 Discussion and conclusions

3.2.1 Comparison of identified recovery times to observations and previous studies

The effects of forest conversion to croplands or pastures are relatively well studied. Tilled croplands typically show large depletions of soil C compared to natural forest vegetation, but the picture for pasture is more diverse (Davidson and Ackerman, 1993, Don *et al.*, 2011, Guo and Gifford, 2002). Table 3.2 summarises recent reviews about observed soil C changes in agriculture compared to our results. LPJ-GUESS tends to simulate lower C loss in croplands than commonly reported in observations. We attribute this to a combination of the observation's focus on the top soil (while in LPJ-GUESS soil C is implicitly averaged over the whole soil column) and our relatively high fertiliser rates increasing productivity and thereby C input to the soil. Pugh *et al.* (2015) studied the C dynamics of soils in managed lands in LPJ-GUESS and found C accumulation even after 100 years of grazed pasture at some locations, especially for low atmospheric CO_2 concentrations. However, they used the C-only version of the model, thereby neglecting C-N interactions and increased N limitation on grass growth with time due to N removal by harvest. Croplands were explicitly represented by a number of managed, but unfertilised, CFTs in Pugh *et al.* (2015). They found soil C reductions in Europe and Africa of ~50% after 100 years of cultivation, whereas in our study C losses are much smaller (~12%), possibly partly due to different tillage effects in the two soil models applied.

In contrast to studies of LU effects compared to previously natural ecosystems, the regeneration of ecosystems after agricultural abandonment has been studied less, and a direct comparison to our simulations is challenging, either because limited information about former LU or reference conditions was provided in these studies or because there are important differences from our setup in terms of management and LU duration or other site-specific characteristics. Additionally, most of the available studies were conducted in Amazonia or North America (Don *et al.*, 2011) and there is large variability in physical and biotic characteristics as well as in land management (Kauffman *et al.*, 2009). Many

studies focus on the recovery of biodiversity or species richness (Cramer *et al.*, 2008, Queiroz *et al.*, 2014), but these variables cannot be adequately captured by our large-scale PFT approach. It is often assumed that the ecosystem will gradually return to its previous state and that intensive LU delays recovery but the time scales are widely unknown and differ across variables and regions, e.g. tropical species composition recovers much slower than forest structure and soil nutrients (Chazdon, 2003). Different recovery processes are strongly interlinked, e.g. vegetation accumulation and turnover are key factors in the replenishment of soil quality and nutrients which in turn determine plant productivity, and post-agricultural soil C and N dynamics have been shown to correlate during the regeneration of ecosystems (Knops and Tilman, 2000, Li *et al.*, 2012).

Table 3.2: Observations and LPJ-GUESS results of soil C changes during agriculture (cropland or pasture) and vegetation and soil C recovery after agricultural abandonment.

Observation type	Biome	Observation value	Closest simulations in terms of LU history	Average model value for the specific biome	Reference
Soil C changes during agriculture					
Soil C change averaged over different depths	global	42% loss for forest-cropland conversions, 8% gain for forest-pasture conversions	P20, P60, P100, C20, C60, C100	7-17% loss in forest biomes for croplands, 2% gain to 7% loss for pastures	Guo and Gifford (2002)
Soil C change at 36 cm	tropical forest	25% loss for cropland, 12% loss for pasture/ grassland	C20, C60, P20, P60	11-12% loss for croplands, 2% gain to 4% loss for pastures	Don *et al.* (2011)
Soil C change at 29 cm	temperate forest	new equilibrium after 23 years	C100	C loss throughout the entire cropland duration	Poeplau *et al.* (2011)
Vegetation recovery after agricultural abandonment					
Above-ground vegetation recovery time	tropical forest	189 years	C20	121 years	Saldarriaga *et al.* (1988)
Above-ground vegetation recovery rate	tropical forest	slowdown with time, recovery slower for pasture than for cropland	P20, P60, P100, C20, C60, C100	(slight) slowdown, pasture recovery slower only for long durations (P100/C100)	Silver *et al.* (2000)
Total and vegetation C recovery rate	temperate forest	linear with time	P60, P100	(slight) slowdown	Hooker and Compton (2003)
Vegetation recovery rate	temperate forest	linear with time	C20, C60	(slight) slowdown	Poulton *et al.* (2003)
Above-ground vegetation	tropical forest	recovery speed inversely related	P20, P60, P100	recovery speed inversely related to	Uhl *et al.* (1988)

recovery rate		to LU duration		LU duration	
Above-ground vegetation recovery rate and time	tropical forest	73 years, recovery speed inversely related to LU duration	C20, C60, C100	121-139 years, recovery speed inversely related to LU duration	Hughes *et al.* (1999)
Maximum tree height recovery rate	tropical forest	recovery speed inversely related to LU duration	C20, C60, C100	recovery speed inversely related to LU duration	Randriamalala *et al.* (2012)
Vegetation height recovery rate	tropical forest	slower for pasture than for cropland	P20, P60, P100, C20, C60, C100	slower only for long durations (C100/P100)	Moran *et al.* (2000)
Above-ground vegetation recovery rate	tropical forest	slower for pasture than for cropland	P20, C20	faster for P20 than for C20	Wandelli and Fearnside (2015)
Soil C recovery after agricultural abandonment					
Soil C recovery at up to 30 cm	global	large variation across studies, tendency to lose C in the first years for pastures, immediate accumulation for croplands	P20, P60, P100, C20, C60, C100	tendency to lose C in the first years for pastures, immediate accumulation for croplands	Paul *et al.* (2002)
Soil C recovery at 34 cm	global	more accumulation for croplands than for pastures, no accumulation in boreal zone	P20, P60, P100, C20, C60, C100	more accumulation for croplands than for pastures, slower accumulation in boreal zone	Laganiere *et al.* (2010)
Soil C recovery at 28/40 cm	temperate forest	linear accumulation, no equilibrium after 120 years	C20	linear accumulation, no equilibrium after 120 years	Poeplau *et al.* (2011)
Soil C recovery time at 0-60 cm	grassland	158 years	C100	198 years	Potter *et al.* (1999)
Soil C recovery time at 0-60 cm	savanna/ temperate forest	230 years	C20	85 (savanna) / 237 (temperate forest) years	Knops and Tilman (2000)
Soil C recovery time 0-10 cm	temperate forest	>100 years	C20, C60, C100	237-261 years	Foote and Grogan (2010)
Soil C recovery time 0-25 cm	tropical forest	50-60 years	P20, P60, P100, C20, C60, C100	49-80 years	Silver *et al.* (2000)

Table 3.2 includes several studies about ecosystem vegetation and soil recovery after agricultural abandonment. Overall, the studies that looked at vegetation recovery upon abandonment indicate that biomass accumulation slows down after some decades and that accumulation rates correlate negatively with agricultural duration. Our simulations show that the rate of vegetation C sequestration indeed declines over time and that longer LU durations delay recovery in each of the analysed biomes. Obser-

vations also indicate that use of land for pasture delays recovery in the tropics upon pasture abandonment compared to cropping, but in our simulations this seems to be the case only after long agricultural durations. For studies about soil C dynamics after agricultural abandonment, interpretation is often hindered by combining different soil layers or aggregating different LU types (Li *et al.*, 2012) and by large variations observed across studies (Post and Kwon, 2000). Nevertheless, most of the observed patterns are reproduced in our simulations, suggesting that LPJ-GUESS captures the salient processes: after abandonment, croplands accumulate C faster than pastures, and recovery often takes more than a century. The impact of LU duration has rarely been studied. However, our results suggest that even though longer agricultural durations mostly result in greater initial soil C depletions, recovery can occur at similar or even faster speed in the sub-tropics and tropics. In temperate and boreal forests long LU durations tend to delay recovery.

The LPJ-GUESS model has been successfully tested against a range of observations and observation-based products, including vegetation distribution, vegetation dynamics, and soil C response to changes in vegetation cover (Hickler *et al.*, 2004, Miller *et al.*, 2008, Pugh *et al.*, 2015, Smith *et al.*, 2014). In our simulations, we used only two different agricultural land-cover types (intensive grazing and fertilised, tilled crops). Our analysis would therefore not identify effects of, for instance, clearing technique (e.g. burning compared to mechanical removal) or different land management practices (e.g. repeated burning or irrigation) within one land-cover type. For example, recovery of species richness and maximum tree height of secondary forests occurs faster under no tillage compared to heavy tillage (Randriamalala *et al.*, 2012).

Our study is intended as an idealised experiment to highlight the importance of LU history on ecosystem state and fluxes across biomes. Still, some processes with the potential to affect post-agricultural ecosystem recovery, at least regionally, are not currently included in LPJ-GUESS. One aspect is the phosphorus cycle, which is not implemented in LPJ-GUESS, even though it can be significantly altered by LUC (MacDonald *et al.*, 2012, McLauchlan, 2006). Moreover, while C and N cycles interact in LPJ-GUESS (Smith *et al.*, 2014), the uniform annual fertiliser rate we applied in this study might be realistic in some regions, such as parts of Europe, but exceeds present-day fertiliser use in Africa (Potter *et al.*, 2010). Seed availability, remnant trees, and resprouting from surviving roots are important factors during initial stages of tree colonisation following agricultural cessation (Bellemare *et al.*, 2002, Cramer *et al.*, 2008). While LPJ-GUESS does not account for these effects explicitly, seedling establishment is limited by a suitable growth environment, such that effects like re-sprouting or remnant trees as seed sources are mimicked. The model has been shown to, for example, reproduce vegetation recolonisation in northern Europe during the Holocene well (Miller *et al.*, 2008) as well as canopy structural changes as a function of forest age (Smith *et al.*, 2014). What is more, by using a prescribed climate in our simulations, hydrological biosphere-atmosphere interactions and feedbacks are not captured (Eltahir and Bras, 1996, Giambelluca, 2002), which could alter regional climate in

response to land-cover change, potentially affecting recovery rates, especially in tropical regions. Biophysical effects are not restricted to modifications of the water cycle but also include changes in surface albedo and roughness length as a function of ecosystem structure and composition, thereby affecting air mixing and heat transfer. While forests generally absorb more sunlight than grasslands (e.g. Culf *et al.*, 1995), differences amongst tree species and age classes exist as well. Substantial impacts related to realistic LU have been found at local-to-regional scales (Alkama and Cescatti, 2016, Peng *et al.*, 2014). Whether or not the locally observed changes translate to a significant global radiative forcing is still debated as the direction of change differs across regions in some climate models, which may cancel when integrated globally (Pielke *et al.*, 2011). Additionally, while we focus on C sequestration rates in our analysis, there might be biogeochemical implications beyond C. For instance, the emissions of BVOCs to the atmosphere vary greatly amongst plant species (Kesselmeier and Staudt, 1999). BVOCs affect atmospheric composition and climate via O_3 production, lengthening the lifetime of atmospheric CH_4, and contributing to secondary organic aerosol formation (Penuelas and Staudt, 2010, Wu *et al.*, 2012). BVOC emission factors might also be drastically influenced by wildfires (Ciccioli *et al.*, 2014), which in turn are driven by species composition and vegetation density. Thus, different successional trajectories of ecosystem structure and composition recovery have the potential to directly modify air quality and climatic conditions under which regrowth occurs, potentially creating positive or negative climate system feedbacks.

3.2.2 Implications of recovery definition

The term recovery is subjective and, in the absence of a universal definition amongst ecologists, several definitions currently exist. The definition used in this study examines recovery from a C sequestration perspective which does not capture situations, for example, where the system approaches a new equilibrium (as soil C did in some regions in the cropland simulations). In order to obtain a better understanding of the uncertainties related to our definition we therefore explored four alternative plausible recovery definitions.

When applying a mean minus 2 σ threshold (instead of a mean minus 1 σ threshold), recovery times are generally shorter, e.g. on average 75 instead of 106 years for vegetation C in P60, but the overall geographic patterns are very consistent across both definitions (not shown). For all variables and simulations, notable differences between both definitions occur in regions with longest recovery times, especially for sub-tropical soil C in the pasture simulations.

Recovery based on percentage change results in more heterogeneous patterns across variables when compared to our standard recovery definition (Fig. 3.9). Applying a threshold of 95% of the mean, instead of a mean minus 1 σ threshold, produces slightly longer dominant PFT recovery times in parts of the temperate and tropical forests, and shorter recovery times in grasslands, especially for the pasture simulations. Vegetation C shows similar patterns to the dominant PFT. However, the differences

to our standard definition are more pronounced. Soil C recovery times generally decrease dramatically, especially outside the tropics. NBP recovery times generally increase, particularly in forest ecosystems.

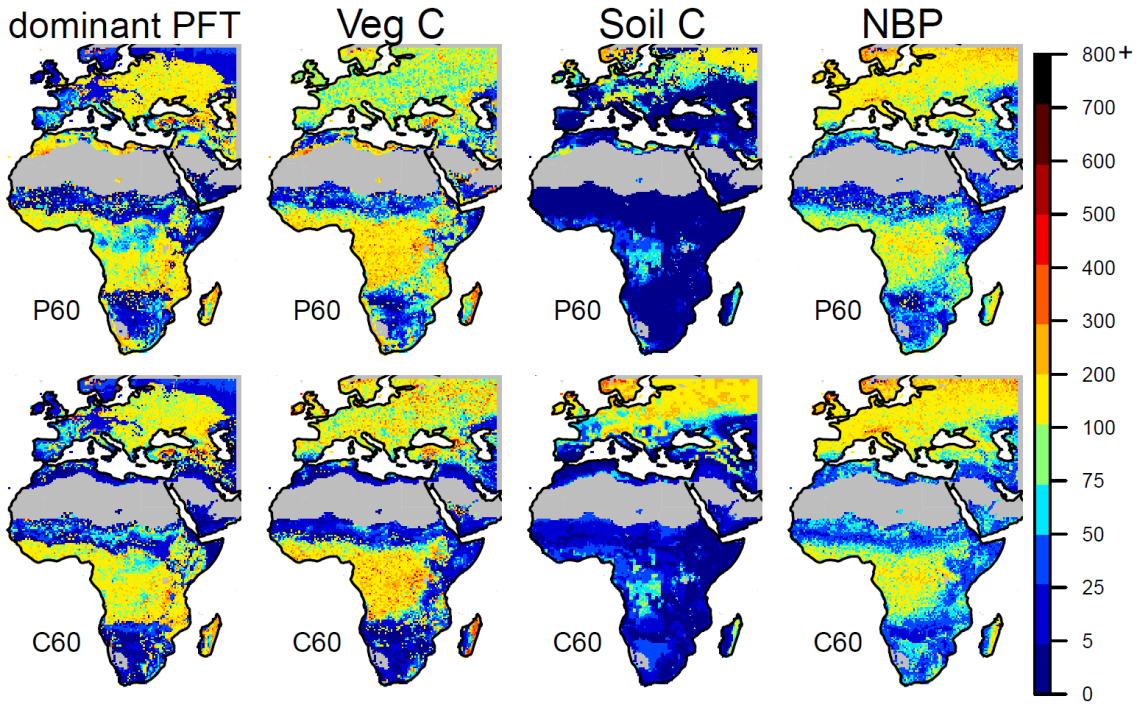

Figure 3.9: Maps of recovery time for the dominant PFT, vegetation C, soil C, and NBP with an alternative recovery definition (compared to Fig. 3.3) for the P60 and C60 simulations. The definition is the same as our standard definition but with a mean · 0.95 threshold instead of mean - 1 σ.

By expanding our standard recovery definition by an upper threshold (reference mean plus 1 σ), and with the "minimum rule" also applied to the maximum (see Section 2.2.5), one can test whether some ecosystems recover from higher rather than lower values than in the reference simulation. Mostly grasslands are affected by this alternative definition (Fig. 3.10). Dominant PFT recovery under this definition takes slightly longer throughout the African grasslands for the pasture simulations, and considerably longer in parts of northern and southern Africa for the cropland simulations. Patterns are similar for vegetation C but the increase in vegetation C recovery times is often larger than the increase in dominant PFT recovery times, especially for croplands. Soil C recovery is notably longer in sub-tropical and eastern African grasslands. The recovery times of NBP are hardly affected. However, we do not use an upper threshold in the primary definition used in this study because in this case the ecosystem is already operating at a level of service above that which the undisturbed ecosystem would have provided and our aim here was to investigate recovery from a depletion perspective.

Finally, when using the mean ± 1 σ definition and additionally checking whether the variable is still in the mean ± 1 σ range at the end of the simulation period (not shown), many grid-cells do not recover even within the set maximum cut-off of 800 years. Elements of random fluctuations due to natural variability arising from stochastic processes and disturbances and responding C, N, and water dynam-

ics make a clear identification of recovery period difficult in that case. In particular for soil C, no recovery is found for parts of eastern and sub-tropical Africa. The system converges towards a new equilibrium state in these regions which lies above reference values. NBP stays within background levels everywhere.

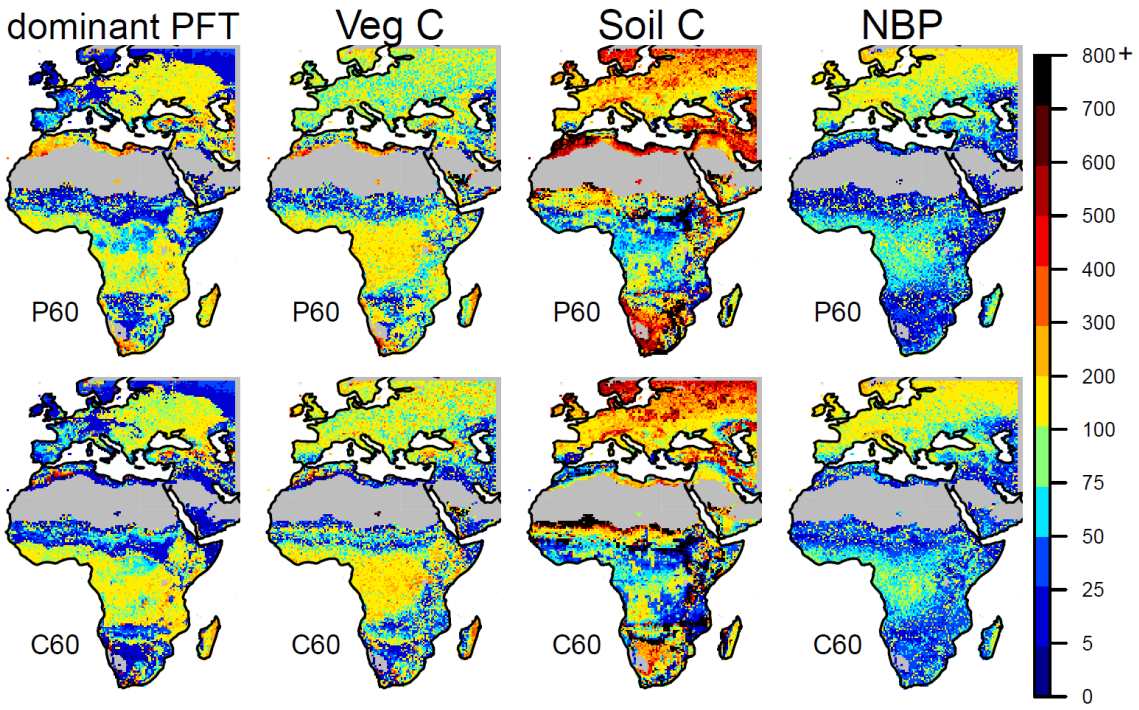

Figure 3.10: Maps of recovery time for the dominant PFT, vegetation C, soil C and NBP with an alternative recovery definition (compared to Fig. 3.3) for the P60 and C60 simulations. The definition is the same as our standard definition but with a mean ± 1 σ threshold and the minimum check also applied to the maximum instead of a mean - 1 σ threshold and only checking the minimum.

Altogether, the alternative recovery definitions agree on the general findings when applying our standard definition, especially in terms of relative recovery rates. For all definitions, vegetation C and dominant PFT recover faster in grasslands than in forest-dominated ecosystems, and soil C recovery takes much longer in higher latitudes. However, some areas, especially in the sub-tropics, "recover" from values higher than in the reference simulation, and these cases are not captured by our standard definition. Additionally, in the tropics, soil C accumulation sometimes does not stop once background values are reached and soil C leaves the reference range. When recovery is defined based on standard deviation, NBP recovery is often quicker than recovery of the C pools. This inconsistency emphasises the importance of both recovery definition and selected variables when studying the recovery of ecosystems (Jones and Schmitz, 2009). This is particularly relevant for flux tower measurements, where an underlying long-term trend caused by the recovery from previous, often unquantified or unknown LUC, might be overlooked due to a large inter-annual variability in net ecosystem exchange.

3.2.3 Conclusions from Section 3

Most studies which have explored the effects of distant human activities on present-day ecosystems were restricted by sampling difficulties, small spatial scales, short time periods since abandonment, and little information about background conditions or the specific LU history of the site. Here, we use a model-based approach to study the legacy effects of agricultural LU history (type and duration) on ecosystem regeneration and C sink capacity after the cessation of agriculture in a range of biomes across Europe and Africa. The model reproduces qualitatively the response found at study locations, including distinct differences in recovery between different variables of the terrestrial C cycle. Long-lasting legacy effects of former agricultural intensity emerge as important for present-day ecosystem functions. These findings have implications for various scientific applications:

1. Long-term monitoring sites (e.g. FLUXNET) and Earth observation systems need to collect and maintain detailed information about past and present land cover and land management to adequately interpret their data.
2. Assessments of trends in data from sites that seek to identify impacts of climate change and/or increasing atmospheric CO_2 concentration need to make sure that legacy effects of past LU are not confounding the observed trends.
3. Simulation experiments need to move beyond deforestation but also represent, in a more detailed manner, regrowth dynamics following agricultural abandonment at the sub-grid level. At the moment a few DGVMs have started to do so (Shevliakova *et al.*, 2009, Stocker *et al.*, 2014, Wilkenskjeld *et al.*, 2014) based on model products of tropical shifting cultivation (Hurtt *et al.*, 2011), but accounting for gross land-cover changes is also important in other regions like Europe (Fuchs *et al.*, 2015). Failure to consider LU history may lead to errors in the simulation of vegetation properties, potentially resulting in biases in C sequestration or energy balance calculations, with subsequent implications for simulations of regional and global climate. Our study suggests that, for vegetation and soil C studies, accounting for LUC over the last 100-150 years is sufficient in the tropics, while more than 200 years might be necessary in the temperate and boreal zone; studies restricted to vegetation should not have to account for LUC more than 150 years ago in any major climatic zone.
4. Assessing the efficiency of climate mitigation through large-scale reforestation or afforestation projects will require knowledge about the type and duration of previous LU. Our simulations suggest that the potential to rapidly sequester C in biomass and soil is greatest in tropical forests following short periods of cropland, while boreal forests accumulate C slowest, especially when previously used for pasture. Special attention should be paid to monitoring changes in below-ground C, as in most places the accumulation of soil C is much more sensitive to LU history than C accumulation in regrowing trees.

5. In terms of soil C, our results suggest that some sub-tropical regions might not recover at all on time scales relevant for humans. However, given the low absolute amounts of C “missing” in these soils, implications for the global C cycle are expected to be small.

4 Large uncertainty in carbon uptake potential of land-based climate-change mitigation efforts

In this section we run four DGVMs forced by land-based mitigation LUC scenarios from the two LUMs (for information about the LUC scenarios and their implementation into the DGVMs see Section 2.3). We compare the C uptake achieved in the DGVMs via bioenergy cultivation combined with C capture and storage or avoided deforestation and afforestation to the C uptake targeted and achieved in the LUMs to assess the potential contribution of negative emissions to climate stabilisation.

4.1 Results

Present-day C pools as simulated by IMAGE and MAgPIE are 440 and 484 GtC in global vegetation, and 1121 and 1981 GtC in the soils (including litter), respectively. Vegetation C simulated by the DGVMs ranges between 275 and 425 GtC, and soil C between 1315 and 1954 GtC (Fig. 4.1). For the two non-mitigation BASE scenarios, in all DGVMs except LPJmL the land acts as a net C sink between the years 2000 and 2099 (Fig. 4.1). The magnitude and direction of change in C pools is determined by the DGVM's response to RCP2.6 climate change, CO_2 fertilisation, and baseline LUC.

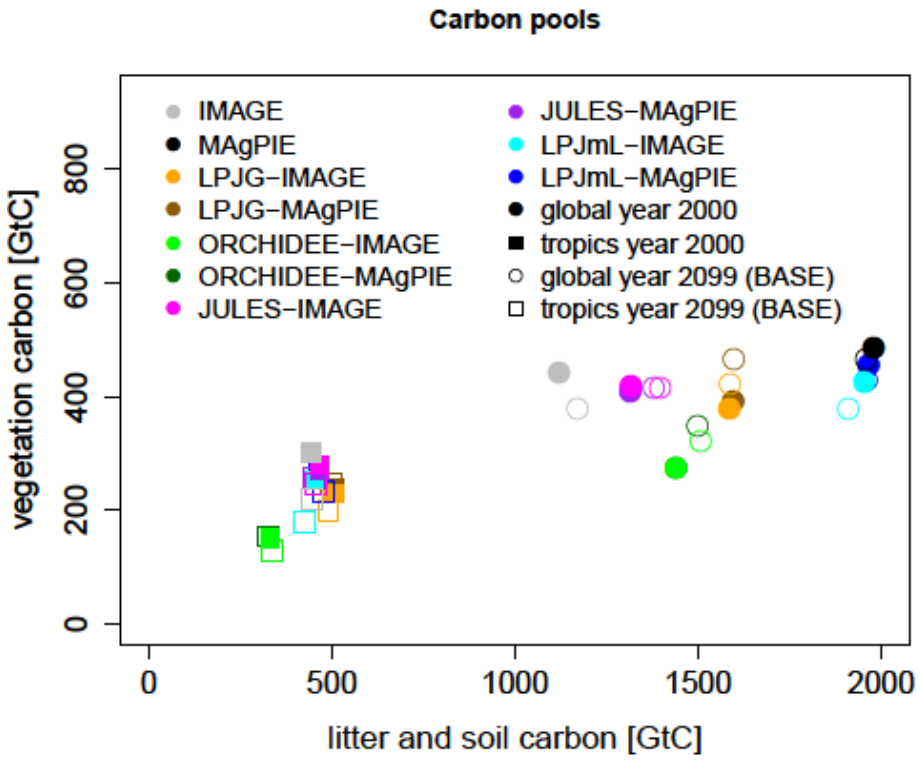

Figure 4.1: Global (circles) and tropical (30°S-30°N; squares) vegetation and litter and soil C pools [GtC] in the LUMs and DGVMs for the years 2000 and 2099 (BASE scenario). Tropical C stocks were not available from MAgPIE. Note that presented C pools are affected by LUC and thus do not represent potential C pools.

4.1.1 Total carbon uptake in the mitigation scenarios

Total additional C uptake in the mitigation scenarios is here calculated as the sum of changes in vegetation C, soil and litter C, and (relatively negligible) product pool C, plus cumulative CCS (all relative to BASE). While an uptake target of 130 GtC was set in both LUMs, actual total C uptake in the LUMs in most cases deviates somewhat from this number. For the ADAFF scenarios, the simplicity of the afforestation implementation in IMAGE was unable to exactly meet the target. In MAgPIE, afforestation decision-making was based on present-day potential C pools. Potential impacts of climate change and CO_2 fertilisation on the terrestrial C storage capacity were therefore not considered, which leads to a mismatch between intended and actual sequestration. The realised C uptake between year 2005 and 2099 for ADAFF is 141 GtC in IMAGE and 120 GtC in MAgPIE (Fig. 4.2a-b, Fig. 4.3a). Around 49% of the total C increase in IMAGE ADAFF can be attributed to avoided deforestation and 51% to afforestation (for MAgPIE spatial C stocks were not available but afforestation is certainly much more important due to the limited decline in forest area in MAgPIE BASE). For BECCS (and the BECCS component of the BECCS&ADAFF scenario), in both LUMs the CDR target was implemented as a gross CCS target which included the harvested C from bioenergy crops and a fractional (80%; Klein *et al.*, 2014) capture and storage of this harvest. Cumulative CCS reaches 128 GtC in year 2099 in both LUMs (see Section 4.1.4) so the implemented CDR/CCS target is reached. However, calculations of the target in the LUMs originally neglected terrestrial C losses from deforestation for bioenergy cultivation. When these are included, cumulative CCS combined with ecosystem C losses from deforestation result in a net total C uptake of 86 and 107 GtC, thus below the sought target due to emissions from LUC. The total C uptake in the LUMs for the combined bioenergy and afforestation scenario (BECCS&ADAFF) is 129 and 122 GtC (Fig. 4.3a).

In contrast to the two LUMs, total C uptake is typically lower in the DGVM simulations forced by the same LU patterns, with total C uptake in the DGVMs ranging between 19 and 130 GtC (Fig. 4.2a-b, Fig. 4.3a). Unsurprisingly (as LPJmL represents the vegetation component of the LUMs), the closest agreement exists between the LUMs and LPJmL. ORCHIDEE simulates the lowest uptake for ADAFF and JULES the lowest uptake for BECCS. BECCS&ADAFF usually results in uptake rates that lie between the ADAFF and the BECCS cases. The maximum yearly total C uptake per decade (2000-2009, 2010-2019,…) ranges from 1.9 GtC yr^{-1} (IMAGE ADAFF) to 3.5 GtC yr^{-1} (MAgPIE ADAFF) in the LUMs and from 0.4 GtC yr^{-1} (ORCHIDEE IMAGE-ADAFF) to 2.0 GtC yr^{-1} (LPJmL IMAGE-BECCS) in the DGVMs. Spatially, total C uptake is concentrated in the tropics for ADAFF (except in ORCHIDEE which simulates substantial emissions in some regions), while patterns are more diverse for BECCS (Fig. 4.4). The largest agreement in total C uptake across DGVMs is found in tropical Africa for the ADAFF scenarios (Fig. 4.5). The contributions of vegetation, soil, and cumulative CCS to model discrepancies in total C uptake are analysed in the following subsections.

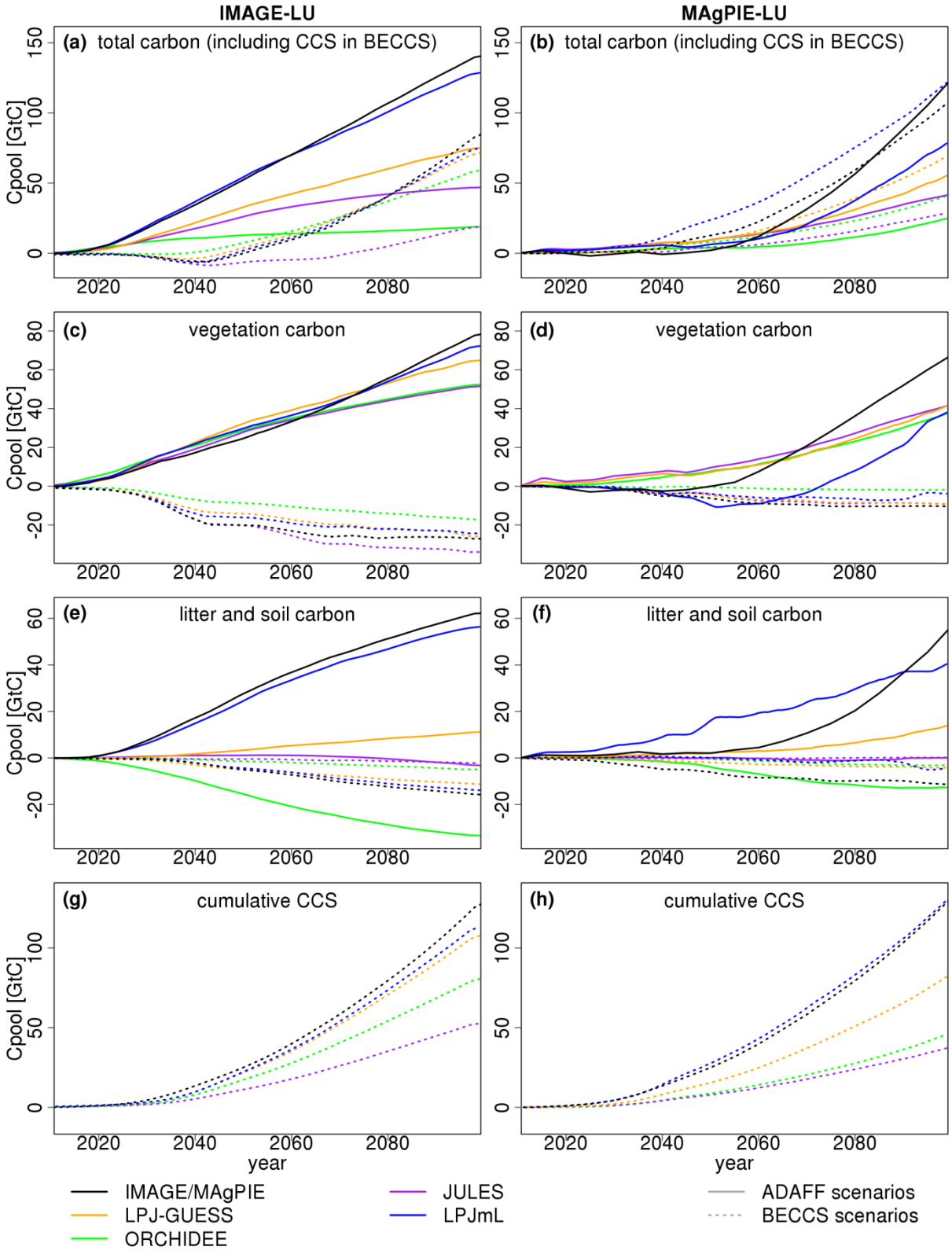

Figure 4.2: Time-series (2010-2099) of simulated C uptake (total of all grid-cells) in the LUMs and DGVMs for the ADAFF and BECCS simulations (compared to the respective BASE simulation), for IMAGE-LU patterns (left, 5-year running means) and MAgPIE-LU patterns (right). a+b) total C (including cumulative CCS), c+d) vegetation C, e+f) litter and soil C, g+h) cumulative CCS. C uptake in the BECCS&ADAFF simulations usually lies between BECCS and ADAFF and is therefore not shown.

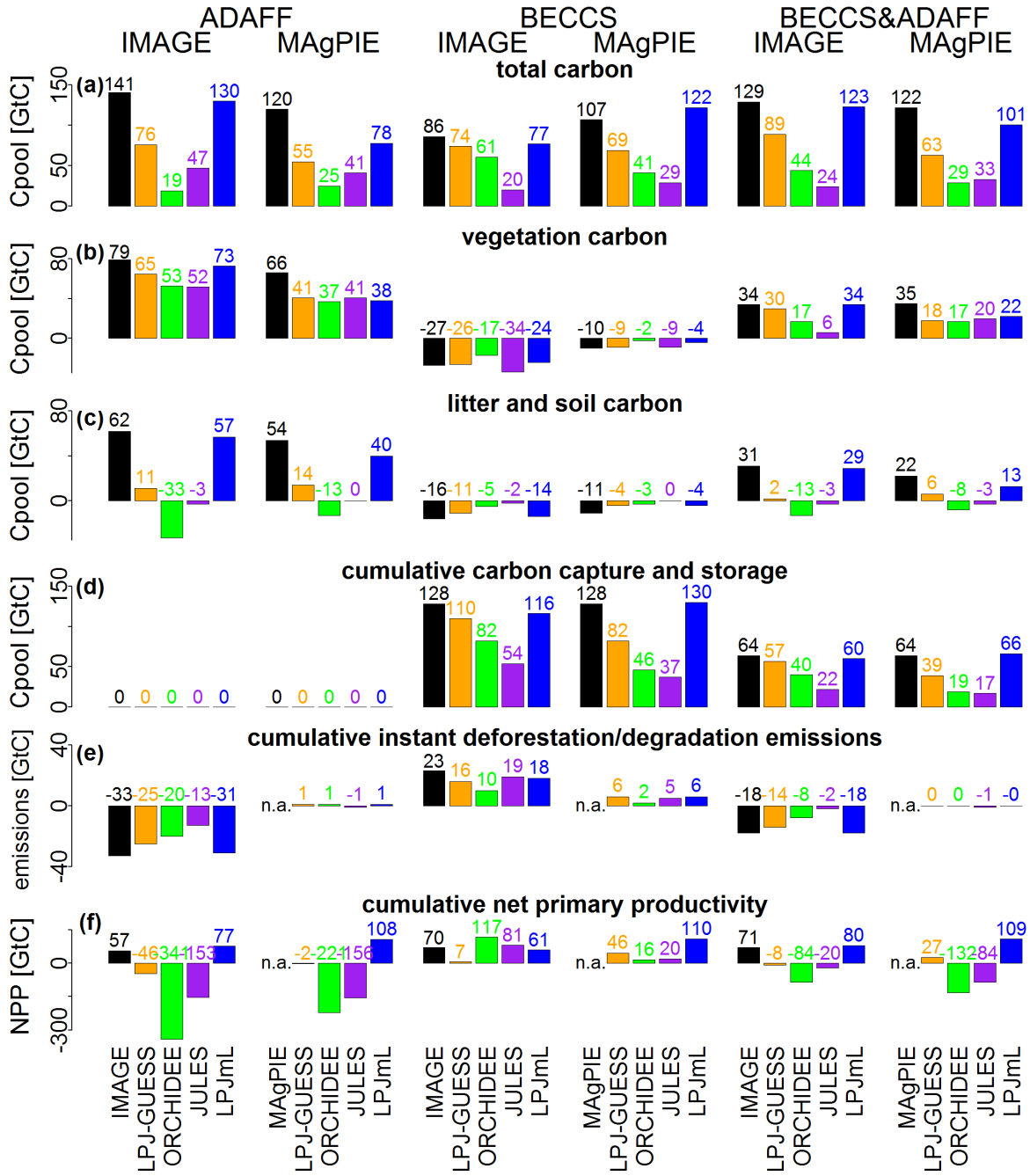

Figure 4.3: Simulated change in total C (a), vegetation C (b), litter and soil C (c), cumulative CCS (d), cumulative instant (oxidized in the same year) deforestation/degradation emissions (e), and cumulative NPP (f) between year 2005 and 2099 for the mitigation simulations (compared to the respective BASE simulation) in IMAGE/MAgPIE (as simulated by the LUMs in the LUC scenarios), LPJ-GUESS, ORCHIDEE, JULES and LPJmL.

4.1.2 Vegetation carbon

As intended, the simulations with the ADAFF scenarios result in increasing biomass over the 21st century compared to the BASE simulations for all LUMs and DGVMs. Vegetation C uptake in year 2099 is 79 and 66 GtC in IMAGE and MAgPIE and ranges between 39 and 73 GtC in the DGVMs (Fig. 4.2c-d, Fig. 4.3b), with generally larger uptake for IMAGE scenarios than for MAgPIE scenarios

due to the earlier start of ADAFF activities in IMAGE (Fig. 2.3). Biomass accumulation occurs at a relatively steady rate in the DGVMs but accelerates during the second half of the century in the LUMs (Fig. 4.2c-d). There is a drop in vegetation C uptake for LPJmL MAgPIE around mid-century. As agricultural land has low vegetation C pools in LPJmL this decline seems to be related to a decreasing vegetation C density in forests, which is not compensated for by the simultaneous increase in forest area. Tree PFTs in LPJmL are represented by a single individual (representing the average of all trees belonging to this PFT), and the individual's properties are changed when afforestation occurs in a grid-cell. These changes in the PFT's properties might in some regions reduce its ability to compete or make it more vulnerable to disturbances so that tree mortality is increased compared to the BASE scenario in which no afforestation took place.

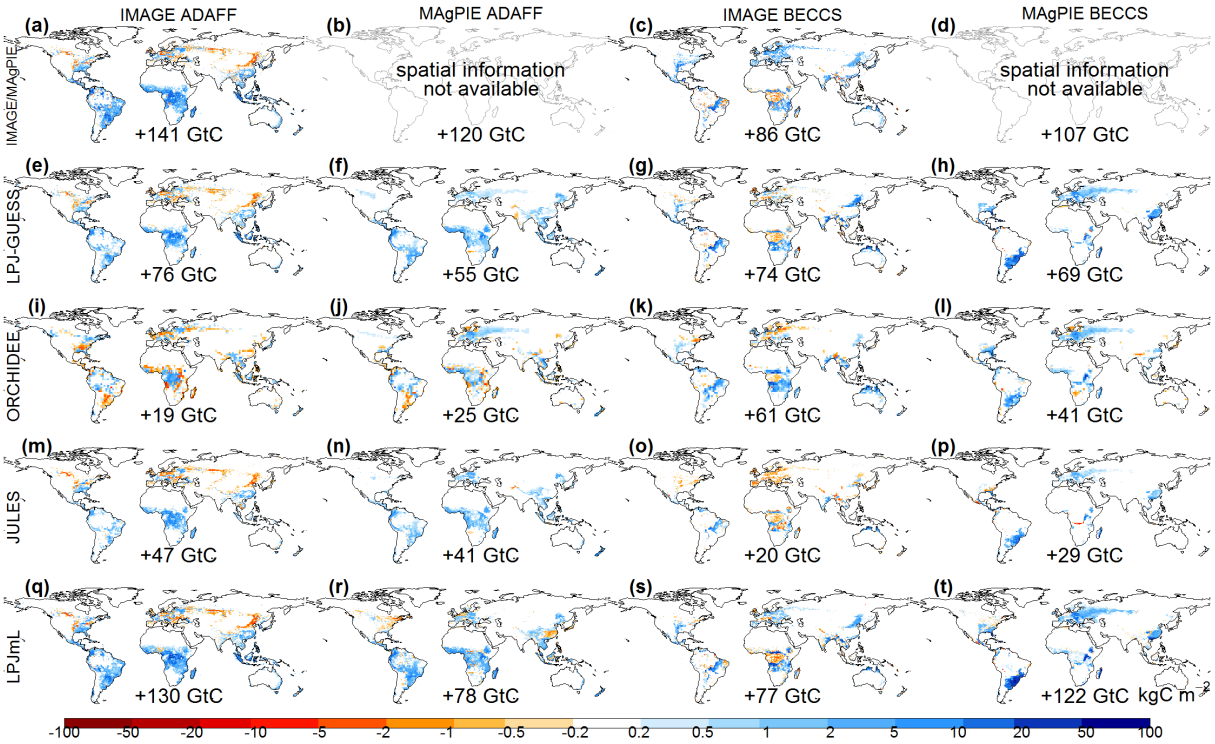

Figure 4.4: Maps of total C uptake [kgC m^{-2}] in the LUMs (a-d) and DGVMs (e-t) for the ADAFF and BECCS simulations (compared to BASE) between year 2005 and 2099 for IMAGE ADAFF (1st column), MAgPIE ADAFF (2nd column), IMAGE BECCS (3rd column) and MAgPIE BECCS (4th column). Numbers are global totals.

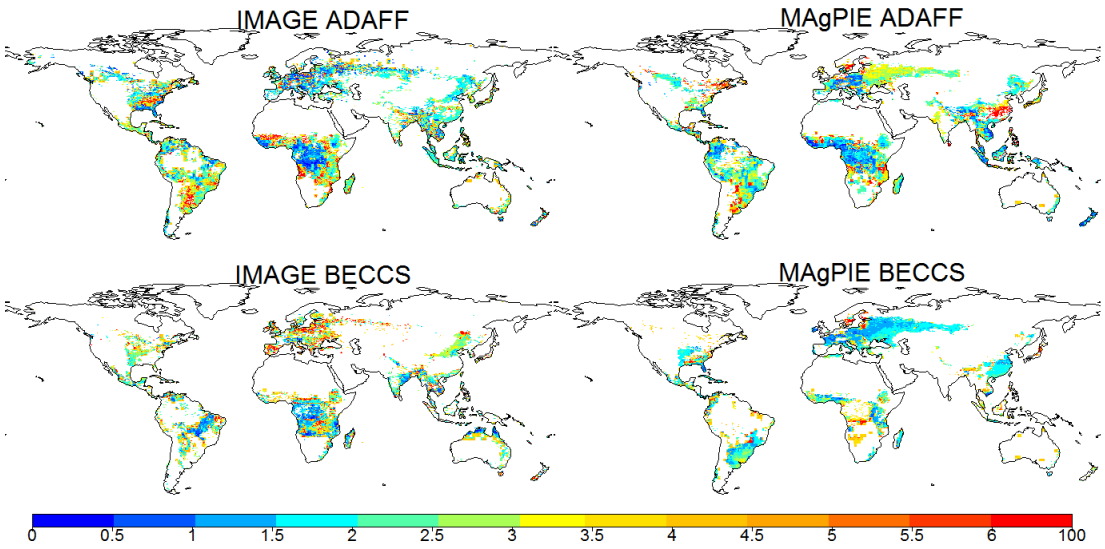

Figure 4.5: Maps of the absolute value of the range divided by the mean (|(max-min)/$\bar{x}$ |) in total C uptake across DGVMs by year 2099. Red colours indicate regions of highest uncertainty in total C uptake. Regions where the absolute mean total C uptake across models is below 0.1 kgC m^{-2} are masked.

The vegetation C uptake in IMAGE can be equally attributed to avoided deforestation and to afforestation (Table 4.1). No quantification is possible in MAgPIE because spatial C stocks were not available. In the DGVMs, the contribution of avoided deforestation to the vegetation C uptake in ADAFF is generally larger for IMAGE-LU than for MAgPIE-LU (Table 4.1), confirming the much larger role of afforestation compared to avoided deforestation in MAgPIE. For BECCS, all LUMs and DGVMs simulate deforestation-driven decreases in vegetation C. JULES simulates the largest biomass losses upon deforestation and ORCHIDEE the smallest losses. Since global vegetation C stocks are similar across DGVMs (with the exception of ORCHIDEE; Fig. 4.1), differences in C losses arise from spatial variations in biomass which DGVMs (and presumably also LUMs) are known to not capture well (Johnson *et al.*, 2016). BECCS deforestation emissions are generally larger for IMAGE-LU patterns than for MAgPIE-LU patterns, reflecting the much larger decline in forest area (Fig. 2.3, Table 2.2).

Table 4.1: Relative contribution of avoided deforestation (compared to afforestation) to the vegetation carbon uptake in the LUMs and DGVMs for the ADAFF simulations.

	IMAGE-LU	MAgPIE-LU
IMAGE/MAgPIE	50%	not available
LPJ-GUESS	55%	25%
ORCHIDEE	60%	10%
JULES	67%	14%
LPJmL	55%	18%

Site-level comparisons can help us to better understand differences across models. Therefore, in order to understand local responses better and to use these to interpret the simulated global totals, we applied the models at a number of grid locations (for IMAGE scenarios as spatial information were not availa-

ble from MAgPIE), selected because a large fraction of the grid-cells' area underwent land-cover transitions within the 21st century. However, there are substantial variations in the models' response to LUC across different sites, making it difficult to choose representative grid-cells and to draw universal conclusions from this comparison. Figure 4.6 shows three relatively representative example sites. As expected for a 0.5° resolution, there are substantial differences on grid-cell level across models in terms of initial vegetation C densities. All models simulate increasing biomass in response to afforestation (Fig. 4.6a-b; taken from the ADAFF simulations) and biomass losses upon deforestation (Fig. 4.6c; taken from the BECCS simulations). However, JULES does not simulate forest degradation (Fig. 4.6c; see Section 2.3.1 for more information about degraded forests in IMAGE), contributing to the lower vegetation C uptake compared to the other DGVMs for the IMAGE ADAFF (and IMAGE BECCS&ADAFF) scenario.

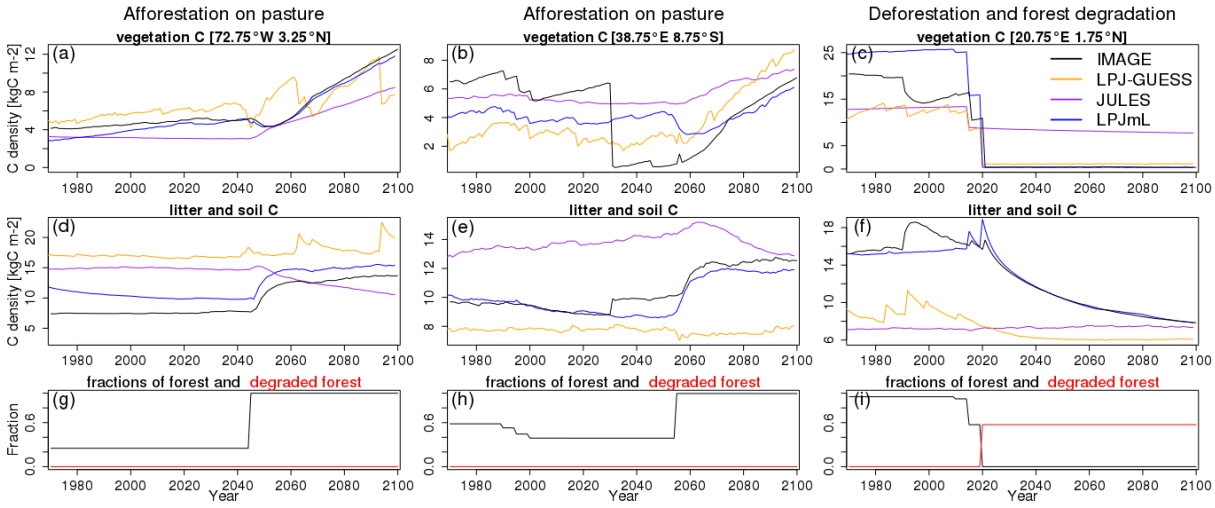

Figure 4.6: Three example sites showing vegetation C [kgC m^{-2}] (a-c) and litter and soil C [kgC m^{-2}] (d-f) trajectories in IMAGE and the DGVMs for different LUC (prescribed by IMAGE; g-i): afforestation on pasture (left and middle) and deforestation for agriculture and forest degradation (right). Note that ORCHIDEE was run on 2° x 2° resolution and is thus excluded.

For MAgPIE scenarios, site-level comparisons are not shown because MAgPIE only reported global C pools. For the MAgPIE ADAFF scenario, global vegetation C uptake is very similar in all DGVMs but lower than in MAgPIE (Fig. 4.2d). It seems that one reason for this divergence is different assumptions about potential vegetation C stocks (available for MAgPIE and LPJ-GUESS; see Fig. 4.7). An additional factor explaining the divergence is the pace of the regrowth curve. In contrast to the other models, MAgPIE assumes a single response function per biome, irrespective of spatial differences in climate and soil conditions within a biome, and thus ignores the effects of spatial differences within a biome, e.g. in terms of annual precipitation or soil fertility on forest regrowth (Poorter *et al.*, 2016). Additionally, MAgPIE does not account for disturbances. When looking at forest regrowth rates averaged over different biomes it seems that tropical regrowth occurs much faster in MAgPIE than, for example, in LPJ-GUESS (Fig. 4.8a).

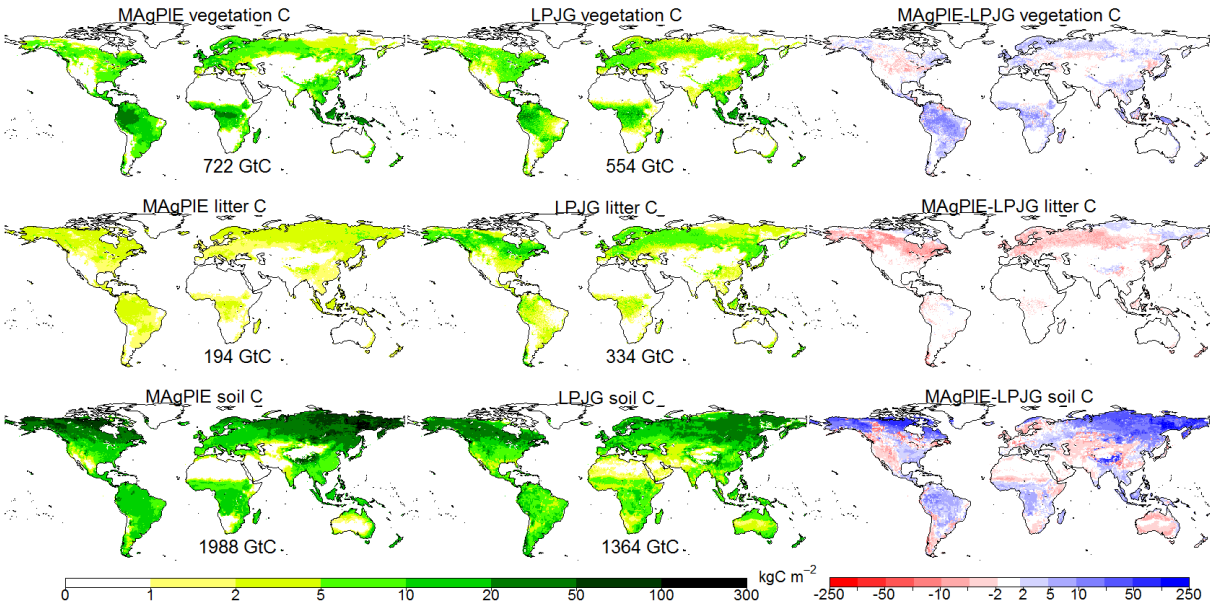

Figure 4.7: Potential vegetation C (top), litter C (middle), and soil (bottom) C stocks [kgC m^{-2}] in the year 1995 for MAgPIE (left) and LPJ-GUESS (middle), and the difference between the two models (right). Note the logarithmic scales. Numbers are global totals.

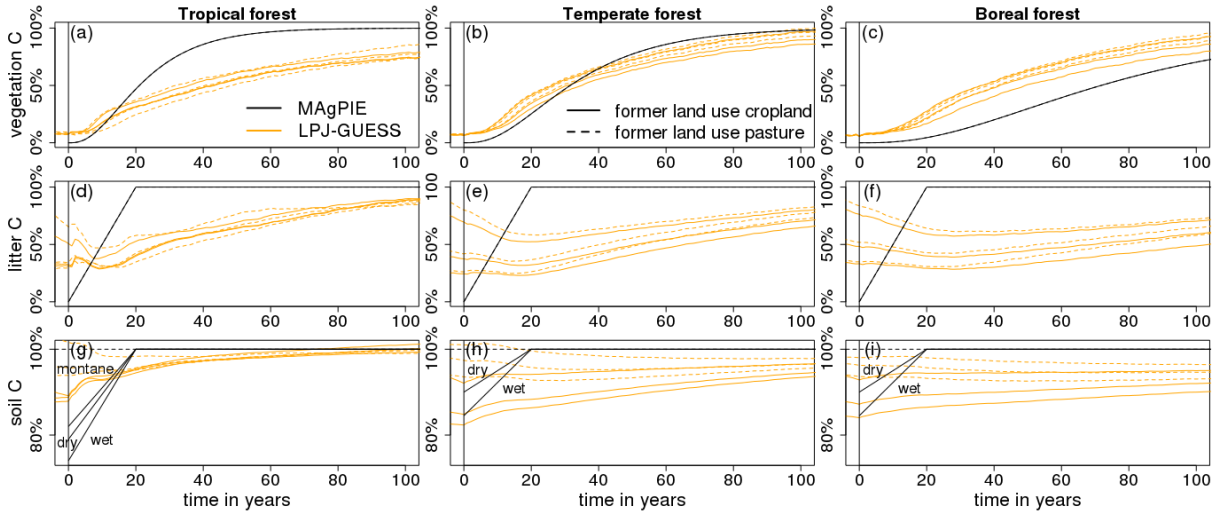

Figure 4.8: Comparison of (relative) changes in vegetation C (a-c), litter C (d-f), and soil C (g-i) following afforestation in MAgPIE and LPJ-GUESS, averaged over different biomes. The orange lines correspond to LPJ-GUESS simulations of different former agriculture durations adopted from Section 3. These LPJ-GUESS simulations in Section 3 only cover regions in Africa and Europe below 63°N and the model version differs from the version used in Section 4 (specific CFTs are not included and croplands are represented as intensively managed grassland; grasses have a larger below-ground/above-ground biomass ratio than CFTs so that less C is removed during harvest and more C is transferred to the litter and soil; consequently initial litter and soil C depletions would likely be lower in the LPJ-GUESS version used in Section 4). Biome classifications are also slightly different between MAgPIE and LPJ-GUESS, e.g. MAgPIE also includes a "temperate-boreal" class (not shown).

4.1.3 Soil carbon

Compared to vegetation, modelled soil C changes in response to ADAFF activities are much more diverse, with some DGVMs simulating net soil C losses upon afforestation (Fig. 4.2e-f, Fig. 4.3c). Soil C uptake in ADAFF is 62 GtC in IMAGE and 54 GtC in MAgPIE which is comparable to vegetation C uptake. In contrast, soil C changes in the DGVMs range between -33 and +57 GtC. Soil C accumulation in LPJmL for the MAgPIE ADAFF scenario starts significantly earlier than in the other models. As afforestation on pastures is common in MAgPIE until around year 2070, this indicates a large soil C uptake potential in LPJmL for pasture-forests transitions, which is also apparent in the LPJmL simulations driven by the IMAGE ADAFF LU patterns. For BECCS, all models simulate small soil C losses (up to -16 GtC) which are generally larger in the LUMs than in the DGVMs. In both ADAFF and BECCS, model differences in soil C changes are more pronounced for IMAGE-LU patterns than for MAgPIE-LU patterns.

The soil C emissions in JULES and ORCHIDEE for the ADAFF scenarios (and the relatively low emissions for BECCS) might be partly caused by the simplistic representation of agricultural management processes in these models. While LPJmL and LPJ-GUESS represent croplands by specific CFTs and growing seasons, ORCHIDEE and JULES grow crops as harvested grass (modified natural grass in ORCHIDEE, natural grass in JULES; see Table 2.4). Additionally, ORCHIDEE does not include grazing of pastures, resulting in more biomass C being transferred to the litter when the grass dies. Consequently, pastures and croplands have larger soil C pools in ORCHIDEE and JULES, respectively, than if those management processes were accounted for, resulting in less soil C accumulation potential upon afforestation. To test further how different representations of agriculture in the DGVMs affect soil C changes upon afforestation we performed two sensitivity simulations with LPJ-GUESS in which we simplified the representation of management processes following Pugh *et al.* (2015). In these simulations, the rate of change in LPJ-GUESS soil C pools is reduced by 57% in the MAgPIE ADAFF scenario (compared to the soil C uptake in the "standard" LPJ-GUESS simulations) when croplands are represented by pastures (mimicking the representation of croplands in JULES), and by 49% in the IMAGE ADAFF case when pastures are not harvested (mimicking the representation of pastures in ORCHIDEE, not shown). Furthermore, in contrast to IMAGE and LPJmL, LPJ-GUESS, JULES, and particularly ORCHIDEE simulate a widespread decline in NPP upon afforestation (Fig. 4.3f, Fig. 4.9) because in these models tropical grasslands (or croplands) are often more productive than tropical forests. Even though the fraction of NPP transferred to the soil might differ across models (e.g. due to different mortality in secondary forests), this suggests that the lower productivity of regrowing forests compared to agriculture also plays an important role for the limited soil C accumulation (or emissions) in LPJ-GUESS, JULES, and ORCHIDEE.

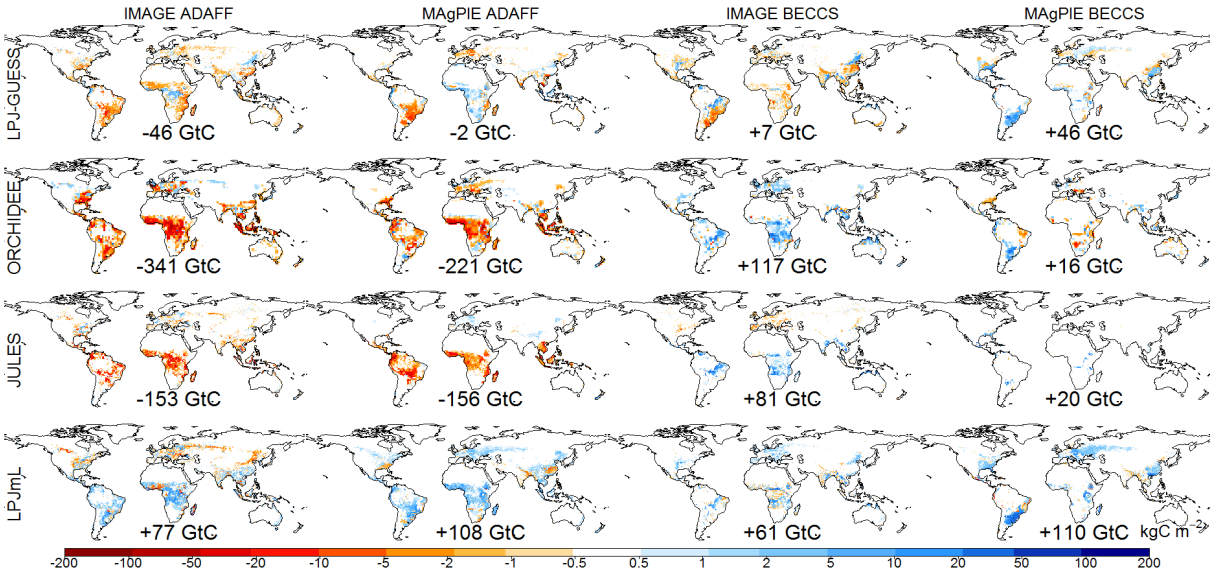

Figure 4.9: Maps of cumulative NPP differences for the mitigation scenarios (compared to BASE) in the DGVMs by year 2099 for IMAGE ADAFF (1st column), MAgPIE ADAFF (2nd column), IMAGE BECCS (3rd column) and MAgPIE BECCS (4th column). Numbers are global totals.

4.1.4 Cumulative carbon capture and storage

CCS is calculated by multiplying the harvested C of bioenergy crops by a capture efficiency of 80% before geologic storage. A prescribed CCS trajectory was implemented in both LUMs, which means that annual global CCS rates are the same in both LUMs (Fig. 4.2g+h). Cumulative CCS reaches 128 GtC in both LUMs by year 2099 (Fig. 4.3d). In the DGVMs, cumulative CCS ranges from 37 to 130 GtC by year 2099 (Fig. 4.3d). As the DGVMs used bioenergy production area from the LUMs and also the same assumptions about capture efficiency and storage capacity, the lower CCS calculated in most of the DGMVs has to arise mainly from differences in simulated bioenergy yields, including differences in the harvest index. Both LUMs assume rain-fed perennial and fast-growing second generation bioenergy crops (such as Miscanthus) to fulfil CCS demand. LPJmL is the only DGVM representing bioenergy crops explicitly, but like the other DGVMs does not assume technological yield increases, which means the slightly larger cumulative CCS than in MAgPIE originates from higher initial yields. In contrast, LPJ-GUESS grows bioenergy as maize (with residues included for CCS), ORCHIDEE as crop grass, and JULES as natural grass (for harvest assumptions see Table 2.4). Consequently, average bioenergy yields are highest in LPJmL followed by LPJ-GUESS and then ORCHIDEE and JULES (Fig. 4.10). Cumulative CCS in all DGVMs apart from LPJmL is higher for IMAGE-LU patterns than for MAgPIE-LU patterns (Fig. 4.3d) because the larger cultivation area in IMAGE (Fig. 2.4) outweighs lower average yields (Fig. 4.10). In the LUMs, the same trade-off between land expansion and yields results in equivalent global CCS rates in both LUMs.

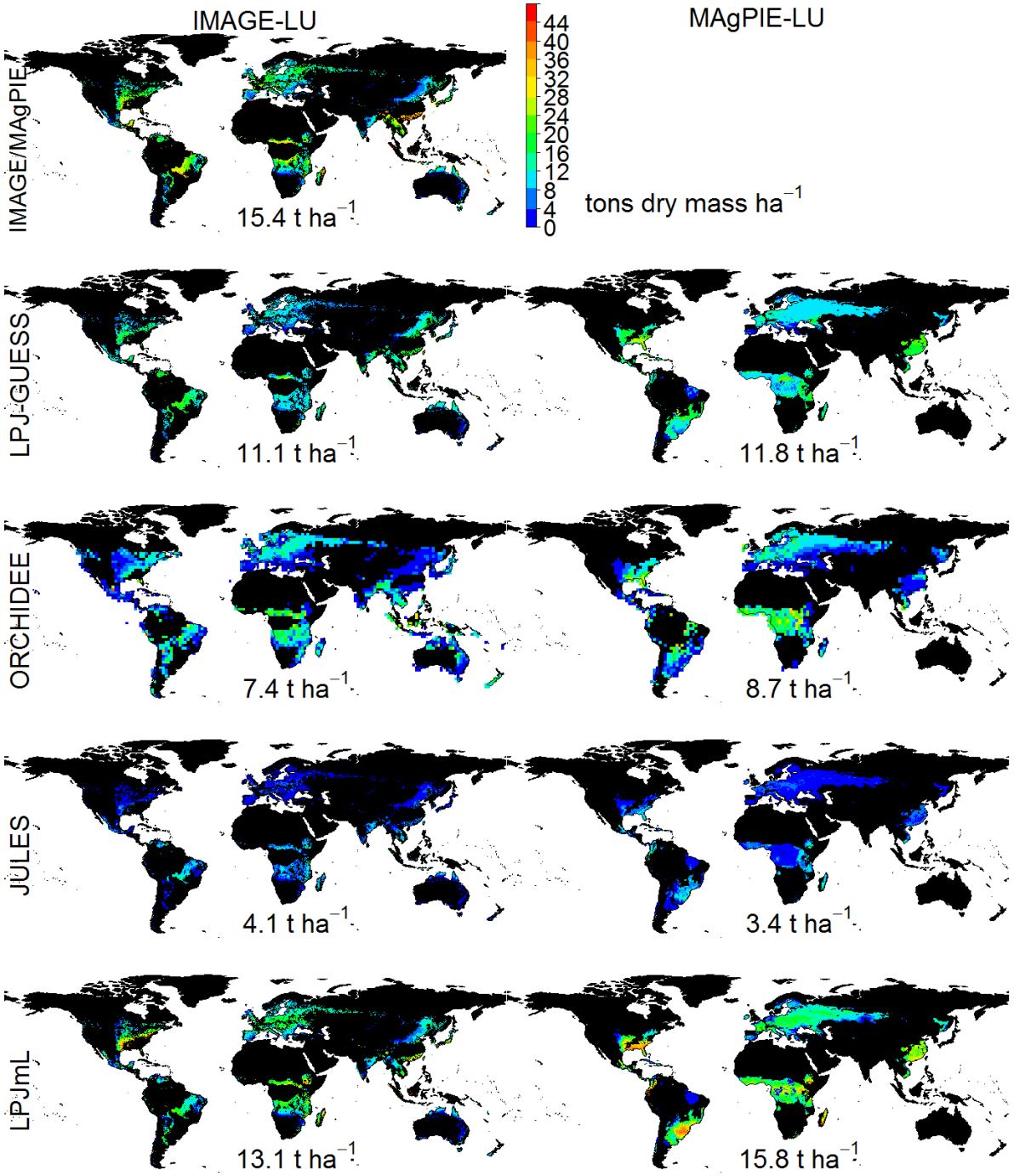

Figure 4.10: Maps of bioenergy crop yields [tons dry mass ha^{-1}, assuming a 45% C content] in BECCS (IMAGE-LU left, MAgPIE-LU right) as simulated by IMAGE (1st row), LPJ-GUESS (2nd row), ORCHIDEE (3rd row), JULES (4th row) and LPJmL (5th row) for year 2099. Note that yields are per-cropland area rather than per-grid-cell area. Spatial information were not available for MAgPIE. Areas in black do not grow bioenergy crops. Numbers are global averages (not weighted by grid-cell differences in bioenergy area).

4.2 Discussion and conclusions

4.2.1 Discussion

Cumulative LUC emissions over the 1750-2015 period were ~190 GtC (Le Quere *et al.*, 2016), with a very large uncertainty arising from how different forms of land management are considered in the simulations (Arneth *et al.*, 2017) but also due to different LUC hindcasts (Bayer *et al.*, 2017). Considering that a possibly large fraction of agricultural area will be needed for future food production (Boysen *et al.*, 2017a, Popp *et al.*, 2017), and assuming that CO_2 fertilizing effects on forest growth will be limited in RCP2.6, this suggests that achieving 130 GtC net uptake via ADAFF might be challenging, consistent with results from the DGVMs here. Several earlier studies estimated an upper limit of afforestation storage capacity of ~150 GtC within this century, despite very different methods and assumptions (Lenton, 2010, and references therein). Sitch *et al.* (in preparation) report 40-180 GtC from the same DGVMs as used in this study when applying stylised alternative afforestation scenarios (achieved e.g. via a C price rather than aiming for a specific CDR target) from IMAGE and MAgPIE. A large C uptake (215 GtC compared to a reference scenario) was found by Sonntag *et al.* (2016) in a coupled ESM for a high emission scenario (RCP8.5) when using RCP4.5 LU (afforestation, -700 Mha agricultural land) instead of RCP8.5 LU (deforestation, +800 Mha agricultural land; Hurtt *et al.*, 2011) in the reference scenario. The C uptake was thus higher than in our study, but so were baseline deforestation rates, climate impacts, and, particularly, differences in CO_2 fertilisation; the high levels of CO_2 fertilisation under RCP8.5 typically causes DGVMs to simulate much larger C uptake in forests.

Some of the discrepancy in total C uptake between the LUMs and the DGVMs in the ADAFF scenarios originates from differences in vegetation C uptake, especially for MAgPIE. Natural forest regrowth upon agricultural abandonment is implemented in all DGVMs and IMAGE, while MAgPIE assumes managed afforestation towards the biomass of potential natural vegetation. Observational studies differ substantially in reported forest regrowth rates and trajectories towards a steady state (see Section 3.2.1 and references therein). Biomass accumulation in tropical forests has often been reported to slow down a few decades after agricultural cessation, with above-ground biomass levels (representing ~80% of total biomass, Cairns *et al.*, 1997) of mature tropical forests being reached within ca. 66-90 years (Anderson-Teixeira *et al.*, 2016, Poorter *et al.*, 2016), and below-ground biomass needing more time to recover, especially following shifting agriculture (Martin *et al.*, 2013). Poorter *et al.* (2016) also found slower accumulation rates in dry (<1500 mm) compared to wet (>2500 mm) environments. In comparison, tropical (22°S-20°N as in Poorter *et al.*) afforestation in the MAgPIE ADAFF scenario occurs in relatively dry regions, with an average precipitation of 1682 mm. In our study, tropical recovery times, i.e. the time secondary forests need to reach 90% of old forest biomass, are 47 years for MAgPIE and ~150 years for LPJ-GUESS (Fig. 4.8a). The similar vegetation C uptake across all DGVMs for the ADAFF scenarios suggests that 150 years are also a reasonable estimation for the other DGVMs, even though no stylised simulations were available to verify this number. Given that

the observational studies mentioned above point towards typical recovery times that lie in the middle of this range suggests that tropical biomass accumulation rates might be underestimated in the DGVMs. This would suggest an actually higher vegetation C uptake potential via ADAFF than calculated by our DGVMs. In contrast, if most of the afforestation occurs as natural regrowth or if forest management is unable to substantially accelerate forest regrowth, tropical biomass accumulation rates might be overestimated in MAgPIE.

Degraded forests also represent an uncertainty in our IMAGE scenarios. JULES represented degraded forests as natural vegetation, whereas the other DGVMs, simply for consistency, followed the IMAGE assumption of degraded forests being grassland. In reality, degraded forests likely represents a mixture between both approaches, with above-ground biomass estimated to be 70% lower than in undisturbed forests (Asner *et al.*, 2010). Clearly, assuming a degraded forest being a grassland will overestimate vegetation C uptake potential in these regions (in IMAGE ~50% of the avoided deforestation and afforestation area by the end of the century is from degraded forests; see Table 2.2). Additionally, the mismatch between forest loss and agricultural gain, i.e. the rate of forest loss exceeding agricultural expansion rates reported by FAO (based on which the degraded forest class was introduced in IMAGE) might be largely explained by shifting cultivation (Houghton and Nassikas, 2017). However, most LUMs/DGVMs so far cannot simulate adequately shifting cultivation due to not representing different age classes amongst trees. The representation of forest degradation thus remains a challenge for LUMs and DGVMs.

Soil C changes contribute most to variations in total C uptake across models. Differences in simulated present-day soil C stocks are hardly surprising as global soil C estimates are very uncertain (Scharlemann *et al.*, 2014) and large variations across DGVMs and ESMs have been reported before (Anav *et al.*, 2013, Tian *et al.*, 2015, Todd-Brown *et al.*, 2013). Todd-Brown *et al.* (2013) showed that soil C stocks in ESMs are closely coupled to simulated NPP. In our simulations, simulated changes in NPP in response to ADAFF activities are very different across models which, along with differing representations of harvest, likely explains much of the differences in soil C accumulation. Substantial divergence in simulated productivity in response to LUC are also reported by Sitch *et al.* (in preparation) who attribute this behaviour to different representations of agriculture in the DGVMs. Modelling work by DeFries (2002) suggests that regional impacts of LUC on NPP are highly variable depending on management intensity and original vegetation cover, and that cropland productivity is higher compared to forests in temperate regions. The relatively high productivity of temperate crops seems to be confirmed for European studies (Ciais *et al.*, 2010, Luyssaert *et al.*, 2010), but estimates are highly dependent on the data source from which NPP is derived. In the tropics, observations suggest crop productivity at many locations to be lower than for forests (Cleveland *et al.*, 2015, Monfreda *et al.*, 2008). As afforestation in our scenarios is mostly concentrated in the tropics, the NPP decrease fol-

lowing afforestation in most DGVMs (due to the high productivity of C_4 grasslands/croplands compared to forests) seems to be unrealistic.

Numerous studies explored soil C changes following LUC (Smith *et al.*, 2016b, and references therein), but there is still substantial disagreement in terms of the direction and magnitude of change for most land-cover transitions. While studies agree that transitions from forests to croplands reduce soil C (and vice versa), patterns are more diverse for conversions to/from grassland, depending on management intensity, climate, and soils (McSherry and Ritchie, 2013, Powers *et al.*, 2011). The picture is further complicated by evidence that the existing field observations in the tropics (where most ADAFF activities occur in our scenarios) might not be representative for many tropical landscapes (Powers *et al.*, 2011). The LUC scenarios from the LUMs differ in terms of converted land-cover types: in MAgPIE, afforestation partly takes place on former croplands (especially before year 2025 and after 2070). MAgPIE assumes initial litter C (both in croplands and pastures) to be completely depleted and, based on IPCC guidelines, to be replenished within 20 years following agricultural abandonment. Soil C in former croplands is assumed to increase from the grid-cell specific average soil C density of cropland and natural vegetation towards the soil C density of natural vegetation within 20 years (Humpenöder *et al.*, 2014). However, a litter C density of zero and an assumed time frame of 20 years until soil C reaches equilibrium appear questionable. In fact, some studies report soil C to decrease during the first years after cropland cessation (Deng *et al.*, 2016), and subsequent C accumulation is usually slow and proceeds over several decades or even centuries (Silver *et al.*, 2000). In contrast to the prescribed recovery implemented in MAgPIE, IMAGE simulates soil C changes dynamically within LPJmL. However, the contribution of soils to total C uptake is comparable to MAgPIE even though ADAFF activities in IMAGE are largely restricted to pasture-forest transitions. In reality, afforestation on grassland (or avoided conversion from forest to grassland) has even less soil C uptake potential than on croplands; soil C depletions in pastures/grasslands relative to forests are generally low (Don *et al.*, 2011, Laganiere *et al.*, 2010) and in many cases pastures/grasslands even store more soil C than the replacing forests (Li *et al.*, submitted; Guo and Gifford, 2002, Poeplau *et al.*, 2011, Powers *et al.*, 2011). Additionally, declines in soil C have been reported during the first years of forest regrowth before accumulation occurs and net accumulation is often only achieved after several decades (Paul *et al.*, 2002, Poeplau *et al.*, 2011). Consequently, the large soil C uptake in the LUMs for the ADAFF scenarios is likely overoptimistic.

As shown above, limited soil C accumulation (compared to vegetation C) in response to afforestation as simulated by some DGVMs seems more realistic than the rapid soil C uptake in the LUMs. However, historic agriculture has likely resulted in substantial net soil C emissions (Sanderman *et al.*, 2017, Smith *et al.*, 2016b), so large losses in response to afforestation as simulated by ORCHIDEE are also unlikely, especially for the MAgPIE ADAFF scenario (where croplands are preferentially afforested). Besides differences in simulated changes in NPP, the amount of C removed from agricultural land

likely also plays an important role. The recovery of soil C following agricultural cessation is analysed in Section 3 with a different version of LPJ-GUESS (croplands are represented by tilled, fertilised, and harvested grassland rather than specific CFTs) and shows reasonable agreement with observations (see Section 3.2.1). ORCHIDEE and JULES represent fewer management processes and therefore may underestimate soil C uptake potential in ADAFF (but also losses in BECCS); the incorporation of harvest (not included in ORCHIDEE pastures) and the representation of crops by specific CFTs (including tillage), instead of grasses, substantially increases soil C depletions on agricultural land in LPJ-GUESS (Pugh *et al.*, 2015). However, there are also observations suggesting that moderately intensive grazing might actually increase soil C stocks in C_4-dominated grasslands (McSherry and Ritchie, 2013, Navarrete *et al.*, 2016), a process the DGVMs likely do not capture well.

The LUMs did not include deforestation emissions ("carbon debt", Fargione *et al.*, 2008) in their BECCS CDR target. This is a common procedure in BECCS scenarios (or at least LUC emissions are often not seperated from fossil fuel emissions, e.g. Smith *et al.*, 2016a). For two bioenergy scenarios (600 and 800 Mha production area made available via either deforestation or agricultural abandonment, RCP2.6 climate) comparable in terms of production area and climate changes to our scenarios, a modelling study by Wiltshire and Davies-Barnard (2015) estimated vegetation C losses of 70 and 0 GtC and, using average depletions from Guo and Gifford (2002), soil C losses of 20 and 60 GtC. In our simulations, vegetation and soil emissions are relatively small, but our study still confirms that these emissions should not be neglected when considering bioenergy as an option to achieve negative emissions.

Cumulative CCS in BECCS differs substantially across models, ranging between 37 GtC and 130 GtC in the DGVMs, and reaching 128 GtC in both LUMs. By comparison, Wiltshire and Davies-Barnard (2015) found 75 and 200 GtC for the two comparable scenarios, which is similar to the 100-230 GtC range reported by Smith *et al.* (2016a) for IAM scenarios consistent with the 2°C target. Recently, Boysen *et al.* (2017a) estimated land availability for bioenergy production in LPJmL. They found that for substantial reductions in yield gaps and a global population of 6.5 billion people in year 2020, more than 2000 Mha of agricultural land could be abandoned for biomass plantations. In this extreme case, C removal from these plantations could deliver up to 350 GtC between 2020 and 2100. However, much less land would be available for more realistic assumptions about closing yield gaps and population growth, and potentially more if plantations would replace natural ecosystems. In our study, bioenergy area was prescribed by the LUMs and differences in CCS across models originate from simulated bioenergy crop yields. The LUMs and LPJmL represent these crops as dedicated bioenergy crops, mimicking characteristics of perennial energy crops like switchgrass or Miscanthus. Bioenergy yields in LPJmL have recently been evaluated against observations and showed reasonable results but were hindered by limited experimental data in the tropics (Heck *et al.*, 2016). The other DGVMs grew bioenergy crops as maize (LPJ-GUESS), productive crop grass (ORCHIDEE), or natural grass

(JULES). JULES and ORCHIDEE also did not increase the harvest index for bioenergy crops relative to food crops. Additionally, the LUMs assumed technological yield increases and closing yield gaps over time, resulting in higher average yields than in most DGVMs. While research of dedicated bioenergy crops is just in its infancy and thus on the one hand promises high potential, there is also evidence that yield increases observed over the last decades for cereals have recently slowed down (Alexandratos and Bruinsma, 2012). In fact, much of the historic yield increase was achieved via increasing the harvest index and fertiliser application, processes that are unlikely to substantially affect bioenergy yields (Searle and Malins, 2014). It also remains to be seen what bioenergy yield will be attainable in more marginal lands compared to sites where these crops are typically grown today (Searle and Malins, 2014). Consequently, what bioenergy yields we can expect in the future is controversial, with the optimistic assumptions made in IAMs/LUMs being plausible, but towards the upper bound of uncertainty (Creutzig, 2016).

4.2.2 Conclusions from Section 4

Based on results from four DGVMs driven by LU patterns from two LUMs we conclude that forest maintenance and expansion, as well as large-scale bioenergy production combined with CCS, offer the potential to remove substantial amounts of C from the atmosphere and thus can help to mitigate climate change. However, the size of the removal is highly uncertain, and may be much less than previously assumed in IAM/LUM scenarios consistent with the 2°C target (Boysen *et al.*, 2017b, Rogelj *et al.*, 2015, Smith *et al.*, 2016a, Tavoni and Socolow, 2013, Wiltshire and Davies-Barnard, 2015); the C uptake simulated by the LUMs is only achieved in one out of 24 combinations of mitigation LUC scenarios and DGVMs. The main reasons for the typically lower C uptake in the DGVMs as initially implemented in the LUMs are slower soil C accumulation (or even losses) following afforestation, different assumptions on potential/maximum vegetation C stocks, lower growth rates of forests, and lower bioenergy crop yields. Clearly the per-area C uptake (and thus the land demand) in land-based mitigation scenarios depends on assumptions made about vegetation and soil processes in the IAMs/LUMs. An improved implementation of land-based CDR options in both kinds of models, LUMs and DGVMs, as well as a deeper interaction between both is necessary to draw more robust conclusions about the potential contribution of land management to climate stabilisation. While the LUMs should emphasise the large uncertainty in assumed yields from bioenergy plantations, the DGVMs need to improve the parameterisations of managed herbaceous vegetation, particularly bioenergy crops (and also woody bioenergy), as well as regrowth of managed forests for afforestation. Field observations should focus on studying bioenergy crop yields under commercial production conditions. Additionally, the LUMs and some DGVMs need to reconsider their assumptions about soil C sequestration rates following afforestation. More detailed information about grazing intensities on grasslands, and a clear differentiation between natural grasslands and intensively managed pastures in observa-

tional studies might also help to reduce the uncertainty in soil C changes following LUC (Navarrete *et al.*, 2016).

In this section we only address the uncertainty in land-based mitigation arising from potential C uptake for a prescribed, realistically available area. However, the establishment of negative emissions from land management could also be hindered by unacceptable social or ecological side effects (Kartha and Dooley, 2016, Smith *et al.*, 2016a), biophysical and biogeochemical climate impacts beyond C (Boysen *et al.*, 2017a, Smith *et al.*, 2016a), irreversible effects of overshooting CO_2 concentrations (Kartha and Dooley, 2016, Tokarska and Zickfeld, 2015), or simply because CCS turns out to be technologically infeasible at commercial scale. There is also strong evidence that the time scales for shifts in farming systems to be realised may be of the order of several decades, substantially delaying the onset of negative emissions from BECCS (Alexander *et al.*, 2013, Brown *et al.*, submitted). Combining these unknowns and caveats with the large uncertainty in C uptake potential identified in this section suggests that relying on negative emissions to mitigate climate change is a very high-risk strategy, and reducing GHG emissions is a far safer and more reliable option. Ecological impacts from land-based mitigation are analysed in the following section.

5 Global consequences of afforestation and bioenergy cultivation on ecosystem service indicators

In this section, we use LPJ-GUESS simulations forced by mitigation LUC scenarios from the two LUMs (for information about the LUC scenarios and their implementation into LPJ-GUESS see Section 2.3) to study the impacts of land-based mitigation (bioenergy cultivation combined with C capture and storage; avoided deforestation and afforestation) on a range of associated ecosystem functions within a consistent modelling framework: C storage, surface albedo, evapotranspiration, water runoff, crop production, N loss, and BVOC emissions (see also Section 2.4).

In the following, the expressions "$LPJG_{IMAGE}$" and "$LPJG_{MAgPIE}$" refer to results from LPJ-GUESS simulations driven by LU patterns from the IMAGE and MAgPIE models, plus climate, CO_2, and N deposition following RCP2.6. At some points we refer to output directly taken from the IMAGE and MAgPIE scenarios, in which case this is explicitly stated ("in the original results/directly from the LUMs /the LUMs report").

5.1 Results

5.1.1 Carbon storage

Total global C pools simulated with LPJ-GUESS are generally lower for $LPJG_{IMAGE}$ than for $LPJG_{MAgPIE}$ for all scenarios (Table 5.1, Fig. 5.1a). This difference is mainly a result of the representation of degraded forests as grasslands in IMAGE-LU patterns (see Section 2.3.1 and Table 2.2), while MAgPIE does not include degraded forests. Moreover, some temperate croplands that are specified in the MAgPIE-LU patterns to grow fodder are represented in LPJ-GUESS by rain-fed or irrigated, harvested grass. This crop type increases soil C relative to cereal crops because the larger below-ground/above-ground biomass ratio results in less C being removed during harvest and thus more C input to the soil. C sequestration is calculated by LPJ-GUESS for both BASE simulations within the 21st century, resulting in total C pools of 1995 ($LPJG_{IMAGE}$) and 2047 ($LPJG_{MAgPIE}$) GtC by 2090-2099 (Table 5.1). The combined effects of LU, changing climate, N deposition, and atmospheric CO_2 levels thus enhance total C pools by 1.7 and 3.2% (33 and 64 Gt) between the beginning and the end of the century (Fig. 5.2a).

As expected from the overall scenario objective, total, vegetation, and soil C pools are higher in the ADAFF simulations relative to the respective BASE at the end of the century (Table 5.1, Fig. 5.1a-c). The additional C uptake for ADAFF is larger for $LPJG_{IMAGE}$ (3.6% or 72 GtC in year 2090-2099, 76 GtC in year 2099) than for $LPJG_{MAgPIE}$ (2.4% or 49 GtC in year 2090-2099, 55 GtC in year 2099, Fig. 5.2b). This reflects the larger afforestation area and earlier afforestation activities in IMAGE (Fig. 2.1,

Fig. 2.2b). The largest changes in total C are found in tropical regions, especially in Africa (+15 and +9%, Fig. 5.3b) and/or tropical forests (+13 and +8%, Fig. 5.4b), mostly due to increases in vegetation C.

Table 5.1: Global net total values ± standard deviations (over 10 years) of all analysed ecosystem functions as simulated by LPJ-GUESS for all scenarios and different time periods and for $LPJG_{IMAGE}$ (top) and $LPJG_{MAgPIE}$ (bottom). Total C is the sum of vegetation C, soil C, product C (wood removed during deforestation but not immediately oxidised), and cumulative CCS.

Ecosystem function	BASE		ADAFF	BECCS&ADAFF	BECCS
	2000-2009	2090-2099			
Vegetation C [GtC]	380 ± 1 393 ± 2	415 ± 2 459 ± 2	478 ± 4 496 ± 5	444 ± 3 476 ± 3	391± 2 450 ± 2
Soil and litter C [GtC]	1575 ± 1 1585 ± 1	1578 ± 1 1587 ± 1	1588 ± 1 1599 ± 2	1580 ± 1 1592 ± 2	1567 ± 1 1583 ± 1
Product C [GtC]	5.7 ± 0.4 4.6 ± 0.2	1.5 ± 0.1 0.3 ± 0.0	0.4 ± 0.0 0.4 ± 0.0	1.0 ± 0.1 0.3 ± 0.0	2.4 ± 0.2 0.6 ± 0.1
Cumulative CCS [GtC]	- -	- -	- -	52.1 ± 3.4 34.7 ± 2.5	100.0 ± 6.6 73.5 ± 5.6
Total C [GtC]	1961 ± 2 1983 ± 2	1995 ± 3 2047 ± 3	2067 ± 5 2096 ± 7	2077 ± 7 2103 ± 7	2060 ± 7 2108 ± 8
January albedo	0.250 ± 0.004 0.249 ± 0.004	0.240 ± 0.002 0.240 ± 0.002	0.237 ± 0.002 0.238 ± 0.002	0.238 ± 0.002 0.240 ± 0.002	0.241 ± 0.002 0.240 ± 0.002
July albedo	0.182 ± 0.001 0.182 ± 0.001	0.179 ± 0.001 0.179 ± 0.001	0.177 ± 0.001 0.177 ± 0.001	0.178 ± 0.001 0.178 ± 0.001	0.180 ± 0.001 0.179 ± 0.001
Evapotranspiration [1000 km^3 yr^{-1} [a]]	58.6 ± 0.7 58.9 ± 0.7	57.9 ± 1.2 58.8 ± 1.2	59.1 ± 1.2 59.5 ± 1.2	58.6 ± 1.2 59.3 ± 1.2	57.7 ± 1.2 58.9 ± 1.2
Annual runoff [1000 km^3 yr^{-1}]	52.5 ± 3.1 52.2 ± 3.1	55.1 ± 2.8 54.3 ± 2.8	53.9 ± 2.8 53.7 ± 2.8	54.4 ± 2.8 53.9 ± 2.8	55.3 ± 2.8 54.2 ± 2.8
Peak monthly runoff [1000 km^3 $month^{-1}$]	17.9 ± 1.0 17.9 ± 1.0	18.9 ± 1.2 18.8 ± 1.2	18.7 ± 1.2 18.6 ± 1.2	18.8 ± 1.2 18.7 ± 1.2	19.0 ± 1.2 18.8 ± 1.2
Crop production [Ecal]	28.9 ± 0.5 27.5 ± 0.9	35.9 ± 0.5 45.2 ± 0.4	34.7 ± 0.5 29.3 ± 2.0	34.0 ± 0.5 35.5 ± 0.7	33.5 ± 0.5 40.8 ± 0.5
N loss [TgN yr^{-1}]	60.3 ± 7.1 73.3 ± 6.8	109.7± 13.2 119.0 ± 8.0	102.3 ± 12.5 103.2 ± 8.4	103.6 ± 12.3 108.1 ± 7.9	98.4 ± 11.5 110.0 ± 7.0
Isoprene emissions [TgC yr^{-1}]	477 ± 8 503 ± 9	419 ± 9 495 ± 10	529 ± 11 578 ± 13	469 ± 10 532 ± 11	382 ± 8 483 ± 10
Monoterpene emissions [TgC yr^{-1}]	40.7 ± 0.6 41.9 ± 0.7	38.9 ± 0.9 40.5 ± 0.9	40.2 ± 1.0 41.6 ± 1.0	39.4 ± 0.9 40.9 ± 0.9	38.2 ± 0.9 40.4 ± 0.9

[a] 1000 km^3 are equal to 1 Eg of water.

The BECCS scenario focusing on bioenergy crops and CCS as a climate change mitigation strategy removes slightly less C from the atmosphere than ADAFF for $LPJG_{IMAGE}$ but removes more C for $LPJG_{MAgPIE}$ (Table 5.1, Fig. 5.2c). Interestingly, $LPJG_{IMAGE}$ ADAFF accumulates more C than $LPJG_{IMAGE}$ BECCS within the first half of the century, while BECCS catches up during the second half of the century (Fig. 5.1a). This acceleration of the BECCS sink is related to a steady increase in bioenergy area throughout the century. The additional total C storage achieved by the period 2090-

2099 (compared to BASE 2090-2099) is 66 GtC (74 GtC in year 2099) for $LPJG_{IMAGE}$ and 61 GtC (69 GtC in year 2099) for $LPJG_{MAgPIE}$. Within these totals, cumulative C storage via CCS (harvested C from bioenergy crops multiplied by a capture efficiency of 80%) is 100 and 74 GtC by the end of the century (Table 5.1), but total C uptake is less than cumulative CCS as LPJ-GUESS simulates a loss of vegetation and soil C from expanded agricultural land. C storage in the combined bioenergy-avoided deforestation and afforestation case (BECCS&ADAFF) mostly lies between the BECCS and the ADAFF case but for $LPJG_{IMAGE}$ exceeds both ADAFF and BECCS by the end of the century (Table 5.1, Fig. 5.1a, Fig. 5.2d, Fig. 5.5).

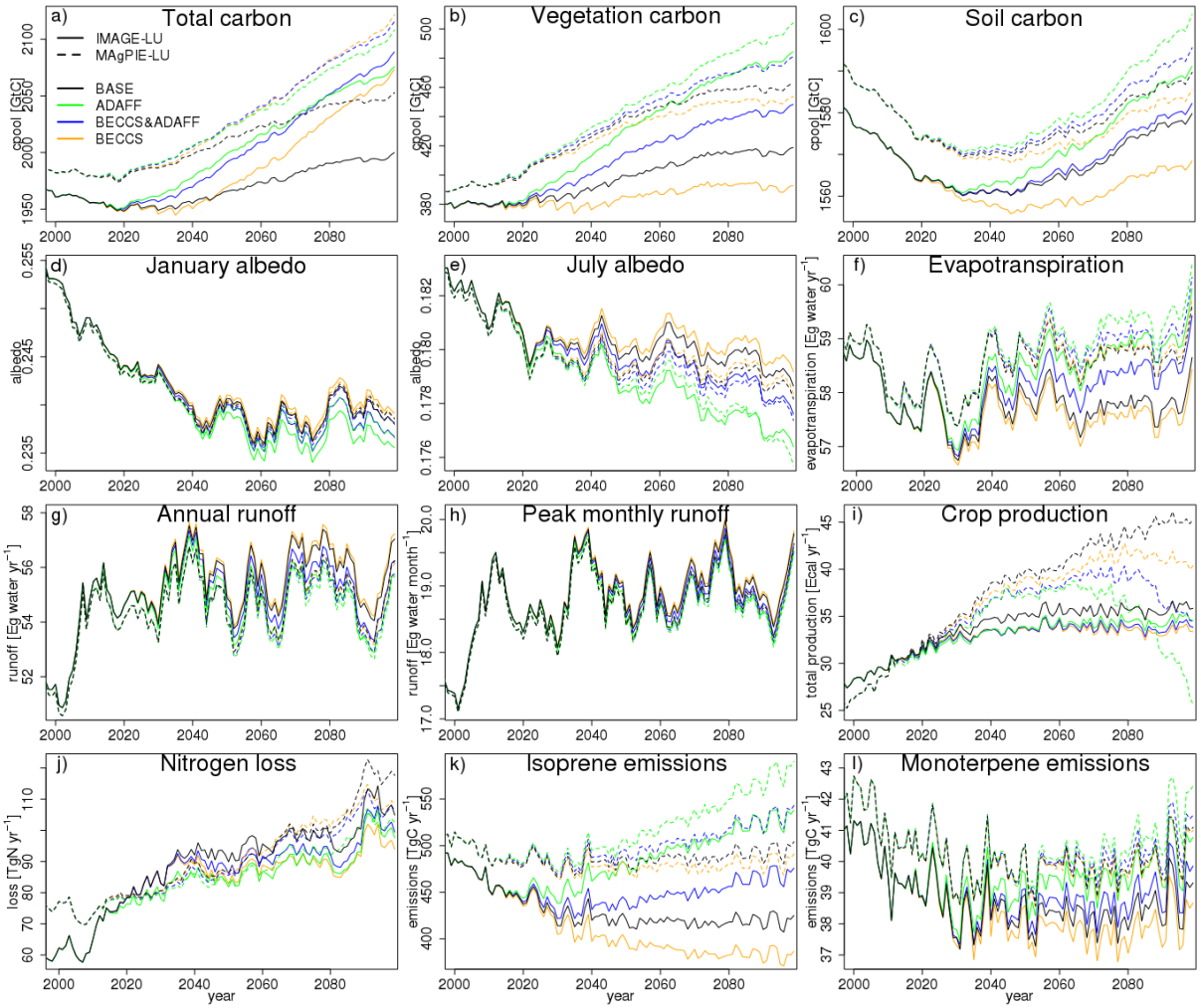

Figure 5.1: Time series (2000-2099) of ecosystem functions as simulated by LPJ-GUESS for all scenarios, area-weighted and summed/averaged over all grid-cells. a) total C pool (terrestrial C, including CCS for bioenergy scenarios), b) vegetation C pool, c) soil and litter C pool, d) January albedo (5-year running mean), e) July albedo (5-year running mean), f) evapotranspiration (5-year running mean), g) annual runoff (5-year running mean), h) peak monthly runoff (5-year running mean), i) crop production, j) N loss (5-year running mean), k) isoprene emissions, l) monoterpene emissions.

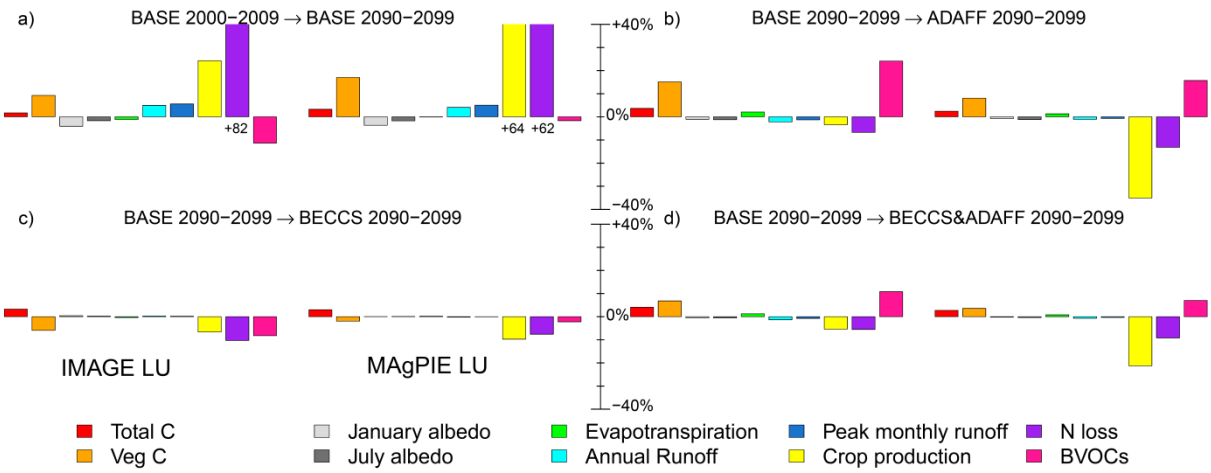

Figure 5.2: Global relative changes in analysed ecosystem functions simulated by LPJ-GUESS for different LU scenarios from IMAGE and MAgPIE. Changes are capped at ±40% for clarity reasons, and values exceeding 40% are written below the bar. a) changes in the BASE simulation from 2000-2009 to 2090-2099. b) changes from BASE to ADAFF by the 2090-2099 period. c) same as b) but from BASE to BECCS. d) same as b) but from BASE to BECCS&ADAFF.

5.1.2 Albedo

Globally averaged January albedo under present-day conditions is significantly higher (~0.25) than July albedo (~0.18) due to the extensive northern hemisphere snow cover in January. Both values decrease throughout the 21st century in the BASE simulations, but more so for January (-4.1 and -3.7% for $LPJG_{IMAGE}$ and $LPJG_{MAgPIE}$, respectively) than for July (-1.7 and -1.8%) as a result of northward vegetation shifts and reductions in snow cover (Table 5.1, Fig. 5.1d-e, Fig. 5.2a). Regionally, for both months and both LUMs, the greatest reductions occur in high latitudes (Fig. 5.3a).

An increase in forested area as in the ADAFF scenario results in further albedo reductions that are - at least for July albedo - comparable in magnitude to the changes in BASE throughout the century (Table 5.1, Fig. 5.2b). Only small increases compared to BASE occur in the BECCS simulations (Fig. 5.2c) as the land demand for bioenergy crop cultivation is relatively small. BECCS&ADAFF results in a decrease in January and July albedo for both LUMs.

5.1.3 Evapotranspiration

Global evapotranspiration in the BASE simulations decreases much more for $LPJG_{IMAGE}$ (-1.2%) than for $LPJG_{MAgPIE}$ (-0.1%; Table 5.1, Fig. 5.1f, Fig 5.2a) due to different deforestation rates. There is large spatial variability with evapotranspiration decreasing in some regions but increasing in others (Fig. 5.3a), mainly driven by shifting rainfall patterns (not shown).

As expected from the generally high evapotranspiration rates of forests, end-of-century evapotranspiration in ADAFF is 2.1 and 1.3% higher than in BASE for $LPJG_{IMAGE}$ and $LPJG_{MAgPIE}$, respectively (Fig. 5.2b), with the largest increase occurring in Africa (Fig. 5.3b). BECCS results in a change of -0.4 and +0.2% ($LPJG_{IMAGE}$ and $LPJG_{MAgPIE}$), and BECCS&ADAFF in an increase of 1.3 and 0.8%.

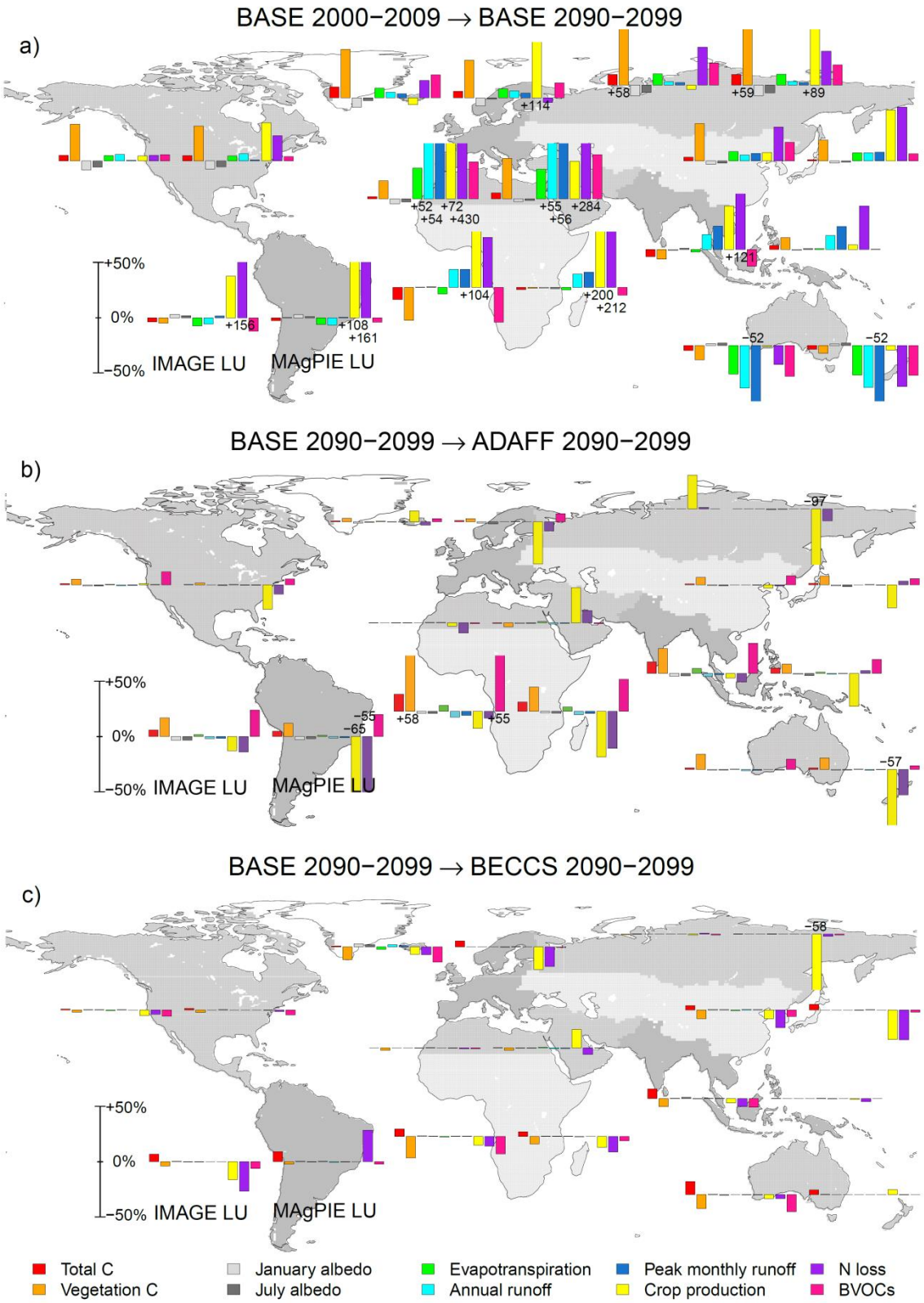

Figure 5.3: Regional relative changes in analysed ecosystem functions as simulated by LPJ-GUESS for IMAGE-LU (left) and MAgPIE-LU (right). Changes are capped at ±50% for clarity reasons, values exceeding ±50% are written upon or below the bar. Regions are aggregated Global Fire Emissions Database (GFED) regions (Giglio *et al.*, 2010) and are North America, South America, Europe, Middle East, Africa, North Asia, Central Asia, South Asia, and Oceania. a) changes in the BASE simulation from 2000-2009 to 2090-2099. b) changes from BASE to ADAFF by the 2090-2099 period. c) same as b) but from BASE to BECCS.

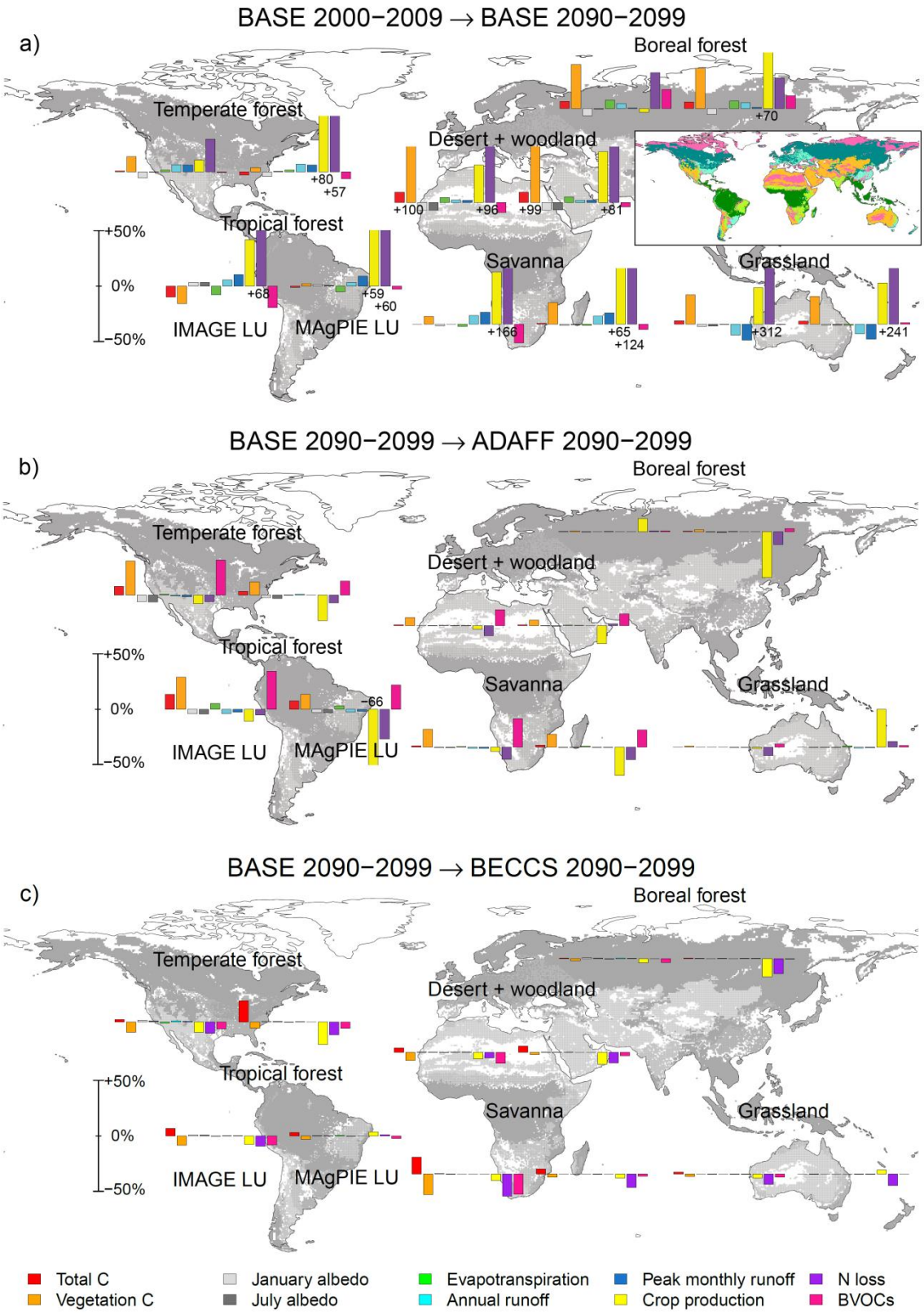

Figure 5.4: Same as Fig. 5.3 but changes shown for different biomes rather than GFED regions. Biomes are aggregated from the biomes used in Smith *et al.* (2014): tundra+desert+woodland+ shrubland; dry+moist savanna; dry and tall grassland; tropical forest; temperate forest; boreal+temperate/boreal mixed forest. The LAI map used for the biome classification was taken from the $LPJG_{MAgPIE}$ BASE simulation and the 2000-2009 period. The coloured snapshot in a) shows the same biomes as the grey-coloured biomes in the larger maps to facilitate differentiation.

5.1.4 Runoff

In the BASE simulations, global annual runoff increases by 4.9 and 4.1% by the end of the century for $LPJG_{IMAGE}$ and $LPJG_{MAgPIE}$, respectively, with a slightly larger increase of 5.2 and 5.0% in peak monthly runoff (Table 5.1, Fig. 5.1g-h, Fig. 5.2a). This increase is mainly driven by precipitation changes, but forest loss and increased water use efficiency simulated under elevated CO_2 levels also play a role. Similar to evapotranspiration, spatial patterns are heterogeneous, with generally larger changes in annual runoff than in peak monthly runoff in high latitudes and reverse patterns in parts of the (sub-)tropics (Fig. 5.3a, Fig. 5.4a).

Changes in runoff in the mitigation simulations are opposite to evapotranspiration changes (Fig. 5.2b-d, Fig. 5.3b-c, Fig. 5.4b-c), and the effects of land-based mitigation on annual runoff are often larger than on peak monthly runoff. ADAFF reduces annual runoff by 2.2 and 1.1% ($LPJG_{IMAGE}$ and $LPJG_{MAgPIE}$) and peak monthly runoff by 1.3 and 0.7% compared to BASE, while BECCS increases annual runoff by 0.3 and 0.2% and peak monthly runoff by 0.2 and 0.0%.

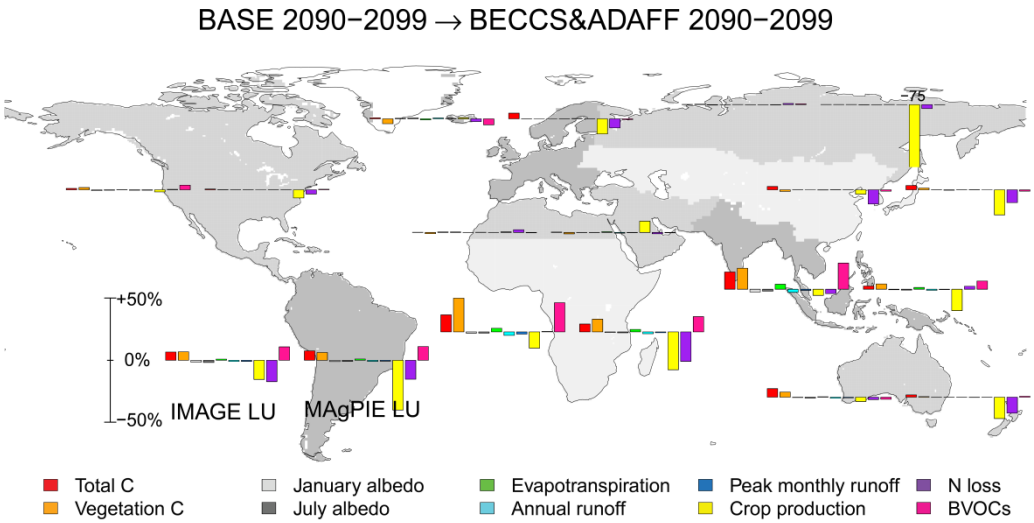

Figure 5.5: Regional relative changes in analysed ecosystem functions as simulated by LPJ-GUESS for IMAGE-LU (left) and MAgPIE-LU (right) from BASE to BECCS&ADAFF by the 2090-2099 period. Changes are capped at ±50% for clarity reasons, values exceeding ±50% are written upon the bar. The decrease in crop production might occur if increases in crop yields cannot be realised. Regions are aggregated GFED regions (Giglio *et al.*, 2010).

5.1.5 Crop production

Globally, total crop production simulated by LPJ-GUESS averages ~29 and 27 exa-calories (Ecal) yr^{-1} over the years 2000-2009 and increases by 24 and 64% to 36 and 45 Ecal yr^{-1} by the end of the century for the $LPJG_{IMAGE}$ and $LPJG_{MAgPIE}$ BASE simulations, respectively (Table 5.1, Fig. 5.1i). For comparison, the increase is 78 and 96% in the original IMAGE and MAgPIE results, respectively. The large differences in crop production increase between $LPJG_{IMAGE}$ and $LPJG_{MAgPIE}$ can be explained by variations in management and crop types (e.g. whether the LUMs assume C_3 or C_4 crops to be grown in certain regions), and the area and location of managed land, which differs considerably by the end

of the century, especially in Africa (not shown). Sensitivity simulations in which N fertiliser rates, cropland area, atmospheric CO_2 mixing ratio, or the dynamic PHU calculation (i.e. adaption to climate change via selecting suitable crop varieties; see Section 2.1) were fixed at year 2009 levels indicate that around 62 and 39% ($LPJG_{IMAGE}$ and $LPJG_{MAgPIE}$, respectively) of the crop production increase in the BASE simulations can be attributed to increases in N fertiliser rates, 22 and 74% to cropland expansion, 26 and 10% to increased atmospheric CO_2 levels, and 9 and 4% to dynamic PHU calculation (Fig. 5.6a). The numbers do not add up to 100% due to non-linear effects, interdependencies between variables (crop area/fertilisation), and additional influences we did not analyse (e.g. climate, N deposition, crop types, and irrigation).

Crop production calculated with LPJ-GUESS is reduced in all mitigation simulations compared to BASE, in contrast to a set requirement in the LUMs to retain annual production at similar levels to BASE: in the LUMs this is achieved through further technology increases (for example through improved management, inputs, pest control, and better crop varieties) compared to BASE. The decline simulated in LPJ-GUESS, which is larger for $LPJG_{MAgPIE}$ than for $LPJG_{IMAGE}$, especially for ADAFF ($LPJG_{IMAGE}$ -3% for the 2090-2099 period compared to 2090-2099 BASE; $LPJG_{MAgPIE}$ -35%), occurs because LPJ-GUESS captures only yield increases achieved through higher N input, which only covers a part of the additional technological yield increase assumed by the LUMs for the mitigation scenarios (and which therefore allows for shrinking production area; see Table 2.2).

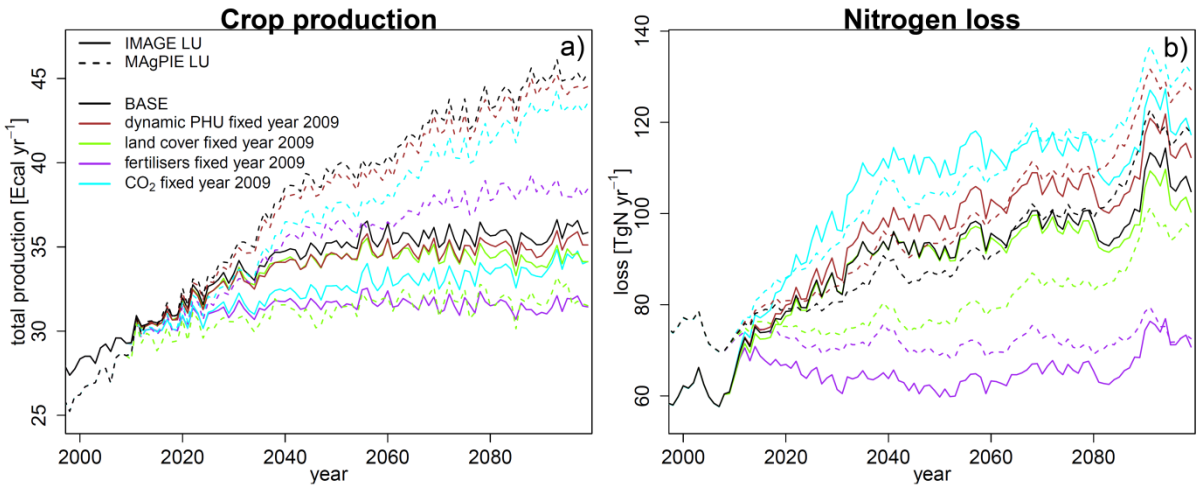

Figure 5.6: Impacts of fixing dynamic PHU calculation (i.e. adaption to climate change via selecting suitable varieties), crop area, nitrogen fertilisers, and atmospheric CO_2 mixing ratio at year 2009 levels on LPJ-GUESS crop production (a) and nitrogen loss (b), for the BASE simulations.

5.1.6 Nitrogen loss

Global N loss in the BASE simulations increases strongly over the 21st century by 82% for $LPJG_{IMAGE}$ and 62% for $LPJG_{MAgPIE}$ (Fig. 5.1j, Fig. 5.2a). Most of the increase is caused by fertilisation but increasing N deposition contributes as well (+19% over the century). N loss is higher for $LPJG_{MAgPIE}$

than for $LPJG_{IMAGE}$ at the beginning and end of the 21st century, but higher for $LPJG_{IMAGE}$ around mid-century (Table 5.1, Fig. 5.1j). As total fertiliser application is higher for $LPJG_{MAgPIE}$ throughout the entire century these differences can be explained by spatial heterogeneity (e.g. in India, where fertilisation has a large impact on N loss, fertiliser rates are generally higher for $LPJG_{IMAGE}$ than for $LPJG_{MAgPIE}$). Increases in N losses correspond roughly to increases in N application, and to crop production increases in the original LUMs. This indicates that crops in LPJ-GUESS approach N saturation, and cannot use the additional N for higher yields, and thus, that N application rates, while consistent with LUM yield levels, are too high for LPJ-GUESS yields. Sensitivity simulations indicate that most of the N loss increase between 2000-2009 and 2090-2099 is induced by increased fertiliser application and cropland expansions, while increasing atmospheric CO_2 and the dynamic PHU calculation reduce N loss (Fig. 5.6b).

N loss in ADAFF decreases by 6.7% for $LPJG_{IMAGE}$ and 13.2% for $LPJG_{MAgPIE}$ compared to BASE 2090-2099 (Fig. 5.2b), but with large variability across regions (Fig. 5.3b, Fig. 5.4b). The decrease can be attributed to lower global fertiliser amounts in ADAFF than in BASE for both LUMs, as forests are not fertilised. In the BECCS simulations the decrease is larger for $LPJG_{IMAGE}$ (-10.3%) than for $LPJG_{MAgPIE}$ (-7.6%), including substantial regional variations, especially in South America (Fig. 5.3c). The fertilisation of bioenergy crops (for which low fertiliser rates are assumed in the LUMs) adds N to the system. However, crop N uptake and subsequent removal during harvest are also enhanced, resulting in a net N removal in LPJ-GUESS (and thus less N available to leave the system via leaching or in gaseous form). N loss reductions in BECCS&ADAFF lie between ADAFF and BECCS for $LPJG_{MAgPIE}$ (-9.2%) but are smallest amongst all mitigation simulations for $LPJG_{IMAGE}$ (-5.5%).

5.1.7 Biogenic volatile organic compounds

Changes in BVOC emissions are dominated by isoprene emissions, which are, by weight, an order of magnitude higher than those of monoterpenes (Table 5.1, Fig. 5.1k-l). In the BASE simulations, total BVOC emissions from 2000-2009 to 2090-2099 decrease by 11% for $LPJG_{IMAGE}$ but only by 2% for $LPJG_{MAgPIE}$ (Fig. 5.2a). Spatially, BVOC emissions generally increase in high latitudes but decrease in the tropics (Fig. 5.3a), corresponding to northward forest shifts and deforestation or forest degradation concentrated in low latitudes (not shown). The tropics dominate the overall response due to much higher typical emission rates.

As expected from the generally high emission potential of woody vegetation (compared with herbaceous), BVOC emissions increase in the ADAFF simulations (by 24 and 16% for $LPJG_{IMAGE}$ and $LPJG_{MAgPIE}$, respectively). Following the spatial change in forest cover, the increase mainly occurs in the tropics (Fig. 5.3b). In the BECCS simulations, BVOC emissions decrease by 8% for $LPJG_{IMAGE}$ and by 2% for $LPJG_{MAgPIE}$ (Fig. 5.2c) due to the low emissions of grassy bioenergy crops (grown as

maize in LPJ-GUESS). BECCS&ADAFF results in 11 and 7% higher emissions for $LPJG_{IMAGE}$ and $LPJG_{MAgPIE}$, respectively (Fig. 5.2d).

5.2 Discussion and conclusions

5.2.1 Modelling uncertainties under present-day and future climate

The ES indicators analysed in this study are subject to uncertainties arising from knowledge gaps, simplified modelling assumptions, and the need to use parameterisations suited for global simulations. LPJ-GUESS has been extensively evaluated against present-day C fluxes and stocks, both for natural and agricultural systems, at site scale and against global estimates (e.g. Fleischer *et al.*, 2015, Piao *et al.*, 2013, Pugh *et al.*, 2015, Smith *et al.*, 2014). The use of forcing climate data from only one climate model can be a major source of uncertainty as shown by the large variability in future terrestrial C stocks introduced by different climate change realisations even for the same emissions pathway (Ahlstrom *et al.*, 2012). As we use the low-emission scenario RCP2.6 here, we expect this effect to be relatively small. The albedo calculation in this study was not used previously but patterns simulated by LPJ-GUESS under present-day conditions (Fig. 5.7) broadly agree with Fig. 3 in Boisier *et al.* (2013). Evapotranspiration and runoff in LPJ were evaluated by Gerten *et al.* (2004). Global total runoff calculated in this study for the 1961-1990 period is 26% higher than their results. Simulation biases against global estimates and observations from large river basins in the Gerten *et al.* study were mainly attributed to uncertainties in climate input data and to human activities such as LUC (which is now accounted for) and human water withdrawal. Spatial runoff patterns as simulated by the current LPJ-GUESS version (Fig. 5.8) seem to reveal some improvements compared to the biases reported in Gerten *et al.* (2004) in mid- and high latitudes, but the model still overestimates runoff in parts of the tropics. With respect to crop production, simulated crop yields in LPJ-GUESS are constrained by N and water limitation, but not by local management decisions, crop varieties or breeds, diseases, and weeds (Lindeskog *et al.*, 2013, Olin *et al.*, 2015b), and future improvement in plant breeding are ignored. While we accounted for the additional restrictions by scaling simulated present-day yields to observations, applying the unscaled LPJ-GUESS yield changes into the future might create substantial underestimation of future yields and crop production, as the only yield-augmenting factor for a given crop type in LPJ-GUESS is increased N input. Global N-leaching rates are highly uncertain but the annual rate simulated with LPJ-GUESS (if all N losses are assumed to be via leaching) is within the range of published studies (Olin *et al.*, 2015a). Future modelled N leaching may also be affected by ignoring improvements in plant breeds, as the current representation of crops may not be able to absorb the N input computed in the LUMs for improved varieties and management. For BVOCs, global datasets for evaluation are not available (Arneth *et al.*, 2007, Schurgers *et al.*, 2009). Spatial emission patterns are in good agreement with other simulations (Hantson *et al.*, 2017).

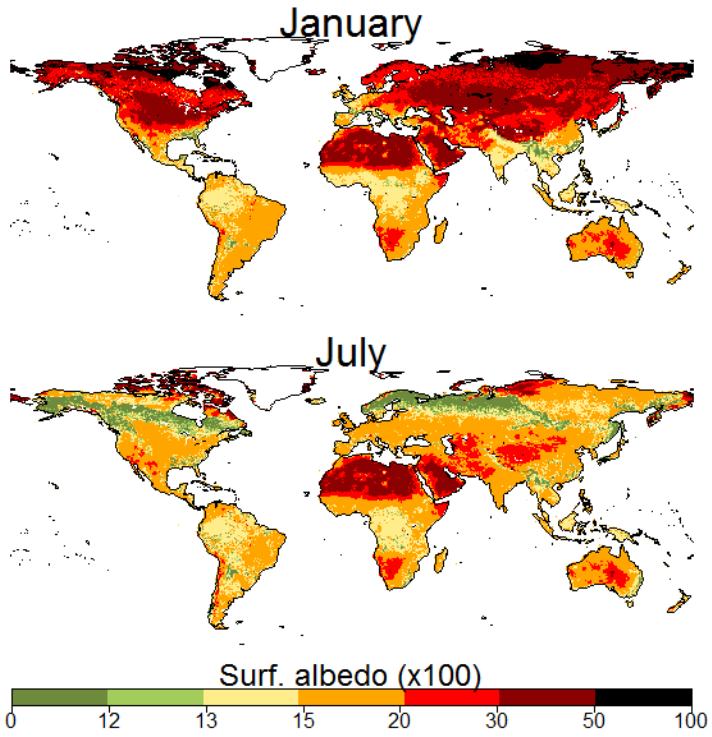

Figure 5.7: Maps of mean surface albedo in January (top) and July (bottom) in $LPJG_{IMAGE}$ BASE (2000-2011). The scale is the same as in Boisier *et al.* (2013).

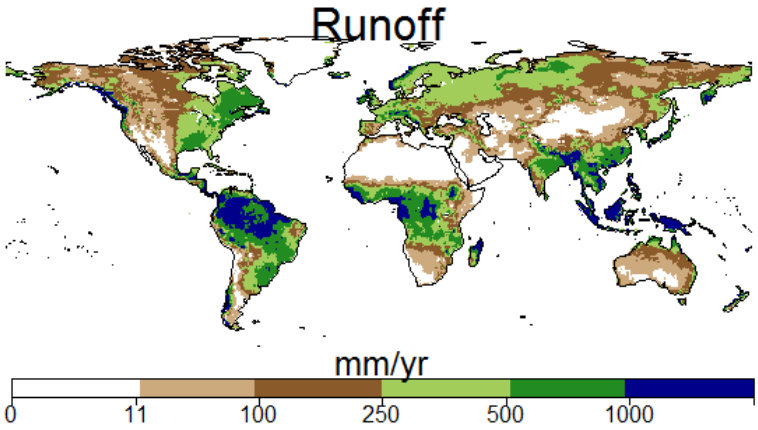

Figure 5.8: Map of total annual runoff in $LPJG_{IMAGE}$ BASE (1961-1990). The scale is the same as in Gerten *et al.* (2004).

While LPJ-GUESS has thus been evaluated as comprehensively as possible, a further next step for multi-process evaluation would be adopting a formalised benchmarking system that also allows to score model performance (Kelley *et al.*, 2013). Likewise, large uncertainties reside in the actual LUMs, which differ to a large degree in their estimates of main land-cover classes for the present day (Alexander *et al.*, 2017b, Prestele *et al.*, 2016), and for which evaluation against observations has been identified as a challenge (van Vliet *et al.*, 2016).

5.2.2 Climate regulation via biogeochemical and biophysical effects

Our $LPJG_{IMAGE}$ simulations are slightly more effective than the $LPJG_{MAgPIE}$ simulations in terms of simulated C uptake, but all simulations diverge from the CDR target initially implemented in the LUMs (see Section 5.2.7 and Section 4). Land-based mitigation might also impact the emissions of other GHGs (e.g. N_2O; see Table 2.5), but future fertiliser application rates and emissions from bioenergy crops are highly uncertain (Davidson and Kanter, 2014). While N_2O contributes to global warming, the net effect of reactive N might be a cooling when accounting for short-lived pollutants and interactions with the C cycle (Erisman *et al.*, 2011). In our LPJ-GUESS simulations, reductions in N losses suggest a decrease in gaseous N emissions for both ADAFF and BECCS. However, no quantifications are possible as LPJ-GUESS does not yet differentiate between different forms of N losses.

Climate effects of well-mixed GHG are global, whereas biophysical effects are primarily felt on the local scale (Alkama and Cescatti, 2016). Surface albedo in regions with seasonal snow cover is expected to decrease significantly for afforestation scenarios (Bala *et al.*, 2007, Bathiany *et al.*, 2010, Betts, 2000, Davies-Barnard *et al.*, 2014), thereby opposing the biogeochemical cooling effect. Effects of enhanced forest cover are less pronounced in lower latitudes (Li *et al.*, 2015) and for BECCS scenarios (Smith *et al.*, 2016). A modelling study by Hallgren *et al.* (2013) found that while albedo effects and C emissions from deforestation for biofuel production might balance on the global scale, biophysical effects can be large locally. In our BECCS simulations, albedo changes are relatively small. However, we find noticeable albedo reductions in ADAFF despite the fact that for both LUMs afforestation was concentrated in snow-free regions, where satellites rarely observe albedo differences between forests and open land exceeding 0.05 (Li *et al.*, 2015).

High evapotranspiration rates, often observed in forests, cool the local surface. In tropical regions, this cooling effect exceeds the warming effect from lower albedo (Alkama and Cescatti, 2016, Li *et al.*, 2015). Current anthropogenic land-cover changes have been estimated to reduce terrestrial evapotranspiration by ~5% (Sterling *et al.*, 2013). In our simulations, impacts of land-based mitigation on global evapotranspiration range from -0.4 to +2.1% ($LPJG_{IMAGE}$ BECCS and $LPJG_{IMAGE}$ ADAFF, respectively). On the regional scale this can translate to absolute changes of more than 100 mm yr^{-1} in some tropical areas (e.g. central Africa). While these changes seem relatively small compared to the mean differences between forests and non-forests reported by Li *et al.* (2015) (141 mm yr^{-1} 20°N-50°N, 238 mm yr^{-1} 20°S-50°S, 428 mm yr^{-1} 20°S-20°N), our results still suggest that reducing emissions from deforestation and forest degradation (REDD) activities would not only help mitigate global climate change via avoided C losses but could provide additional local cooling, serving as a "payback" for tropical countries. The simulated evaporative water loss due to ADAFF at the end of the century (~1200 km^3 yr^{-1} for $LPJG_{IMAGE}$ and 750 km^3 yr^{-1} for $LPJG_{MAgPIE}$ for a C sequestration rate of ~0.8 and 1.4 GtC yr^{-1}, respectively) is higher than estimated by Smith *et al.* (2016a) (370 km^3 yr^{-1} for a C sequestration rate of ~1.1 GtC yr^{-1}). Furthermore, Smith *et al.* (2016a) assumed that dedicated rain-fed

bioenergy crops consume more water than the replaced vegetation (with additional water required for CCS), while in our simulations bioenergy crops had little impact on evapotranspiration as they were represented as maize. LU-driven changes in evapotranspiration rates can also modify the amount of atmospheric water vapour and cloud cover, with consequences for direct radiative forcing, planetary albedo, and precipitation (e.g. Sampaio *et al.*, 2007; see also Table 2.5); however, such interactions cannot be captured by our model setup.

BVOCs influence climate via their influence on tropospheric O_3, CH_4, and secondary organic aerosol formation (Arneth *et al.*, 2010, Scott *et al.*, 2014), which depend strongly on local conditions such as levels of nitrogen oxides (NO_X) or background aerosol (Carslaw *et al.*, 2010, Rosenkranz *et al.*, 2015). BVOC emissions also impact climate directly by reducing terrestrial C stocks but the magnitude is small (<0.5%) compared to total GPP. While enhanced leaf-level BVOC emissions are driven by warmer temperatures, uncertainties arise from additional CO_2 effects (which suppress leaf emissions). On the canopy scale, isoprene emissions generally decrease for deforestation scenarios (Hantson *et al.*, 2017) but increase for woody biofuel plantations, which tend to use high-emission tree species (Rosenkranz *et al.*, 2015). In our simulations, we find increases in BVOC emissions for ADAFF but not so for BECCS as bioenergy crops were mostly grown as low-emission maize. The high spatial and temporal variability of the BVOC emissions, complications of atmospheric transport, and gaps in our knowledge of the reactions involved make it difficult to judge whether an increase in BVOC emissions results in a warming or cooling. The global effect (assuming present-day air pollution in 1850 and excluding aerosol-cloud interactions) of historic (1850s-2000s) reductions in BVOC emissions (20-25%) due to deforestation has been estimated to be a cooling of -0.11 ± 0.17 W m^{-2} (Unger, 2014). Accordingly, the substantial increase in BVOC emissions in our ADAFF simulations (16 and 24%) might induce a warming of similar magnitude.

5.2.3 Water availability

Forests generally reduce local river flow compared to grass- and croplands. Based on 26 catchment datasets including 504 observations worldwide, Farley *et al.* (2005) reported an average decrease of 44 and 31% in annual stream flow caused by woody plantations replacing grasslands and shrublands, respectively, with large variability across different plantation ages. Simulations by Sterling *et al.* (2013) suggest that historic land-cover changes were responsible for a 7% increase in total runoff. The reduction in global annual runoff due to ADAFF (1200 and 600 km^3 yr^{-1} compared to BASE 2090-2099 for IMAGE and MAgPIE, respectively) corresponds to around 16-32% of human runoff withdrawal (Oki and Kanae, 2006), which could be seen as a potential risk to freshwater supply. Regional changes range from -5.2 to +0.4% across all scenarios, but in many cases impacts on irrigation (the largest consumer of freshwater) potential in fact might be small: modelling work suggests that renewable water supply will exceed the irrigation demand in most regions by the end of the century for

RCP8.5 (Elliott *et al.*, 2014). However, Elliott *et al.* (2014) also found that regions with the largest potential for yield increases from increased irrigation are also the regions most likely to suffer from water limitations. Patterns will be different in an RCP2.6 world as CO_2 fertilisation significantly reduced global irrigation demand (8-15% on presently irrigated area) in the Elliott *et al.* crop models and climate impacts are expected to be less severe in RCP2.6.

In uncoupled simulations, such as those carried out here, atmospheric feedbacks related to higher evapotranspiration cannot be captured. At regional or continental scale, there is evidence that afforestation might actually increase runoff as the larger evapotranspiration rates enhance precipitation (Ellison *et al.*, 2012). However, based on regional climate modelling, Jackson *et al.* (2005) concluded that atmospheric feedbacks were not likely to offset water losses in temperate regions, where the additional atmospheric moisture cannot be lifted high enough to form clouds.

Changing runoff affects water supply but can also contribute to changes in flood risks. Bradshaw *et al.* (2007), using a multi-model approach and data from 56 developing countries, calculated a 4-28% increase in flood frequency and a 4-8% increase in flood duration for a hypothetical reduction of 10% natural forest cover, while van Dijk *et al.* (2009), for example, questioned forest potential to reduce large-scale flooding and argued that the frequency of reported floods can be mainly explained by population density. Ferreira and Ghimire (2012) extended the original Bradshaw sample to all countries (129) that reported at least one large flood between 1990 and 2009 and included socio-economic factors in their analyses. They did not find a statistically significant correlation between forest cover and reported floods. In our simulations, peak monthly runoff is generally reduced for ADAFF. However, given maximum regional changes of -3.6% (Africa, $LPJG_{IMAGE}$ ADAFF) and presuming that floods are largely controlled by other factors than forest cover, we expect LU effects on flooding to be limited.

5.2.4 Food production

Increasing food production in a sustainable way to feed a growing population is a major challenge of the modern world (Tilman *et al.*, 2002). Population and income growth (in SSP2 population peaks in 2070 at 9.4 billion people, and per capita GDP continues to increase until 2100 (Dellink *et al.*, 2017, Samir and Lutz, 2017)) are projected to be accompanied by an increased need of total calories and shifts in diets (Popp *et al.*, 2017). For SSP2, economic modelling suggests that global food crop demand will increase by 50-97% between 2005 and 2050 (Valin *et al.*, 2014). In the present study, the corresponding increase reported directly from the LUMs is 38% for IMAGE and 52% for MAgPIE in 2050 (78 and 96% in year 2100). In our LPJ-GUESS BASE simulations we find crop production increases of 22 and 45% ($LPJG_{IMAGE}$ and $LPJG_{MAgPIE}$, respectively) by 2050 and 24 and 64% by the end of the century (corresponding to a per capita increase for MAgPIE but a decrease for IMAGE). However, the production increase is significantly reduced in the mitigation simulations, especially for

$LPJG_{MAgPIE}$ ADAFF due to production shifts and the abandonment of croplands for afforestation. Similar results have been reported by Reilly *et al.* (2012) who found that afforestation substantially increases prices for agricultural products, while the cultivation of biofuels has little impact on agricultural prices due to benefits of avoided environmental damage offsetting higher mitigation costs. Crop yields in LPJ-GUESS are a function of environmental conditions, fertilisers, irrigation, and adaption to climate change by selecting suitable varieties. In our BASE simulations, the combined effect is an average yield increase of 17 and 41% ($LPJG_{IMAGE}$ and $LPJG_{MAgPIE}$) between 2000-2009 and 2090-2099. In the LUMs, the mitigation scenarios are characterised by additional yield increases compared to BASE, triggered by increased land prices. This intensification is to some extent reflected in the fertiliser rates (derived from yields) provided by the LUMs. However, other management improvements and investments in research and development leading to higher-yielding varieties also impact future yield increases. Additional assumptions about yield increases driven by technological progress can thus not be captured by LPJ-GUESS. The simulated decline in productivity in response to shrinking cropland area in the mitigation scenarios suggests that, when adapting N fertilisation, irrigation, and cropland area and location from the LUMs, additional yield increases of up to 6.6 and 35% ($LPJG_{IMAGE}$ and $LPJG_{MAgPIE}$) would be required between the 2000s and the 2090s to produce the same amount of food crops as in the BASE scenario, equivalent to ~0.07 and 0.33% per year.

5.2.5 Water and air quality

Managed agricultural systems directly impact freshwater quality. Historically, approximately 20% of reactive N moved into aquatic ecosystems (Galloway *et al.*, 2004), causing drinking water pollution and eutrophication. As N loss in LPJ-GUESS is largely driven by fertilisation (Blanke *et al.*, 2017), the much higher future fertilisation rates compared to present-day (+78% for $LPJG_{IMAGE}$; +95% for $LPJG_{MAgPIE}$) lead to an increase in N loss of 82 and 62% in BASE. Such a large increase would have severe impacts on waterways and coastal zones, where current levels of N pollution are already having substantial effects (Camargo and Alonso, 2006). However, as discussed above, the N application rates are derived from crop yields in the LUMs, and can only be partially utilised by LPJ-GUESS due to its lower yield levels. Increasing crop yields by increased N inputs leads to a strong decline in nutrient use efficiency and declining returns on yields (Cassman *et al.*, 2002, Mueller *et al.*, 2017). In contrast to the BASE simulations, the mitigation simulations result in somewhat lower N losses because less fertiliser is applied (ADAFF) or because bioenergy harvest removes more N than is added via bioenergy crop fertilisation (BECCS). Simulated N losses in LPJ-GUESS are affected by different assumptions about N fertilisers and inconsistencies between the models: fertiliser rates in the LUMs were calculated to support the estimated crop yields (and hence the ensuing N demand). The resulting grid-cell averages available to LPJ-GUESS did not take into account differences in N application across crop types in a grid-cell (Mueller *et al.*, 2012). Additionally, IMAGE and MAgPIE simulate further

increases in crop productivity and N use efficiency and therefore nutrient recovery in harvested biomass, which may only be partly captured by LPJ-GUESS (see Section 5.2.4).

Although we do not explicitly simulate emissions of N gases, increased N losses suggest an excess of soil N, which increases the likelihood of gaseous reactive N emissions such as NO_X and ammonia (NH_3) pollution, contributing to particulate matter formation, visibility degradation, and atmospheric N deposition (Behera *et al.*, 2013). The chemical form and level of these emissions will strongly depend on soil water status (Liu *et al.*, 2007). Improvements in air quality, e.g. via reductions in tropospheric O_3, are not only relevant for human health but can also enhance plant productivity and crop yields (Wilkinson *et al.*, 2012). The response of O_3 to BVOC emissions changes depends on the local NO_X:BVOC ratio (Sillman, 1999). An increase in BVOC emissions slightly suppresses O_3 concentration in regions of low NO_X background but promotes it in polluted regions (Pyle *et al.*, 2011). Ganzeveld *et al.* (2010) used a chemistry-climate model to study the effects of LUC in the SRES A2 scenario (tropical deforestation) on atmospheric chemistry. By year 2050, they found increases in boundary layer O_3 mixing ratios of up to 9 ppb (20%). Changes in the concentration of the hydroxyl radical resulting from deforestation (the primary atmospheric oxidant, and main determinant of atmospheric CH_4 lifetime) are much less clear due to uncertainties in isoprene oxidation chemistry (Fuchs *et al.*, 2013, Hansen *et al.*, 2017b, Lelieveld *et al.*, 2008), but O_3 concentrations were not sensitive to this uncertainty (Pugh *et al.*, 2010). ADAFF describes a reverse scenario, with forest expansion being largely concentrated in the tropics. The sign of changes in the ADAFF simulations is reverse to changes in Ganzeveld *et al.*: by mid-century, global N loss in ADAFF decreases by 8 and 4% and isoprene emissions increase by 14 and 4% compared to BASE. Consequently, we would expect tropospheric O_3 burden in ADAFF to decrease in the tropics but to increase in large parts of the mid-latitudes. However, changes in overall air quality will likely be dominated by anthropogenic emissions rather than LUC (Val Martin *et al.*, 2015). BVOC emissions might also increase in bioenergy scenarios (Rosenkranz *et al.*, 2015) but this does not happen in our study as the LUMs assumed grasses to be the predominant bioenergy crop type.

5.2.6 Potential impacts on biodiversity

Global-scale approaches that link changes in LU, climate, and other drivers to effects on biodiversity are scarce, and burdened with high uncertainty, though some approaches exist (Alkemade *et al.*, 2009, Visconti *et al.*, 2011). Biodiversity, whether it is being perceived as a requisite for the provision of ESs or an ES per se, with its own intrinsic value (Liang *et al.*, 2016, Mace *et al.*, 2012), has not been considered in our analysis. Nevertheless, it is evident that biodiversity can be in critical conflict with demands for land resources such as food or timber (Behrman *et al.*, 2015, Murphy and Romanuk, 2014). LUC has been the most critical driver of recent species loss (Jantz *et al.*, 2015, Newbold *et al.*, 2014). This has led to substantial concerns that land requirements for bioenergy crops would be com-

peting with conservation areas directly or indirectly. Santangeli *et al.* (2016) found around half of today's global bioenergy production potential to be located either in already protected areas or in land that has highest priority for protection, indicating a high risk for biodiversity in the absence of strong regulatory conservation efforts.

In principle, avoided deforestation and afforestation should maintain and enhance habitat and species richness, since forests are amongst the most diverse ecosystems (Liang *et al.*, 2016). Forestation could also support the restoration of degraded ecosystems. However, success of large-scale afforestation programs under a C-uptake as well as a biodiversity perspective will depend critically on the types of forests promoted and so far show mixed results (Cunningham *et al.*, 2015, Hua *et al.*, 2016). Likewise, even under a globally implemented forest conservation scheme there may be cropland expansion into non-forested regions that could well be C-rich (implying reduced overall C mitigation) but also diverse such as savannas or natural grasslands.

5.2.7 Role of model assumptions on carbon uptake via land-based mitigation and implications for other ecosystem services

Our simulations show that trade-offs between C uptake and other ESs are to be expected. Consequently, the question of whether land-based mitigation projects should be realised depends not only on the effects on ESs, but also on the magnitude of C uptake that will be achieved. However, our study suggests that potential C uptake is highly model-dependent: C uptake in the three land-based mitigation options in LPJ-GUESS is lower than the target value used in the LUMs (see Section 4 for a quantitative analysis). When the underlying reasons for model-model discrepancies are explored, a number of reasons can be identified such as bioenergy yields, forest regrowth, legacy effects from past LUC, and recovery of soil C in response to afforestation. Additionally, for the BECCS scenarios the CDR target was implemented as a CCS target which does not account for additional LUC emissions, partly explaining the lower CDR values.

For forest regrowth, the current model configuration of LPJ-GUESS simulates natural forest succession, including the representation of different age classes. In Section 3 it is shown that the recovery of C in ecosystems following different agricultural LU histories broadly agrees with site-based measurements. LPJ-GUESS also has N (and soil water availability) as an explicit constraint on forest growth and has been successfully tested against a broad range of observations (Fleischer *et al.*, 2015, Smith *et al.*, 2014). These studies indicate an overall realistic rate of forest growth under natural succession. However, much of the afforestation may occur with management facilitating fast built-up of C stocks (as assumed in MAgPIE), but LPJ-GUESS does not implement plantations and has thus not been evaluated against this type of regrowth. Forest (re)growth is simulated very differently in LPJ-GUESS (where different age classes and their competition are simulated), IMAGE (where in this study the dynamically coupled LPJmL DGVM simulates natural regrowth in one individual per PFT), and

MAgPIE (where managed regrowth is prescribed towards potential C densities from LPJmL; see Section 2.3.1). LPJmL also does not yet consider N constraints on vegetation regrowth. C losses from deforestation and maximum C uptake following afforestation depend on potential C densities which are likely different in LPJmL and LPJ-GUESS. In the LUMs, the model's algorithm adopts C pools from LPJmL and can thus decide to afforest the most suitable areas, while in LPJ-GUESS other regions might have more afforestation potential. Finally, soil C sequestration rates are likely different between LPJ-GUESS and LPJmL, especially for MAgPIE-LPJmL, where the assumption of soil C recovering within 20 years is likely overoptimistic (see Sections 3 and 4).

For BECCS, LPJ-GUESS simulates CCS rates of 2.2 and 1.8 GtC yr^{-1} ($LPJG_{IMAGE}$ and $LPJG_{MAgPIE}$, respectively) by the end of the 21st century, compared to 2.8 GtC yr^{-1} reported directly from the LUMs. The number from the LUMs is close to the mean removal rate of 3.3 GtC yr^{-1} reported in Smith *et al.* (2016a) for scenarios of similar production area (380-700 *vs.* 493 and 363 Mha in our IMAGE and MAgPIE BECCS scenarios, respectively) and slightly larger CO_2 levels (430-480 ppmv *vs.* 424 ppmv). Discrepancies between the models arise mainly from differences in assumptions about bioenergy crop yields. In our LPJ-GUESS simulations we grew bioenergy crops as maize (i.e. a CFT with parameters taken from maize). By the 2090-2099 period, simulated bioenergy yields are higher for $LPJG_{MAgPIE}$ BECCS (on average 13.8 t dry mass ha^{-1} yr^{-1}, 10% of total above-ground biomass remaining on-site) than for $LPJG_{IMAGE}$ BECCS (12.2 t dry mass ha^{-1} yr^{-1}) due to different fertiliser rates and production locations. Bioenergy crop yields in LPJ-GUESS might be influenced by inconsistencies between the models about fertilisation of bioenergy crops: while the LUMs generally assume high N application, fertiliser rates are reduced in areas used for bioenergy production because bioenergy crops are less N-demanding. Consequently, the fertiliser rates from the LUMs might be insufficient to fulfil the N demand of the maize-based bioenergy crop in LPJ-GUESS, which responds strongly to fertilisation (Blanke *et al.*, 2017). In contrast, bioenergy crops in the LUMs were represented by dedicated lignocellulosic energy grasses. Reported yields of dedicated bioenergy crops under present-day conditions show large variability (switchgrass: 1-35 t dry mass ha^{-1} yr^{-1}; miscanthus × giganteus: 5-44 t ha^{-1} yr^{-1}; woody species: 0-51 t ha^{-1} yr^{-1}), depending on location, plot size, and management (Searle and Malins, 2014). By the end of the century, the LUMs report average bioenergy yields of ~15.0 t ha^{-1} yr^{-1} (IMAGE) and ~20.3 t ha^{-1} yr^{-1} (MAgPIE), but how bioenergy yields will evolve in reality when averaged across regions (including more marginal land) is highly uncertain (Creutzig, 2016, Searle and Malins, 2014, Slade *et al.*, 2014).

Legacy effects from historic LU might also impact future C uptake as the soil C balance continues to respond to LUC decades or even centuries after (Pugh *et al.*, 2015; see also Section 3). We assessed the contribution of legacy effects by comparing an LPJ-GUESS simulation in which LU (but not climate and CO_2) was held constant from year 1970 for IMAGE and 1995 for MAgPIE (consistent with the scenario starting years in each model) with a run with fixed LU from year 1901 on. The

differences then seen over the 21st century between these two simulations would arise chiefly from legacy fluxes of 20th century LUC. These were found to be 17-18 GtC (not shown), accounting for part of the difference in uptake between LPJ-GUESS and the LUMs. In the LUMs, harmonisation to history has been done with respect to land cover, but this was not possible with respect to changes in vegetation and soil C pools (prior to 1970/1995).

Our results show that assumptions about forest growth and C densities, bioenergy crop yields, and time scales of soil processes can critically influence the C removal potential of land-based mitigation. Large uncertainties about forest regrowth trajectories in different DGVMs (Pongratz *et al.*, in preparation) and BECCS potential to remove C from the atmosphere (Creutzig *et al.*, 2015, Kemper, 2015) have been reported before, including the importance of second-generation bioenergy crops (Kato and Yamagata, 2014) and LU-driven C losses in vegetation and soils (Wiltshire and Davies-Barnard, 2015). This is clearly an important subject for future research. Additional analyses about the difference in C removal between the LUMs and LPJ-GUESS, including results from additional DGVMs, are presented in Section 4.

5.2.8 Conclusions from Section 5

Terrestrial ecosystems provide us with many valuable services like climate and air quality regulation, water and food provision, or flood protection. While substantial changes in ecosystem functions are likely to occur within the 21st century even in the absence of land-based climate change mitigation, additional impacts are to be expected from land management for negative emissions. In all mitigation simulations, what might generally be perceived as beneficial effects on some ecosystem functions and their services (e.g. decreased N loss improving water and air quality) are counteracted by negative effects on others (e.g. reduced crop production), including substantial temporal and regional variations. Environmental side effects in our ADAFF simulations are usually larger than in BECCS, presumably reflecting the larger area affected by land-cover transitions in ADAFF. Without a valuation exercise it is not possible to state whether one option would be "better" than the other. All mitigation approaches might reduce crop production (in the absence of assumptions about large technology-related yield increases) but potentially improve air and water quality via reduced N loss. Impacts on climate via biophysical effects and on water availability and flood risks via changes in runoff are found to be relatively small in terms of percentage changes when averaged over large areas, but this does not exclude the possibility of significant impacts e.g. on the scale of large catchments.

Policy makers should be aware of manifold side effects - be they positive or negative - when discussing and evaluating the feasibility and effects of different climate mitigation options, possibly involving the prioritisation of individual ESs at the costs of exacerbating other challenges. Our analysis makes some of these trade-offs explicit, but there are many other services offered by ecosystems much more difficult to quantify, particularly relating to cultural services, which also need to be considered. Any

discussion about land-based climate change mitigation efforts should take into account their effects on ESs beyond C storage in order to avoid unintended negative consequences, which would be intrinsically undesirable and may also affect the effective delivery of climate mitigation through societal feedbacks.

6 General conclusions and outlook

This thesis studied the importance and effects of future LUC - in particular the implementation of large-scale land-based climate change mitigation - on the C cycle and associated ecosystem functions. The following paragraphs aim to summarise the key results of this thesis, highlight major sources of uncertainty, and propose possible directions of future model development.

6.1 Answers to the underlying research questions

Sections 3-5 provide answers to the main research questions addressed in this thesis.

- **What are the impacts of land-use and land-cover changes on the terrestrial carbon cycle and to what degree are these impacts reversible?**

The findings of this thesis confirm earlier studies that found historic LUC activities have caused drastic alterations of the terrestrial C cycle (e.g. Le Quere *et al.*, 2016) and will continue to do so in the future (e.g. Pugh *et al.*, 2015). Depending on the type of land management, the land can continue to act as a C sink within the 21st century and even take up additional C. However, the reversal of historic LUC (e.g. deforestation) is a slow process and in some cases the legacy effects continue to impact the recovery of ecosystems even after many centuries, suggesting that model simulations (especially for afforestation scenarios) should start at least one century before the period of interest begins.

- **Can large-scale land-based mitigation efforts contribute to climate stabilisation by removing substantial amounts of carbon from the atmosphere?**

The amount of negative emissions achievable from land-based mitigation is highly uncertain. Avoided deforestation and afforestation as well as bioenergy cultivation combined with C capture and storage are widely used by the IAM/LUM community to achieve ambitious climate change mitigation targets. Even though the findings of this thesis suggest that negative emissions from land-based mitigation (both via ADAFF or BECCS) could delay the implementation of large emission reductions by a few years, the large role land-based mitigation plays in climate stabilisation scenarios appears worrying. Climate change mitigation scenarios typically assume that large-scale applications of negative emissions (mainly from BECCS) could boost our remaining emission budget of 140-320 GtC (Rockstrom *et al.*, 2017, Rogelj *et al.*, 2016b) by a factor of around 1.6-2.0 (Fuss *et al.*, 2014, Rogelj *et al.*, 2015), thereby effectively almost halving the required fossil fuel emission reductions to stay below 2°C. However, this thesis suggests that potential CDR rates might well be lower than typically assumed by IAMs/LUMs, and cumulative CDR will likely not exceed 100 GtC by the end of the century due to

limited C uptake per unit land area, limited land availability, trade-offs with other ESs, and other constraints not explicitly investigated in this thesis.

- **What would be the environmental side effects of land-based climate change mitigation?**

There are always side effects from land-based mitigation on associated ecosystem functions, which are likely to enhance or reduce the supply of derived ESs, with large differences across scenarios, variables, regions, and time scales. While some impacts (changes in albedo, evapotranspiration, runoff, BVOC emissions) were expected, others (reductions in crop production and N loss) were less obvious and to some degree an outcome of inconsistencies in terms of process representation between the LUMs and LPJ-GUESS, thereby complicating the interpretation of the results and emphasizing the necessity of a better integration between the models to better assess changes in ESs. Afforestation generally induces larger changes in ES indicators than BECCS due to the larger area affected. One major concern of land-based mitigation is the potential conflict with food production. In the LUMs, technological progress is assumed to allow for the abandonment of agricultural areas for land-based climate change mitigation. However, this thesis suggests that if agricultural efficiency cannot be increased as expected, land-based mitigation will pose substantial risks to food security, especially in the case of land-intensive mitigation via afforestation. On the other hand, afforestation could have beneficial effects on biodiversity if managed properly, a major concern in large-scale BECCS scenarios.

- **How do different representations of agricultural processes in vegetation models affect the results?**

This thesis reveals large uncertainties in future terrestrial C cycling due to very different responses to LUC in the LUMs and DGVMs, and thus confirms earlier studies reporting large differences in LUC fluxes due to different representations of land cover and land management (Arneth *et al.*, 2017, Pugh *et al.*, 2015). Simulated total C uptake in the LUMs/DGVMs ranges between 19 GtC and 141 GtC, including large model disagreement in terms of total C uptake for both ADAFF as well as BECCS simulations. These differences are induced by assumptions about forest regrowth, potential vegetation and soil C pools, the direction and magnitude of soil C changes following LUC, and bioenergy crop yields. The analysis is hindered by differences in model structures, different implementations of LU patterns into the DGVMs, and incomplete data reporting. In many cases it is difficult to judge which model simulates the most realistic C uptake because observational data that can be used for model evaluation are scarce or provide an inconsistent picture.

6.2 Limitations

This thesis identifies numerous sources of uncertainties which emerge from limited process understanding and data availability, limited computational resources and storage capacities, and inconsistencies and incomplete transparency across models. One salient limitation of the models used in this thesis (and other models simulating the global C cycle) is the still very rudimentary representation of LUC processes. While some basic management techniques are accounted for by at least some models (different crop types, fertilisation, irrigation, tillage, growing seasons, cropland and pasture harvest), other processes are typically ignored (pesticides, soil compaction, salinisation, and erosion). In any case, reliable large-scale observational datasets are often not available (Erb *et al.*, 2017). Uncertainty is also large for bioenergy crop yields. Most DGVMs, including LPJ-GUESS, so far do not represent dedicated bioenergy CFTs which have very different physiologies and different growth requirements than food crops. LPJmL represents dedicated grassy or woody bioenergy crops but field observations do not provide a comprehensive picture about what bioenergy yields can be expected at larger scales in more marginal land and how much potential there is in terms of yield improvements. Adopting yields typically achieved in highly managed field trials as a benchmark bears the risk of a substantial overestimation of future bioenergy production. In addition, high yields require substantial amounts of management, water, and fertiliser input (especially if first generation bioenergy crops were to be grown), thereby increasing costs but also raising other issues like water consumption, water pollution, and N_2O emissions (Creutzig, 2016, Crutzen *et al.*, 2008, Lisboa *et al.*, 2011, Smith *et al.*, 2016a).

It is also apparent that most models used here are not particularly suitable for the simulation of C removal via afforestation due to the typical representation of PFTs by just one single individual. LPJ-GUESS is an exception as it explicitly simulates competition amongst trees of different age/size classes. Additionally, LPJ-GUESS is one of the few DGVMs accounting for nutrient (at least N) limitation on plant growth. Consequently, DGVMs such as LPJ-GUESS are arguably more suited to study forest regrowth after natural or anthropogenic disturbances, and to assess the potential contribution of C sequestration via afforestation to climate change mitigation. However, this thesis also shows that not only do the models have substantial limitations, but also that observational data for model evaluation in terms of C uptake via afforestation are quite scarce or contradictory. This includes growth rates in (managed) secondary forests, but particularly the direction and magnitude of changes in soil C in response to grassland-forest transitions.

Another source of uncertainty is the forcing data for the DGVMs, especially climate. The simulations for Section 3 were performed with repeated cycles of present-day CRU climate. This dataset is derived from statistical interpolation of weather station data and is thus quite inaccurate in regions were measurements are sparse (e.g. Africa). The simulations analysed in Sections 4 and 5 were driven by the same simulated meteorological variables for the LUMs and DGVMs, thereby ensuring consistency between simulations. However, we only used climate forcing from one single climate model and one

emission scenario (RCP2.6). While climate change is expected to be relatively moderate for RCP2.6, different climate models still simulate quite different rates of warming/precipitation changes and consequently influence C uptake potential (Ahlstrom *et al.*, 2012). For example, global temperature increase in the five ISI-MIP climate models ranges between 1.4 and 2.4°C for RCP2.6 (Warszawski *et al.*, 2014). The findings of this thesis could thus be modified by the use of additional climate models. Moreover, the C removal achieved via BECCS or ADAFF could be quite different in alternative emission scenarios, e.g. increased CO_2 fertilisation could substantially enhance forest or bioenergy crop growth in a scenario in which negative emissions are needed to limit global warming below 3°C rather than 2°C.

6.3 Future work

As discussed above, the models need to further improve the representation of management practices, including (bioenergy) CFTs. All DGVMs (and LUMs) apart from LPJ-GUESS would benefit from a representation of different age classes amongst trees to account for heterogeneity at the landscape level. Biomass accumulation in secondary forests depends on forest age (Poorter *et al.*, 2016, Yang *et al.*, 2011), so the representation of all trees in a grid-cell by a single individual per PFT is likely a serious oversimplification. The implementation of age cohorts, along with bioenergy crops, is work-in-progress for the ORCHIDEE DGVM. However, LPJ-GUESS also needs to be further improved to be able to simulate a wider range of forest management techniques. IAMs/LUMs increasingly focus on assisted regrowth and forest plantations to achieve more negative emissions via afforestation. Possible LPJ-GUESS features could thus comprise the introduction of new, fast-growing PFTs (and possibly preventing the growth of competitors in these regions), simulating tree planting via regrowth from an initial biomass, resprouting after wood harvest, and N (and phosphorus) fertilisation in forests.

There is also a need to study additional variables in land-based mitigation impact assessments on top of the ones explored in this thesis. For example, biodiversity deserves protection not only because it is directly linked to ecosystem functioning, but also to secure genetic variety. However, the inclusion of biodiversity in DGVMs even at a very rudimentary level is challenging. The explicit simulation of N_2O emissions is work-in-progress in LPJ-GUESS, which would allow for a better separation between aquatic and gaseous N losses. Additionally, LPJ-GUESS is currently being developed to simulate additional BVOC types and N-fixing crops.

Finally, the evaluation of simulated CDR via land-based mitigation relies on comprehensive observational datasets, which are often scarce or not available. In particular, there is a clear lack of observations for bioenergy crop yields in the (sub-)tropics (Heck *et al.*, 2016, Searle and Malins, 2014). More data are available with respect to the rate of tropical forest regrowth, however, it remains largely unclear to what extent management can accelerate C accumulation in secondary forests compared to

natural regrowth. Studies addressing these issues could therefore help to identify the most suitable locations for land-based mitigation and to minimise conflicts with other forms of LU.

6.4 Final remarks

Climate change likely represents a great challenge for human societies within the 21st century, and its impacts in a business-as-usual scenario might pose a serious threat to the world we know today. This thesis emphasises the large uncertainties in potential C removal and environmental side effects from land-based climate change mitigation efforts, which encourages focusing on rapid reductions in GHG emissions to prevent dangerous climate change. However, it appears highly unlikely that conventional mitigation efforts alone will be able to limit global warming below 2°C or even 1.5°C. Even relatively small amounts of negative emissions could thus help to dampen effects of climate change, regardless of whether global warming will reach 2°C, 3°C, or more. Consequently, scientists should continue to pursue the feasibility of land-based mitigation and also explore the potentials and risks of alternative approaches like direct air capture.

Acknowledgements

At the end of my thesis I would like to thank all those people who made this work possible. In particular, I want to thank the following people:

First of all I am very grateful to my supervisor Almut Arneth who spent countless hours on the success of this thesis despite her many other duties. Almut, thanks so much for your guidance, inspiration, patience, and shared knowledge over the last years. You have been a great supervisor.

I am also very thankful for my co-advisor Thomas Pugh for his help with the LPJ-GUESS model, his many suggestions on structuring, writing, and presenting my work, and his constant encouragement.

The same is also true for my co-advisor Anita Bayer. Again, thanks a lot for all the help, recommendations, motivation, and time you invested into this thesis.

Special thanks go to Peter Anthoni for his help with the LPJ-GUESS model code and to Benjamin Quesada for his help with R.

I also want to thank the other members of the PAI group at IMK-IFU, the LPJ-GUESS developers at Lund University, and all of our collaborators within the LUC4C project.

Furthermore, I am grateful to Mark Rounsevell and Anja Rammig for reviewing this thesis.

Finally, I want to thank my friends and my family for their unlimited support, especially my mother who did not live to see the submission of this thesis. Her memory will always be with me.

This thesis was funded by the European Commission's Seventh Framework Programme, under grant agreement numbers 603542 (LUC4C) and 308393 (OPERAs), and the International Research Group CLUCIE.

Literature

Ahlstrom A, Raupach MR, Schurgers G *et al.* (2015) The dominant role of semi-arid ecosystems in the trend and variability of the land CO2 sink. *Science,* **348**, 895-899, doi:10.1126/science.aaa1668.

Ahlstrom A, Schurgers G, Arneth A, Smith B (2012) Robustness and uncertainty in terrestrial ecosystem carbon response to CMIP5 climate change projections. *Environmental Research Letters,* **7**, doi:10.1088/1748-9326/7/4/044008.

Alexander P, Brown C, Arneth A, Finnigan J, Moran D, Rounsevell MDA (2017a) Losses, inefficiencies and waste in the global food system. *Agricultural Systems,* **153**, 190-200, doi:10.1016/j.agsy.2017.01.014.

Alexander P, Brown C, Arneth A, Finnigan J, Rounsevell MDA (2016) Human appropriation of land for food: The role of diet. *Global Environmental Change-Human and Policy Dimensions,* **41**, 88-98, doi:10.1016/j.gloenvcha.2016.09.005.

Alexander P, Moran D, Rounsevell MDA, Smith P (2013) Modelling the perennial energy crop market: the role of spatial diffusion. *Journal of the Royal Society Interface,* **10**, doi:10.1098/Rsif.2013.0656.

Alexander P, Prestele R, Verburg PH *et al.* (2017b) Assessing uncertainties in land cover projections. *Global Change Biology,* **23**, 767-781, doi:10.1111/gcb.13447.

Alexandratos N, Bruinsma J (2012) World agriculture towards 2030/2050: the 2012 revision. Rome, FAO.

Alkama R, Cescatti A (2016) Biophysical climate impacts of recent changes in global forest cover. *Science,* **351**, 600-604, doi:10.1126/science.aac8083.

Alkemade R, Van Oorschot M, Miles L, Nellemann C, Bakkenes M, Ten Brink B (2009) GLOBIO3: A framework to investigate options for reducing global terrestrial biodiversity loss. *Ecosystems,* **12**, 374–390, doi:10.1007/s10021-009-9229-5.

Allen CD, Breshears DD, Mcdowell NG (2015) On underestimation of global vulnerability to tree mortality and forest die-off from hotter drought in the Anthropocene. *Ecosphere,* **6**, doi:10.1890/Es15-00203.1.

Anagnostou E, John EH, Edgar KM *et al.* (2016) Changing atmospheric CO2 concentration was the primary driver of early Cenozoic climate. *Nature,* **533**, 380-384, doi:10.1038/nature17423.

Anav A, Friedlingstein P, Kidston M *et al.* (2013) Evaluating the Land and Ocean Components of the Global Carbon Cycle in the CMIP5 Earth System Models. *Journal of Climate,* **26**, 6801-6843, doi:10.1175/Jcli-D-12-00417.1.

Anderson-Teixeira KJ, Miller AD, Mohan JE, Hudiburg TW, Duval BD, Delucia EH (2013) Altered dynamics of forest recovery under a changing climate. *Global Change Biology,* **19**, 2001-2021, doi:10.1111/gcb.12194.

Anderson-Teixeira KJ, Wang MMH, Mcgarvey JC, Lebauer DS (2016) Carbon dynamics of mature and regrowth tropical forests derived from a pantropical database (TropForC-db). *Global Change Biology,* **22**, 1690-1709, doi:10.1111/gcb.13226.

Anderson K (2015) Duality in climate science. *Nature Geoscience,* **8**, 898-900, doi:10.1038/ngeo2559.

Anderson K, Peters G (2016) The trouble with negative emissions. *Science,* **354**, 182-183, doi:10.1126/science.aah4567.

Arneth A, Harrison SP, Zaehle S *et al.* (2010) Terrestrial biogeochemical feedbacks in the climate system. *Nature Geoscience,* **3**, 525-532, doi:10.1038/ngeo905.

Arneth A, Niinemets U, Pressley S *et al.* (2007) Process-based estimates of terrestrial ecosystem isoprene emissions: incorporating the effects of a direct CO2-isoprene interaction. *Atmospheric Chemistry and Physics,* **7**, 31-53, doi:10.5194/acp-7-31-2007.

Arneth A, Sitch S, Pongratz J *et al.* (2017) Historical carbon dioxide emissions caused by land-use changes are possibly larger than assumed. *Nature Geoscience,* **10**, 79-84, doi:10.1038/NGEO2882.

Arora VK, Montenegro A (2011) Small temperature benefits provided by realistic afforestation efforts. *Nature Geoscience,* **4**, 514-518, doi:10.1038/NGEO1182.

Ashworth K, Folberth G, Hewitt CN, Wild O (2012) Impacts of near-future cultivation of biofuel feedstocks on atmospheric composition and local air quality. *Atmospheric Chemistry and Physics*, **12**, 919-939, doi:10.5194/acp-12-919-2012.

Asner GP, Powell GVN, Mascaro J *et al.* (2010) High-resolution forest carbon stocks and emissions in the Amazon. *Proceedings of the National Academy of Sciences of the United States of America*, **107**, 16738-16742, doi:10.1073/pnas.1004875107.

Bajzelj B, Richards KS, Allwood JM, Smith P, Dennis JS, Curmi E, Gilligan CA (2014) Importance of food-demand management for climate mitigation. *Nature Climate Change*, **4**, 924-929, doi:10.1038/Nclimate2353.

Bala G, Caldeira K, Wickett M, Phillips TJ, Lobell DB, Delire C, Mirin A (2007) Combined climate and carbon-cycle effects of large-scale deforestation. *Proceedings of the National Academy of Sciences of the United States of America*, **104**, 6550-6555, doi:10.1073/pnas.0608998104.

Ban-Weiss GA, Bala G, Cao L, Pongratz J, Caldeira K (2011) Climate forcing and response to idealized changes in surface latent and sensible heat. *Environmental Research Letters*, **6**, doi:10.1088/1748-9326/6/3/034032.

Barnett TP, Adam JC, Lettenmaier DP (2005) Potential impacts of a warming climate on water availability in snow-dominated regions. *Nature*, **438**, 303-309, doi:10.1038/nature04141.

Barnosky AD, Matzke N, Tomiya S *et al.* (2011) Has the Earth's sixth mass extinction already arrived? *Nature*, **471**, 51-57, doi:10.1038/nature09678.

Bathiany S, Claussen M, Brovkin V, Raddatz T, Gayler V (2010) Combined biogeophysical and biogeochemical effects of large-scale forest cover changes in the MPI earth system model. *Biogeosciences*, **7**, 1383-1399, doi:10.5194/bg-7-1383-2010.

Bayer AD, Lindeskog M, Pugh TaM, Anthoni PM, Fuchs R, Arneth A (2017) Uncertainties in the land-use flux resulting from land-use change reconstructions and gross land transitions. *Earth System Dynamics*, **8**, 91-111, doi:10.5194/esd-8-91-2017.

Bayer AD, Pugh TaM, Krause A, Arneth A (2015) Historical and future quantification of terrestrial carbon sequestration from a Greenhouse-Gas-Value perspective. *Global Environmental Change-Human and Policy Dimensions*, **32**, 153-164, doi:10.1016/j.gloenvcha.2015.03.004.

Becker K, Wulfmeyer V, Berger T, Gebel J, Munch W (2013) Carbon farming in hot, dry coastal areas: an option for climate change mitigation. *Earth System Dynamics*, **4**, 237-251, doi:10.5194/esd-4-237-2013.

Beer C, Reichstein M, Tomelleri E *et al.* (2010) Terrestrial Gross Carbon Dioxide Uptake: Global Distribution and Covariation with Climate. *Science*, **329**, 834-838, doi:10.1126/science.1184984.

Behera SN, Sharma M, Aneja VP, Balasubramanian R (2013) Ammonia in the atmosphere: a review on emission sources, atmospheric chemistry and deposition on terrestrial bodies. *Environmental Science and Pollution Research*, **20**, 8092-8131, doi:10.1007/s11356-013-2051-9.

Behrman KD, Juenger TE, Kiniry JR, Keitt TH (2015) Spatial land use trade-offs for maintenance of biodiversity, biofuel, and agriculture. *Landscape Ecology*, **30**, 1987-1999, doi:10.1007/s10980-015-0225-1.

Bellassen V, Luyssaert S (2014) Managing forests in uncertain times. *Nature*, **506**, 153-155,

Bellemare J, Motzkin G, Foster DR (2002) Legacies of the agricultural past in the forested present: an assessment of historical land-use effects on rich mesic forests. *Journal of Biogeography*, **29**, 1401-1420, doi:10.1046/j.1365-2699.2002.00762.x.

Bereiter B, Eggleston S, Schmitt J *et al.* (2015) Revision of the EPICA Dome C CO2 record from 800 to 600kyr before present. *Geophysical Research Letters*, **42**, 542-549, doi:10.1002/2014GL061957.

Beringer T, Lucht W, Schaphoff S (2011) Bioenergy production potential of global biomass plantations under environmental and agricultural constraints. *Global Change Biology Bioenergy*, **3**, 299-312, doi:10.1111/j.1757-1707.2010.01088.x.

Best MJ, Pryor M, Clark DB *et al.* (2011) The Joint UK Land Environment Simulator (JULES), model description - Part 1: Energy and water fluxes. *Geoscientific Model Development*, **4**, 677-699, doi:10.5194/gmd-4-677-2011.

Betts RA (2000) Offset of the potential carbon sink from boreal forestation by decreases in surface albedo. *Nature*, **408**, 187-190, doi:10.1038/35041545.

Betts RA, Falloon PD, Goldewijk KK, Ramankutty N (2007) Biogeophysical effects of land use on climate: Model simulations of radiative forcing and large-scale temperature change. *Agricultural and Forest Meteorology,* **142**, 216-233, doi:10.1016/j.agrformet.2006.08.021.

Bindoff NL, Stott PA, Achutarao KM *et al.* (2013) Detection and Attribution of Climate Change: from Global to Regional. In: *Climate Change 2013: The Physical Science Basis. Contribution of Working Group I to the Fifth Assessment Report of the Intergovernmental Panel on Climate Change.* (eds Stocker TF, Qin D, Plattner G-K, Tignor M, Allen SK, Boschung J, Nauels A, Xia Y, Bex V, Midgley PM), Cambridge, United Kingdom and New York, NY, USA, Cambridge University Press.

Blanke JH, Olin S, Stürck J, Sahlin U, Lindeskog M, Helming J, Lehsten V (2017) Assessing the impact of changes in land-use intensity and climate on simulated trade-offs between crop yield and nitrogen leaching. *Agriculture, Ecosystems and Environment,* **239**, 385-398, doi:10.1016/j.agee.2017.01.038.

Boisier JP, De Noblet-Ducoudre N, Ciais P (2013) Inferring past land use-induced changes in surface albedo from satellite observations: a useful tool to evaluate model simulations. *Biogeosciences,* **10**, 1501-1516, doi:10.5194/bg-10-1501-2013.

Bonan GB (2008) Forests and climate change: Forcings, feedbacks, and the climate benefits of forests. *Science,* **320**, 1444-1449, doi:10.1126/science.1155121.

Bondeau A, Smith PC, Zaehle S *et al.* (2007) Modelling the role of agriculture for the 20th century global terrestrial carbon balance. *Global Change Biology,* **13**, 679-706, doi:10.1111/j.1365-2486.2006.01305.x.

Boucher O, Myhre G, Myhre A (2004) Direct human influence of irrigation on atmospheric water vapour and climate. *Climate Dynamics,* **22**, 597-603, doi:10.1007/s00382-004-0402-4.

Boysen LR, Lucht W, Gerten D (2017a) Trade-offs for food production, nature conservation and climate limit the terrestrial carbon dioxide removal potential. *Global Change Biology,* doi:10.1111/gcb.13745.

Boysen LR, Lucht W, Gerten D, Heck V (2016) Impacts devalue the potential of large-scale terrestrial CO2 removal through biomass plantations. *Environmental Research Letters,* **11**, doi:10.1088/1748-9326/11/9/095010.

Boysen LR, Lucht W, Gerten D, Heck V, Lenton TM, Schellnhuber HJ (2017b) The limits to global-warming mitigation by terrestrial carbon removal. *Earths Future,* **5**, 463-474, doi:10.1002/2016EF000469.

Bradshaw CJA, Sodhi NS, Peh KSH, Brook BW (2007) Global evidence that deforestation amplifies flood risk and severity in the developing world. *Global Change Biology,* **13**, 2379-2395, doi:10.1111/j.1365-2486.2007.01446.x.

Bright RM, Davin E, O'halloran T, Pongratz J, Zhao KG, Cescatti A (2017) Local temperature response to land cover and management change driven by non-radiative processes. *Nature Climate Change,* **7**, doi:10.1038/Nclimate3250.

Brovkin V, Boysen L, Arora VK *et al.* (2013) Effect of Anthropogenic Land-Use and Land-Cover Changes on Climate and Land Carbon Storage in CMIP5 Projections for the Twenty-First Century. *Journal of Climate,* **26**, 6859-6881, doi:10.1175/Jcli-D-12-00623.1.

Brown C, Alexander P, Rounsevell M (submitted) Empirical evidence for the diffusion of knowledge in land use change.

Brown RA, Rosenberg NJ, Hays CJ, Easterling WE, Mearns LO (2000) Potential production and environmental effects of switchgrass and traditional crops under current and greenhouse-altered climate in the central United States: a simulation study. *Agriculture Ecosystems & Environment,* **78**, 31-47, doi:10.1016/S0167-8809(99)00115-2.

Bugmann H (2001) A review of forest gap models. *Climatic Change,* **51**, 259-305, doi:10.1023/A:1012525626267.

Cai C, Yin XY, He SQ *et al.* (2016) Responses of wheat and rice to factorial combinations of ambient and elevated CO2 and temperature in FACE experiments. *Global Change Biology,* **22**, 856-874, doi:10.1111/gcb.13065.

Cairns MA, Brown S, Helmer EH, Baumgardner GA (1997) Root biomass allocation in the world's upland forests. *Oecologia,* **111**, 1-11, doi:10.1007/s004420050201.

Camargo JA, Alonso A (2006) Ecological and toxicological effects of inorganic nitrogen pollution in aquatic ecosystems: A global assessment. *Environment International*, **32**, 831-849, doi:10.1016/j.envint.2006.05.002.

Campbell JE, Lobell DB, Genova RC, Field CB (2008) The global potential of bioenergy on abandoned agriculture lands. *Environmental Science & Technology*, **42**, 5791-5794, doi:10.1021/es800052w.

Carslaw KS, Boucher O, Spracklen DV, Mann GW, Rae JGL, Woodward S, Kulmala M (2010) A review of natural aerosol interactions and feedbacks within the Earth system. *Atmospheric Chemistry and Physics*, **10**, 1701-1737, doi:10.5194/acp-10-1701-2010.

Cassman KG, Dobermann A, Walters DT (2002) Agroecosystems, nitrogen-use efficiency, and nitrogen management. *Ambio*, **31**, 132-140, doi:10.1639/0044-7447(2002)031[0132:Anuean]2.0.Co;2.

Challinor AJ, Watson J, Lobell DB, Howden SM, Smith DR, Chhetri N (2014) A meta-analysis of crop yield under climate change and adaptation. *Nature Climate Change*, **4**, 287-291, doi:10.1038/Nclimate2153.

Chatskikh D, Hansen S, Olesen JE, Petersen BM (2009) A simplified modelling approach for quantifying tillage effects on soil carbon stocks. *European Journal of Soil Science*, **60**, 924-934, doi:10.1111/j.1365-2389.2009.01185.x.

Chazdon RL (2003) Tropical forest recovery: legacies of human impact and natural disturbances. *Perspectives in Plant Ecology Evolution and Systematics*, **6**, 51-71, doi:10.1078/1433-8319-00042.

Chazdon RL (2014) *Second Growth: The Promise of Tropical Forest Regeneration in an Age of Deforestation*, Chicago, Illinois, USA, University of Chicago Press.

Chazdon RL, Broadbent EN, Rozendaal DMA *et al.* (2016) Carbon sequestration potential of second-growth forest regeneration in the Latin American tropics. *Science Advances*, **2**, doi:10.1126/sciadv.1501639.

Choat B, Jansen S, Brodribb TJ *et al.* (2012) Global convergence in the vulnerability of forests to drought. *Nature*, **491**, 752-755, doi:10.1038/nature11688.

Ciais P, Sabine C, Bala G *et al.* (2013) Carbon and Other Biogeochemical Cycles. In: *Climate Change 2013: The Physical Science Basis. Contribution of Working Group I to the Fifth Assessment Report of the Intergovernmental Panel on Climate Change.* (eds Stocker TF, Qin D, Plattner G-K, Tignor M, Allen SK, Boschung J, Nauels A, Xia Y, Bex V, Midgley PM), Cambridge, United Kingdom and New York, NY, USA, Cambridge University Press.

Ciais P, Wattenbach M, Vuichard N *et al.* (2010) The European carbon balance. Part 2: croplands. *Global Change Biology*, **16**, 1409-1428, doi:10.1111/j.1365-2486.2009.02055.x.

Ciccioli P, Centritto M, Loreto F (2014) Biogenic volatile organic compound emissions from vegetation fires. *Plant Cell and Environment*, **37**, 1810-1825, doi:10.1111/pce.12336.

Clark DB, Mercado LM, Sitch S *et al.* (2011) The Joint UK Land Environment Simulator (JULES), model description - Part 2: Carbon fluxes and vegetation dynamics. *Geoscientific Model Development*, **4**, 701-722, doi:10.5194/gmd-4-701-2011.

Clark PU, Shakun JD, Marcott SA *et al.* (2016) Consequences of twenty-first-century policy for multi-millennial climate and sea-level change. *Nature Climate Change*, **6**, 360-369, doi:10.1038/Nclimate2923.

Cleveland CC, Taylor P, Chadwick KD *et al.* (2015) A comparison of plot-based satellite and Earth system model estimates of tropical forest net primary production. *Global Biogeochemical Cycles*, **29**, 626-644, doi:10.1002/2014GB005022.

Cramer VA, Hobbs RJ, Standish RJ (2008) What's new about old fileds? Land abandonment and ecosystem assembly. *Trends in Ecology & Evolution*, **23**, 104-112, doi:10.1016/j.tree.2007.10.005.

Cramer W, Bondeau A, Woodward FI *et al.* (2001) Global response of terrestrial ecosystem structure and function to CO2 and climate change: results from six dynamic global vegetation models. *Global Change Biology*, **7**, 357-373, doi:10.1046/j.1365-2486.2001.00383.x.

Creutzig F (2016) Economic and ecological views on climate change mitigation with bioenergy and negative emissions. *Global Change Biology Bioenergy*, **8**, 4-10, doi:10.1111/gcbb.12235.

Creutzig F, Ravindranath NH, Berndes G *et al.* (2015) Bioenergy and climate change mitigation: an assessment. *Global Change Biology Bioenergy*, **7**, 916-944, doi:10.1111/gcbb.12205.

Cru (2013) CRU TS3.21: Climatic Research Unit (CRU) Time-Series (TS) Version 3.21 of High Resolution Gridded Data of Month-by-month Variation in Climate (Jan. 1901 - Dec. 2012). *NCAS British Atmospheric Data Centre,* **2013**, doi:10.5285/D0E1585D-3417-485F-87AE-4FCECF10A992.

Crutzen PJ, Mosier AR, Smith KA, Winiwarter W (2008) N2O release from agro-biofuel production negates global warming reduction by replacing fossil fuels. *Atmospheric Chemistry and Physics,* **8**, 389-395, doi:10.5194/acp-8-389-2008.

Culf AD, Fisch G, Hodnett MG (1995) The Albedo of Amazonian Forest and Ranch Land. *Journal of Climate,* **8**, 1544-1554, doi:10.1175/1520-0442(1995)008<1544:Taoafa>2.0.Co;2.

Cunningham SC, Mac Nally R, Baker PJ, Cavagnaro TR, Beringer J, Thomson JR, Thompson RM (2015) Balancing the environmental benefits of reforestation in agricultural regions. *Perspectives in Plant Ecology Evolution and Systematics,* **17**, 301-317, doi:10.1016/j.ppees.2015.06.001.

Davidson EA, Ackerman IL (1993) Changes in Soil Carbon Inventories Following Cultivation of Previously Untilled Soils. *Biogeochemistry,* **20**, 161-193, doi:10.1007/Bf00000786.

Davidson EA, Kanter D (2014) Inventories and scenarios of nitrous oxide emissions. *Environmental Research Letters,* **9**, doi:10.1088/1748-9326/9/10/105012.

Davies-Barnard T, Valdes PJ, Singarayer JS, Pacifico FM, Jones CD (2014) Full effects of land use change in the representative concentration pathways. *Environmental Research Letters,* **9**, doi:10.1088/1748-9326/9/11/114014.

De Noblet-Ducoudre N, Boisier JP, Pitman A *et al.* (2012) Determining Robust Impacts of Land-Use-Induced Land Cover Changes on Surface Climate over North America and Eurasia: Results from the First Set of LUCID Experiments. *Journal of Climate,* **25**, 3261-3281, doi:10.1175/Jcli-D-11-00338.1.

Dean R, Ellis JE, Rice RW, Bement RE (1975) Nutrient Removal by Cattle from a Shortgrass Prairie. *Journal of Applied Ecology,* **12**, 25-29, doi:10.2307/2401715.

Defries R (2002) Past and future sensitivity of primary production to human modification of the landscape. *Geophysical Research Letters,* **29**, doi:10.1029/2001gl013620.

Dellink R, Chateau J, Lanzi E, Magne B (2017) Long-term economic growth projections in the Shared Socioeconomic Pathways. *Global Environmental Change-Human and Policy Dimensions,* **42**, 200-214, doi:10.1016/j.gloenvcha.2015.06.004.

Deng L, Zhu G, Tang Z, Shangguan Z (2016) Global patterns of the effects of land-use changes on soil carbon stocks. *Global Ecology and Conservation,* **5**, 127-138, doi:10.1016/j.gecco.2015.12.004.

Devaraju N, Bala G, Nemani R (2015) Modelling the influence of land-use changes on biophysical and biochemical interactions at regional and global scales. *Plant Cell and Environment,* **38**, 1931-1946, doi:10.1111/pce.12488.

Dlugokencky E, Tans P (2017) ESRL Global Monitoring Division - Global Greenhouse Gas Reference Network.

Doelman JC, Stehfest E, Tabeau A *et al.* (2018) Exploring SSP land-use dynamics using the IMAGE model: Regional and gridded scenarios of land-use change and land-based climate change mitigation. *Global Environmental Change,* **48**, 119-135, doi:10.1016/j.gloenvcha.2017.11.014.

Don A, Schumacher J, Freibauer A (2011) Impact of tropical land-use change on soil organic carbon stocks - a meta-analysis. *Global Change Biology,* **17**, 1658-1670, doi:10.1111/j.1365-2486.2010.02336.x.

Doney SC, Fabry VJ, Feely RA, Kleypas JA (2009) Ocean Acidification: The Other CO2 Problem. *Annual Review of Marine Science,* **1**, 169-192, doi:10.1146/annurev.marine.010908.163834.

Edmonds J, Luckow P, Calvin K *et al.* (2013) Can radiative forcing be limited to 2.6 Wm(-2) without negative emissions from bioenergy AND CO2 capture and storage? *Climatic Change,* **118**, 29-43, doi:10.1007/s10584-012-0678-z.

Eitelberg DA, Van Vliet J, Verburg PH (2015) A review of global potentially available cropland estimates and their consequences for model-based assessments. *Global Change Biology,* **21**, 1236-1248, doi:10.1111/gcb.12733.

Elliott J, Deryng D, Mueller C *et al.* (2014) Constraints and potentials of future irrigation water availability on agricultural production under climate change. *Proceedings of the National*

Academy of Sciences of the United States of America, **111**, 3239-3244, doi:10.1073/pnas.1222474110.
Ellis EC, Kaplan JO, Fuller DQ, Vavrus S, Goldewijk KK, Verburg PH (2013) Used planet: A global history. *Proceedings of the National Academy of Sciences of the United States of America,* **110**, 7978-7985, doi:10.1073/pnas.1217241110.
Ellison D, Futter MN, Bishop K (2012) On the forest cover-water yield debate: from demand- to supply-side thinking. *Global Change Biology,* **18**, 806-820, doi:10.1111/j.1365-2486.2011.02589.x.
Eltahir EaB, Bras RL (1996) Precipitation recycling. *Reviews of Geophysics,* **34**, 367-378, doi:10.1029/96rg01927.
Erb KH, Kastner T, Luyssaert S, Houghton RA, Kuemmerle T, Olofsson P, Haberl H (2013) COMMENTARY: Bias in the attribution of forest carbon sinks. *Nature Climate Change,* **3**, 854-856, doi:10.1038/nclimate2004.
Erb KH, Lauk C, Kastner T, Mayer A, Theurl MC, Haberl H (2016) Exploring the biophysical option space for feeding the world without deforestation. *Nature Communications,* **7**, doi:10.1038/Ncomms11382.
Erb KH, Luyssaert S, Meyfroidt P *et al.* (2017) Land management: data availability and process understanding for global change studies. *Global Change Biology,* **23**, 512-533, doi:10.1111/gcb.13443.
Erisman JW, Galloway J, Seitzinger S, Bleeker A, Butterbach-Bahl K (2011) Reactive nitrogen in the environment and its effect on climate change. *Current Opinion in Environmental Sustainability,* **3**, 281-290, doi:10.1016/j.cosust.2011.08.012.
Fargione J, Hill J, Tilman D, Polasky S, Hawthorne P (2008) Land clearing and the biofuel carbon debt. *Science,* **319**, 1235-1238, doi:10.1126/science.1152747.
Farley KA, Jobbagy EG, Jackson RB (2005) Effects of afforestation on water yield: a global synthesis with implications for policy. *Global Change Biology,* **11**, 1565-1576, doi:10.1111/j.1365-2486.2005.01011.x.
Ferreira S, Ghimire R (2012) Forest cover, socioeconomics, and reported flood frequency in developing countries. *Water Resources Research,* **48**, doi:10.1029/2011wr011701.
Field CB, Mach KJ (2017) Rightsizing carbon dioxide removal. *Science,* **356**, 706-707, doi:10.1126/science.aam9726.
Figueres C, Schellnhuber HJ, Whiteman G, Rockstrom J, Hobley A, Rahmstorf S (2017) Three years to safeguard our climate. *Nature,* **546**, 593-595,
Fleischer K, Warlind D, Van Der Molen MK *et al.* (2015) Low historical nitrogen deposition effect on carbon sequestration in the boreal zone. *Journal of Geophysical Research-Biogeosciences,* **120**, 2542-2561, doi:10.1002/2015JG002988.
Foley JA, Costa MH, Delire C, Ramankutty N, Snyder P (2003) Green surprise? How terrestrial ecosystems could affect earth's climate. *Frontiers in Ecology and the Environment,* **1**, 38-44, doi:10.2307/3867963.
Foley JA, Defries R, Asner GP *et al.* (2005) Global consequences of land use. *Science,* **309**, 570-574, doi:10.1126/science.1111772.
Foley JA, Ramankutty N, Brauman KA *et al.* (2011) Solutions for a cultivated planet. *Nature,* **478**, 337-342, doi:10.1038/nature10452.
Foote RL, Grogan P (2010) Soil Carbon Accumulation During Temperate Forest Succession on Abandoned Low Productivity Agricultural Lands. *Ecosystems,* **13**, 795-812, doi:10.1007/s10021-010-9355-0.
Foster GL, Royer DL, Lunt DJ (2017) Future climate forcing potentially without precedent in the last 420 million years. *Nature Communications,* **8**, doi:10.1038/Ncomms14845.
Friedlingstein P, Meinshausen M, Arora VK, Jones CD, Anav A, Liddicoat SK, Knutti R (2014) Uncertainties in CMIP5 Climate Projections due to Carbon Cycle Feedbacks. *Journal of Climate,* **27**, 511-526, doi:10.1175/Jcli-D-12-00579.1.
Fuchs H, Hofzumahaus A, Rohrer F *et al.* (2013) Experimental evidence for efficient hydroxyl radical regeneration in isoprene oxidation. *Nature Geoscience,* **6**, 1023-1026, doi:10.1038/NGEO1964.

Fuchs R, Herold M, Verburg PH, Clevers JGPW, Eberle J (2015) Gross changes in reconstructions of historic land cover/use for Europe between 1900 and 2010. *Global Change Biology*, **21**, 299-313, doi:10.1111/gcb.12714.

Fuss S, Canadell JG, Peters GP *et al.* (2014) COMMENTARY: Betting on negative emissions. *Nature Climate Change*, **4**, 850-853, doi:10.1038/nclimate2392.

Fuss S, Jones CD, Kraxner F *et al.* (2016) Research priorities for negative emissions. *Environmental Research Letters*, **11**, doi:10.1088/1748-9326/11/11/115007.

Galloway JN, Dentener FJ, Capone DG *et al.* (2004) Nitrogen cycles: past, present, and future. *Biogeochemistry*, **70**, 153-226, doi:10.1007/s10533-004-0370-0.

Ganzeveld L, Bouwman L, Stehfest E, Van Vuuren DP, Eickhout B, Lelieveld J (2010) Impact of future land use and land cover changes on atmospheric chemistry-climate interactions. *Journal of Geophysical Research-Atmospheres*, **115**, doi:10.1029/2010jd014041.

Gasser T, Guivarch C, Tachiiri K, Jones CD, Ciais P (2015) Negative emissions physically needed to keep global warming below 2 degrees C. *Nature Communications*, **6**, doi:10.1038/Ncomms8958.

Gerten D, Schaphoff S, Haberlandt U, Lucht W, Sitch S (2004) Terrestrial vegetation and water balance - hydrological evaluation of a dynamic global vegetation model. *Journal of Hydrology*, **286**, 249-270, doi:10.1016/j.jhydrol.2003.09.029.

Giambelluca TW (2002) Hydrology of altered tropical forest. *Hydrological Processes*, **16**, 1665-1669, doi:10.1002/Hyp.5021.

Giglio L, Randerson JT, Van Der Werf GR, Kasibhatla PS, Collatz GJ, Morton DC, Defries RS (2010) Assessing variability and long-term trends in burned area by merging multiple satellite fire products. *Biogeosciences*, **7**, 1171-1186, doi:10.5194/bg-7-1171-2010.

Ginoux P, Prospero JM, Gill TE, Hsu NC, Zhao M (2012) Global-Scale Attribution of Anthropogenic and Natural Dust Sources and Their Emission Rates Based on Modis Deep Blue Aerosol Products. *Reviews of Geophysics*, **50**, doi:10.1029/2012rg000388.

Godfray HCJ, Beddington JR, Crute IR *et al.* (2010) Food Security: The Challenge of Feeding 9 Billion People. *Science*, **327**, 812-818, doi:10.1126/science.1185383.

Guo LB, Gifford RM (2002) Soil carbon stocks and land use change: a meta analysis. *Global Change Biology*, **8**, 345-360, doi:10.1046/j.1354-1013.2002.00486.x.

Haines-Yong R, Potschin M (2013) CICES V4.3 - Revised report prepared following consultation on CICES Version 4, August-December 2012. EEA Framework Contract No EEA/IEA/09/003.

Hallgren W, Schlosser CA, Monier E, Kicklighter D, Sokolov A, Melillo J (2013) Climate impacts of a large-scale biofuels expansion. *Geophysical Research Letters*, **40**, 1624-1630, doi:10.1002/grl.50352.

Hansen J, Satoa M, Ruedy R, Schmidt GA, Lo K, Persin A (2017a) Global Temperature in 2016. In: *Climate Science, Awareness and Solutions.*

Hansen RF, Lewis TR, Graham L, Whalley SK, Seakins PW, Heard DE, Blitz MA (2017b) OH production from the photolysis of isoprene-derived peroxy radicals: cross-sections, quantum yields and atmospheric implications. *Phys. Chem. Chem. Phys*, **19**, 2332-2345, doi:10.1039/c6cp06718b.

Hansis E, Davis SJ, Pongratz J (2015) Relevance of methodological choices for accounting of land use change carbon fluxes. *Global Biogeochemical Cycles*, **29**, 1230-1246, doi:10.1002/2014GB004997.

Hantson S, Knorr W, Schurgers G, Pugh TaM, Arneth A (2017) Global isoprene and monoterpene emissions under changing climate, vegetation, CO2 and land use. *Atmospheric Environment*, **155**, 35-45, doi:10.1016/j.atmosenv.2017.02.010.

Harari YN (2015) *Sapiens: A Brief History of Humankind*, London, Vintage.

Haxeltine A, Prentice IC (1996a) BIOME3: An equilibrium terrestrial biosphere model based on ecophysiological constraints, resource availability, and competition among plant functional types. *Global Biogeochemical Cycles*, **10**, 693-709, doi:10.1029/96gb02344.

Haxeltine A, Prentice IC (1996b) A general model for the light-use efficiency of primary production. *Functional Ecology*, **10**, 551-561, doi:10.2307/2390165.

He F, Vavrus SJ, Kutzbach JE, Ruddiman WF, Kaplan JO, Krumhardt KM (2014) Simulating global and local surface temperature changes due to Holocene anthropogenic land cover change. *Geophysical Research Letters*, **41**, 623-631, doi:10.1002/2013GL058085.

Heck V, Gerten D, Lucht W, Boysen LR (2016) Is extensive terrestrial carbon dioxide removal a 'green' form of geoengineering? A global modelling study. *Global and Planetary Change*, **137**, 123-130, doi:10.1016/j.gloplacha.2015.12.008.

Hempel S, Frieler K, Warszawski L, Schewe J, Piontek F (2013) A trend-preserving bias correction - the ISI-MIP approach. *Earth System Dynamics*, **4**, 219-236, doi:10.5194/esd-4-219-2013.

Hickler T, Smith B, Sykes MT, Davis MB, Sugita S, Walker K (2004) Using a generalized vegetation model to simulate vegetation dynamics in northeastern USA. *Ecology*, **85**, 519-530, doi:10.1890/02-0344.

Hickler T, Vohland K, Feehan J *et al.* (2012) Projecting the future distribution of European potential natural vegetation zones with a generalized, tree species-based dynamic vegetation model. *Global Ecology and Biogeography*, **21**, 50-63, doi:10.1111/j.1466-8238.2010.00613.x.

Holmgren M, Hirota M, Van Nes EH, Scheffer M (2013) Effects of interannual climate variability on tropical tree cover. *Nature Climate Change*, **3**, 755-758, doi:10.1038/Nclimate1906.

Hoogwijk M, Faaija A, Van Den Broek R, Berndes G, Gielen D, Turkenburg W (2003) Exploration of the ranges of the global potential of biomass for energy. *Biomass & Bioenergy*, **25**, 119-133, doi:10.1016/S0961-9534(02)00191-5.

Hooker TD, Compton JE (2003) Forest ecosystem carbon and nitrogen accumulation during the first century after agricultural abandonment. *Ecological Applications*, **13**, 299-313, doi:10.1890/1051-0761(2003)013[0299:Fecana]2.0.Co;2.

Houghton RA (2003a) Revised estimates of the annual net flux of carbon to the atmosphere from changes in land use and land management 1850-2000. *Tellus Series B-Chemical and Physical Meteorology*, **55**, 378-390, doi:10.1034/j.1600-0889.2003.01450.x.

Houghton RA (2003b) Why are estimates of the terrestrial carbon balance so different? *Global Change Biology*, **9**, 500-509, doi:10.1046/j.1365-2486.2003.00620.x.

Houghton RA (2007) Balancing the global carbon budget. *Annual Review of Earth and Planetary Sciences*, **35**, 313-347, doi:10.1146/annurev.earth.35.031306.140057.

Houghton RA, Byers B, Nassikas AK (2015) COMMENTARY: A role for tropical forests in stabilizing atmospheric CO2. *Nature Climate Change*, **5**, 1022-1023, doi:10.1038/nclimate2869.

Houghton RA, House JI, Pongratz J *et al.* (2012) Carbon emissions from land use and land-cover change. *Biogeosciences*, **9**, 5125-5142, doi:10.5194/bg-9-5125-2012.

Houghton RA, Nassikas AA (2017) Negative emissions from stopping deforestation and forest degradation, globally. *Global Change Biology*, 1-10, doi:10.1111/gcb.13876.

Houldcroft CJ, Grey WMF, Barnsley M, Taylor CM, Los SO, North PRJ (2009) New Vegetation Albedo Parameters and Global Fields of Soil Background Albedo Derived from MODIS for Use in a Climate Model. *Journal of Hydrometeorology*, **10**, 183-198, doi:10.1175/2008JHM1021.1.

Hua FY, Wang XY, Zheng XL *et al.* (2016) Opportunities for biodiversity gains under the world's largest reforestation programme. *Nature Communications*, **7**, doi:10.1038/Ncomms12717.

Hughes RF, Kauffman JB, Jaramillo VJ (1999) Biomass, carbon, and nutrient dynamics of secondary forests in a humid tropical region of Mexico. *Ecology*, **80**, 1892-1907, doi:10.1890/0012-9658(1999)080[1892:BCANDO]2.0.CO;2.

Humpenöder F, Popp A, Dietrich JP *et al.* (2014) Investigating afforestation and bioenergy CCS as climate change mitigation strategies. *Environmental Research Letters*, **9**, doi:10.1088/1748-9326/9/6/064029.

Hurtt GC, Chini LP, Frolking S *et al.* (2011) Harmonization of land-use scenarios for the period 1500-2100: 600 years of global gridded annual land-use transitions, wood harvest, and resulting secondary lands. *Climatic Change*, **109**, 117-161, doi:10.1007/s10584-011-0153-2.

Ito A (2011) A historical meta-analysis of global terrestrial net primary productivity: are estimates converging? *Global Change Biology*, **17**, 3161-3175, doi:10.1111/j.1365-2486.2011.02450.x.

Jackson RB, Jobbagy EG, Avissar R *et al.* (2005) Trading water for carbon with biological sequestration. *Science*, **310**, 1944-1947, doi:10.1126/science.1119282.

Jackson RB, Randerson JT, Canadell JG *et al.* (2008) Protecting climate with forests. *Environmental Research Letters*, **3**, doi:10.1088/1748-9326/3/4/044006.

Jagermeyr J, Gerten D, Heinke J, Schaphoff S, Kummu M, Lucht W (2015) Water savings potentials of irrigation systems: global simulation of processes and linkages. *Hydrology and Earth System Sciences*, **19**, 3073-3091, doi:10.5194/hess-19-3073-2015.

Jantz SM, Barker B, Brooks TM *et al.* (2015) Future habitat loss and extinctions driven by land-use change in biodiversity hotspots under four scenarios of climate-change mitigation. *Conservation Biology*, **29**, 1122-1131, doi:10.1111/cobi.12549.

Johnson MO, Galbraith D, Gloor M *et al.* (2016) Variation in stem mortality rates determines patterns of above-ground biomass in Amazonian forests: implications for dynamic global vegetation models. *Global Change Biology*, **22**, 3996-4013, doi:10.1111/gcb.13315.

Jones CD, Ciais P, Davis SJ *et al.* (2016) Simulating the Earth system response to negative emissions. *Environmental Research Letters*, **11**, doi:10.1088/1748-9326/11/9/095012.

Jones CD, Hughes JK, Bellouin N *et al.* (2011) The HadGEM2-ES implementation of CMIP5 centennial simulations. *Geoscientific Model Development*, **4**, 543-570, doi:10.5194/gmd-4-543-2011.

Jones HP, Schmitz OJ (2009) Rapid Recovery of Damaged Ecosystems. *Plos One*, **4**, doi:10.1371/journal.pone.0005653.

Kampa M, Castanas E (2008) Human health effects of air pollution. *Environmental Pollution*, **151**, 362-367, doi:10.1016/j.envpol.2007.06.012.

Kaplan JO, Krumhardt KM, Ellis EC, Ruddiman WF, Lemmen C, Goldewijk KK (2011) Holocene carbon emissions as a result of anthropogenic land cover change. *Holocene*, **21**, 775-791, doi:10.1177/0959683610386983.

Kartha S, Dooley K (2016) The risks of relying on tomorrow's 'negative emissions' to guide today's mitigation action. Stockholm Environment Institute.

Kato E, Yamagata Y (2014) BECCS capability of dedicated bioenergy crops under a future land-use scenario targeting net negative carbon emissions. *Earths Future*, **2**, 421-439, doi:10.1002/2014EF000249.

Kauffman JB, Hughes RF, Heider C (2009) Carbon pool and biomass dynamics associated with deforestation, land use, and agricultural abandonment in the neotropics. *Ecological Applications*, **19**, 1211-1222, doi:10.1890/08-1696.1.

Keenan TF, Prentice IC, Canadell JG, Williams CA, Wang H, Raupach M, Collatz GJ (2016) Recent pause in the growth rate of atmospheric CO2 due to enhanced terrestrial carbon uptake. *Nature Communications*, **7**, doi:10.1038/Ncomms13428.

Keller DP, Feng EY, Oschlies A (2014) Potential climate engineering effectiveness and side effects during a high carbon dioxide-emission scenario. *Nature Communications*, **5**, doi:10.1038/ncomms4304.

Kelley DI, Prentice IC, Harrison SP, Wang H, Simard M, Fisher JB, Willis KO (2013) A comprehensive benchmarking system for evaluating global vegetation models. *Biogeosciences*, **10**, 3313-3340, doi:10.5194/bg-10-3313-2013.

Kemper J (2015) Biomass and carbon dioxide capture and storage: A review. *International Journal of Greenhouse Gas Control*, **40**, 401-430, doi:10.1016/j.ijggc.2015.06.012.

Kesselmeier J, Staudt M (1999) Biogenic volatile organic compounds (VOC): An overview on emission, physiology and ecology. *Journal of Atmospheric Chemistry*, **33**, 23-88, doi:10.1023/A:1006127516791.

Klein D, Luderer G, Kriegler E *et al.* (2014) The value of bioenergy in low stabilization scenarios: an assessment using REMIND-MAgPIE. *Climatic Change*, **123**, 705-718, doi:10.1007/s10584-013-0940-z.

Klein Goldewijk K, Beusen A, Doelman J, Stehfest E (2016) New anthropogenic land use estimates for the Holocene; HYDE 3.2 *Earth System Science Data Discussion*, doi:10.5194/essd-2016-58.

Klein Goldewijk K, Beusen A, Van Drecht G, De Vos M (2011) The HYDE 3.1 spatially explicit database of human-induced global land-use change over the past 12,000 years. *Global Ecology and Biogeography*, **20**, 73-86, doi:10.1111/j.1466-8238.2010.00587.x.

Kloster S, Mahowald NM, Randerson JT *et al.* (2010) Fire dynamics during the 20th century simulated by the Community Land Model. *Biogeosciences*, **7**, 1877-1902, doi:10.5194/bg-7-1877-2010.

Knops JMH, Tilman D (2000) Dynamics of soil nitrogen and carbon accumulation for 61 years after agricultural abandonment. *Ecology,* **81**, 88-98, doi:10.1890/0012-9658(2000)081[0088:Dosnac]2.0.Co;2.

Knutti R, Rogelj J, Sedlacek J, Fischer EM (2016) A scientific critique of the two-degree climate change target. *Nature Geoscience,* **9**, 13-18, doi:10.1038/NGEO2595.

Krinner G, Viovy N, De Noblet-Ducoudre N *et al.* (2005) A dynamic global vegetation model for studies of the coupled atmosphere-biosphere system. *Global Biogeochemical Cycles,* **19**, doi:10.1029/2003gb002199.

Laganiere J, Angers DA, Pare D (2010) Carbon accumulation in agricultural soils after afforestation: a meta-analysis. *Global Change Biology,* **16**, 439-453, doi:10.1111/j.1365-2486.2009.01930.x.

Lamarque JF, Bond TC, Eyring V *et al.* (2010) Historical (1850-2000) gridded anthropogenic and biomass burning emissions of reactive gases and aerosols: methodology and application. *Atmospheric Chemistry and Physics,* **10**, 7017-7039, doi:10.5194/acp-10-7017-2010.

Lamarque JF, Dentener F, Mcconnell J *et al.* (2013) Multi-model mean nitrogen and sulfur deposition from the Atmospheric Chemistry and Climate Model Intercomparison Project (ACCMIP): evaluation of historical and projected future changes. *Atmospheric Chemistry and Physics,* **13**, 7997-8018, doi:10.5194/acp-13-7997-2013.

Lamarque JF, Kyle GP, Meinshausen M *et al.* (2011) Global and regional evolution of short-lived radiatively-active gases and aerosols in the Representative Concentration Pathways. *Climatic Change,* **109**, 191-212, doi:10.1007/s10584-011-0155-0.

Lauenroth WK, Milchunas DG (1992) Shortgrass steppe. In: *Natural Grasslands: Introduction and Western Hemisphere.* (ed Coupland RT). Amsterdam, Elsevier Science.

Laurance WF, Sayer J, Cassman KG (2014) Agricultural expansion and its impacts on tropical nature. *Trends in Ecology & Evolution,* **29**, 107-116, doi:10.1016/j.tree.2013.12.001.

Le Quere C, Andrew RM, Canadell JG *et al.* (2016) Global Carbon Budget 2016. *Earth System Science Data,* **8**, 605-649, doi:10.5194/essd-8-605-2016.

Lelieveld J, Butler TM, Crowley JN *et al.* (2008) Atmospheric oxidation capacity sustained by a tropical forest. *Nature,* **452**, 737-740, doi:10.1038/nature06870.

Lenton TM (2010) The potential for land-based biological CO2 removal to lower future atmospheric CO2 concentration. *Carbon Management,* **1**, 145-160, doi:10.4155/Cmt.10.12.

Lenton TM, Vaughan NE (2009) The radiative forcing potential of different climate geoengineering options. *Atmospheric Chemistry and Physics,* **9**, 5539-5561, doi:10.5194/acp-9-5539-2009.

Levis S, Bonan GB, Kluzek E, Thornton PE, Jones A, Sacks WJ, Kucharik CJ (2012) Interactive Crop Management in the Community Earth System Model (CESM1): Seasonal Influences on Land-Atmosphere Fluxes. *Journal of Climate,* **25**, 4839-4859, doi:10.1175/Jcli-D-11-00446.1.

Levis S, Hartman MD, Bonan GB (2014) The Community Land Model underestimates land-use CO2 emissions by neglecting soil disturbance from cultivation. *Geoscientific Model Development,* **7**, 613-620, doi:10.5194/gmd-7-613-2014.

Lewis SL, Maslin MA (2015) Defining the Anthropocene. *Nature,* **519**, 171-180, doi:10.1038/nature14258.

Li DJ, Niu SL, Luo YQ (2012) Global patterns of the dynamics of soil carbon and nitrogen stocks following afforestation: a meta-analysis. *New Phytologist,* **195**, 172-181, doi:10.1111/j.1469-8137.2012.04150.x.

Li W, Ciais P, Guenet B *et al.* (submitted) Temporal response of soil organic carbon after grassland-related land-use change.

Li Y, Zhao MS, Motesharrei S, Mu QZ, Kalnay E, Li SC (2015) Local cooling and warming effects of forests based on satellite observations. *Nature Communications,* **6**, doi:10.1038/Ncomms7603.

Liang JJ, Crowther TW, Picard N *et al.* (2016) Positive biodiversity-productivity relationship predominant in global forests. *Science,* **354**, 196, doi:10.1126/science.aaf8957.

Lieberman D (2014) *The Story of the Human Body: Evolution, Health and Disease,* New York, Pantheon Books.

Lindeskog M, Arneth A, Bondeau A, Waha K, Seaquist J, Olin S, Smith B (2013) Implications of accounting for land use in simulations of ecosystem carbon cycling in Africa. *Earth System Dynamics,* **4**, 385-407, doi:10.5194/esd-4-385-2013.

Lisboa CC, Butterbach-Bahl K, Mauder M, Kiese R (2011) Bioethanol production from sugarcane and emissions of greenhouse gases - known and unknowns. *Global Change Biology Bioenergy*, **3**, 277-292, doi:10.1111/j.1757-1707.2011.01095.x.

Liu GD, Li YC, Alva AK (2007) Moisture quotients for ammonia volatilization from four soils in potato production regions. *Water Air and Soil Pollution*, **183**, 115-127, doi:10.1007/s11270-007-9361-9.

Lotze-Campen H, Muller C, Bondeau A, Rost S, Popp A, Lucht W (2008) Global food demand, productivity growth, and the scarcity of land and water resources: a spatially explicit mathematical programming approach. *Agricultural Economics*, **39**, 325-338, doi:10.1111/j.1574-0862.2008.00336.x.

Luderer G, Bertram C, Calvin K, De Cian E, Kriegler E (2016) Implications of weak near-term climate policies on long-term mitigation pathways. *Climatic Change*, **136**, 127-140, doi:10.1007/s10584-013-0899-9.

Luthi D, Le Floch M, Bereiter B *et al.* (2008) High-resolution carbon dioxide concentration record 650,000-800,000 years before present. *Nature*, **453**, 379-382, doi:10.1038/nature06949.

Luyssaert S, Ciais P, Piao SL *et al.* (2010) The European carbon balance. Part 3: forests. *Global Change Biology*, **16**, 1429-1450, doi:10.1111/j.1365-2486.2009.02056.x.

Luyssaert S, Schulze ED, Borner A *et al.* (2008) Old-growth forests as global carbon sinks. *Nature*, **455**, 213-215, doi:10.1038/nature07276.

Macdonald GK, Bennett EM, Taranu ZE (2012) The influence of time, soil characteristics, and land-use history on soil phosphorus legacies: a global meta-analysis. *Global Change Biology*, **18**, 1904-1917, doi:10.1111/j.1365-2486.2012.02653.x.

Mace GM, Norris K, Fitter AH (2012) Biodiversity and ecosystem services: a multilayered relationship. *Trends in Ecology & Evolution*, **27**, 19-26, doi:10.1016/j.tree.2011.08.006.

Mackey B, Prentice IC, Steffen W, House JI, Lindenmayer D, Keith H, Berry S (2013) Untangling the confusion around land carbon science and climate change mitigation policy. *Nature Climate Change*, **3**, 552-557, doi:10.1038/Nclimate1804.

Malmqvist B, Rundle S (2002) Threats to the running water ecosystems of the world. *Environmental Conservation*, **29**, 134-153, doi:10.1017/S0376892902000097.

Marcott SA, Shakun JD, Clark PU, Mix AC (2013) A Reconstruction of Regional and Global Temperature for the Past 11,300 Years. *Science*, **339**, 1198-1201, doi:10.1126/science.1228026.

Martin PA, Newton AC, Bullock JM (2013) Carbon pools recover more quickly than plant biodiversity in tropical secondary forests. *Proceedings of the Royal Society B-Biological Sciences*, **280**, doi:10.1098/Rspb.2013.2236.

Mayer D (2017) Potentials and Side-Effects of Herbaceous Biomass Plantations for Climate Change Mitigation. PhD thesis, University of Hamburg, Hamburg.

Mcgrath JM, Lobell DB (2013) Regional disparities in the CO2 fertilization effect and implications for crop yields. *Environmental Research Letters*, **8**, doi:10.1088/1748-9326/8/1/014054.

Mclauchlan K (2006) The nature and longevity of agricultural impacts on soil carbon and nutrients: A review. *Ecosystems*, **9**, 1364-1382, doi:10.1007/s10021-005-0135-1.

Mcsherry ME, Ritchie ME (2013) Effects of grazing on grassland soil carbon: a global review. *Global Change Biology*, **19**, 1347-1357, doi:10.1111/gcb.12144.

Meinshausen M, Smith SJ, Calvin K *et al.* (2011) The RCP greenhouse gas concentrations and their extensions from 1765 to 2300. *Climatic Change*, **109**, 213-241, doi:10.1007/s10584-011-0156-z.

Millar RJ, Fuglestvedt JS, Friedlingstein P *et al.* (2017) Emission budgets and pathways consistent with limiting warming to 1.5°C. *Nature Geoscience*, **10**, 741–747, doi:10.1038/ngeo3031.

Millennium Ecosystem Assessment (2005) Ecosystems and Human Well-being: Synthesis. Washington, DC.

Miller PA, Giesecke T, Hickler T *et al.* (2008) Exploring climatic and biotic controls on Holocene vegetation change in Fennoscandia. *Journal of Ecology*, **96**, 247-259, doi:10.1111/j.1365-2745.2007.01342.x.

Monfreda C, Ramankutty N, Foley JA (2008) Farming the planet: 2. Geographic distribution of crop areas, yields, physiological types, and net primary production in the year 2000. *Global Biogeochemical Cycles*, **22**, doi:10.1029/2007gb002947.

Moran EF, Brondizio ES, Tucker JM, Da Silva-Forsberg MC, Mccracken S, Falesi I (2000) Effects of soil fertility and land-use on forest succession in Amazonia. *Forest Ecology and Management*, **139**, 93-108, doi:10.1016/S0378-1127(99)00337-0.

Mueller ND, Gerber JS, Johnston M, Ray DK, Ramankutty N, Foley JA (2012) Closing yield gaps through nutrient and water management. *Nature*, **490**, 254-257, doi:10.1038/nature11420.

Mueller ND, Lassaletta L, Runck BC, Billen G, Garnier J, Gerber JS (2017) Declining spatial efficiency of global cropland nitrogen allocation. *Global Biogeochemical Cycles*, **31**, 245-257, doi:10.1002/2016GB005515.

Murphy GEP, Romanuk TN (2014) A meta-analysis of declines in local species richness from human disturbances. *Ecology and Evolution*, **4**, 91-103, doi:10.1002/ece3.909.

Navarrete D, Sitch S, Aragao LEOC, Pedroni L (2016) Conversion from forests to pastures in the Colombian Amazon leads to contrasting soil carbon dynamics depending on land management practices. *Global Change Biology*, **22**, 3503-3517, doi:10.1111/gcb.13266.

Neumann M, Mues V, Moreno A, Hasenauer H, Seidl R (2017) Climate variability drives recent tree mortality in Europe. *Global Change Biology*, 1-10, doi:10.1111/gcb.13724.

Newbold T, Hudson LN, Phillips HRP *et al.* (2014) A global model of the response of tropical and sub-tropical forest biodiversity to anthropogenic pressures. *Proceedings of the Royal Society B-Biological Sciences*, **281**, doi:10.1098/Rspb.2014.1371.

O'neill BC, Kriegler E, Riahi K *et al.* (2014) A new scenario framework for climate change research: the concept of shared socioeconomic pathways. *Climatic Change*, **122**, 387-400, doi:10.1007/s10584-013-0905-2.

Oki T, Kanae S (2006) Global hydrological cycles and world water resources. *Science*, **313**, 1068-1072, doi:10.1126/science.1128845.

Olin S, Lindeskog M, Pugh TaM *et al.* (2015a) Soil carbon management in large-scale Earth system modelling: implications for crop yields and nitrogen leaching. *Earth System Dynamics*, **6**, 745-768, doi:10.5194/esd-6-745-2015.

Olin S, Schurgers G, Lindeskog M *et al.* (2015b) Modelling the response of yields and tissue C : N to changes in atmospheric CO2 and N management in the main wheat regions of western Europe. *Biogeosciences*, **12**, 2489-2515, doi:10.5194/bg-12-2489-2015.

Ornstein L, Aleinov I, Rind D (2009) Irrigated afforestation of the Sahara and Australian Outback to end global warming. *Climatic Change*, **97**, 409-437, doi:10.1007/s10584-009-9626-y.

Pan YD, Birdsey RA, Fang JY *et al.* (2011) A Large and Persistent Carbon Sink in the World's Forests. *Science*, **333**, 988-993, doi:10.1126/science.1201609.

Parton WJ, Scurlock JMO, Ojima DS *et al.* (1993) Observations and Modeling of Biomass and Soil Organic-Matter Dynamics for the Grassland Biome Worldwide. *Global Biogeochemical Cycles*, **7**, 785-809, doi:10.1029/93gb02042.

Paul KI, Polglase PJ, Nyakuengama JG, Khanna PK (2002) Change in soil carbon following afforestation. *Forest Ecology and Management*, **168**, 241-257, doi:10.1016/S0378-1127(01)00740-X.

Peng SS, Ciais P, Maignan F, Li W, Chang JF, Wang T, Yue C (2017) Sensitivity of land use change emission estimates to historical land use and land cover mapping. *Global Biogeochemical Cycles*, **31**, 626-643, doi:10.1002/2015GB005360.

Peng SS, Piao SL, Zeng ZZ *et al.* (2014) Afforestation in China cools local land surface temperature. *Proceedings of the National Academy of Sciences of the United States of America*, **111**, 2915-2919, doi:10.1073/pnas.1315126111.

Penuelas J, Staudt M (2010) BVOCs and global change. *Trends in Plant Science*, **15**, 133-144, doi:10.1016/j.tplants.2009.12.005.

Perugini L, Caporaso L, Marconi S *et al.* (2017) Biophysical effects on temperature and precipitation due to land cover change. *Environmental Research Letters*, **12**, doi:10.1088/1748-9326/Aa6b3f.

Peters GP, Andrew RM, Canadell JG *et al.* (2017) Key indicators to track current progress and future ambition of the Paris Agreement. *Nature Climate Change*, **7**, 118-123, doi:10.1038/Nclimate3202.

Piao SL, Ciais P, Friedlingstein P, De Noblet-Ducoudre N, Cadule P, Viovy N, Wang T (2009) Spatiotemporal patterns of terrestrial carbon cycle during the 20th century. *Global Biogeochemical Cycles*, **23**, doi:10.1029/2008gb003339.

Piao SL, Sitch S, Ciais P *et al.* (2013) Evaluation of terrestrial carbon cycle models for their response to climate variability and to CO2 trends. *Global Change Biology*, **19**, 2117-2132, doi:10.1111/gcb.12187.

Pielke RA, Pitman A, Niyogi D *et al.* (2011) Land use/land cover changes and climate: modeling analysis and observational evidence. *Wiley Interdisciplinary Reviews-Climate Change*, **2**, 828-850, doi:10.1002/wcc.144.

Pimm SL, Jenkins CN, Abell R *et al.* (2014) The biodiversity of species and their rates of extinction, distribution, and protection. *Science*, **344**, 987-997, doi:10.1126/Science.1246752.

Pitman AJ, De Noblet-Ducoudre N, Cruz FT *et al.* (2009) Uncertainties in climate responses to past land cover change: First results from the LUCID intercomparison study. *Geophysical Research Letters*, **36**, doi:10.1029/2009gl039076.

Poeplau C, Don A, Vesterdal L, Leifeld J, Van Wesemael B, Schumacher J, Gensior A (2011) Temporal dynamics of soil organic carbon after land-use change in the temperate zone - carbon response functions as a model approach. *Global Change Biology*, **17**, 2415-2427, doi:10.1111/j.1365-2486.2011.02408.x.

Pongratz J, Reick C, Raddatz T, Claussen M (2008) A reconstruction of global agricultural areas and land cover for the last millennium. *Global Biogeochemical Cycles*, **22**, doi:10.1029/2007gb003153.

Pongratz J, Reick CH, Raddatz T, Caldeira K, Claussen M (2011) Past land use decisions have increased mitigation potential of reforestation. *Geophysical Research Letters*, **38**, doi:10.1029/2011gl047848.

Pongratz J, Reick CH, Raddatz T, Claussen M (2010) Biogeophysical versus biogeochemical climate response to historical anthropogenic land cover change. *Geophysical Research Letters*, **37**, doi:10.1029/2010gl043010.

Poorter L, Ongers FB, Aide TM *et al.* (2016) Biomass resilience of Neotropical secondary forests. *Nature*, **530**, 211-214, doi:10.1038/nature16512.

Popp A, Calvin K, Fujimori S *et al.* (2017) Land-use futures in the shared socio-economic pathways. *Global Environmental Change-Human and Policy Dimensions*, **42**, 331-345, doi:10.1016/j.gloenvcha.2016.10.002.

Popp A, Humpenoder F, Weindl I *et al.* (2014) Land-use protection for climate change mitigation. *Nature Climate Change*, **4**, 1095-1098, doi:10.1038/Nclimate2444.

Post WM, Kwon KC (2000) Soil carbon sequestration and land-use change: processes and potential. *Global Change Biology*, **6**, 317-327, doi:10.1046/j.1365-2486.2000.00308.x.

Posthumus H, Morris J, Hess TM, Neville D, Phillips E, Baylis A (2009) Impacts of the summer 2007 floods on agriculture in England. *Journal of Flood Risk Management*, **2**, 182-189, doi:10.1111/j.1753-318X.2009.01031.x.

Potter KN, Torbert HA, Johnson HB, Tischler CR (1999) Carbon storage after long-term grass establishment on degraded soils. *Soil Science*, **164**, 718-725, doi:10.1097/00010694-199910000-00002.

Potter P, Ramankutty N, Bennett EM, Donner SD (2010) Characterizing the Spatial Patterns of Global Fertilizer Application and Manure Production. *Earth Interactions*, **14**, doi:10.1175/2009ei288.1.

Poulter B, Frank D, Ciais P *et al.* (2014) Contribution of semi-arid ecosystems to interannual variability of the global carbon cycle. *Nature*, **509**, 600-603, doi:10.1038/nature13376.

Poulton PR, Pye E, Hargreaves PR, Jenkinson DS (2003) Accumulation of carbon and nitrogen by old arable land reverting to woodland. *Global Change Biology*, **9**, 942-955, doi:10.1046/j.1365-2486.2003.00633.x.

Powers JS, Corre MD, Twine TE, Veldkamp E (2011) Geographic bias of field observations of soil carbon stocks with tropical land-use changes precludes spatial extrapolation. *Proceedings of the National Academy of Sciences of the United States of America*, **108**, 6318-6322, doi:10.1073/pnas.1016774108.

Prentice IC, Bondeau A, Cramer W *et al.* (2007) Dynamic Global Vegetation Modeling: Quantifying Terrestrial Ecosystem Responses to Large-Scale Environmental Change. In: *Terrestrial Ecosystems in a Changing World.* (eds Canadell JG, Pataki DE, Pitelka LF). Springer Berlin Heidelberg.

Prestele R, Alexander P, Rounsevell MDA *et al.* (2016) Hotspots of uncertainty in land-use and land-cover change projections: a global-scale model comparison. *Global Change Biology*, **22**, 3967-3983, doi:10.1111/gcb.13337.

Prestele R, Arneth A, Bondeau A *et al.* (2017) Current challenges of implementing anthropogenic land-use and land-cover change in models contributing to climate change assessments. *Earth System Dynamics*, **8**, 369-386, doi:10.5194/esd-8-369-2017.

Pretty J (2008) Agricultural sustainability: concepts, principles and evidence. *Philosophical Transactions of the Royal Society B-Biological Sciences*, **363**, 447-465, doi:10.1098/rstb.2007.2163.

Pugh TaM, Arneth A, Olin S *et al.* (2015) Simulated carbon emissions from land use change are substantially enhanced by accounting for agricultural management. *Environmental Research Letters*, **10**, doi:10.1088/1748-9326/10/12/124008.

Pugh TaM, Mackenzie AR, Hewitt CN *et al.* (2010) Simulating atmospheric composition over a South-East Asian tropical rainforest: performance of a chemistry box model. *Atmospheric Chemistry and Physics*, **10**, 279-298, doi:10.5194/acp-10-279-2010.

Pugh TaM, Muller C, Elliott J *et al.* (2016) Climate analogues suggest limited potential for intensification of production on current croplands under climate change. *Nature Communications*, **7**, doi:10.1038/Ncomms12608.

Pyle JA, Warwick NJ, Harris NRP *et al.* (2011) The impact of local surface changes in Borneo on atmospheric composition at wider spatial scales: coastal processes, land-use change and air quality. *Philosophical Transactions of the Royal Society B-Biological Sciences*, **366**, 3210-3224, doi:10.1098/rstb.2011.0060.

Queiroz C, Beilin R, Folke C, Lindborg R (2014) Farmland abandonment: threat or opportunity for biodiversity conservation? A global review. *Frontiers in Ecology and the Environment*, **12**, 288-296, doi:10.1890/120348.

Quesada B, Devaraju N, De Noblet-Ducoudre N, Arneth A (2017) Reduction of monsoon rainfall in response to past and future land use and land cover changes. *Geophysical Research Letters*, **44**, 1041-1050, doi:10.1002/2016GL070663.

Quillet A, Peng CH, Garneau M (2010) Toward dynamic global vegetation models for simulating vegetation-climate interactions and feedbacks: recent developments, limitations, and future challenges. *Environmental Reviews*, **18**, 333-353, doi:10.1139/A10-016.

Ramankutty N, Foley JA (1999) Estimating historical changes in global land cover: Croplands from 1700 to 1992. *Global Biogeochemical Cycles*, **13**, 997-1027, doi:10.1029/1999gb900046.

Randriamalala JR, Herve D, Randriamboavonjy JC, Carriere SM (2012) Effects of tillage regime, cropping duration and fallow age on diversity and structure of secondary vegetation in Madagascar. *Agriculture Ecosystems & Environment*, **155**, 182-193, doi:10.1016/j.agee.2012.03.020.

Ray DK, Mueller ND, West PC, Foley JA (2013) Yield Trends Are Insufficient to Double Global Crop Production by 2050. *Plos One*, **8**, doi:10.1371/journal.pone.0066428.

Ray DK, Ramankutty N, Mueller ND, West PC, Foley JA (2012) Recent patterns of crop yield growth and stagnation. *Nature Communications*, **3**, doi:10.1038/Ncomms2296.

Reilly J, Melillo J, Cai YX *et al.* (2012) Using Land To Mitigate Climate Change: Hitting the Target, Recognizing the Trade-offs. *Environmental Science & Technology*, **46**, 5672-5679, doi:10.1021/es2034729.

Rieu R, Allen PA, Plotze M, Pettke T (2007) Climatic cycles during a Neoproterozoic "snowball" glacial epoch. *Geology*, **35**, 299-302, doi:10.1130/G23400a.1.

Rockstrom J, Gaffney O, Rogelj J, Meinshausen M, Nakicenovic N, Schellnhuber HJ (2017) CLIMATE POLICY A roadmap for rapid decarbonization. *Science*, **355**, 1269-1271, doi:10.1126/science.aah3443.

Rockstrom J, Steffen W, Noone K *et al.* (2009) A safe operating space for humanity. *Nature*, **461**, 472-475, doi:10.1038/461472a.

Rogelj J, Den Elzen M, Hohne N *et al.* (2016a) Paris Agreement climate proposals need a boost to keep warming well below 2 degrees C. *Nature*, **534**, 631-639, doi:10.1038/nature18307.

Rogelj J, Luderer G, Pietzcker RC, Kriegler E, Schaeffer M, Krey V, Riahi K (2015) Energy system transformations for limiting end-of-century warming to below 1.5 degrees C. *Nature Climate Change*, **5**, 519–527, doi:10.1038/nclimate2572.

Rogelj J, Schaeffer M, Friedlingstein P *et al.* (2016b) Differences between carbon budget estimates unravelled. *Nature Climate Change,* **6**, 245-252, doi:10.1038/Nclimate2868.

Rolinski S, Müller C, Heinke J *et al.* (2017) Modeling vegetation and carbon dynamics of managed grasslands at the global scale with LPJmL 3.6. *Geoscientific Model Development Discussion,* doi:10.5194/gmd-2017-26.

Rosenkranz M, Pugh TaM, Schnitzler JP, Arneth A (2015) Effect of land-use change and management on biogenic volatile organic compound emissions - selecting climate-smart cultivars. *Plant Cell and Environment,* **38**, 1896-1912, doi:10.1111/pce.12453.

Rosenzweig C, Elliott J, Deryng D *et al.* (2014) Assessing agricultural risks of climate change in the 21st century in a global gridded crop model intercomparison. *Proceedings of the National Academy of Sciences of the United States of America,* **111**, 3268-3273, doi:10.1073/pnas.1222463110.

Rounsevell MDA, Arneth A, Alexander P *et al.* (2014) Towards decision-based global land use models for improved understanding of the Earth system. *Earth System Dynamics,* **5**, 117-137, doi:10.5194/esd-5-117-2014.

Ruddiman WF (2006) Orbital changes and climate. *Quaternary Science Reviews,* **25**, 3092-3112, doi:10.1016/j.quascirev.2006.09.001.

Saldarriaga JG, West DC, Tharp ML, Uhl C (1988) Long-Term Chronosequence of Forest Succession in the Upper Rio Negro of Colombia and Venezuela. *Journal of Ecology,* **76**, 938-958, doi:10.2307/2260625.

Samir KC, Lutz W (2017) The human core of the shared socioeconomic pathways: Population scenarios by age, sex and level of education for all countries to 2100. *Global Environmental Change-Human and Policy Dimensions,* **42**, 181-192, doi:10.1016/j.gloenvcha.2014.06.004.

Sampaio G, Nobre C, Costa MH, Satyamurty P, Soares BS, Cardoso M (2007) Regional climate change over eastern Amazonia caused by pasture and soybean cropland expansion. *Geophysical Research Letters,* **34**, doi:10.1029/2007gl030612.

Sanderman J, Hengl T, Fiske GJ (2017) Soil carbon debt of 12,000 years of human land use. *Proceedings of the National Academy of Sciences of the United States of America,* **114**, 9575-9580, doi:10.1073/pnas.1706103114.

Sanderson BM, O'neill BC, Tebaldi C (2016) What would it take to achieve the Paris temperature targets? *Geophysical Research Letters,* **43**, 7133-7142, doi:10.1002/2016GL069563.

Santangeli A, Toivonen T, Pouzols FM, Pogson M, Hastings A, Smith P, Moilanen A (2016) Global change synergies and trade-offs between renewable energy and biodiversity. *Global Change Biology Bioenergy,* **8**, 941-951, doi:10.1111/gcbb.12299.

Schaphoff S, Heyder U, Ostberg S, Gerten D, Heinke J, Lucht W (2013) Contribution of permafrost soils to the global carbon budget. *Environmental Research Letters,* **8**, doi:10.1088/1748-9326/8/1/014026.

Scharlemann JPW, Tanner EVJ, Hiederer R, Kapos V (2014) Global soil carbon: understanding and managing the largest terrestrial carbon pool. *Carbon Management,* **5**, 81-91, doi:10.4155/Cmt.13.77.

Schauberger B, Archontoulis S, Arneth A *et al.* (2017) Consistent negative response of US crops to high temperatures in observations and crop models. *Nature Communications,* **8**, doi:10.1038/ncomms13931.

Schimel DS, House JI, Hibbard KA *et al.* (2001) Recent patterns and mechanisms of carbon exchange by terrestrial ecosystems. *Nature,* **414**, 169-172, doi:10.1038/35102500.

Schleussner CF, Rogelj J, Schaeffer M *et al.* (2016) Science and policy characteristics of the Paris Agreement temperature goal. *Nature Climate Change,* **6**, 827-835, doi:10.1038/Nclimate3096.

Scholze M, Knorr W, Arnell NW, Prentice IC (2006) A climate-change risk analysis for world ecosystems. *Proceedings of the National Academy of Sciences of the United States of America,* **103**, 13116-13120, doi:10.1073/pnas.0601816103.

Schueler V, Fuss S, Steckel JC, Weddige U, Beringer T (2016) Productivity ranges of sustainable biomass potentials from non-agricultural land. *Environmental Research Letters,* **11**, doi:10.1088/1748-9326/11/7/074026.

Schurer AP, Mann ME, Hawkins E, Tett SFB, Hegerl GC (2017) Importance of the pre-industrial baseline for likelihood of exceeding Paris goals. *Nature Climate Change,* **7**, 563-567, doi:10.1038/Nclimate3345.

Schurgers G, Arneth A, Holzinger R, Goldstein AH (2009) Process-based modelling of biogenic monoterpene emissions combining production and release from storage. *Atmospheric Chemistry and Physics*, **9**, 3409-3423, doi:10.5194/acp-9-3409-2009.

Scott CE, Rap A, Spracklen DV *et al.* (2014) The direct and indirect radiative effects of biogenic secondary organic aerosol. *Atmospheric Chemistry and Physics*, **14**, 447-470, doi:10.5194/acp-14-447-2014.

Searle SY, Malins CJ (2014) Will energy crop yields meet expectations? *Biomass & Bioenergy*, **65**, 3-12, doi:10.1016/j.biombioe.2014.01.001.

Seidl R, Schelhaas MJ, Rammer W, Verkerk PJ (2014) Increasing forest disturbances in Europe and their impact on carbon storage. *Nature Climate Change*, **4**, 806-810, doi:10.1038/Nclimate2318.

Shevliakova E, Pacala SW, Malyshev S *et al.* (2009) Carbon cycling under 300 years of land use change: Importance of the secondary vegetation sink. *Global Biogeochemical Cycles*, **23**, doi:10.1029/2007gb003176.

Sillman S (1999) The relation between ozone, NOx and hydrocarbons in urban and polluted rural environments. *Atmospheric Environment*, **33**, 1821-1845, doi:10.1016/S1352-2310(98)00345-8.

Silver WL, Ostertag R, Lugo AE (2000) The potential for carbon sequestration through reforestation of abandoned tropical agricultural and pasture lands. *Restoration Ecology*, **8**, 394-407, doi:10.1046/j.1526-100x.2000.80054.x.

Sitch S, Friedlingstein P, Gruber N *et al.* (2015) Recent trends and drivers of regional sources and sinks of carbon dioxide. *Biogeosciences*, **12**, 653-679, doi:10.5194/bg-12-653-2015.

Sitch S, Smith B, Prentice IC *et al.* (2003) Evaluation of ecosystem dynamics, plant geography and terrestrial carbon cycling in the LPJ dynamic global vegetation model. *Global Change Biology*, **9**, 161-185, doi:10.1046/j.1365-2486.2003.00569.x.

Slade R, Bauen A, Gross R (2014) Global bioenergy resources. *Nature Climate Change*, **4**, 99-105, doi:10.1038/Nclimate2097.

Smith B, Prentice IC, Sykes MT (2001) Representation of vegetation dynamics in the modelling of terrestrial ecosystems: comparing two contrasting approaches within European climate space. *Global Ecology and Biogeography*, **10**, 621-637, doi:10.1046/j.1466-822X.2001.t01-1-00256.x.

Smith B, Warlind D, Arneth A, Hickler T, Leadley P, Siltberg J, Zaehle S (2014) Implications of incorporating N cycling and N limitations on primary production in an individual-based dynamic vegetation model. *Biogeosciences*, **11**, 2027-2054, doi:10.5194/bg-11-2027-2014.

Smith P, Davis SJ, Creutzig F *et al.* (2016a) Biophysical and economic limits to negative CO2 emissions. *Nature Climate Change*, **6**, 42-50, doi:10.1038/Nclimate2870.

Smith P, House JI, Bustamante M *et al.* (2016b) Global change pressures on soils from land use and management. *Global Change Biology*, **22**, 1008-1028, doi:10.1111/gcb.13068.

Sonntag S, Pongratz J, Reick CH, Schmidt H (2016) Reforestation in a high-CO2 world-Higher mitigation potential than expected, lower adaptation potential than hoped for. *Geophysical Research Letters*, **43**, 6546-6553, doi:10.1002/2016GL068824.

Spiegl TC, Paeth H, Frimmel HE (2015) Evaluating key parameters for the initiation of a Neoproterozoic Snowball Earth with a single Earth System Model of intermediate complexity. *Earth and Planetary Science Letters*, **415**, 100-110, doi:10.1016/j.epsl.2015.01.035.

Stehfest E, Van Vuuren D, Kram T *et al.* (2014) Integrated Assessment of Global Environmental Change with IMAGE 3.0 : Model description and policy applications. The Hague: PBL Netherlands Environmental Assessment Agency.

Sterling SM, Ducharne A, Polcher J (2013) The impact of global land-cover change on the terrestrial water cycle. *Nature Climate Change*, **3**, 385-390, doi:10.1038/Nclimate1690.

Stoate C, Boatman ND, Borralho RJ, Carvalho CR, De Snoo GR, Eden P (2001) Ecological impacts of arable intensification in Europe. *Journal of Environmental Management*, **63**, 337-365, doi:10.1006/jema.2001.0473.

Stocker BD, Feissli F, Strassmann KM, Spahni R, Joos F (2014) Past and future carbon fluxes from land use change, shifting cultivation and wood harvest. *Tellus Series B-Chemical and Physical Meteorology*, **66**, doi:10.3402/Tellusb.V66.23188.

Swann ALS, Fung IY, Chiang JCH (2012) Mid-latitude afforestation shifts general circulation and tropical precipitation. *Proceedings of the National Academy of Sciences of the United States of America,* **109**, 712-716, doi:10.1073/pnas.1116706108.

Tavoni M, Socolow R (2013) Modeling meets science and technology: an introduction to a special issue on negative emissions. *Climatic Change,* **118**, 1-14, doi:10.1007/s10584-013-0757-9.

Thomas CD, Cameron A, Green RE *et al.* (2004) Extinction risk from climate change. *Nature,* **427**, 145-148, doi:10.1038/nature02121.

Thonicke K, Venevsky S, Sitch S, Cramer W (2001) The role of fire disturbance for global vegetation dynamics: coupling fire into a Dynamic Global Vegetation Model. *Global Ecology and Biogeography,* **10**, 661-677, doi:10.1046/j.1466-822x.2001.00175.x.

Tian HQ, Lu CQ, Ciais P *et al.* (2016) The terrestrial biosphere as a net source of greenhouse gases to the atmosphere. *Nature,* **531**, 225-228, doi:10.1038/nature16946.

Tian HQ, Lu CQ, Yang J *et al.* (2015) Global patterns and controls of soil organic carbon dynamics as simulated by multiple terrestrial biosphere models: Current status and future directions. *Global Biogeochemical Cycles,* **29**, 775-792, doi:10.1002/2014GB005021.

Tilman D, Cassman KG, Matson PA, Naylor R, Polasky S (2002) Agricultural sustainability and intensive production practices. *Nature,* **418**, 671-677, doi:10.1038/nature01014.

Todd-Brown KEO, Randerson JT, Post WM, Hoffman FM, Tarnocai C, Schuur EaG, Allison SD (2013) Causes of variation in soil carbon simulations from CMIP5 Earth system models and comparison with observations. *Biogeosciences,* **10**, 1717-1736, doi:10.5194/bg-10-1717-2013.

Tokarska KB, Zickfeld K (2015) The effectiveness of net negative carbon dioxide emissions in reversing anthropogenic climate change. *Environmental Research Letters,* **10**, doi:10.1088/1748-9326/10/9/094013.

Tubiello FN, Salvatore M, Ferrara AF *et al.* (2015) The Contribution of Agriculture, Forestry and other Land Use activities to Global Warming, 1990-2012. *Global Change Biology,* **21**, 2655-2660, doi:10.1111/gcb.12865.

Uhl C, Buschbacher R, Serrao EaS (1988) Abandoned Pastures in Eastern Amazonia .1. Patterns of Plant Succession. *Journal of Ecology,* **76**, 663-681, doi:10.2307/2260566.

Unger N (2014) Human land-use-driven reduction of forest volatiles cools global climate. *Nature Climate Change,* **4**, 907-910, doi:10.1038/nclimate2347.

United Nations, Department of Economic and Social Affairs, Population Division (2015) World Population Prospects: The 2015 Revision, Key Findings and Advance Tables. New York.

Val Martin M, Heald CL, Lamarque JF, Tilmes S, Emmons LK, Schichtel BA (2015) How emissions, climate, and land use change will impact mid-century air quality over the United States: a focus on effects at national parks. *Atmospheric Chemistry and Physics,* **15**, 2805-2823, doi:10.5194/acp-15-2805-2015.

Valin H, Sands RD, Van Der Mensbrugghe D *et al.* (2014) The future of food demand: understanding differences in global economic models. *Agricultural Economics,* **45**, 51-67, doi:10.1111/agec.12089.

Van Dijk AIJM, Van Noordwijk M, Calder IR, Bruijnzeel SLA, Schellekens J, Chappell NA (2009) Forest-flood relation still tenuous - comment on 'Global evidence that deforestation amplifies flood risk and severity in the developing world' by Bradshaw et al. *Global Change Biology,* **15**, 110-115, doi:10.1111/j.1365-2486.2008.01708.x.

Van Vliet J, Bregt AK, Brown DG, Van Delden H, Heckbert S, Verburg PH (2016) A review of current calibration and validation practices in land-change modeling. *Environmental Modelling & Software,* **82**, 174-182, doi:10.1016/j.envsoft.2016.04.017.

Visconti P, Pressey RL, Giorgini D *et al.* (2011) Future hotspots of terrestrial mammal loss. *Philosophical Transactions of the Royal Society B: Biological Sciences,* **366**, 2693–2702, doi:10.1098/rstb.2011.0105.

Waha K, Van Bussel LGJ, Muller C, Bondeau A (2012) Climate-driven simulation of global crop sowing dates. *Global Ecology and Biogeography,* **21**, 247-259, doi:10.1111/j.1466-8238.2011.00678.x.

Wandelli EV, Fearnside PM (2015) Secondary vegetation in central Amazonia: Land-use history effects on aboveground biomass. *Forest Ecology and Management,* **347**, 140-148, doi:10.1016/j.foreco.2015.03.020.

Wang Z, Zeng XB (2010) Evaluation of Snow Albedo in Land Models for Weather and Climate Studies. *Journal of Applied Meteorology and Climatology,* **49**, 363-380, doi:10.1175/2009JAMC2134.1.

Warlind D, Smith B, Hickler T, Arneth A (2014) Nitrogen feedbacks increase future terrestrial ecosystem carbon uptake in an individual-based dynamic vegetation model. *Biogeosciences,* **11**, 6131-6146, doi:10.5194/bg-11-6131-2014.

Warszawski L, Frieler K, Huber V, Piontek F, Serdeczny O, Schewe J (2014) The Inter-Sectoral Impact Model Intercomparison Project (ISI-MIP): Project framework. *Proceedings of the National Academy of Sciences of the United States of America,* **111**, 3228-3232, doi:10.1073/pnas.1312330110.

Watts N, Adger WN, Agnolucci P *et al.* (2015) Health and climate change: policy responses to protect public health. *Lancet,* **386**, 1861-1914, doi:10.1016/S0140-6736(15)60854-6.

Whitehead PG, Wilby RL, Battarbee RW, Kernan M, Wade AJ (2009) A review of the potential impacts of climate change on surface water quality. *Hydrological Sciences Journal-Journal Des Sciences Hydrologiques,* **54**, 101-123, doi:10.1623/hysj.54.1.101.

Wilkenskjeld S, Kloster S, Pongratz J, Raddatz T, Reick CH (2014) Comparing the influence of net and gross anthropogenic land-use and land-cover changes on the carbon cycle in the MPI-ESM. *Biogeosciences,* **11**, 4817-4828, doi:10.5194/bg-11-4817-2014.

Wilkinson S, Mills G, Illidge R, Davies WJ (2012) How is ozone pollution reducing our food supply? *Journal of Experimental Botany,* **63**, 527-536, doi:10.1093/jxb/err317.

Williamson P (2016) Scrutinize CO2 removal methods. *Nature,* **530**, 153-155, doi:10.1038/530153a.

Wiltshire A, Davies-Barnard T (2015) Planetary limits to BECCS negative emissions. In: *AVOID 2 WPD.2a Report 1*.

Wu S, Mickley LJ, Kaplan JO, Jacob DJ (2012) Impacts of changes in land use and land cover on atmospheric chemistry and air quality over the 21st century. *Atmospheric Chemistry and Physics,* **12**, 1597-1609, doi:10.5194/acp-12-1597-2012.

Xu M, Hoffman F (2015) Evaluations of CMIP5 simulations over cropland. *Proc. SPIE 9610, Remote Sensing and Modeling of Ecosystems for Sustainability XII,* **961003**, doi:10.1117/12.2192586.

Xu YY, Ramanathan V (2017) Well below 2 degrees C: Mitigation strategies for avoiding dangerous to catastrophic climate changes. *Proceedings of the National Academy of Sciences of the United States of America,* **114**, 10315-10323, doi:10.1073/pnas.1618481114.

Yang YH, Luo YQ, Finzi AC (2011) Carbon and nitrogen dynamics during forest stand development: a global synthesis. *New Phytologist,* **190**, 977-989, doi:10.1111/j.1469-8137.2011.03645.x.

Zachos J, Pagani M, Sloan L, Thomas E, Billups K (2001) Trends, rhythms, and aberrations in global climate 65 Ma to present. *Science,* **292**, 686-693, doi:10.1126/science.1059412.

Zachos JC, Dickens GR, Zeebe RE (2008) An early Cenozoic perspective on greenhouse warming and carbon-cycle dynamics. *Nature,* **451**, 279-283, doi:10.1038/nature06588.

Zaehle S, Ciais P, Friend AD, Prieur V (2011) Carbon benefits of anthropogenic reactive nitrogen offset by nitrous oxide emissions. *Nature Geoscience,* **4**, 601-605, doi:10.1038/ngeo1207.

Zemp DC, Schleussner CF, Barbosa HMJ *et al.* (2014) On the importance of cascading moisture recycling in South America. *Atmospheric Chemistry and Physics,* **14**, 13337-13359, doi:10.5194/acp-14-13337-2014.

Zhu ZC, Piao SL, Myneni RB *et al.* (2016) Greening of the Earth and its drivers. *Nature Climate Change,* **6**, 791–795, doi:10.1038/Nclimate3004.

Appendix

The original papers published in open access journals are attached in the following.

Earth Syst. Dynam., 7, 745–766, 2016
www.earth-syst-dynam.net/7/745/2016/
doi:10.5194/esd-7-745-2016

Earth System Dynamics
Open Access
EGU

Impacts of land-use history on the recovery of ecosystems after agricultural abandonment

Andreas Krause[1], **Thomas A. M. Pugh**[1,2], **Anita D. Bayer**[1], **Mats Lindeskog**[3], **and Almut Arneth**[1]

[1]Karlsruhe Institute of Technology, Institute of Meteorology and Climate Research – Atmospheric Environmental Research (IMK-IFU), Kreuzeckbahnstr. 19, 82467 Garmisch-Partenkirchen, Germany
[2]School of Geography, Earth & Environmental Science and Birmingham Institute of Forest Research, University of Birmingham, Birmingham, B15 2TT, UK
[3]Department of Physical Geography and Ecosystem Science, Lund University, 22362 Lund, Sweden

Correspondence to: Andreas Krause (andreas.krause@kit.edu)

Received: 16 March 2016 – Published in Earth Syst. Dynam. Discuss.: 14 April 2016
Revised: 26 August 2016 – Accepted: 29 August 2016 – Published: 15 September 2016

Abstract. Land-use changes have been shown to have large effects on climate and biogeochemical cycles, but so far most studies have focused on the effects of conversion of natural vegetation to croplands and pastures. By contrast, relatively little is known about the long-term influence of past agriculture on vegetation regrowth and carbon sequestration following land abandonment. We used the LPJ-GUESS dynamic vegetation model to study the legacy effects of different land-use histories (in terms of type and duration) across a range of ecosystems. To this end, we performed six idealized simulations for Europe and Africa in which we made a transition from natural vegetation to either pasture or cropland, followed by a transition back to natural vegetation after 20, 60 or 100 years. The simulations identified substantial differences in recovery trajectories of four key variables (vegetation composition, vegetation carbon, soil carbon, net biome productivity) after agricultural cessation. Vegetation carbon and composition typically recovered faster than soil carbon in subtropical, temperate and boreal regions, and vice versa in the tropics. While the effects of different land-use histories on recovery periods of soil carbon stocks often differed by centuries across our simulations, differences in recovery times across simulations were typically small for net biome productivity (a few decades) and modest for vegetation carbon and composition (several decades). Spatially, we found the greatest sensitivity of recovery times to prior land use in boreal forests and subtropical grasslands, where post-agricultural productivity was strongly affected by prior land management. Our results suggest that land-use history is a relevant factor affecting ecosystems long after agricultural cessation, and it should be considered not only when assessing historical or future changes in simulations of the terrestrial carbon cycle but also when establishing long-term monitoring networks and interpreting data derived therefrom, including analysis of a broad range of ecosystem properties or local climate effects related to land cover changes.

1 Introduction

Historically, many natural forests or grasslands on Earth have been cleared or cultivated for grazing, timber, food production, mining or settlements. However, land-use change (LUC) in these areas has rarely been continuous, and land cover and management have often changed for a variety of reasons (Burgi and Turner, 2002). Based on the HYDE dataset, Campbell et al. (2008) estimated that 269 Mha of cropland and 479 Mha of pasture have been abandoned between 1700 and 2000. Recently, agricultural cessation rates have risen globally, especially in the temperate region. For example, during the last decades, large areas in Europe previously used for pasture or crop cultivation have been abandoned (e.g., Schierhorn et al., 2013; Smith et al., 2005). Following agricultural abandonment, and in the absence of fur-

ther anthropogenic influence, natural vegetation recolonizes in a typical succession from herbaceous vegetation to shrubland and forests, if environmental conditions are suitable for tree growth. These secondary forests act as an important carbon (C) sink during the years of regrowth, thereby reducing the growth rate of global atmospheric CO_2 concentration (Pan et al., 2011).

The immediate effects of land-use (LU) practices on C fluxes and nutrient cycles have been studied in some detail over recent decades. Generally, agriculture significantly reduces C and, in the absence of supplementary sources, nitrogen (N) pools due to initial deforestation, reduced soil litter input, and accelerated soil decomposition and erosion (Davidson and Ackerman, 1993; Fujisaki et al., 2015; Guo and Gifford, 2002; McLauchlan, 2006; Murty et al., 2002). Pasture soils can be an exception as they have been found to accumulate C, depending on location and management (McSherry and Ritchie, 2013; Milchunas and Lauenroth, 1993). The long-term importance of past LU on ecosystems, however, was recognized only recently, and much less effort has been put so far into the investigation of legacy effects of LU history on ecosystem processes, how long these effects persist, or whether they may even be irreversible (Chazdon, 2014; Compton and Boone, 2000; Cramer et al., 2008; Hobbs et al., 2009; McLauchlan, 2006). This is important not only for understanding present-day ecological systems but also because, due to demographical, social, technological, economic and environmental changes, LUC and land abandonment will continue to occur in the future (Hurtt et al., 2011).

Most observational studies that looked at the recovery of ecosystems after agricultural cessation focused on the first years of succession. Analyses of the long-term effects of historical LU are often limited by the availability of adequate LU information and the absence of undisturbed ecosystems, and usually rely on chronosequences (Chazdon, 2003; Knops and Tilman, 2000). Only a few long-term observational study plots like the one maintained at the Rothamsted Experimental Station (e.g., Poulton et al., 2003) exist. Differences between (near) pristine and post-agricultural forests or grasslands have been reported to persist for decades or centuries after agricultural abandonment for various variables, including soil pH (Falkengren-Grerup et al., 2006); microbial communities (Fichtner et al., 2014); soil C, N and phosphorus (Compton and Boone, 2000); and other nutrients (Wall and Hytonen, 2005). Furthermore, aboveground (ag) biomass (Wandelli and Fearnside, 2015), percentage vegetation cover (Lesschen et al., 2008), biodiversity (Vellend, 2004), species composition (Aide et al., 2000) and structure (Bellemare et al., 2002) remained affected for years to decades, or even longer. These effects have consequences, not only for the C sink capacity of the ecosystem but also for water and energy exchange between the land and the atmosphere (Foley et al., 2003), which also has important, albeit still highly uncertain, implications for regional climate change (e.g., Arora and Montenegro, 2011; Brovkin et al., 2013; de Noblet-Ducoudre et al., 2012). Some studies have detected an influence of ancient agriculture on forest composition and diversity even thousands of years later (Dambrine et al., 2007; Dupouey et al., 2002; Willis et al., 2004). However, the persistence of legacy effects varies considerably with former LU, geographical location, sampling methods and examined variables, making recovery trajectories often hard to predict (Cramer et al., 2008; Foster et al., 2003; Guariguata and Ostertag, 2001; Norden et al., 2015; Post and Kwon, 2000; Suding et al., 2004).

In this study, we performed idealized simulations with the LPJ-GUESS dynamic global vegetation model (DGVM) to explore the importance of agricultural LU history in terms of type and duration for the regeneration of ecosystems and C stocks and fluxes under a range of environmental conditions. We converted natural vegetation to either pasture or cropland, followed by a re-transition to natural vegetation after time periods of 20, 60 and 100 years. While there are numerous variables suitable to measure recovery (Chazdon, 2003; Martin et al., 2016), we analyzed recovery times for vegetation composition (represented here by the dominant plant functional type), vegetation C, soil C, and net biome productivity to evaluate the longevity of the effects of LU history on the C cycle component of ecosystems and to ascertain whether the system eventually recovers to its pre-disturbance state.

2 Methods

2.1 LPJ-GUESS

LPJ-GUESS is a process-based DGVM that is driven by climate, atmospheric CO_2 concentration and N input (Smith et al., 2014). Plants are attributed to one of 11 plant functional types (PFTs, nine groups of tree species and two grasses) which are distinguished, for instance, in terms of their climate preferences for establishment and survival, photosynthetic pathways, growth rates, and growth strategies (see Table A1 for PFT acronyms and names). Vegetation dynamics and composition at a given location result from competition between plants for light and soil resources in a number of independent replicate patches (50 in this study), averaged per $0.5° \times 0.5°$ grid cell. Wildfire is included in the model and, additionally, stochastic disturbances kill all the biomass in a patch, representing, for example, storm or insect damages, with a typical return period of 100 years (Smith et al., 2014). Recent model updates include the representation of LUC (Lindeskog et al., 2013) and the implementation of the N cycle in natural vegetation and grasses (Smith et al., 2014). The representation of the N cycle is crucial for this study because previous agricultural N dynamics, such as extraction through harvest and input through fertilization, can greatly affect ecosystems even after many decades (Richter et al., 2000).

Conversion of natural to managed land in LPJ-GUESS is characterized by the initial killing of all living vegetation in the affected area. The corresponding woody biomass is partly oxidized immediately (67–76 %) and partly transferred to the product (21 %) or litter (3–12 %) pool. Ten percent of the leaves are oxidized, while the rest of the leaves and the fine roots enter the litter pool. Only the litter thus remains in the ecosystem subsequent to land conversion. Pastures are represented by preventing tree establishment and wildfires and by splitting the aboveground biomass of the grasses equally between atmosphere (harvest) and litter at the end of each year. Crops were represented by grass PFTs modified to mimic aspects of cropland important for the C and N cycles. Settings for croplands and pastures were as follows:

1. For transitions from natural vegetation to cropland, we transferred only 3 % of the cleared woody biomass to the litter instead of 12 % for natural vegetation–pasture transitions. This accounts for the practice that farmers would try to remove as many coarse roots as possible before planting of crops.

2. Harvest efficiency (in this study: fraction of aboveground biomass that is oxidized) was $0.5\,\mathrm{yr}^{-1}$ for pasture, representing the net effect of grazing processes (Lindeskog et al., 2013). For crop simulations we changed the harvest efficiency to $0.8\,\mathrm{yr}^{-1}$, representing simplified crop harvest, as in Lindeskog et al. (2013).

3. While we removed 100 % of harvested N biomass for croplands, we changed this value to 65 % for pastures. That accounts for significant urine N regain from animals fed on pastures (Dean et al., 1975; Lauenroth and Milchunas, 1992).

4. Root turnover rate was $0.7\,\mathrm{yr}^{-1}$ for pasture and was adapted to $1.0\,\mathrm{yr}^{-1}$ for croplands to represent the annual plant types used in most croplands.

5. In croplands we estimated tillage effects by increasing heterotrophic respiration by a factor of 1.94 (Pugh et al., 2015).

6. We simulated N fertilization in croplands by applying $75\,\mathrm{kg\,ha}^{-1}\,\mathrm{yr}^{-1}$ equally throughout the year to sustain crop productivity with time. This value represents a compromise between higher values presently found in parts of Europe and lower values in most of Africa (e.g., Potter et al., 2010).

After patch-destroying disturbances or managed land converting back to natural vegetation, there is a typical succession from grasses to light-demanding pioneer trees, eventually followed in many ecosystems by the establishment of shade-tolerant PFTs. It has been shown that LPJ-GUESS is able to realistically simulate observed succession pathways and species variations (Hickler et al., 2004; Smith et al., 2014).

2.2 Simulation setup

During spin-up (500 years) and the simulation period (900 years), we forced LPJ-GUESS with temperature-detrended, repeated 1981–2000 climate from the University of East Anglia Climate Research Unit 3.21 dataset (CRU, 2013), 1990s mean N deposition (Lamarque et al., 2013) and a fixed atmospheric CO_2 mixing ratio of 356 ppmv. We ran the model for Europe and Africa (33° E to 55° W), covering a wide range of environmental conditions. These regions include all major biomes (Smith et al., 2014). We chose Africa and Europe for the simulation domain because the original LU version of the model was evaluated against observations in Africa (Lindeskog et al., 2013) and to limit the computational expense of the simulations. We did not intend to realistically represent typical crop and pasture management across the domain (i.e., the spatial variability in fertilizer use, multiple cropping systems, or irrigation). For all simulations we used potential natural vegetation cover to spin up the model, followed by a transition to either pasture or croplands directly after spin-up and a transition back to natural vegetation after time periods of 20, 60 and 100 years. This resulted in three pasture (P20, P60, P100) and three cropland (C20, C60, C100) simulations. Additionally, we performed a reference simulation in which natural vegetation was retained throughout the whole simulation period.

2.3 Analyzed grid cells and biome classification

To facilitate the interpretation, we classified each grid cell to one biome. We used the same classification rules as Smith et al. (2014), aggregated to eight biomes as in Bayer et al. (2015). Afterwards, we excluded grid cells from the analyses which were classified as desert or tundra, had a mean net primary productivity (NPP) below $0.1\,\mathrm{kg\,C\,m}^{-2}\,\mathrm{yr}^{-1}$, or were located above 62.5° N, making the assumption that the relevance of these low-production areas for agriculture is negligible.

2.4 Analyzed variables and definition of recovery

We studied the influence of LU history on ecosystems by analyzing four key variables: dominant PFT, vegetation C, soil C (excluding litter) and net biome productivity (NBP). NBP is the net atmosphere–land carbon flux after C losses associated with respiratory fluxes, fire, harvest, land clearing and decomposition of LUC product pools are subtracted from gross primary productivity. We investigated the legacy effects of LU history by calculating a recovery time for each variable, simulation and grid cell after the conversion back to natural vegetation. For vegetation C, soil C and NBP, recovery time was defined as the year in which the 20-year running mean of the variable exceeded the threshold of one standard deviation (σ) below the mean of the reference simulation (full simulation period) for the first time after agricultural abandonment. σ was calculated on the 20-year running

mean of the reference simulation. To avoid "false-positive" identifications of recovery in cases for which the variable of interest was initially within 1σ but then exhibited dynamics taking it outside this range (e.g., soil C in Fig. A1), we applied an additional criterion of whether the minimum after the transition to natural vegetation occurred in the first 200 years and if it was below the mean minus 1σ threshold. If that was the case, the condition was expanded so that the variable could only be defined as recovered after the year in which the minimum occurred ("minimum rule"). A 200-year window was chosen because the minimum occurred within the first 200 years for all biome averages of all variables and simulations. If the minimum was located after 200 years, we assumed the minimum to be a result of natural variability and recovery was achieved as soon as the variable in question exceeded the threshold of 1σ below the reference mean. Figure A1 shows an example of how soil C recovery was calculated for one site.

For the dominant PFT recovery, we first identified which PFT dominates each grid cell in the reference simulation based on the annual maximum leaf area index (LAI) amongst PFTs. We then checked for dominant PFT recovery in the same way as we did for vegetation C, soil C and NBP (i.e., whether its LAI exceeded the threshold of 1σ below the reference simulation mean; condition 1) but additionally checked whether its LAI was also larger than the LAI of any other PFT in the same simulation and year (i.e., the dominant PFT is the same as in the reference simulation, condition 2). Thus, dominant PFT recovery was only possible if both conditions were fulfilled. For example, if the temperate broadleaved evergreen (TeBS) tree was the dominant PFT in the reference simulation (with an average maximum LAI of, for example, 3.0 and standard deviation of ± 0.2), dominant PFT recovery in a specific LU simulation (e.g., P20) would occur once the LAI of TeBS in this simulation (a) hits the threshold of 2.8 ($3.0 - 0.2$, condition 1) and (b) is larger than the LAI of any other PFT in P20 in the specific year – i.e., TeBS is the dominant PFT in the grid cell (condition 2). For all variables, the recovery time was capped at 800 years after reconversion to natural vegetation, the point when simulations ended. Recovery times of 800 years thus represent a lower limit. However, the actual recovery time in these cases could theoretically lie between 801 years and infinity.

3 Results

3.1 Reference simulation

Maps of simulated vegetation and soil C, as well as dominant PFT and biomes derived from PFT composition for the reference simulation, are shown in Fig. 1. The salient features of biome and C storage distribution at the regional scale are captured (Haxeltine and Prentice, 1996; Scharlemann et al., 2014). Vegetation C reaches its highest values in tropical forests of central Africa and decreases towards the deserts of southern and northern Africa. Patterns are more homogeneous in Europe, where most areas store 5–10 $\mathrm{kg\,C\,m^{-2}}$. Similar to vegetation C, soil C in the (sub)tropics also decreases with drier conditions; however, the differences are small, with typical values of 5–10 $\mathrm{kg\,C\,m^{-2}}$. Soils in the temperate and southern boreal ecosystems of Europe generally store more C (usually $> 10\,\mathrm{kg\,C\,m^{-2}}$), especially in colder environments. While Europe is mostly dominated by woody PFTs (e.g., TeBS is the acronym for temperate broadleaved summergreen tree), in Africa there is a shift from C_3 and C_4 grasses in the dry regions to trees in the humid tropics. This gradient also appears in the corresponding biome map: in Africa and the Arabian Peninsula, LPJ-GUESS reproduces the transition from grasslands to savannas and tropical forests (TrFo) as the Equator is approached. Europe is mostly classified as temperate forests (TeFo), with some boreal forests (BoFo) in the north and some shrublands/savannas in the south.

3.2 Dominant PFT recovery

The LAI of the dominant PFT recovers on average within around one century for all LU histories (Fig. 2). Maps of the recovery time (Fig. 3) show distinct geographical patterns which occur in all simulations. Most subtropical grasslands and savannas, and parts of the temperate and boreal forests, recover within several decades, some grasslands even within 5 years. In contrast, recovery times are clearly longer (> 100 years) in other parts of the temperate forests and in the tropical forests. Long recovery is associated with woody successional vegetation dynamics, as slow-recovering areas are usually dominated by temperate broadleaved summergreen and tropical broadleaved evergreen forests (compare PFT distribution in Fig. 1). These are shade-tolerant PFTs that establish only slowly after disturbances. For 84 % of all analyzed grid cells, condition 1 (LAI recovery) was the delaying condition for dominant PFT recovery (numbers exemplified for the P60 simulation), compared to only 3 % for condition 2 (dominance recovery). For the remaining grid cells, both conditions were fulfilled in the same year.

Overall, differences across simulations of different LU histories are moderate, with generally only small differences in temperate forests, savannas and shrublands (Fig. 3; see also biome averages in Table 1 and the histogram in Fig. A2). Areas of major differences are central Africa, where P20 recovers faster than other simulations because post-agricultural net mineralization rates are higher in this region for P20 than for the other simulations (Fig. 4), thereby relatively increasing post-agricultural N availability compared to the other simulations (Fig. 5), and the African Mediterranean coast, where croplands recover much faster because the reduced C : N ratio in the soil (not shown) enhances N mineralization and thus plant N availability compared to pastures. Furthermore, in parts of the boreal zone recovery takes several hundred years for C100 instead of a few decades for the other sim-

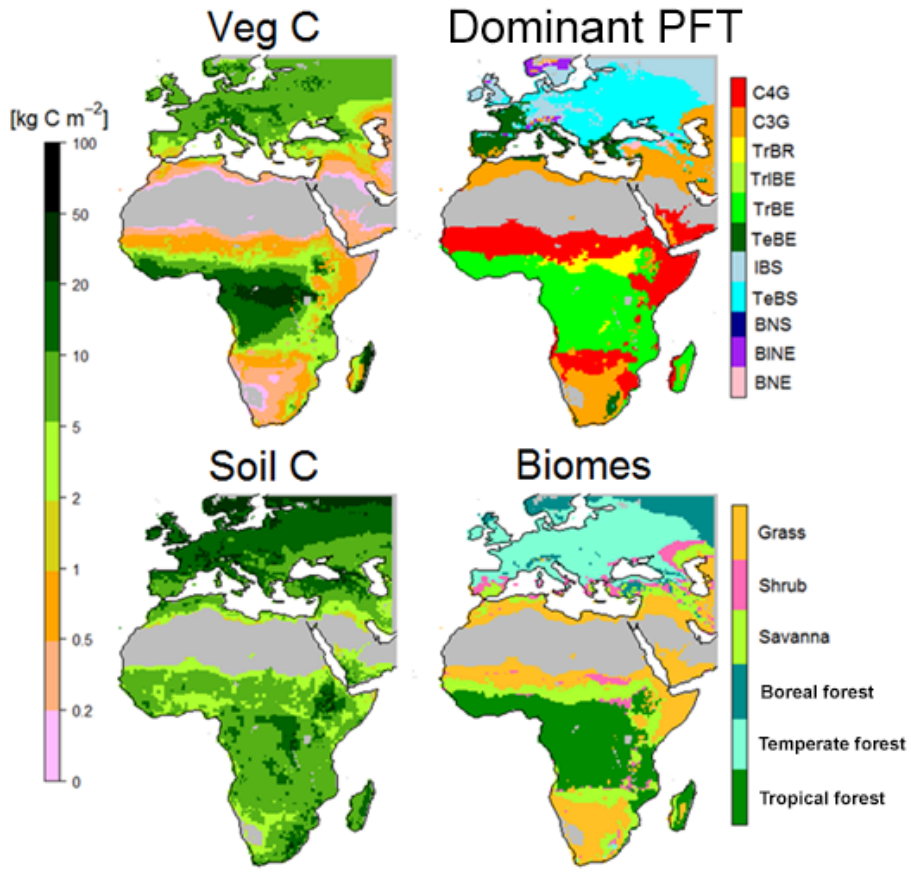

Figure 1. Vegetation C (kg C m^{-2}) for the reference simulation, averaged over the whole simulation period of 900 years (upper left panel), soil C (kg C m^{-2}) (lower left panel), dominant PFT (upper right panel), and corresponding biomes (lower right panel). Grid cells with a NPP below 0.1 kg C m^{-2} yr^{-1}, deserts and tundra, and latitudes above 62.5° N are masked in grey. PFT abbreviations are given in Table A1.

ulations because lower available N levels relatively reduce the growth of IBS (the dominant PFT in this region) compared to other woody PFTs. Figure 6 shows the maximum differences between recovery times across all simulations per biome (black dots), as well as across a subset of simulations (colored squares and triangles). The differences were first calculated for each grid cell and only then averaged over biomes, thereby providing an estimate of the relative importance of former LU duration versus former LU type on recovery times. While substantial differences occur across the pasture simulations (P20, P60, P100) in tropical forests, savannas and grasslands, and across cropland simulations (C20, C60, C100) in boreal forests (emphasizing the importance of LU duration in these regions), major differences between P100 and C100 occur in boreal forests and grasslands (emphasizing the importance of LU type if agricultural duration was long). On the other hand, in our simulations, dominant PFT recovery in temperate forests is hardly influenced by the type of former LU or, conversely, pasture duration has negligible effects on boreal forest recovery. Interestingly, temperate forests recover faster for P100 and C100 then for P20 and C20. This pattern is generally restricted to areas where the TeBS PFT dominates. We interpret this behavior as reduced soil N favoring TeBS in the competition with other tree PFTs, thereby reaching its background LAI levels earlier.

3.3 Vegetation C recovery

Compared to dominant PFT, recovery occurs slightly later for vegetation C (Fig. 2, Table 1). Spatial patterns look more homogeneous than for the dominant PFT (Fig. 3). While most grasslands recover within a few decades for all simulations, in particular so for post-cropland recovery, recovery occurs only after several decades or centuries in forest ecosystems. Lower standard deviations for the mean differences in vegetation C recovery times compared to the standard deviations for the mean differences in dominant PFT recovery times for most biomes (Fig. 6a and b) reflect the spatially more uniform response of vegetation C recovery. Exceptions are tropical forests and grasslands, where the standard deviation is higher for vegetation C recovery compared to dominant PFT recovery.

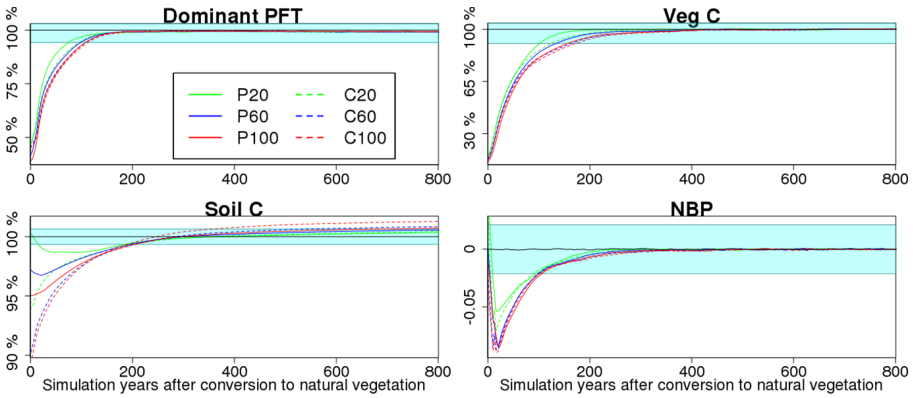

Figure 2. Time series (20-year running mean) of dominant PFT, vegetation C, soil C and NBP for the different experiments, starting from the time of reconversion to natural vegetation and area-averaged over all grid cells. Dominant PFT, vegetation C and soil C are shown in relative values compared to reference simulation mean, while NBP is shown as absolute values ($kg\,C\,m^{-2}\,yr^{-1}$) because values cannot be presented relative to a zero background. The cyan-shaded area corresponds to reference simulation mean $\pm\,1\sigma$. Note the different scales on the y axes.

Significant differences in recovery times occur between simulations of different LU types that have the same duration, and between simulations of the same LU type but with different duration. For example, in the grasslands and savannas of southern, eastern and northern Africa, former croplands recover much faster than former pastures (see also Table 1 and Fig. A2) because post-agricultural N availability is enhanced in these regions (Fig. 5). In former croplands in these environments, the combined effect of fertilizing and harvest is a net N flux to the ecosystem (not shown) and mineralization rates are enhanced after cropland abandonment (Fig. 4). This net N flux can partially be explained by high levels of water stress in these savannas and grasslands, resulting in greater C and N allocation to roots relative to leaves and thereby decreased harvest removal in this region (Fig. A3). Conversely, recovery in northern European forests is delayed for C60 and, to an even greater extent, C100 because in this region N removal by annual harvest exceeds N addition through fertilization during the agricultural period (not shown) and post-agricultural N mineralization rates in this region are substantially reduced compared to the other simulations many decades or even a few centuries after abandonment (Fig. 4). Differences in vegetation recovery times resulting from agricultural duration are mostly found in temperate and boreal forests for the cropland simulations (here longer durations result in longer recovery times due to reduced N availability, Fig. 5) and in tropical forests and shrublands for the pasture simulations, emphasizing the importance of agricultural duration in these regions (see also Fig. 6b).

3.4 Soil C recovery

Relative depletion of soil C content under crop and pasture LU is not as large (loss of 0–11 % compared to the reference simulation) as for vegetation C (Fig. 2). However, regeneration proceeds over longer timescales due to slower C accumulation in soils than in vegetation. C depletion is generally more pronounced for former crops than for pastures due to the greater harvest efficiency, which leads to more biomass removed each year, and the effect of tillage enhancing soil respiration (Sect. 2.1). Upon re-conversion, soil C accumulation is delayed for the pasture simulations compared to the cropland simulations, especially for P20, where the residual roots and other litter left after the original deforestation event continue to decay and soil C decreases for some decades. The general delay for pastures is associated with larger heterotrophic respiration rates (not shown) compared to rates calculated in recovering croplands.

Soil C recovery rates are highly latitude-dependent (Fig. 3), being much slower in temperate ($\sim$ 250 years) and boreal forests ($\sim$ 400 years) than in the tropics ($<$ 100 years, sometimes even within 5 years). Initial soil C depletions are larger in higher latitudes, while these regions also suffer from low productivity, thereby reducing C input to the soil upon regrowth. Additionally, in the intensive LU simulations (P100, C60, C100), vegetation productivity in the boreal region is further reduced compared to the reference simulation in the first 200 years of regrowth (not shown) due to N limitation (Smith et al., 2014), reducing litter input to the soil even further.

Soil C recovery times differ substantially between simulations in many areas. LU type is particularly important in grasslands and non-tropical forests. While croplands tend to recover faster than pastures in grasslands of southern and northern Africa, the opposite occurs in most temperate and boreal forests but also the northern Sahel, where soil C after re-conversion from croplands does not recover at all. Post-agricultural N availability is enhanced in parts of the Sahel for the cropland simulations due to increased

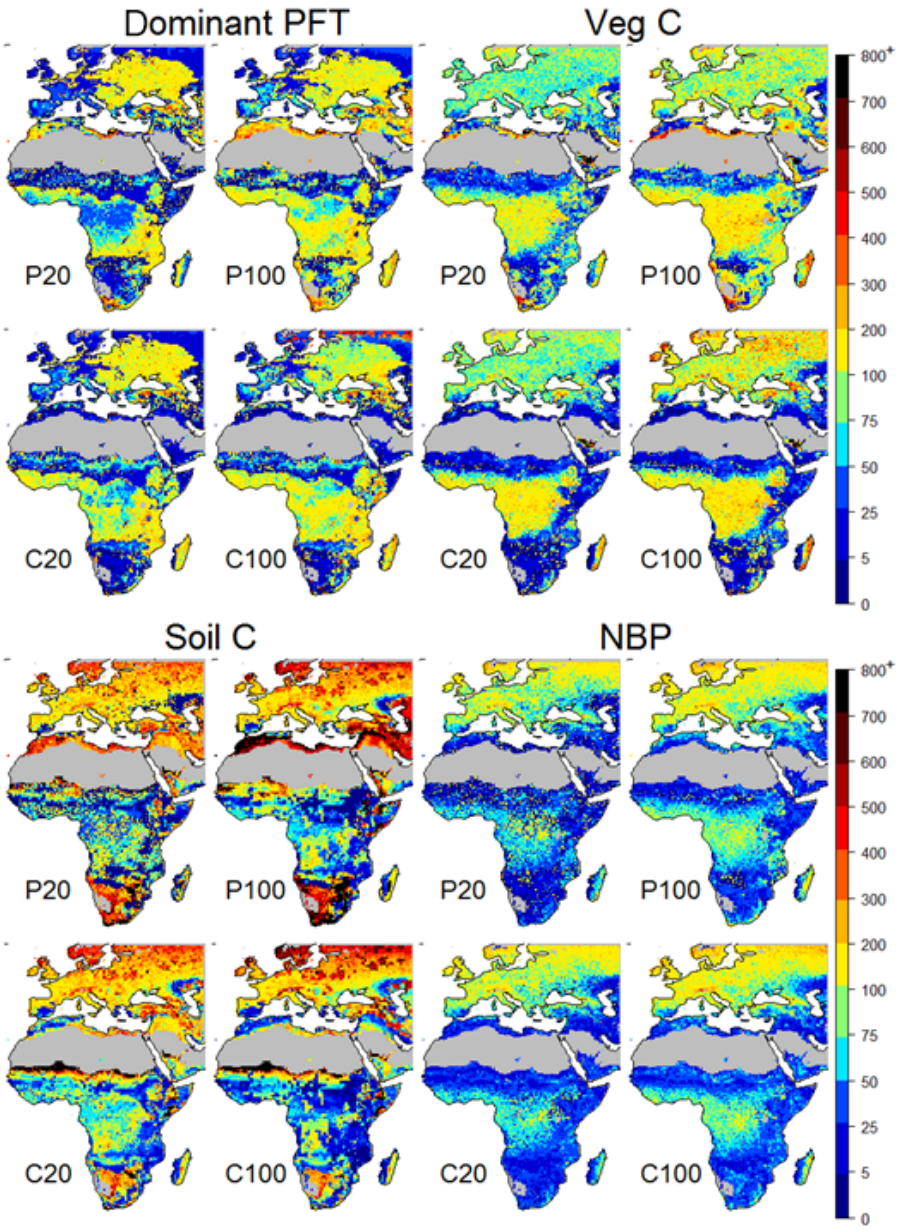

Figure 3. Maps of recovery times in years for the dominant PFT, vegetation C, soil C, and NBP for the P20, P100, C20, and C100 simulations.

N mineralization rates (Figs. 4 and 5), and trees benefit more than grasses, leading to a shift in the equilibrium vegetation state towards woody species (not shown), which results in an overall lower soil C pool size. It should be noted that even though some regions do not recover within 800 years, a large fraction of the original C loss is already replenished after a few centuries, thereby limiting implications for the C cycle. Counter to a priori expectations, for tropical and temperate forests and for shrublands, the difference between P20 and C20 is usually higher than between P60 and C60 or P100 and C100 (Fig. 6c). Pasture duration is relevant for speed of soil C recovery in most ecosystems and, apart from in the tropics, a longer duration usually delays recovery, mainly due to substantial initial depletions after long pasture durations (Fig. 2). For croplands, longer durations tend to delay recovery in temperate and boreal forests but accelerate soil C recovery in the (sub)tropics. This is somewhat unexpected for the tropical forest biome, where longer cropland durations usually do not increase N availability upon abandonment in our simulations (Fig. 5). However, while tropical soils lose large amounts of C during the first decades of cropland use, slow C accumulation takes place thereafter, resulting in higher soil C values at the end of the agricultural period for C100 than for C20 in large

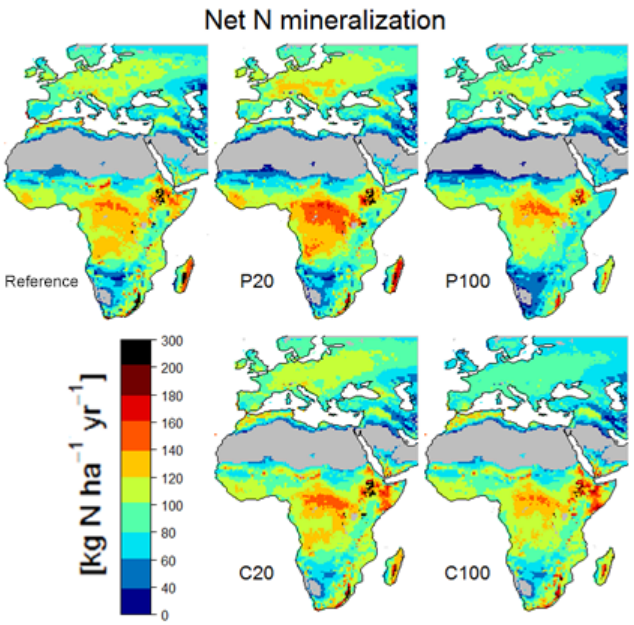

Figure 4. Average net N mineralization rates (kg N ha^{-1} yr^{-1}) in the soil for the reference simulation (full simulation period) and during the first 100 years of regrowth for the P20, P100, C20, and C100 simulations.

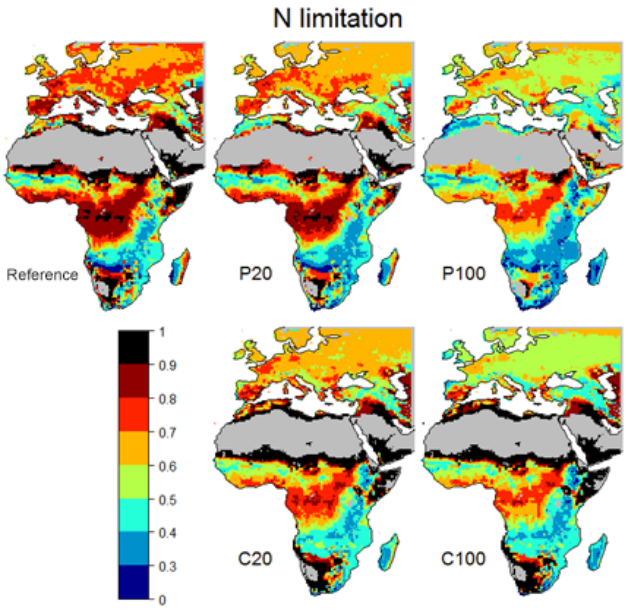

Figure 5. Average N limitation on vegetation RuBisCO capacity (and thus on gross primary production) for the reference simulation (full simulation period) and during the first 100 years of regrowth for the P20, P100, C20, and C100 simulations. N limitation is a number scaling from 0 (completely N-limited) to 1 (no N limitation) (Smith et al., 2014).

parts of eastern Africa. This occurs because tillage-driven C losses in more labile soil pools, which dominate the system's response during the first decades, are eventually supplanted as the dominant process by accumulation in more stable pools. This is different to temperate and boreal forest, where soil C decreases throughout the entire cropland period. Overall, the greatest sensitivity of soil C recovery times to different LU histories is found in boreal forests and grasslands, where maximum differences across simulations are often several centuries (Fig. 6c). The maximum differences across all simulations (P20/P60/P100/C20/C60/C100) in boreal forests are mainly due to differences across simulations of same LU type but different duration (e.g., P20/P60/P100), whereas the sensitivity of grasslands mainly reflects differences across simulations of different LU type but same duration (e.g., P100/C100), emphasizing the importance of duration and type of agriculture in a range of biomes.

3.5 NBP recovery

NBP switches from being a C source to the atmosphere during the period of land management to a C sink after reconversion to natural vegetation (Fig. 2). The sink capacity of the recovering ecosystem is greatest during the first decades and then gradually returns to the NBP levels of the reference simulation. P20 and, to a lesser extent, C20 act as a smaller sink than the other simulations at least during the first 100 years of regrowth. Recovery generally occurs slower in temperate and boreal regions than in the tropics for all simulations (Fig. 3). Apart from boreal forests, standard deviations of mean differences in recovery times are very small in all biomes compared to the other variables (Fig. 6d). Recovery times are often somewhat lower than those which would be expected from vegetation and soil C recovery times. This is because the greater standard deviation of NBP in our reference simulation (Fig. 2) reduces the threshold value in our recovery definition, thereby making it easier to reach recovery levels for NBP. We discuss the implications of this further in Sect. 4.2.

Differences in NBP recovery times between simulations are relatively small (typically a few years to decades; see Table 1). The largest differences in recovery times are found in the boreal forests between the cropland simulations, and, as for soil C, the differences are often greater between P20 and C20 than between P100 and C100 (Fig. 6d).

4 Discussion

4.1 Comparison to observations and previous studies

The effects of forest conversion to croplands or pastures are relatively well studied. Tilled croplands typically show large depletions of soil C compared to natural forest vegetation, but the picture for pasture is more diverse (Davidson and Ackerman, 1993; Don et al., 2011; Guo and Gifford, 2002). Table 2 summarizes recent reviews about observed soil C changes in agriculture compared to our results. LPJ-GUESS tends

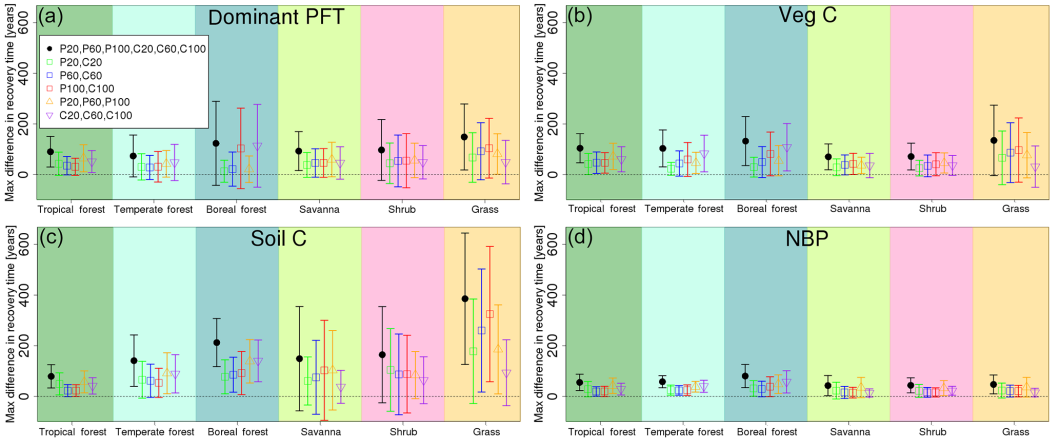

Figure 6. Maximum difference in recovery time (longest recovery time minus shortest recovery time of all selected simulations) for the dominant PFT, vegetation C, soil C, and NBP. Black dots show maximum differences across all six simulations (P20, P60, P100, C20, C60, C100), green squares differences across 20-year pasture and cropland simulations (P20, C20), blue squares differences across 60-year pasture and cropland simulations (P60, C60), red squares differences across 100-year pasture and cropland simulations (P100, C100), orange triangles differences across pasture simulations (P20, P60, P100), and purple triangles differences across cropland simulations (C20, C60, C100). Background colors indicate associated biomes, arrows one standard deviation, and the dashed line 0 years' difference. Thus, the black dots show the sensitivity of recovery times to LU history across all simulations for each biome. The red, blue and green squares indicate the relative contribution of LU type for a specific LU duration to this sensitivity, and the orange and purple squares indicate the relative contributions of pasture and of cropland duration. For example, if recovery times for one variable in one grid cell were to be 50, 60, 65, 90, 100, 110 years (for P20, P60, P100, C20, C60, C100), the maximum difference in recovery time across all simulations (black) would be 60 years, across the 20-year simulations (green) 40 years, across the 60-year simulations (blue) 40 years, across the 100-year simulations (red) 45 years, across the pasture simulations (orange) 15 years and across the cropland simulations (purple) 20 years.

to simulate lower C loss in croplands than commonly reported in observations. We attribute this to a combination of the observation's focus on the top soil (while in LPJ-GUESS soil C is implicitly averaged over the whole soil column) and our relatively high fertilizer rates increasing productivity and thereby C input to the soil. Pugh et al. (2015) studied the C dynamics of soils in managed lands in LPJ-GUESS and found C accumulation even after 100 years of grazed pasture at some locations, especially for low atmospheric CO_2 concentrations. However, they used the C-only version of the model, thereby neglecting C–N interactions and increased N limitation on grass growth with time due to N removal by harvest. Croplands were explicitly represented by a number of managed, but unfertilized, crop functional types in Pugh et al. (2015). They found soil C reductions in Europe and Africa of $\sim 50\,\%$ after 100 years of cultivation, whereas in our study C losses were much smaller ($\sim 12\,\%$), possibly partly due to different tillage effects in the two soil models applied.

In contrast to studies of LU effects compared to previously natural ecosystems, the regeneration of ecosystems after agricultural abandonment has been studied less, and a direct comparison to our simulations is challenging, either because limited information about former LU or reference conditions was provided in these studies or because there are important differences from our setup in terms of management and LU duration or other site-specific characteristics. Additionally, most of the available studies were conducted in Amazonia or North America (Don et al., 2011) and there is large variability in physical and biotic characteristics as well as in land management (Kauffman et al., 2009). Many studies focus on the recovery of biodiversity or species richness (Cramer et al., 2008; Queiroz et al., 2014), but these variables cannot be adequately captured by our large-scale PFT approach. It is often assumed that the ecosystem will gradually return to its previous state and that intensive LU delays recovery but the timescales are widely unknown and differ across variables and regions, e.g., tropical species composition recovers much slower than forest structure and soil nutrients (Chazdon, 2003). Different recovery processes are strongly interlinked, e.g., vegetation accumulation and turnover are key factors in the replenishment of soil quality and nutrients which in turn determine plant productivity, and post-agricultural soil C and N dynamics have been shown to correlate during the regeneration of ecosystems (Knops and Tilman, 2000; Li et al., 2012).

Table 2 includes several studies about ecosystem vegetation and soil recovery after agricultural abandonment. Overall, the studies that looked at vegetation recovery upon abandonment indicate that biomass accumulation slows down after some decades and that accumulation rates correlate negatively with agricultural duration. Our simulations show that the rate of vegetation C sequestration indeed declines over time and that longer LU durations delay recovery in each of the analyzed biomes. Observations also indicate that use of

Table 1. Average recovery times and standard deviations per biome and for each simulation. Recovery times are depicted in Fig. 3.

Biome	Simulation					
	P20	P60	P100	C20	C60	C100
	Dominant PFT recovery time, averaged per biome					
Tropical forest	90 ± 55	112 ± 48	121 ± 50	113 ± 54	125 ± 52	126 ± 51
Temperate forest	102 ± 74	96 ± 63	93 ± 57	99 ± 71	89 ± 61	92 ± 69
Boreal forest	47 ± 89	52 ± 97	53 ± 90	47 ± 95	60 ± 111	145 ± 178
Savanna	47 ± 71	57 ± 74	62 ± 77	50 ± 65	57 ± 73	59 ± 76
Shrub	95 ± 93	104 ± 101	108 ± 100	103 ± 100	109 ± 112	109 ± 112
Grassland	76 ± 108	102 ± 109	115 ± 109	45 ± 77	55 ± 97	58 ± 100
Total	80 ± 85	93 ± 84	99 ± 84	77 ± 78	83 ± 85	90 ± 95
	Vegetation C recovery time, averaged per biome					
Tropical forest	106 ± 50	137 ± 61	150 ± 65	121 ± 65	138 ± 73	139 ± 74
Temperate forest	84 ± 24	93 ± 31	108 ± 46	91 ± 29	124 ± 59	149 ± 79
Boreal forest	102 ± 47	113 ± 57	127 ± 71	111 ± 55	144 ± 79	187 ± 107
Savanna	49 ± 37	61 ± 44	66 ± 46	35 ± 40	42 ± 43	43 ± 44
Shrub	73 ± 40	86 ± 48	96 ± 51	60 ± 38	69 ± 48	73 ± 54
Grassland	96 ± 136	119 ± 140	126 ± 138	40 ± 98	43 ± 102	45 ± 105
Total	88 ± 80	106 ± 87	117 ± 90	75 ± 74	92 ± 87	101 ± 98
	Soil C recovery time, averaged per biome					
Tropical forest	74 ± 60	69 ± 43	66 ± 45	80 ± 46	64 ± 46	49 ± 43
Temperate forest	207 ± 98	229 ± 105	241 ± 117	237 ± 108	261 ± 133	260 ± 144
Boreal forest	327 ± 107	381 ± 122	421 ± 140	362 ± 112	425 ± 132	454 ± 161
Savanna	84 ± 132	132 ± 191	162 ± 233	85 ± 112	83 ± 125	74 ± 126
Shrub	107 ± 140	129 ± 161	135 ± 168	137 ± 173	139 ± 183	125 ± 183
Grassland	286 ± 234	366 ± 262	422 ± 283	239 ± 227	219 ± 229	198 ± 228
Total	182 ± 176	220 ± 209	245 ± 236	182 ± 171	183 ± 186	174 ± 194
	NBP recovery time, averaged per biome					
Tropical forest	57 ± 37	65 ± 26	71 ± 27	56 ± 28	64 ± 24	65 ± 24
Temperate forest	97 ± 29	108 ± 29	113 ± 31	102 ± 30	112 ± 31	119 ± 36
Boreal forest	136 ± 55	146 ± 56	152 ± 58	139 ± 54	151 ± 59	169 ± 71
Savanna	31 ± 40	34 ± 30	36 ± 26	29 ± 18	32 ± 17	33 ± 17
Shrub	51 ± 37	58 ± 31	59 ± 29	52 ± 27	58 ± 26	59 ± 25
Grassland	25 ± 37	31 ± 31	35 ± 30	27 ± 15	34 ± 20	36 ± 22
Total	59 ± 51	66 ± 49	71 ± 49	60 ± 45	68 ± 47	72 ± 52

land for pasture delays recovery in the tropics upon pasture abandonment compared to cropping, but in our simulations this seems to be the case only after long agricultural durations. For studies about soil C dynamics after agricultural abandonment, interpretation is often hindered by combining different soil layers or aggregating different LU types (Li et al., 2012) and by large variations observed across studies (Post and Kwon, 2000). Nevertheless, most of the observed patterns are reproduced in our simulations, suggesting that LPJ-GUESS captures the salient processes: after abandonment, croplands accumulate C faster than pastures, and recovery often takes more than a century. The impact of LU duration has rarely been studied; however, our results suggest that even though longer agricultural durations mostly result in greater initial soil C depletions, recovery can occur at similar or even faster speed in the subtropics and tropics. In temperate and boreal forests long LU durations tend to delay recovery.

The LPJ-GUESS model has been successfully tested against a range of observations and observation-based products, including vegetation distribution and dynamics and soil C response to changes in vegetation cover (Hickler et al., 2004; Miller et al., 2008; Pugh et al., 2015; Smith et al., 2014). In our simulations, we used only two different agricultural land cover types (intensive grazing and fertilized, tilled crops). Our analysis would therefore not identify effects of, for instance, clearing technique (e.g., burning compared to mechanical removal) or different land management practices (e.g., repeated burning or irrigation) within one land cover type. For example, recovery of species richness and

Table 2. Observations and LPJ-GUESS results of soil C changes during agriculture (cropland and/or pasture) and vegetation and soil C recovery after abandonment.

Observation type	Biome	Observation value	Closest simulations in terms of LU history	Average model value for the specific biome	Reference
Soil C changes during agriculture					
Soil C change averaged over different depths	global	42 % loss for forest–cropland conversions, 8 % gain for forest–pasture conversions	P20, P60, P100, C20, C60, C100	7–17 % loss in forest biomes for croplands, 2 % gain to 7 % loss for pastures	Guo and Gifford (2002)
Soil C change at 36 cm	tropical forest	25 % loss for cropland, 12 % loss for pasture/grassland	C20, C60, P20, P60	11–12 % loss for croplands, 2 % gain to 4 % loss for pastures	Don et al. (2011)
Soil C change at 29 cm	temperate forest	new equilibrium after 23 years	C100	C loss throughout the entire cropland duration	Poeplau et al. (2011)
Vegetation recovery after agricultural abandonment					
ag* vegetation recovery time	tropical forest	189 years	C20	121 years	Saldarriaga et al. (1988)
ag vegetation recovery rate	tropical forest	slowdown with time, recovery slower for pasture than for cropland	P20, P60, P100, C20, C60, C100	(slight) slowdown, pasture recovery slower only for long durations (P100/C100)	Silver et al. (2000)
Total and vegetation C recovery rate	temperate forest	linear with time	P60, P100	(slight) slowdown	Hooker and Compton (2003)
Vegetation recovery rate	temperate forest	linear with time	C20, C60	(slight) slowdown	Poulton et al. (2003)
ag vegetation recovery rate	tropical forest	recovery speed inversely related to LU duration	P20, P60, P100	recovery speed inversely related to LU duration	Uhl et al. (1988)
ag vegetation recovery rate and time	tropical forest	73 years, recovery speed inversely related to LU duration	C20, C60, C100	121–139 years, recovery speed inversely related to LU duration	Hughes et al. (1999)
Maximum tree height recovery rate	tropical forest	recovery speed inversely related to LU duration	C20, C60, C100	recovery speed inversely related to LU duration	Randriamalala et al. (2012)
Vegetation height recovery rate	tropical forest	slower for pasture than for cropland	P20, P60, P100, C20, C60, C100	slower only for long durations (C100/P100)	Moran et al. (2000)
ag vegetation recovery rate	tropical forest	slower for pasture than for cropland	P20, C20	faster for P20 than for C20	Wandelli and Fearnside (2015)
Soil C recovery after agricultural abandonment					
Soil C recovery at up to 30 cm	global	large variation across studies, tendency to lose C in the first years for pastures, immediate accumulation for croplands	P20, P60, P100, C20, C60, C100	tendency to lose C in the first years for pastures, immediate accumulation for croplands	Paul et al. (2002)

* ag = aboveground.

Table 3. Observations and LPJ-GUESS results of soil C changes during agriculture (cropland and/or pasture) and vegetation and soil C recovery after abandonment.

Observation type	Biome	Observation value	Closest simulations in terms of LU history	Average model value for the specific biome	Reference
Soil C recovery at 34 cm	global	more accumulation for croplands than for pastures, no accumulation in boreal zone	P20, P60, P100, C20, C60, C100	more accumulation for croplands than for pastures, slower accumulation in boreal zone	Laganiere et al. (2010)
Soil C recovery at 28/40 cm	temperate forest	linear accumulation, no equilibrium after 120 years	C20	linear accumulation, no equilibrium after 120 years	Poeplau et al. (2011)
Soil C recovery time at 0–60 cm	grassland	158 years	C100	198 years	Potter et al. (1999)
Soil C recovery time at 0–60 cm	savanna/ temperate forest	230 years	C20	85 (savanna)/237 (temperate forest) years	Knops and Tilman (2000)
Soil C recovery time 0–10 cm	temperate forest	> 100 years	C20, C60, C100	237–261 years	Foote and Grogan (2010)
Soil C recovery time 0–25 cm	tropical forest	50–60 years	P20, P60, P100, C20, C60, C100	49–80 years	Silver et al. (2000)

maximum tree height of secondary forests occurs faster under no tillage compared to heavy tillage (Randriamalala et al., 2012).

Our study is intended as an idealized experiment to highlight the importance of LU history on ecosystem state and fluxes across biomes. Still, some processes with the potential to affect post-agricultural ecosystem recovery, at least regionally, are not currently included in LPJ-GUESS. One aspect is the phosphorus cycle, which is not implemented in LPJ-GUESS, even though it can be significantly altered by LUC (MacDonald et al., 2012; McLauchlan, 2006). Moreover, while C and N cycles interact in LPJ-GUESS (Smith et al., 2014), the uniform annual fertilizer rate we applied in this study might be realistic in some regions, such as parts of Europe, but exceeds present-day fertilizer use in Africa (Potter et al., 2010). Seed availability, remnant trees and resprouting from surviving roots are important factors during initial stages of tree colonization following agricultural cessation (Bellemare et al., 2002; Cramer et al., 2008). While LPJ-GUESS does not account for these effects explicitly, seedling establishment is limited by a suitable growth environment, such that effects like re-sprouting or remnant trees as seed sources are mimicked. The model has been shown to, for example, reproduce vegetation recolonization in northern Europe during the Holocene well (Miller et al., 2008), as well as canopy structural changes as a function of forest age (Smith et al., 2014). What is more, by using a prescribed climate in our simulations, hydrological biosphere–atmosphere interactions and feedbacks are not captured (Eltahir and Bras, 1996; Giambelluca, 2002), which could alter regional climate in response to land cover change, potentially affecting recovery rates, especially in tropical regions. Biophysical effects are not restricted to modifications of the water cycle but also include changes in surface albedo and roughness length as a function of ecosystem structure and composition, thereby affecting air mixing and heat transfer. While forests generally absorb more sunlight than grasslands (e.g., Culf et al., 1995), differences amongst tree species and age classes exist as well. Substantial impacts related to realistic land-use have been found on local-to-regional scales (Alkama and Cescatti, 2016; Peng et al., 2014). Whether or not the locally observed changes translate to a significant global radiative forcing is still debated as the direction of change differs across regions in some climate models, which may cancel when integrated globally (Pielke et al., 2011). Additionally, while we focus on C sequestration rates in our analysis, there might be biogeochemical implications beyond C. For instance, the emissions of biogenic volatile organic compounds (BVOCs) to the atmosphere vary greatly amongst plant species (Kesselmeier and Staudt, 1999). BVOCs affect atmospheric composition and climate via ozone production, lengthening the lifetime of atmospheric methane, and contributing to secondary organic aerosol formation (Penuelas and Staudt, 2010; Wu et al., 2012). BVOC emission factors might also be drastically

influenced by wildfires (Ciccioli et al., 2014), which in turn are driven by species composition and vegetation density. Thus, different successional trajectories of ecosystem structure and composition recovery have the potential to directly modify air quality and climatic conditions under which regrowth occurs, potentially creating positive or negative climate system feedbacks.

4.2 Implications of recovery definition

The term recovery is subjective and, in the absence of a universal definition amongst ecologists, several definitions currently exist. The definition used in this study examines recovery from a C sequestration perspective which does not capture situations, for example, where the system approaches a new equilibrium (as soil C did in some regions in the cropland simulations). In order to obtain a better understanding of the uncertainties related to our definition we therefore explored four alternative plausible recovery definitions.

When applying a mean minus 2σ threshold (instead of a mean minus 1σ threshold), recovery times are generally shorter, e.g., on average 75 instead of 106 years for vegetation C in P60, but the overall geographic patterns are very consistent across both definitions (not shown). For all variables and simulations, notable differences between both definitions occur in regions with longest recovery times, especially for subtropical soil C in the pasture simulations.

Recovery based on percentage change (Fig. A4) results in more heterogeneous patterns across variables when compared to our standard recovery definition. Applying a threshold of 95 % of the mean, instead of a mean minus 1σ threshold, produces slightly longer dominant PFT recovery times in parts of the temperate and tropical forests, and shorter recovery times in grasslands, especially for the pasture simulations. Vegetation C shows similar patterns to the dominant PFT; however, the differences to our standard definition are more pronounced. Soil C recovery times generally decrease dramatically, especially outside the tropics. NBP recovery times generally increase, particularly in forest ecosystems.

By expanding our standard recovery definition by an upper threshold (reference mean plus 1σ), and with the "minimum rule" also applied to the maximum (see Sect. 2.4), one can test whether some ecosystems recover from higher rather than lower values than in the reference simulation. Mostly grasslands are affected by this alternative definition (Fig. A5). Dominant PFT recovery under this definition takes slightly longer throughout the African grasslands for the pasture simulations, and considerably longer in parts of northern and southern Africa for the cropland simulations. Patterns are similar for vegetation C, but the increase in vegetation C recovery times is often larger than the increase in dominant PFT recovery times, especially for croplands. Soil C recovery is notably longer in subtropical and eastern African grasslands. The recovery times of NBP are hardly affected. However, we do not use an upper threshold in the primary definition used in this study because in this case the ecosystem is already operating at a level of service above that which the undisturbed ecosystem would have provided and our aim here was to investigate recovery from a depletion perspective.

Finally, when using the mean $\pm 1\sigma$ definition and additionally checking whether the variable is still in the mean $\pm 1\sigma$ range at the end of the simulation period (not shown), many grid cells did not recover even within the set maximum cut-off of 800 years. Elements of random fluctuations due to natural variability arising from stochastic processes and disturbances and responding C, N, and water dynamics made a clear identification of recovery period difficult in that case. In particular for soil C, no recovery is found for parts of eastern and subtropical Africa. The system converges towards a new equilibrium state in these regions which lies above reference values. NBP stays within background levels everywhere.

Altogether, the alternative recovery definitions agree on the general findings when applying our standard definition, especially in terms of relative recovery rates. For all definitions, vegetation C and dominant PFT recover faster in grasslands than in forest-dominated ecosystems, and soil C recovery takes much longer in higher latitudes. However, some areas, especially in the subtropics, "recover" from values higher than in the reference simulation, and these cases are not captured by our standard definition. Additionally, in the tropics, soil C accumulation sometimes does not stop once background values are reached and soil C leaves the reference range. When recovery is defined based on standard deviation, NBP recovery is often quicker than recovery of the C pools. This inconsistency emphasizes the importance of both recovery definition and selected variables when studying the recovery of ecosystems (Jones and Schmitz, 2009). This is particularly relevant for flux tower measurements, where an underlying long-term trend caused by the recovery from previous, often unquantified or unknown LU change, might be overlooked due to a large interannual variability in net ecosystem exchange.

5 Conclusions

Most studies which have explored the effects of distant human activities on present-day ecosystems were restricted by sampling difficulties, small spatial scales, short time periods since abandonment, and little information about background conditions or the specific LU history of the site. Here, we use a model-based approach to study the legacy effects of agricultural LU history (type and duration) on ecosystem regeneration and C sink capacity after the cessation of agriculture in a range of biomes across Europe and Africa. The model reproduces qualitatively the response found at study locations, including distinct differences in recovery between different variables of the terrestrial carbon cycle. Long-lasting legacy

effects of former agricultural intensity emerge as important for present-day ecosystem functions. These findings have implications for various scientific applications:

1. Long-term monitoring sites (e.g., FLUXNET) and Earth observation systems need to collect and maintain detailed information about past and present land cover and land management to adequately interpret their data.

2. Assessments of trends in data from sites that seek to identify impacts of climate change and/or increasing atmospheric CO_2 concentration need to make sure that legacy effects of past LU are not confounding the observed trends.

3. Simulation experiments need to move beyond deforestation but also represent, in a more detailed manner, re-growth dynamics following agricultural abandonment at the sub-grid level. At the moment a few DGVMs have started to do so (Shevliakova et al., 2009; Stocker et al., 2014; Wilkenskjeld et al., 2014) based on model products of tropical shifting cultivation (Hurtt et al., 2011), but accounting for gross land cover changes is also important in other regions like Europe (Fuchs et al., 2015). Failure to consider LU history may lead to errors in the simulation of vegetation properties, potentially resulting in biases in carbon sequestration or energy balance calculations, with subsequent implications for simulations of regional and global climate. Our study suggests that, for vegetation and soil C studies, accounting for LUC over the last 100–150 years is sufficient in the tropics, while more than 200 years might be necessary in the temperate and boreal zone; studies restricted to vegetation should not have to account for LUC more than 150 years ago in any major climatic zone.

4. Assessing the efficiency of climate mitigation through large-scale reforestation or afforestation projects will require knowledge about the type and duration of previous LU. Our simulations suggest that the potential to rapidly sequester C in biomass and soil is greatest in tropical forests following short periods of cropland, while boreal forests accumulate C slowest, especially when previously used for pasture. Special attention should be paid to monitoring changes in belowground C, as in most places the accumulation of soil C is much more sensitive to LU history than C accumulation in re-growing trees.

5. In terms of soil C, our results suggest that some subtropical regions might not recover at all on timescales relevant for humans. However, given the low absolute amounts of C "missing" in these soils, implications for the global C cycle are expected to be small.

6 Data availability

Researchers interested in the LPJ-GUESS source code can contact the model developers (http://iis4.nateko.lu.se/lpj-guess/contact.html). The CRU TS 3.21 climate data can be downloaded from http://browse.ceda.ac.uk/browse/badc/cru/data/cru_ts/cru_ts_3.21. The LPJ-GUESS simulation data are stored at the IMK-IFU computing facilities and can be obtained on request (andreas.krause@kit.edu).

Appendix A: Additional tables and figures

Table A1. Plant functional types used in this study.

BNE	Boreal needleleaved evergreen tree
BINE	Boreal shade-intolerant needleleaved evergreen tree
BNS	Boreal needleleaved summergreen tree
TeBS	Shade-tolerant temperate broadleaved summergreen tree
IBS	Shade-intolerant broadleaved summergreen tree
TeBE	Temperate broadleaved evergreen tree
TrBE	Tropical broadleaved evergreen tree
TrIBE	Tropical shade-intolerant broadleaved evergreen tree
TrBR	Tropical broadleaved raingreen tree
C3G	Cool C_3 grass
C4G	Warm C_4 grass

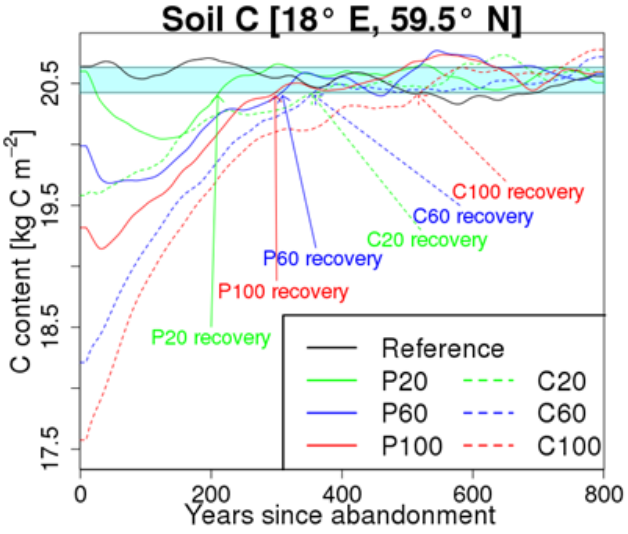

Figure A1. Soil C for the six simulations after conversion to natural vegetation at one single example site to illustrate how recovery time was calculated according to our definition. The cyan-shaded area corresponds to reference simulation mean $\pm 1\sigma$. When soil C exceeds the mean $- 1\sigma$ threshold and the time of the minimum (which in this case is located in the first 200 years and below the mean $- 1\sigma$ threshold for all six simulations) is passed, recovery is achieved.

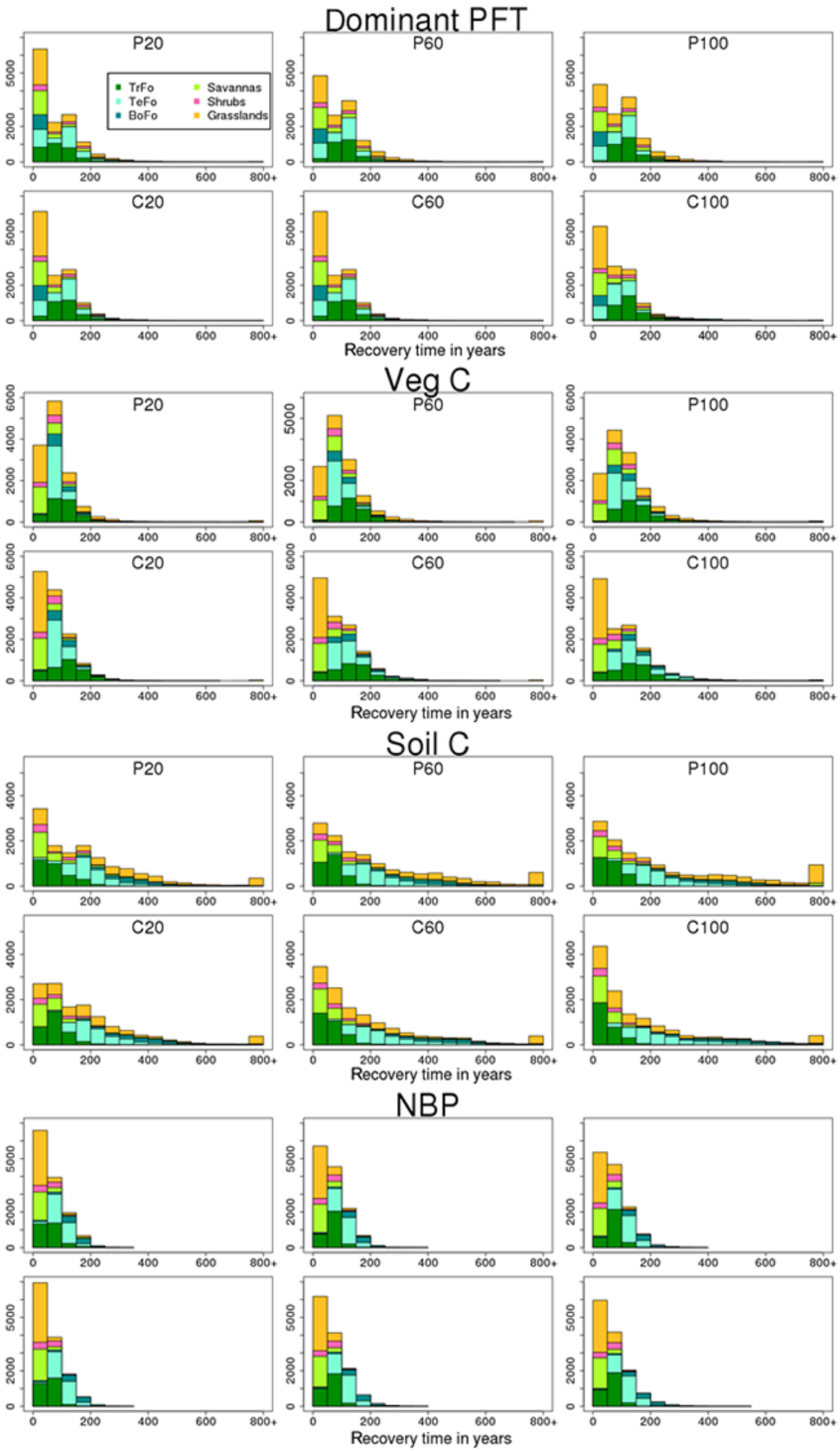

Figure A2. Histograms of recovery times for the dominant PFT, vegetation C, soil C, and NBP for the six experiments. Colors indicate different biomes.

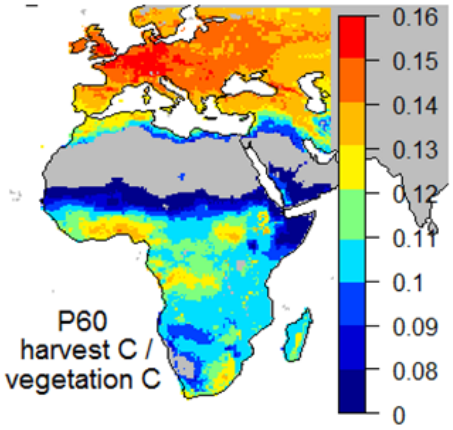

Figure A3. Annual ratio of C removed by harvest and C stored in vegetation, averaged over the whole agricultural period and for P60. As only aboveground biomass is harvested, lower values indicate increased C allocation to roots compared to leaves due to limited water supply.

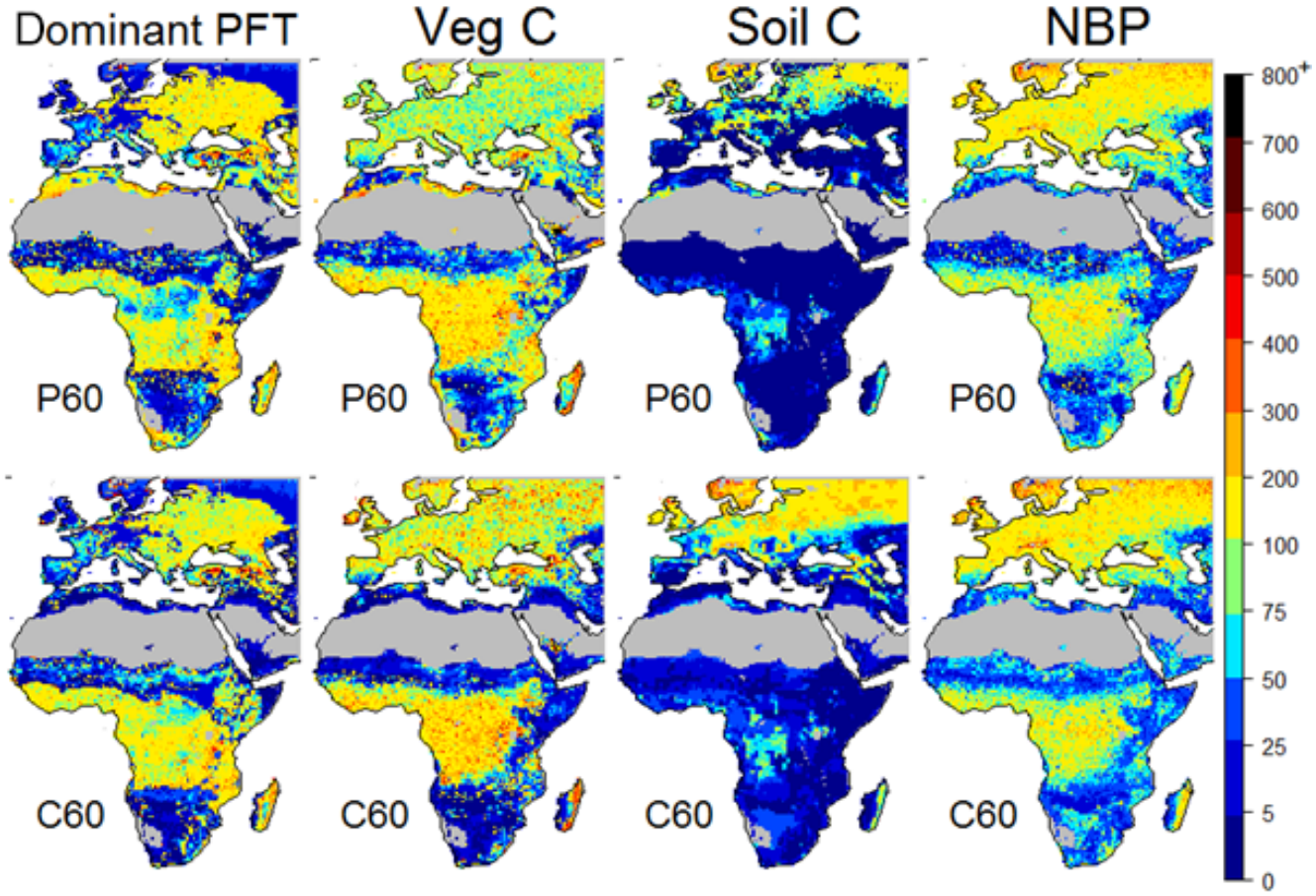

Figure A4. Maps of recovery time for the dominant PFT, vegetation C, soil C and NBP with an alternative recovery definition for the P60 and C60 simulations. The definition is the same as our standard definition but with a mean $\cdot$ 0.95 threshold instead of mean $- 1\sigma$.

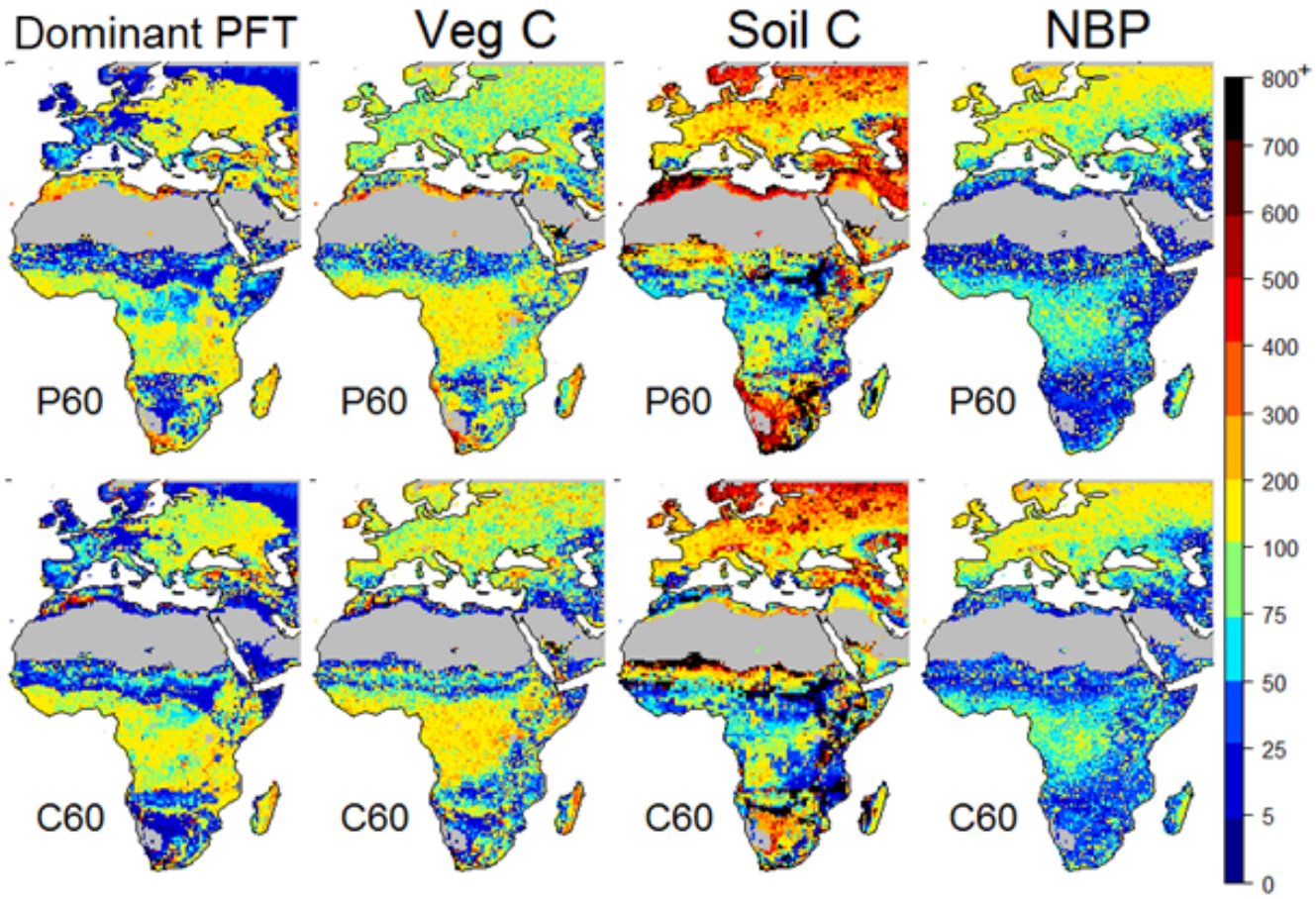

Figure A5. Maps of recovery time for the dominant PFT, vegetation C, soil C and NBP with an alternative recovery definition for the P60 and C60 simulations. The definition is the same as our standard definition but with a mean $\pm 1\sigma$ threshold and the minimum check also applied to the maximum instead of a mean $- 1\sigma$ threshold and only checking the minimum.

Acknowledgements. This work was funded by the Helmholtz Association through the International Research Group CLUCIE and by the European Commission's 7th Framework Programme, under grant agreement number 603542 (LUC4C). A. D. Bayer acknowledges support by the European Commission's 7th Framework Programme, under grant agreement number 308393 (OPERAs). This work was supported, in part, by the German Federal Ministry of Education and Research (BMBF), through the Helmholtz Association and its research program ATMO. It also represents paper number 20 of the Birmingham Institute of Forest Research.

The article processing charges for this open-access publication were covered by a Research Centre of the Helmholtz Association.

Edited by: V. Arora
two anonymous referees

References

Aide, T. M., Zimmerman, J. K., Pascarella, J. B., Rivera, L., and Marcano-Vega, H.: Forest regeneration in a chronosequence of tropical abandoned pastures: Implications for restoration ecology, Restor. Ecol., 8, 328–338, doi:10.1046/j.1526-100x.2000.80048.x, 2000.

Alkama, R. and Cescatti, A.: Biophysical climate impacts of recent changes in global forest cover, Science, 351, 600–604, doi:10.1126/science.aac8083, 2016.

Arora, V. K. and Montenegro, A.: Small temperature benefits provided by realistic afforestation efforts, Nat. Geosci., 4, 514–518, doi:10.1038/NGEO1182, 2011.

Bayer, A. D., Pugh, T. A. M., Krause, A., and Arneth, A.: Historical and future quantification of terrestrial carbon sequestration from a greenhouse-gas-value perspective, Global Environ. Change, 32, 153–164, doi:10.1016/j.gloenvcha.2015.03.004, 2015.

Bellemare, J., Motzkin, G., and Foster, D. R.: Legacies of the agricultural past in the forested present: An assessment of historical land-use effects on rich mesic forests, J. Biogeogr., 29, 1401–1420, doi:10.1046/j.1365-2699.2002.00762.x, 2002.

Brovkin, V., Boysen, L., Arora, V. K., Boisier, J. P., Cadule, P., Chini, L., Claussen, M., Friedlingstein, P., Gayler, V., van den Hurk, B. J. J. M., Hurtt, G. C., Jones, C. D., Kato, E., de Noblet-Ducoudre, N., Pacifico, F., Pongratz, J., and Weiss, M.: Effect of anthropogenic land-use and land-cover changes on climate and land carbon storage in CMIP5 projections for the twenty-first century, J. Climate, 26, 6859–6881, doi:10.1175/Jcli-D-12-00623.1, 2013.

Burgi, M. and Turner, M. G.: Factors and processes shaping land cover and land cover changes along the Wisconsin River, Ecosystems, 5, 184–201, doi:10.1007/s10021-001-0064-6, 2002.

Campbell, J. E., Lobell, D. B., Genova, R. C., and Field, C. B.: The global potential of bioenergy on abandoned agriculture lands, Environ. Sci. Technol., 42, 5791–5794, doi:10.1021/es800052w, 2008.

Chazdon, R. L.: Tropical forest recovery: Legacies of human impact and natural disturbances, Perspect. Plant Ecol., 6, 51–71, doi:10.1078/1433-8319-00042, 2003.

Chazdon, R. L.: Second growth: The promise of tropical forest regeneration in an age of deforestation, University of Chicago Press, Chicago, Illinois, USA, 2014.

Ciccioli, P., Centritto, M., and Loreto, F.: Biogenic volatile organic compound emissions from vegetation fires, Plant Cell Environ., 37, 1810–1825, doi:10.1111/pce.12336, 2014.

Compton, J. E. and Boone, R. D.: Long-term impacts of agriculture on soil carbon and nitrogen in New England forests, Ecology, 81, 2314–2330, 2000.

Cramer, V. A., Hobbs, R. J., and Standish, R. J.: What's new about old fileds? Land abandonment and ecosystem assembly, Trends Ecol. Evol., 23, 104–112, doi:10.1016/j.tree.2007.10.005, 2008.

CRU: CRU TS3.21: Climatic Research Unit (CRU) time-series (TS) version 3.21 of high resolution gridded data of month-by-month variation in climate (Jan. 1901–Dec. 2012), NCAS British Atmospheric Data Centre, doi:10.5285/D0E1585D-3417-485F-87AE-4FCECF10A992, 2013.

Culf, A. D., Fisch, G., and Hodnett, M. G.: The albedo of Amazonian forest and ranch land, J. Climate, 8, 1544–1554, doi:10.1175/1520-0442(1995)008<1544:Taoafa>2.0.Co;2, 1995.

Dambrine, E., Dupouey, J. L., Laut, L., Humbert, L., Thinon, M., Beaufils, T., and Richard, H.: Present forest biodiversity patterns in France related to former Roman agriculture, Ecology, 88, 1430–1439, doi:10.1890/05-1314, 2007.

Davidson, E. A. and Ackerman, I. L.: Changes in soil carbon inventories following cultivation of previously untilled soils, Biogeochemistry, 20, 161–193, doi:10.1007/Bf00000786, 1993.

Dean, R., Ellis, J. E., Rice, R. W., and Bement, R. E.: Nutrient removal by cattle from a shortgrass prairie, J. Appl. Ecol., 12, 25–29, doi:10.2307/2401715, 1975.

de Noblet-Ducoudre, N., Boisier, J. P., Pitman, A., Bonan, G. B., Brovkin, V., Cruz, F., Delire, C., Gayler, V., van den Hurk, B. J. J. M., Lawrence, P. J., van der Molen, M. K., Muller, C., Reick, C. H., Strengers, B. J., and Voldoire, A.: Determining robust impacts of land-use-induced land cover changes on surface climate over North America and Eurasia: Results from the first set of LUCID experiments, J. Climate, 25, 3261–3281, doi:10.1175/Jcli-D-11-00338.1, 2012.

Don, A., Schumacher, J., and Freibauer, A.: Impact of tropical land-use change on soil organic carbon stocks – a meta-analysis, Global Change Biol., 17, 1658–1670, doi:10.1111/j.1365-2486.2010.02336.x, 2011.

Dupouey, J. L., Dambrine, E., Laffite, J. D., and Moares, C.: Irreversible impact of past land use on forest soils and biodiversity, Ecology, 83, 2978–2984, doi:10.2307/3071833, 2002.

Eltahir, E. A. B. and Bras, R. L.: Precipitation recycling, Rev. Geophys., 34, 367–378, doi:10.1029/96rg01927, 1996.

Falkengren-Grerup, U., ten Brink, D. J., and Brunet, J.: Land use effects on soil N, P, C and pH persist over 40–80 years of forest growth on agricultural soils, Forest Ecol. Manage., 225, 74–81, doi:10.1016/j.foreco.2005.12.027, 2006.

Fichtner, A., von Oheimb, G., Hardtle, W., Wilken, C., and Gutknecht, J. L. M.: Effects of anthropogenic disturbances on soil microbial communities in oak forests persist for more than 100 years, Soil Biol. Biochem., 70, 79–87, doi:10.1016/j.soilbio.2013.12.015, 2014.

Foley, J. A., Costa, M. H., Delire, C., Ramankutty, N., and Snyder, P.: Green surprise? How terrestrial ecosystems

could affect earth's climate, Front. Ecol. Environ., 1, 38–44, doi:10.2307/3867963, 2003.

Foote, R. L. and Grogan, P.: Soil carbon accumulation during temperate forest succession on abandoned low productivity agricultural lands, Ecosystems, 13, 795–812, doi:10.1007/s10021-010-9355-0, 2010.

Foster, D., Swanson, F., Aber, J., Burke, I., Brokaw, N., Tilman, D., and Knapp, A.: The importance of land-use legacies to ecology and conservation, Bioscience, 53, 77–88, doi:10.1641/0006-3568(2003)053[0077:Tiolul]2.0.Co;2, 2003.

Fuchs, R., Herold, M., Verburg, P. H., Clevers, J. G. P. W., and Eberle, J.: Gross changes in reconstructions of historic land cover/use for Europe between 1900 and 2010, Global Change Biol., 21, 299–313, doi:10.1111/gcb.12714, 2015.

Fujisaki, K., Perrin, A. S., Desjardins, T., Bernoux, M., Balbino, L. C., and Brossard, M.: From forest to cropland and pasture systems: A critical review of soil organic carbon stocks changes in Amazonia, Global Change Biol., 21, 2773–2786, doi:10.1111/gcb.12906, 2015.

Giambelluca, T. W.: Hydrology of altered tropical forest, Hydrol. Process., 16, 1665–1669, doi:10.1002/Hyp.5021, 2002.

Guariguata, M. R. and Ostertag, R.: Neotropical secondary forest succession: Changes in structural and functional characteristics, Forest Ecol. Manage., 148, 185–206, doi:10.1016/S0378-1127(00)00535-1, 2001.

Guo, L. B. and Gifford, R. M.: Soil carbon stocks and land use change: A meta analysis, Global Change Biol., 8, 345–360, doi:10.1046/j.1354-1013.2002.00486.x, 2002.

Haxeltine, A. and Prentice, I. C.: BIOME3: An equilibrium terrestrial biosphere model based on ecophysiological constraints, resource availability, and competition among plant functional types, Global Biogeochem. Cy., 10, 693–709, doi:10.1029/96gb02344, 1996.

Hickler, T., Smith, B., Sykes, M. T., Davis, M. B., Sugita, S., and Walker, K.: Using a generalized vegetation model to simulate vegetation dynamics in northeastern USA, Ecology, 85, 519–530, doi:10.1890/02-0344, 2004.

Hobbs, R. J., Higgs, E., and Harris, J. A.: Novel ecosystems: Implications for conservation and restoration, Trends Ecol. Evol., 24, 599–605, doi:10.1016/j.tree.2009.05.012, 2009.

Hooker, T. D. and Compton, J. E.: Forest ecosystem carbon and nitrogen accumulation during the first century after agricultural abandonment, Ecol. Appl., 13, 299–313, doi:10.1890/1051-0761(2003)013[0299:Fecana]2.0.Co;2, 2003.

Hughes, R. F., Kauffman, J. B., and Jaramillo, V. J.: Biomass, carbon, and nutrient dynamics of secondary forests in a humid tropical region of Mexico, Ecology, 80, 1892–1907, 1999.

Hurtt, G. C., Chini, L. P., Frolking, S., Betts, R. A., Feddema, J., Fischer, G., Fisk, J. P., Hibbard, K., Houghton, R. A., Janetos, A., Jones, C. D., Kindermann, G., Kinoshita, T., Goldewijk, K. K., Riahi, K., Shevliakova, E., Smith, S., Stehfest, E., Thomson, A., Thornton, P., van Vuuren, D. P., and Wang, Y. P.: Harmonization of land-use scenarios for the period 1500–2100: 600 years of global gridded annual land-use transitions, wood harvest, and resulting secondary lands, Climatic Change, 109, 117–161, doi:10.1007/s10584-011-0153-2, 2011.

Jones, H. P. and Schmitz, O. J.: Rapid recovery of damaged ecosystems, Plos One, 4, e5653, doi:10.1371/journal.pone.0005653, 2009.

Kauffman, J. B., Hughes, R. F., and Heider, C.: Carbon pool and biomass dynamics associated with deforestation, land use, and agricultural abandonment in the Neotropics, Ecol. Appl., 19, 1211–1222, doi:10.1890/08-1696.1, 2009.

Kesselmeier, J. and Staudt, M.: Biogenic volatile organic compounds (VOC): An overview on emission, physiology and ecology, J. Atmos. Chem., 33, 23–88, doi:10.1023/A:1006127516791, 1999.

Knops, J. M. H. and Tilman, D.: Dynamics of soil nitrogen and carbon accumulation for 61 years after agricultural abandonment, Ecology, 81, 88–98, doi:10.1890/0012-9658(2000)081[0088:Dosnac]2.0.Co;2, 2000.

Laganiere, J., Angers, D. A., and Pare, D.: Carbon accumulation in agricultural soils after afforestation: A meta-analysis, Global Change Biol., 16, 439–453, doi:10.1111/j.1365-2486.2009.01930.x, 2010.

Lamarque, J. F., Dentener, F., McConnell, J., Ro, C. U., Shaw, M., Vet, R., Bergmann, D., Cameron-Smith, P., Dalsoren, S., Doherty, R., Faluvegi, G., Ghan, S. J., Josse, B., Lee, Y. H., MacKenzie, I. A., Plummer, D., Shindell, D. T., Skeie, R. B., Stevenson, D. S., Strode, S., Zeng, G., Curran, M., Dahl-Jensen, D., Das, S., Fritzsche, D., and Nolan, M.: Multi-model mean nitrogen and sulfur deposition from the Atmospheric Chemistry and Climate Model Intercomparison Project (ACCMIP): Evaluation of historical and projected future changes, Atmos. Chem. Phys., 13, 7997–8018, doi:10.5194/acp-13-7997-2013, 2013.

Lauenroth, W. K. and Milchunas, D. G.: Shortgrass steppe, in: Natural grasslands: Introduction and western hemisphere, edited by: Coupland, R. T., Elsevier Science, Amsterdam, 1992.

Lesschen, J. P., Cammeraat, L. H., Kooijman, A. M., and van Wesemael, B.: Development of spatial heterogeneity in vegetation and soil properties after land abandonment in a semi-arid ecosystem, J. Arid Environ., 72, 2082–2092, doi:10.1016/j.jaridenv.2008.06.006, 2008.

Li, D. J., Niu, S. L., and Luo, Y. Q.: Global patterns of the dynamics of soil carbon and nitrogen stocks following afforestation: A meta-analysis, New Phytol., 195, 172–181, doi:10.1111/j.1469-8137.2012.04150.x, 2012.

Lindeskog, M., Arneth, A., Bondeau, A., Waha, K., Seaquist, J., Olin, S., and Smith, B.: Implications of accounting for land use in simulations of ecosystem carbon cycling in Africa, Earth Syst. Dynam., 4, 385–407, doi:10.5194/esd-4-385-2013, 2013.

MacDonald, G. K., Bennett, E. M., and Taranu, Z. E.: The influence of time, soil characteristics, and land-use history on soil phosphorus legacies: A global meta-analysis, Global Change Biol., 18, 1904–1917, doi:10.1111/j.1365-2486.2012.02653.x, 2012.

Martin, P., Jung, M., Brearley, F. Q., Ribbons, R. R., Lines, E. R., and Jacob, A. L.: Can we set a global threshold age to define mature forests?, Peer J., 4, E1595, doi:10.7717/Peerj.1595, 2016.

McLauchlan, K.: The nature and longevity of agricultural impacts on soil carbon and nutrients: A review, Ecosystems, 9, 1364–1382, doi:10.1007/s10021-005-0135-1, 2006.

McSherry, M. E. and Ritchie, M. E.: Effects of grazing on grassland soil carbon: A global review, Global Change Biol., 19, 1347–1357, doi:10.1111/gcb.12144, 2013.

Milchunas, D. G. and Lauenroth, W. K.: Quantitative effects of grazing on vegetation and soils over a global range of environments, Ecol. Monogr., 63, 327–366, doi:10.2307/2937150, 1993.

Miller, P. A., Giesecke, T., Hickler, T., Bradshaw, R. H. W., Smith, B., Seppa, H., Valdes, P. J., and Sykes, M. T.: Exploring climatic and biotic controls on Holocene vegetation change in Fennoscandia, J. Ecol., 96, 247–259, doi:10.1111/j.1365-2745.2007.01342.x, 2008.

Moran, E. F., Brondizio, E. S., Tucker, J. M., da Silva-Forsberg, M. C., McCracken, S., and Falesi, I.: Effects of soil fertility and land-use on forest succession in Amazonia, Forest Ecol. Manage., 139, 93–108, doi:10.1016/S0378-1127(99)00337-0, 2000.

Murty, D., Kirschbaum, M. U. F., McMurtrie, R. E., and McGilvray, A.: Does conversion of forest to agricultural land change soil carbon and nitrogen? A review of the literature, Global Change Biol., 8, 105–123, doi:10.1046/j.1354-1013.2001.00459.x, 2002.

Norden, N., Angarita, H. A., Bongers, F., Martinez-Ramos, M., Granzow-de la Cerda, I., Breugel, M., Lebrija-Trejos, E., Meave, J. A., Vandermeer, J., Williamson, G. B., Finegan, B., Mesquita, R., and Chazdon, R. L.: Successional d ynamics in Neotropical forests are as uncertain as they are predictable, P. Natl. Acad. Sci. USA, 112, 8013–8018, doi:10.1073/pnas.1500403112, 2015.

Pan, Y. D., Birdsey, R. A., Fang, J. Y., Houghton, R., Kauppi, P. E., Kurz, W. A., Phillips, O. L., Shvidenko, A., Lewis, S. L., Canadell, J. G., Ciais, P., Jackson, R. B., Pacala, S. W., McGuire, A. D., Piao, S. L., Rautiainen, A., Sitch, S., and Hayes, D.: A large and persistent carbon sink in the world's forests, Science, 333, 988–993, doi:10.1126/science.1201609, 2011.

Paul, K. I., Polglase, P. J., Nyakuengama, J. G., and Khanna, P. K.: Change in soil carbon following afforestation, Forest Ecol. Manage., 168, 241–257, doi:10.1016/S0378-1127(01)00740-X, 2002.

Peng, S. S., Piao, S. L., Zeng, Z. Z., Ciais, P., Zhou, L. M., Li, L. Z. X., Myneni, R. B., Yin, Y., and Zeng, H.: Afforestation in China cools local land surface temperature, P. Natl. Acad. Sci. USA, 111, 2915–2919, doi:10.1073/pnas.1315126111, 2014.

Penuelas, J. and Staudt, M.: BVOCS and global change, Trends Plant Sci., 15, 133–144, doi:10.1016/j.tplants.2009.12.005, 2010.

Pielke, R. A., Pitman, A., Niyogi, D., Mahmood, R., McAlpine, C., Hossain, F., Goldewijk, K. K., Nair, U., Betts, R., Fall, S., Reichstein, M., Kabat, P., and de Noblet, N.: Land use/land cover changes and climate: Modeling analysis and observational evidence, Wires Clim. Change, 2, 828–850, doi:10.1002/wcc.144, 2011.

Poeplau, C., Don, A., Vesterdal, L., Leifeld, J., Van Wesemael, B., Schumacher, J., and Gensior, A.: Temporal dynamics of soil organic carbon after land-use change in the temperate zone – carbon response functions as a model approach, Global Change Biol., 17, 2415–2427, doi:10.1111/j.1365-2486.2011.02408.x, 2011.

Post, W. M. and Kwon, K. C.: Soil carbon sequestration and land-use change: Processes and potential, Global Change Biol., 6, 317–327, doi:10.1046/j.1365-2486.2000.00308.x, 2000.

Potter, K. N., Torbert, H. A., Johnson, H. B., and Tischler, C. R.: Carbon storage after long-term grass establishment on degraded soils, Soil Sci., 164, 718–725, doi:10.1097/00010694-199910000-00002, 1999.

Potter, P., Ramankutty, N., Bennett, E. M., and Donner, S. D.: Characterizing the spatial patterns of global fertilizer application and manure production, Earth Interact., 14, 1–22, doi:10.1175/2009ei288.1, 2010.

Poulton, P. R., Pye, E., Hargreaves, P. R., and Jenkinson, D. S.: Accumulation of carbon and nitrogen by old arable land reverting to woodland, Global Change Biol., 9, 942–955, doi:10.1046/j.1365-2486.2003.00633.x, 2003.

Pugh, T. A. M., Arneth, A., Olin, S., Ahlstrom, A., Bayer, A. D., Goldewijk, K. K., Lindeskog, M., and Schurgers, G.: Simulated carbon emissions from land-use change are substantially enhanced by accounting for agricultural management, Environ. Res. Lett., 10, 124008, doi:10.1088/1748-9326/10/12/124008, 2015.

Queiroz, C., Beilin, R., Folke, C., and Lindborg, R.: Farmland abandonment: Threat or opportunity for biodiversity conservation? A global review, Front. Ecol. Environ., 12, 288–296, doi:10.1890/120348, 2014.

Randriamalala, J. R., Herve, D., Randriamboavonjy, J. C., and Carriere, S. M.: Effects of tillage regime, cropping duration and fallow age on diversity and structure of secondary vegetation in Madagascar, Agr. Ecosyst. Environ., 155, 182–193, doi:10.1016/j.agee.2012.03.020, 2012.

Richter, D. D., Markewitz, D., Heine, P. R., Jin, V., Raikes, J., Tian, K., and Wells, C. G.: Legacies of agriculture and forest regrowth in the nitrogen of old-field soils, Forest Ecol. Manage., 138, 233–248, doi:10.1016/S0378-1127(00)00399-6, 2000.

Saldarriaga, J. G., West, D. C., Tharp, M. L., and Uhl, C.: Long-term chronosequence of forest succession in the upper Rio Negro of Colombia and Venezuela, J. Ecol., 76, 938–958, doi:10.2307/2260625, 1988.

Scharlemann, J. P. W., Tanner, E. V. J., Hiederer, R., and Kapos, V.: Global soil carbon: Understanding and managing the largest terrestrial carbon pool, Carbon Manage., 5, 81–91, doi:10.4155/Cmt.13.77, 2014.

Schierhorn, F., Muller, D., Beringer, T., Prishchepov, A. V., Kuemmerle, T., and Balmann, A.: Post-Soviet cropland abandonment and carbon sequestration in European Russia, Ukraine, and Belarus, Global Biogeochem. Cy., 27, 1175–1185, doi:10.1002/2013GB004654, 2013.

Shevliakova, E., Pacala, S. W., Malyshev, S., Hurtt, G. C., Milly, P. C. D., Caspersen, J. P., Sentman, L. T., Fisk, J. P., Wirth, C., and Crevoisier, C.: Carbon cycling under 300 years of land use change: Importance of the secondary vegetation sink, Global Biogeochem. Cy., 23, GB2022, doi:10.1029/2007gb003176, 2009.

Silver, W. L., Ostertag, R., and Lugo, A. E.: The potential for carbon sequestration through reforestation of abandoned tropical agricultural and pasture lands, Restor. Ecol., 8, 394–407, doi:10.1046/j.1526-100x.2000.80054.x, 2000.

Smith, B., Warlind, D., Arneth, A., Hickler, T., Leadley, P., Siltberg, J., and Zaehle, S.: Implications of incorporating N cycling and N limitations on primary production in an individual-based dynamic vegetation model, Biogeosciences, 11, 2027–2054, doi:10.5194/bg-11-2027-2014, 2014.

Smith, P., Andren, O., Karlsson, T., Perala, P., Regina, K., Rounsevell, M., and van Wesemael, B.: Carbon sequestration potential in European croplands has been overestimated, Global Change Biol., 11, 2153–2163, doi:10.1111/j.1365-2486.2005.01052.x, 2005.

Stocker, B. D., Feissli, F., Strassmann, K. M., Spahni, R., and Joos, F.: Past and future carbon fluxes from land use change,

shifting cultivation and wood harvest, Tellus B, 66, 23188, doi:10.3402/Tellusb.V66.23188, 2014.

Suding, K. N., Gross, K. L., and Houseman, G. R.: Alternative states and positive feedbacks in restoration ecology, Trends Ecol. Evol., 19, 46–53, doi:10.1016/j.tree.2003.10.005, 2004.

Uhl, C., Buschbacher, R., and Serrao, E. A. S.: Abandoned pastures in Eastern Amazonia. 1. Patterns of plant succession, J. Ecol., 76, 663–681, doi:10.2307/2260566, 1988.

Vellend, M.: Parallel effects of land-use history on species diversity and genetic diversity of forest herbs, Ecology, 85, 3043–3055, doi:10.1890/04-0435, 2004.

Wall, A. and Hytonen, J.: Soil fertility of afforested arable land compared to continuously, Plant Soil, 275, 247–260, doi:10.1007/s11104-005-1869-4, 2005.

Wandelli, E. V. and Fearnside, P. M.: Secondary vegetation in central Amazonia: Land-use history effects on aboveground biomass, Forest Ecol. Manage., 347, 140–148, doi:10.1016/j.foreco.2015.03.020, 2015.

Wilkenskjeld, S., Kloster, S., Pongratz, J., Raddatz, T., and Reick, C. H.: Comparing the influence of net and gross anthropogenic land-use and land-cover changes on the carbon cycle in the MPI-ESM, Biogeosciences, 11, 4817–4828, doi:10.5194/bg-11-4817-2014, 2014.

Willis, K. J., Gillson, L., and Brncic, T. M.: How "virgin" is virgin rainforest?, Science, 304, 402–403, doi:10.1126/science.1093991, 2004.

Wu, S., Mickley, L. J., Kaplan, J. O., and Jacob, D. J.: Impacts of changes in land use and land cover on atmospheric chemistry and air quality over the 21st century, Atmos Chem Phys, 12, 1597–1609, doi:10.5194/acp-12-1597-2012, 2012.

Biogeosciences, 14, 4829–4850, 2017
https://doi.org/10.5194/bg-14-4829-2017

Biogeosciences Open Access EGU

Global consequences of afforestation and bioenergy cultivation on ecosystem service indicators

Andreas Krause[1], Thomas A. M. Pugh[1,2,3], Anita D. Bayer[1], Jonathan C. Doelman[4], Florian Humpenöder[5], Peter Anthoni[1], Stefan Olin[6], Benjamin L. Bodirsky[5], Alexander Popp[5], Elke Stehfest[4], and Almut Arneth[1]

[1]Karlsruhe Institute of Technology, Institute of Meteorology and Climate Research – Atmospheric Environmental Research (IMK-IFU), Kreuzeckbahnstr. 19, Garmisch-Partenkirchen, 82467, Germany
[2]School of Geography, Earth & Environmental Science, University of Birmingham, Birmingham, B15 2TT, UK
[3]Birmingham Institute of Forest Research, University of Birmingham, Birmingham, B15 2TT, UK
[4]PBL, Netherlands Environmental Assessment Agency, 2500 GH The Hague, Postbus 30314, the Netherlands
[5]Potsdam Institute for Climate Impact Research (PIK), Telegrafenberg, P.O. Box 60 12 03, Potsdam, 14412, Germany
[6]Department of Physical Geography and Ecosystem Science, Lund University, Lund, 22362, Sweden

Correspondence to: Andreas Krause (andreas.krause@kit.edu)

Received: 26 April 2017 – Discussion started: 19 May 2017
Revised: 21 September 2017 – Accepted: 22 September 2017 – Published: 3 November 2017

Abstract. Land management for carbon storage is discussed as being indispensable for climate change mitigation because of its large potential to remove carbon dioxide from the atmosphere, and to avoid further emissions from deforestation. However, the acceptance and feasibility of land-based mitigation projects depends on potential side effects on other important ecosystem functions and their services. Here, we use projections of future land use and land cover for different land-based mitigation options from two land-use models (IMAGE and MAgPIE) and evaluate their effects with a global dynamic vegetation model (LPJ-GUESS). In the land-use models, carbon removal was achieved either via growth of bioenergy crops combined with carbon capture and storage, via avoided deforestation and afforestation, or via a combination of both. We compare these scenarios to a reference scenario without land-based mitigation and analyse the LPJ-GUESS simulations with the aim of assessing synergies and trade-offs across a range of ecosystem service indicators: carbon storage, surface albedo, evapotranspiration, water runoff, crop production, nitrogen loss, and emissions of biogenic volatile organic compounds.

In our mitigation simulations cumulative carbon storage by year 2099 ranged between 55 and 89 GtC. Other ecosystem service indicators were influenced heterogeneously both positively and negatively, with large variability across regions and land-use scenarios. Avoided deforestation and afforestation led to an increase in evapotranspiration and enhanced emissions of biogenic volatile organic compounds, and to a decrease in albedo, runoff, and nitrogen loss. Crop production could also decrease in the afforestation scenarios as a result of reduced crop area, especially for MAgPIE land-use patterns, if assumed increases in crop yields cannot be realized. Bioenergy-based climate change mitigation was projected to affect less area globally than in the forest expansion scenarios, and resulted in less pronounced changes in most ecosystem service indicators than forest-based mitigation, but included a possible decrease in nitrogen loss, crop production, and biogenic volatile organic compounds emissions.

1 Introduction

If the trend in global carbon dioxide (CO_2) emissions observed over the last 2 decades continues, the atmospheric CO_2 concentration is expected to exceed 900 ppm at the end of the 21st century, resulting in a surface temperature increase of several degrees (Friedlingstein et al., 2014; Le Quéré et al., 2015; Peters et al., 2013). However, during the COP21 climate conference in Paris 2015, participating parties agreed to limit global warming to 2 °C or less relative to the pre-industrial era, and by today, 169 countries have rat-

ified the agreement (http://unfccc.int/paris_agreement/items/9485.php, accessed 2 November 2017). The $< 2\,^{\circ}C$ warming goal requires greenhouse gas (GHG) concentrations to approximately follow or stay below the representative concentration pathway 2.6 (RCP2.6, van Vuuren et al., 2011), which will require serious reductions in CO_2 (and other GHG) emissions across all sectors. Present projections indicate that (1) without substantial net negative CO_2 emissions later this century, the Paris goal will not be achievable (Fuss et al., 2014; Rogelj et al., 2015), and (2) some negative emissions need to be realized in 10–20 years (Anderson and Peters, 2016).

The total carbon dioxide removal (CDR) necessary to achieve the $2\,^{\circ}C$ target is typically around 100–230 GtC (Rogelj et al., 2015; Smith et al., 2016) depending on the future CO_2 emission pathway and including the need to avoid carbon (C) emissions from further land clearance. Two main strategies of land-based climate change mitigation are commonly discussed for CDR: growth of bioenergy crops in combination with carbon capture and storage (BECCS), and avoided deforestation in combination with afforestation and reforestation (ADAFF) (Humpenöder et al., 2014; van Vuuren et al., 2013; Williamson, 2016). BECCS involves the planting of bioenergy crops or trees, which are burned in power stations or converted to biofuels, and the released CO_2 being captured for long-term underground storage in geological reservoirs. ADAFF utilizes the natural C uptake of forest ecosystems in biomass and soil by maintaining and expanding global forest area.

The total land demand and spatial patterns of these mitigation strategies are highly uncertain due to strong dependencies on underlying assumptions about future environmental and socio-economic changes (Boysen et al., 2017; Popp et al., 2017; Slade et al., 2014). BECCS and ADAFF will likely increase pressure on food-producing agricultural areas and, in the case of BECCS, natural ecosystems. Moreover, similar to other mitigation technologies, the feasibility and effectiveness of BECCS and ADAFF are debated (Keller et al., 2014; Williamson, 2016). For instance, in boreal and many temperate regions tree cover reduces surface albedo, thereby causing local warming (Alkama and Cescatti, 2016). Additionally, reduced CO_2 emissions through forest protection and expansion might be counteracted by cropland expansion in non-forest areas (Popp et al., 2014). BECCS includes substantial economic costs in its CCS component (Smith et al., 2016) and is currently far from being deployable at the commercial scale (Peters et al., 2017; Reiner, 2016). It will also require sufficient safe geologic C storage capacities (Scott et al., 2015). Additionally, the efficiency of BECCS might diminish when C emissions from deforestation (Wiltshire and Davies-Barnard, 2015) or nitrous oxide (N_2O) emissions from bioenergy crops (Crutzen et al., 2008) are considered (with the latter often being accounted for in BECCS scenarios, e.g. Humpenöder et al., 2014).

But even if land-based measures were to be successful with respect to their primary goal of permanently and substantially reducing atmospheric CO_2 levels to mitigate climate change, impacts on ecosystems and societies are likely to be complex (Bennett et al., 2009; Creutzig et al., 2015; Foley et al., 2005; Smith and Torn, 2013; Smith et al., 2013; Viglizzo et al., 2012) and include effects far away from the original land-use (LU) location (DeFries et al., 2004; Rodriguez et al., 2006). The multiplicity of environmental implications caused by large-scale CO_2 removal have so far been largely neglected (Williamson, 2016). The relevance of negative emission technologies, combined with our limited knowledge of their feasibility and risks, encourages the exploration of potential synergies and trade-offs between terrestrial ecosystem services (ESs, defined as benefits that people obtain from ecosystems; MEA, 2005) that are affected in land-based mitigation projects. Such work will facilitate decision-making as to whether the realization of such projects is desirable for society.

In this study, we utilize projections of future LU from one integrated assessment model (IAM, IMAGE) and one LU model (MAgPIE), that are created based on three large-scale land-based mitigation options (BECCS, ADAFF, and a combination of both). Each of these target a CDR of 130 GtC (only CO_2 carbon, omitting other greenhouse gases) by the end of the century, which is approximately equivalent to the cumulative deforestation CO_2 emissions from the late 19th century to today, or around 60 ppm (Le Quéré et al., 2015). We use these spatially explicit LU patterns as input for simulations with the LPJ-GUESS dynamic vegetation model to analyse effects on a variety of ecosystem functions that serve as indicators for important ecosystem services. By using LU patterns from two different LU models we explore some of the uncertainty in indicators of ESs arising from different model assumptions concerning the land demand of land-based mitigation. The main research questions we address in this study are as follows.

1. What are the impacts of land management for carbon uptake on other ecosystem service indicators?

2. Do the effects of land-based climate change mitigation on ecosystem service indicators differ based on the mitigation approach (BECCS, ADAFF, or a combination of both)?

3. If so, can a mitigation approach be identified in which trade-offs between other ecosystem service indicators are less pronounced than in the other approaches?

4. What are the spatial and temporal patterns of the impacts of land-based mitigation on ecosystem service indicators?

This is to our knowledge the first time that global LU scenarios are being used as input to a process-based ecosystem

model to assess changes in ecosystem function and effects on multiple ES indicators.

2 Methods

2.1 LPJ-GUESS

The process-based dynamic global vegetation model (DGVM) LPJ-GUESS simulates vegetation dynamics in response to climate, land-use change (LUC), atmospheric CO_2, and nitrogen (N) input (Olin et al., 2015a; Smith et al., 2014). The model distinguishes between natural, pasture and cropland land-cover types (Lindeskog et al., 2013), all of which include C–N dynamics (Olin et al., 2015a; Smith et al., 2014). Vegetation dynamics in natural land cover are characterized by the establishment, competition, and mortality of 12 plant functional types (PFTs, 10 groups of tree species, C_3 and C_4 grasses) in a number of replicate patches (10 in this study for primary vegetation, 2 for abandoned agricultural areas). Vertical forest structure is accounted for by the use of different age classes for woody PFTs. When forests are cleared for agriculture, 20 % of the woody biomass enters a product pool (turnover time of 25 years), with the rest being oxidized (74 %) or transferred to the litter (6 %). Pastures are populated by C_3 or C_4 grasses which are annually harvested (50 % of above-ground biomass) (Lindeskog et al., 2013). Croplands are represented by prescribed fractions of five crop functional types (CFTs, see Table S1 in the Supplement), which are moderately tilled, fertilized, and harvested (Olin et al., 2015a), and are prescribed to be either irrigated or rain-fed (Lindeskog et al., 2013). Specific bioenergy crops are currently not represented. While LPJ-GUESS does not assume yield increases due to technological progress (in contrast to IMAGE and MAgPIE), climate change adaption is simulated by using a dynamic potential heat unit (PHU) calculation (Lindeskog et al., 2013). The PHU sum needed for the full development of a crop determines its harvesting time. For irrigated crops, water supply is assumed to be available as required to fulfil the plant's water demand. Unmanaged cover grass (C_3 or C_4 type depending on climate) is allowed to grow in croplands between growing seasons.

2.2 The IMAGE and MAgPIE models and the provided land-use scenarios

IMAGE is an IAM model framework that includes several sub-models representing the energy system, agricultural economy, LU, natural vegetation, and climate system (Stehfest et al., 2014). Socio-economic parameters are usually calculated for 26 world regions, and most environmental parameters are modelled on a $0.5° \times 0.5°$ grid at annual time steps. LU dynamics are driven by demand for and supply of crops, animal products, and bioenergy. Bioenergy demand to achieve a specific CDR target is determined by the energy system sub-model which uses land availability from the LU sub-model following a set of sustainability criteria (Hoogwijk et al., 2003). For this study, bioenergy crops are included as fast-growing C_4 grasses (Doelman et al., 2017) as these produce higher yields than woody plants in many locations. The level of agricultural intensification required to free up land for afforestation to achieve a specific CDR target is estimated using a stepwise approach of increasing yields and livestock efficiencies. This implies that reduced crop and pasture areas go with higher yields and livestock efficiencies, thereby allowing the same food production as in the baseline. Afforestation is assumed to occur first in grid cells with high potential for forest growth. IMAGE also represents degraded areas (calibrated so that, together with areas cleared for agriculture, FAO deforestation statistics are met) which can be reforested as part of the afforestation activities (Doelman et al., 2017). Natural vegetation regrowth trajectories as well as crop yields, C, and water dynamics are modelled dynamically by the internally coupled DGVM LPJmL (Bondeau et al., 2007; Stehfest et al., 2014).

MAgPIE is a global multi-regional partial equilibrium model of the agricultural sector (Lotze-Campen et al., 2008; Popp et al., 2014). The model aims to minimize the global costs for agricultural production throughout the 21st century at a 5-year time step (recursive dynamic optimization) and is driven by demand for agricultural commodities and associated costs in 10 world regions. The cost minimization is subject to various spatially explicit biophysical factors such as land and water availability as well as crop yields (provided by LPJmL). Major options to fulfil increasing demand are intensification (yield-increasing technologies), expansion (LUC), and international trade. Demand for CDR enters the model at the global scale, while the spatial distribution of bioenergy production or afforestation is derived endogenously in the model (involving economic and biophysical factors). Bioenergy demand is fulfilled chiefly through the growth and harvest of grassy energy crops; woody bioenergy in this study is grown only on less than 1 % of the area used for bioenergy. Actual bioenergy yields are derived from potential LPJmL yields (using information about observed LU intensity and agricultural area for initialization) but can exceed LPJmL yields over time due to technological progress (Humpenöder et al., 2014). Afforestation is assumed to occur as managed regrowth of natural vegetation according to parameterized s-shaped growth curves towards a maximum potential natural vegetation C density as provided by LPJmL, with soil C increasing linearly towards its potential maximum within 20 years (Humpenöder et al., 2014). For simplicity, we refer to both IMAGE and MAgPIE as LU models (LUMs) in the following.

As input to our study we use the baseline projections (without land-based mitigation) from IMAGE and MAgPIE, and three land-based mitigation scenarios, each calculated by both LUMs, based on the assumption of a cumulative CDR target of 130 GtC by the year 2100. In the "BECCS" scenario this is achieved via bioenergy plant cultivation and sub-

sequent CCS, the "ADAFF" scenario involves maintaining and expanding global forest area, and in "BECCS-ADAFF" the CDR demand is fulfilled in equal parts via both options. While the CDR target in ADAFF is achieved via terrestrial C uptake (CDR = Δ vegetation C + Δ soil C + Δ product pool), in BECCS it is fulfilled solely via CCS (CDR = cumulative CCS) and thus did not account for changes in vegetation and soil C. The baseline scenario ("BASE") involves no land-based mitigation but LUC takes place in response to, among other factors, increasing food demand, dependent on population and GDP growth. LUC was provided by the LUMs as net land-cover transitions. Wood harvest was not accounted for in the data provided by the LUMs. All scenarios were developed with RCP2.6 climate produced by the IPSL-CM5A-LR general circulation model (GCM), bias corrected to the 1960–1999 historical period (Hempel et al., 2013). The LU scenarios were created using harmonized assumptions about climate change, atmospheric composition, and socio-economic development and thus did not include C cycle feedbacks. As it seems currently unlikely that the RCP2.6 pathway can be achieved without any land-based mitigation (Fuss et al., 2014), the BASE scenario should rather be regarded as a diagnostic scenario to isolate the LU effects induced by the mitigation scenarios from other factors. CO_2 fertilization effects on plant growth were simulated in the LUMs' crop growth and vegetation models. Both LUMs harmonized their cropland and pasture LU patterns to the spatially explicit HYDE 3.1 dataset (Klein Goldewijk et al., 2011) in the year 1995 (MAgPIE) or 2005 (IMAGE), with small deviations in the area of the land-cover classes occurring due to different land masks and calibration routines. The simulation period was 1970–2100 in IMAGE and 1995–2100 in MAgPIE. Socio-economic developments as input to the LUMs were based on the Shared Socioeconomic Pathway 2 (SSP2, "Middle of the Road") (O'Neill et al., 2014; Popp et al., 2017). We only used spatially explicit LU and land management (irrigation and synthetic plus organic N fertilizer) patterns from the LUMs as input to the LPJ-GUESS simulations; other variables also available from the LUMs (e.g. C stocks or crop production) were calculated with LPJ-GUESS. Details about the conversion of IMAGE and MAgPIE-LU data to LPJ-GUESS input data can be found in Supplement Sect. S1.

Even though MAgPIE and IMAGE derive crop yields and C densities from the same DGVM (LPJmL; Bondeau et al., 2007), the land demand to meet the same CDR target is larger in IMAGE than in MAgPIE. This reflects different model approaches: while in IMAGE bioenergy cultivation can only be established in unproductive regions not needed for food production, in MAgPIE there is a competition for land between food production and land-based mitigation. Concerning afforestation, managed regrowth (according to prescribed growth curves) is assumed in MAgPIE while in IMAGE natural regrowth dynamically calculated within LPJmL is implemented. Consequently, bioenergy production in MAgPIE is located in regions with mostly higher yields compared to IMAGE, and forest regrowth occurs at a faster rate, resulting in less LUC and mitigation actions starting later in the MAgPIE scenarios (Fig. 1, Table S2). In the BASE scenario, the area under natural vegetation decreases throughout the future for both IMAGE and MAgPIE (Fig. 1, Table S2), but more so for IMAGE due to the representation of degraded forests (which are treated as grassland in IMAGE; see Supplement Sect. S1). Substantial regional differences between both LUMs exist by the end of the century in the BASE scenario (Fig. 2a). Avoided deforestation and afforestation in the ADAFF scenarios is chiefly located in the tropics (Fig. 2b) and afforestation typically takes place on pastures or degraded forests in IMAGE but on croplands in MAgPIE (Table S2). Bioenergy production area in BECCS is increased mainly at the expense of natural vegetation in IMAGE but taken also from existing agricultural land in MAgPIE. Total cropland area increases in the scenario combining both strategies (BECCS-ADAFF) compared to BASE for IMAGE but decreases for MAgPIE BECCS-ADAFF (Fig. 1). IMAGE uses a slightly larger grid list than MAgPIE and accounts for the water fraction of a grid cell; but as the impacts on land-based mitigation in LPJ-GUESS turned out to be small (< 2 GtC over the simulation period) we only included grid cells in our simulations for which LU data were provided by both LUMs (assuming 100 % land cover) to facilitate comparison of the results.

2.3 Simulations setup

The LPJ-GUESS simulations were forced by daily atmospheric climate variables (surface temperature, precipitation, shortwave radiation) extracted from bias-corrected simulated IPSL-CM5A-LR RCP2.6 climate (1950–2099) from the first phase of ISI-MIP project (Warszawski et al., 2014). For the historical period we randomly chose years from the period 1950–1959 to generate climate data for the years 1901–1949. A repeating climate cycle from the 1901–1930 period was used for the model's spin-up. The global average surface temperature increase in IPSL-CM5A-LR is 1.3 °C (1.6 °C on land) by the end of the century (2070–2099) compared to present-day (1980–2009) for RCP2.6. This value is in the middle of an ensemble of a wider range of GCM models used in ISI-MIP (Warszawski et al., 2014). Historical (1901–2005) and future (RCP2.6, 2006–2099) atmospheric CO_2 mixing ratios were taken from Meinshausen et al. (2011). The year 1901 value (296 ppmv) was used for the spin-up. Future atmospheric CO_2 mixing ratio peaks at 443 ppmv in year 2052 and drops to $\sim$ 424 ppmv by the end of the century (Meinshausen et al., 2011). Gridded N deposition rates were available as decadal monthly averages for the historical and future (RCP2.6) period (Lamarque et al., 2010, 2011). N deposition for year 1901 was used for the spin-up. Spatially explicit LU patterns and N fertilization were adopted from IMAGE and MAgPIE (see also Supplement Sect. S1). We used the year 1901 land-cover map for the spin-up, thereby

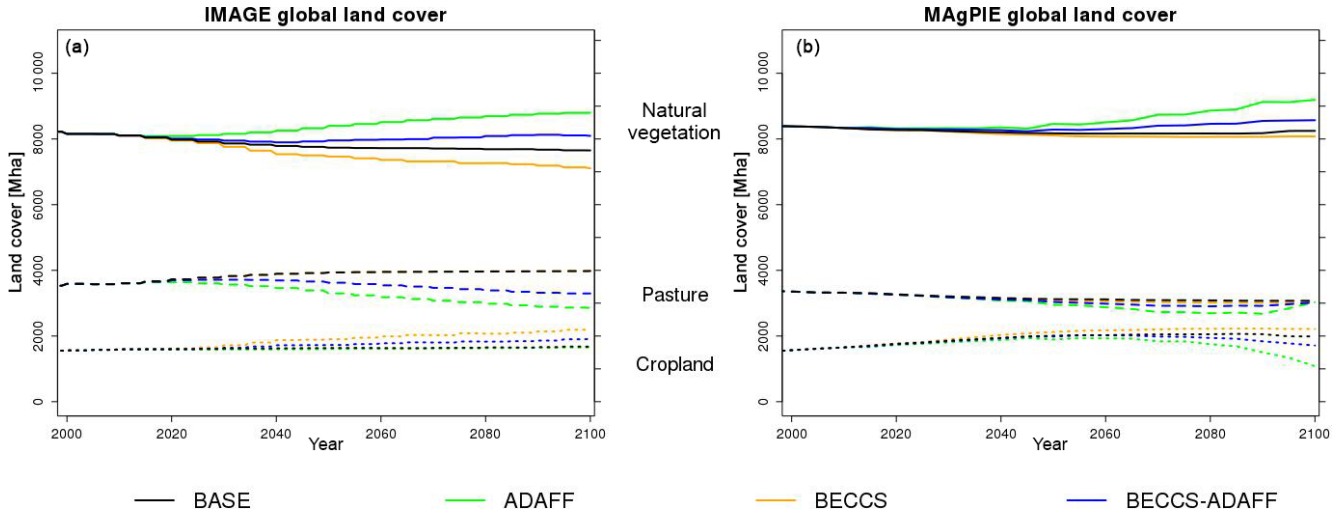

Figure 1. Time series (2000–2100) of area under natural vegetation (including afforested area), pasture (including degraded forest area for IMAGE), and cropland (including bioenergy production area) for the different scenarios, for IMAGE **(a)** and MAgPIE **(b)**.

omitting LUC occurring before the 20th century as we assumed legacy effects from pre-1901 LUC on the future C cycle to be small.

2.4 Analysed ecosystem service indicators

We analysed the implications of future LU patterns for the following ES indicators: C storage (as an indicator for global climate change mitigation), surface albedo and evapotranspiration (indicators for regional climate effects in response to land-cover change), annual runoff (indicator for water availability), peak monthly runoff (indicator for flood protection), crop production (excluding cotton, forage crops, and pasture harvest; indicator for food production), N loss (in LPJ-GUESS currently not differentiated into dissolved N vs. N lost to the atmosphere; indicator for water or air quality, or GHG losses), and emissions of the most common biogenic volatile organic compounds (BVOCs) – isoprene and monoterpenes (indicator for air quality). With the exception of C storage and crop production these variables were not available from the LUMs. Most variables are direct outputs from LPJ-GUESS simulations. Calculations for ES indicators not taken directly from model outputs (C storage via CCS, crop production scaled to EarthStat, albedo) or different from the standard model setup (BVOCs) are provided in the Supplement Sects. S2–S5.

The analysed ES indicators can serve as proxies for several ESs linked to human well-being. Table 1 gives a qualitative overview of how these ES indicators and corresponding ESs are interlinked. We do not aim to value and rank individual ES indicators and thus do not assess here how relative changes could be differently prioritized in decision-making for land management. While this is certainly too simple of a generalization for fully assessing the implications of such scenarios, ranking or prioritizing individual ES indicators is a substantial challenge, which is beyond the scope of this study. A given relative change can be more crucial for some indicators than for others, and their importance can also vary across regions and parties concerned. ESs will be influenced by changes in climate, atmospheric chemistry, and LU even in the absence of land management for C mitigation. To separate these non-mitigation effects from those effects associated with a mitigation approach, we compared changes in ES indicators in the BASE simulations over the 21st century to the changes that occur when a mitigation approach is implemented. Land-based mitigation may thus potentially enhance or degrade ESs to human societies.

3 Results

In the following, the expressions "$LPJG_{IMAGE}$" and "$LPJG_{MAgPIE}$" refer to results from LPJ-GUESS simulations driven by LU patterns from IMAGE and MAgPIE, plus climate, CO_2, and N deposition from RCP2.6. At some points we refer to output directly taken from the IMAGE and MAgPIE scenarios, in which case this is explicitly stated ("in the original results/directly from the LUMs /the LUMs report").

3.1 Carbon storage

Total global C pools simulated with LPJ-GUESS are generally lower for $LPJG_{IMAGE}$ than for $LPJG_{MAgPIE}$ for all scenarios (Table 2, Fig. S1a). This difference is mainly a result of the representation of degraded forests as grasslands in IMAGE-LU patterns (see Table S2), while MAgPIE does not include degraded forests. Moreover, some temperate croplands that are specified in the MAgPIE-LU patterns to grow fodder are represented in LPJ-GUESS by rain-fed or irri-

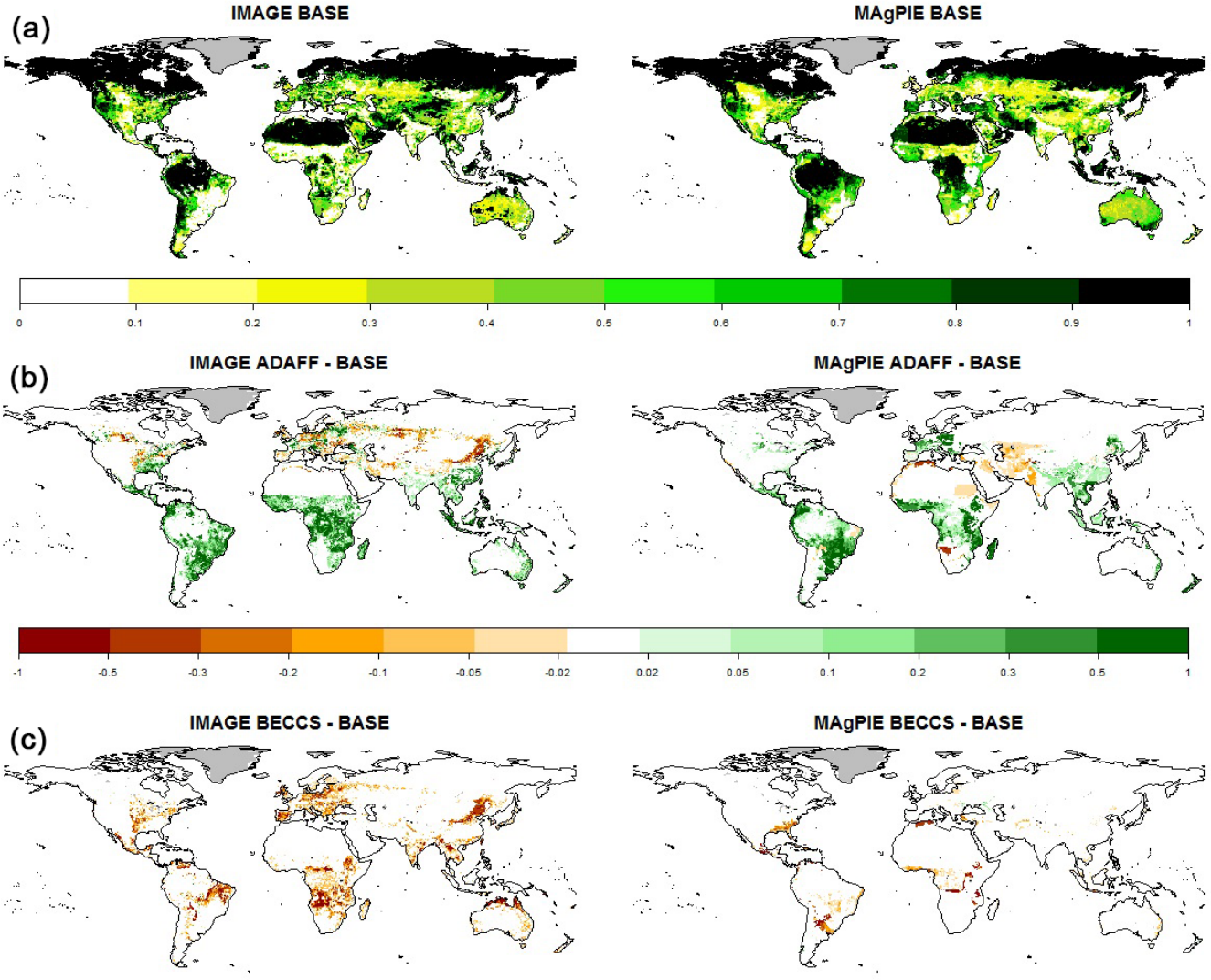

Figure 2. **(a)** Fraction of grid cell under natural vegetation (including afforested area but not degraded forests) by the end of the century (2090–2099) in the BASE scenario for IMAGE (left) and MAgPIE (right). **(b)** Difference in the natural vegetation fraction between the ADAFF and the BASE scenario by the end of the century (2090–2099). **(c)** Same as panel **(b)** but between the BECCS and the BASE scenario.

gated, harvested grass. This crop type increases soil C relative to cereal crops because the larger below-ground / above-ground biomass ratio results in less C being removed during harvest and thus more C input to the soil. C sequestration is calculated by LPJ-GUESS for both BASE simulations within the 21st century, resulting in total C pools of 1995 ($LPJG_{IMAGE}$) and 2047 ($LPJG_{MAgPIE}$) GtC by 2090–2099 (Table 2). The combined effects of LU, changing climate, N deposition, and atmospheric CO_2 levels thus enhance total C pools by 1.7 and 3.2 % (33 and 64 Gt) between the beginning and the end of the century (Fig. 3a).

As expected from the overall scenario objective, total, vegetation, and soil C pools are higher in the ADAFF simulations relative to the respective BASE at the end of the century (Table 2, Fig. S1a–c). The additional C uptake for ADAFF is larger for $LPJG_{IMAGE}$ (3.6 % or 72 GtC in year 2090–2099, 76 GtC in year 2099) than for $LPJG_{MAgPIE}$ (2.4 % or 49 GtC in year 2090–2099, 55 GtC in year 2099, Fig. 3b). This reflects the larger afforestation area and earlier afforestation activities in IMAGE (Figs. 1, 2b). The largest changes in total C are found in tropical regions, especially in Africa (+15 and +9 %, Fig. 4b) and/or tropical forests (+13 and +8 %, Fig. S2b), mostly due to increases in vegetation C.

The BECCS scenario focusing on bioenergy crops and CCS as a climate change mitigation strategy removes slightly less C from the atmosphere than ADAFF for $LPJG_{IMAGE}$ but removes more C for $LPJG_{MAgPIE}$ (Table 2, Fig. 3c). Interestingly, $LPJG_{IMAGE}$ ADAFF accumulates more C than

Table 1. Linking ecosystem functions to ecosystem services (ESs). An increase in an ecosystem function can be interpreted positive (+), negative (−), zero (0), or either positive or negative (+/−), depending on the background conditions or perspective. Effects can be small (+ or −) or large (++ or −−). Regional effects are shown without brackets and global effects, where relevant, in brackets. Indirect effects that are more directly represented by another ecosystem function considered here are not shown. The table is based on evidence from the literature in cases where the link is not directly clear (see footnotes).

Ecosystem function	ES – climate change mitigation	ES – water availability	ES – flood protection	ES – water quality	ES – air quality	ES – food production
C storage ↑	++ (++)					
Surface albedo ↑	++ (+)[a]					
Evapotranspiration ↑	++ (+/−)[b]					
Annual runoff ↑		++	−	0/+[c]		
Peak monthly runoff ↑		0/+[d]	−−	0/−[e]		0/−[f]
Crop production ↑						++ (++)
N loss ↑	+/− (+/−)[g]			−−[g]	− (−)[g]	
BVOC emissions ↑	+/− (+/−)[h]				0/− − (0/−)[i]	

[a] The global effects of LU-driven albedo changes seem to be small (e.g. de Noblet-Ducoudre et al., 2012).
[b] Local surface cooling as heat is needed to evaporate water. On larger scales, the effect could be either a warming due to increases in atmospheric water vapour (Boucher et al., 2004) or a cooling due to increased planetary albedo resulting from more cloudiness (Bala et al., 2007; Ban-Weiss et al., 2011).
[c] High flows imply more volume for dilution, prevent algae growth, and maintain oxygen levels (Whitehead et al., 2009).
[d] Effect of peak monthly runoff on water availability is dependent on seasonal rainfall distribution and regional water storage capacity. Annual runoff is the clearer indicator.
[e] Soil erosion and associated remobilization of metals is enhanced during flood events (Whitehead et al., 2009).
[f] Due to flood damage in croplands (Posthumus et al., 2009).
[g] LPJ-GUESS at present calculates total N loss and does not differentiate between leaching and gaseous loss. Thus, we indicate several effects that would arise from N emitted as N_2O (a greenhouse gas), as NO_X or NH_3 (affecting air quality and aerosol formation), or as dissolved N. The net effect of N loss on climate has been estimated to be a small cooling (Erisman et al., 2011), but uncertainties are large.
[h] The net impact of BVOC emissions is very uncertain. On the global scale, increased BVOC emissions might result in a warming (Unger, 2014).
[i] BVOCs often increase ozone and aerosol formation, primarily locally (Rosenkranz et al., 2015), with principally opposite warming and cooling effects (Unger, 2014).

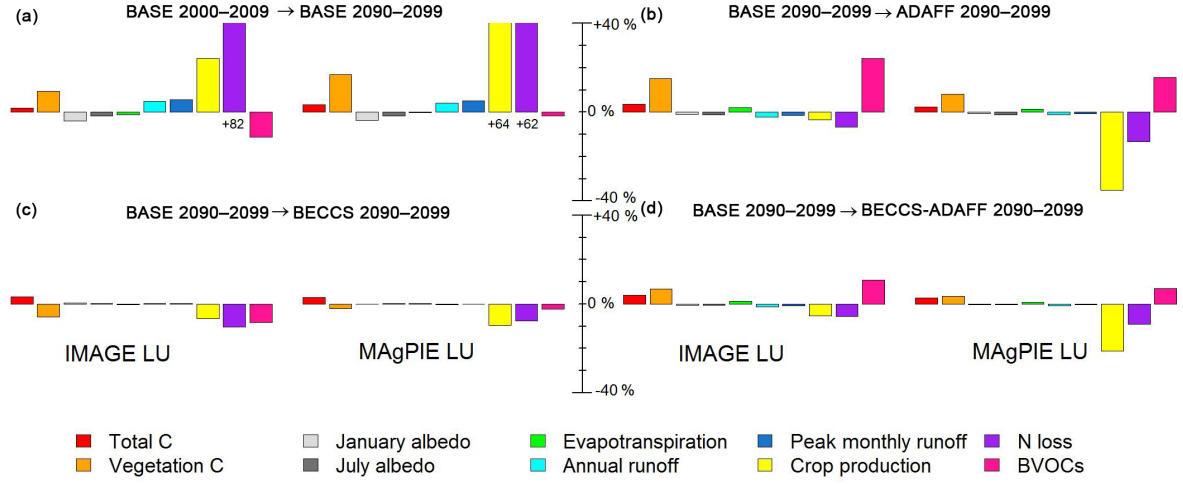

Figure 3. Global relative changes in analysed ecosystem functions simulated by LPJ-GUESS for different LU scenarios from IMAGE and MAgPIE. Changes are capped at ±40 % for clarity reasons, and values exceeding 40 % are written below the bar. **(a)** Changes in the BASE simulation from 2000–2009 to 2090–2099. **(b)** Changes from BASE to ADAFF by the 2090-2099 period. **(c)** Same as panel **(b)** but from BASE to BECCS. **(d)** Same as panel **(b)** but from BASE to BECCS-ADAFF.

$LPJG_{IMAGE}$ BECCS within the first half of the century, while BECCS catches up during the second half of the century (Fig. S1a); this acceleration of the BECCS sink is related to a steady increase in bioenergy area throughout the century. The additional total C storage achieved by the period 2090–2099 (compared to BASE 2090–2099) is 66 GtC (74 GtC in year 2099) for $LPJG_{IMAGE}$ and 61 GtC (69 GtC in year 2099) for $LPJG_{MAgPIE}$. Within these totals, cumulative C storage via CCS (harvested C from bioenergy crops) is 100 and 74 GtC by the end of the century (Table 2), but total C uptake is less than cumulative CCS as LPJ-GUESS simulates a loss of vegetation and soil C from expanded agricultural land. C stor-

Table 2. Global net-total values ± standard deviations (over 10 years) of all analysed ecosystem functions as simulated by LPJ-GUESS for all scenarios and different time periods and for $LPJG_{IMAGE}$ (top) and $LPJG_{MAgPIE}$ (bottom). Total C is the sum of vegetation C, soil C, product C (wood removed during deforestation but not immediately oxidized), and cumulative CCS.

Ecosystem function	BASE		ADAFF	BECCS-ADAFF	BECCS
	2000–2009		2090–2099		
Vegetation C	380 ± 1	415 ± 2	478 ± 4	444 ± 3	391 ± 2
(GtC)	393 ± 2	459 ± 2	496 ± 5	476 ± 3	450 ± 2
Soil and litter C	1575 ± 1	1578 ± 1	1588 ± 1	1580 ± 1	1567 ± 1
(GtC)	1585 ± 1	1587 ± 1	1599 ± 2	1592 ± 2	1583 ± 1
Product C	5.7 ± 0.4	1.5 ± 0.1	0.4 ± 0.0	1.0 ± 0.1	2.4 ± 0.2
(GtC)	4.6 ± 0.2	0.3 ± 0.0	0.4 ± 0.0	0.3 ± 0.0	0.6 ± 0.1
Cumulative CCS	–	–	–	52.1 ± 3.4	100.0 ± 6.6
(GtC)	–	–	–	34.7 ± 2.5	73.5 ± 5.6
Total C	1961 ± 2	1995 ± 3	2067 ± 5	2077 ± 7	2060 ± 7
(GtC)	1983 ± 2	2047 ± 3	2096 ± 7	2103 ± 7	2108 ± 8
January albedo	0.250 ± 0.004	0.240 ± 0.002	0.237 ± 0.002	0.238 ± 0.002	0.241 ± 0.002
	0.249 ± 0.004	0.240 ± 0.002	0.238 ± 0.002	0.240 ± 0.002	0.240 ± 0.002
July albedo	0.182 ± 0.001	0.179 ± 0.001	0.177 ± 0.001	0.178 ± 0.001	0.180 ± 0.001
	0.182 ± 0.001	0.179 ± 0.001	0.177 ± 0.001	0.178 ± 0.001	0.179 ± 0.001
Evapotranspiration	58.6 ± 0.7	57.9 ± 1.2	59.1 ± 1.2	58.6 ± 1.2	57.7 ± 1.2
($1000\,km^3\,yr^{-1}$*)	58.9 ± 0.7	58.8 ± 1.2	59.5 ± 1.2	59.3 ± 1.2	58.9 ± 1.2
Annual runoff	52.5 ± 3.1	55.1 ± 2.8	53.9 ± 2.8	54.4 ± 2.8	55.3 ± 2.8
($1000\,km^3\,yr^{-1}$)	52.2 ± 3.1	54.3 ± 2.8	53.7 ± 2.8	53.9 ± 2.8	54.2 ± 2.8
Peak monthly runoff	17.9 ± 1.0	18.9 ± 1.2	18.7 ± 1.2	18.8 ± 1.2	19.0 ± 1.2
($1000\,km^3\,month^{-1}$)	17.9 ± 1.0	18.8 ± 1.2	18.6 ± 1.2	18.7 ± 1.2	18.8 ± 1.2
Crop production	28.9 ± 0.5	35.9 ± 0.5	34.7 ± 0.5	34.0 ± 0.5	33.5 ± 0.5
(Ecal)	27.5 ± 0.9	45.2 ± 0.4	29.3 ± 2.0	35.5 ± 0.7	40.8 ± 0.5
N loss	60.3 ± 7.1	109.7 ± 13.2	102.3 ± 12.5	103.6 ± 12.3	98.4 ± 11.5
($TgN\,yr^{-1}$)	73.3 ± 6.8	119.0 ± 8.0	103.2 ± 8.4	108.1 ± 7.9	110.0 ± 7.0
Isoprene emissions	477 ± 8	419 ± 9	529 ± 11	469 ± 10	382 ± 8
($TgC\,yr^{-1}$)	503 ± 9	495 ± 10	578 ± 13	532 ± 11	483 ± 10
Monoterpene emissions	40.7 ± 0.6	38.9 ± 0.9	40.2 ± 1.0	39.4 ± 0.9	38.2 ± 0.9
($TgC\,yr^{-1}$)	41.9 ± 0.7	40.5 ± 0.9	41.6 ± 1.0	40.9 ± 0.9	40.4 ± 0.9

* $1000\,km^3$ are equal to 1 Eg of water.

age in the combined bioenergy–avoided deforestation and afforestation case (BECCS–ADAFF) mostly lies between the BECCS and the ADAFF case but for $LPJG_{IMAGE}$ exceeds both ADAFF and BECCS by the end of the century (Table 2, Figs. 3d, S1a, S3).

3.2 Albedo

Globally averaged January albedo under present-day conditions is significantly higher (∼ 0.25) than July albedo (∼ 0.18) due to the extensive northern hemispheric snow cover in January. Both values decrease throughout the 21st century in the BASE simulations, but more so for January (−4.1 and −3.7 % for $LPJG_{IMAGE}$ and $LPJG_{MAgPIE}$, respectively) than for July (−1.7 and −1.8 %) as a result of northward vegetation shifts and reductions in snow cover (Table 2, Figs. 3a, S1d–e). Regionally, for both months and both LUMs, the greatest reductions occur in high latitudes (Fig. 4a).

An increase in forested area as in the ADAFF scenario results in further albedo reductions that are – at least for July albedo – comparable in magnitude to the changes in BASE throughout the century (Table 2, Fig. 3b). Only small increases compared to BASE occur in the BECCS simulations

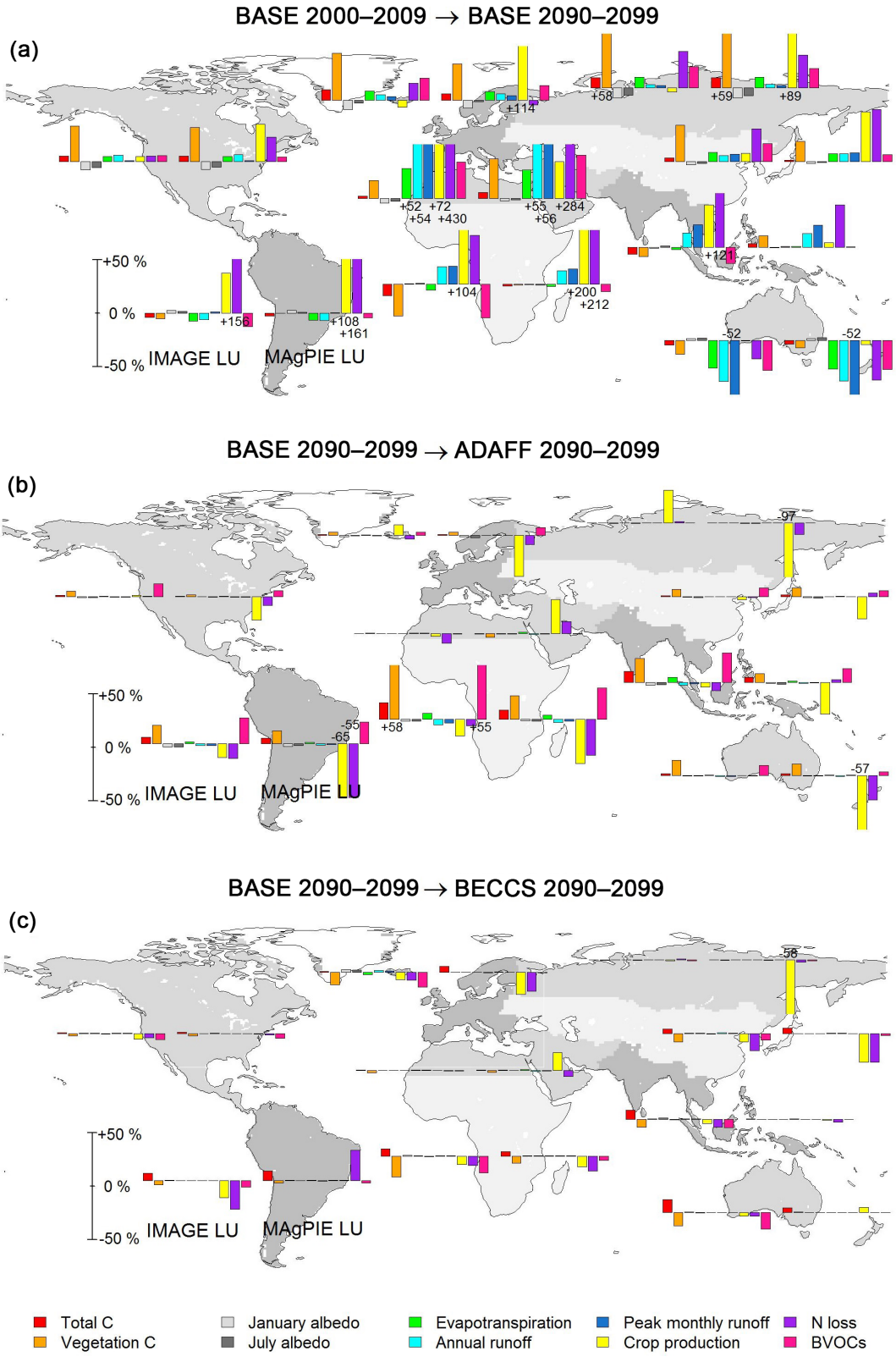

Figure 4. Regional relative changes in analysed ecosystem functions as simulated by LPJ-GUESS for IMAGE-LU (left) and MAgPIE-LU (right). Changes are capped at ±50 % for clarity reasons, values exceeding ±50 % are written upon or below the bar. Regions are aggregated Global Fire Emissions Database regions (Giglio et al., 2010) and are North America, South America, Europe, Middle East, Africa, North Asia, Central Asia, South Asia, and Oceania. **(a)** Changes in the BASE simulation from 2000–2009 to 2090–2099. **(b)** Changes from BASE to ADAFF by the 2090–2099 period. **(c)** Same as panel **(b)** but from BASE to BECCS.

(Fig. 3c) as the land demand for bioenergy crop cultivation is relatively small. BECCS-ADAFF results in a decrease in January and July albedo for both LUMs.

3.3 Evapotranspiration

Global evapotranspiration in the BASE simulations decreases much more for $LPJG_{IMAGE}$ ($-1.2\,\%$) than for $LPJG_{MAgPIE}$ (0.1 %; Table 2, Figs. 3a, S1f) due to different deforestation rates. There is large spatial variability with evapotranspiration decreasing in some regions but increasing in others (Fig. 4a), mainly driven by shifting rainfall patterns (not shown).

As expected from the generally high evapotranspiration rates of forests, end-of-century evapotranspiration in ADAFF is 2.1 and 1.3 % higher than in BASE for $LPJG_{IMAGE}$ and $LPJG_{MAgPIE}$, respectively (Fig. 3b), with the largest increase occurring in Africa (Fig. 4b). BECCS results in a change of -0.4 and $+0.2$ % for $LPJG_{IMAGE}$ and $LPJG_{MAgPIE}$, respectively, and BECCS-ADAFF in an increase of 1.3 and 0.8 % compared to BASE.

3.4 Runoff

In the BASE simulations, global annual runoff increases by 4.9 and 4.1 % by the end of the century for $LPJG_{IMAGE}$ and $LPJG_{MAgPIE}$, respectively, with a slightly larger increase of 5.2 and 5.0 % in peak monthly runoff (Table 2, Fig. 3a). This increase is mainly driven by precipitation changes, but forest loss and increased water use efficiency simulated under elevated CO_2 levels also play a role. Similar to evapotranspiration, spatial patterns are heterogeneous, with generally larger changes in annual runoff than in peak monthly runoff in high latitudes and reverse patterns in parts of the (sub-) tropics (Figs. 4a, S2a).

Changes in runoff in the mitigation simulations are opposite to evapotranspiration changes (Figs. 3b–d, 4b–c), and the effects of land-based mitigation on annual runoff are often larger than on peak monthly runoff. ADAFF reduces annual runoff by 2.2 and 1.1 % ($LPJG_{IMAGE}$ and $LPJG_{MAgPIE}$) and peak monthly runoff by 1.3 and 0.7 %, while BECCS increases annual runoff by 0.3 and 0.2 % and peak monthly runoff by 0.2 and 0.0 %.

3.5 Crop production

Globally, total crop production simulated by LPJ-GUESS averages ~ 29 and $27\,\mathrm{Ecal\,yr^{-1}}$ over the years 2000–2009 and increases by 24 and 64 % to 36 and $45\,\mathrm{Ecal\,yr^{-1}}$ by the end of the century for the $LPJG_{IMAGE}$ and $LPJG_{MAgPIE}$ BASE simulations, respectively (Table 2, Fig. S1i) (for comparison, the increase is 78 and 96 % in the original IMAGE and MAgPIE results, respectively). The large differences in crop production increase between $LPJG_{IMAGE}$ and $LPJG_{MAgPIE}$ can be explained by variations in management and crop types (e.g. whether the LUMs assume C_3 or C_4 crops to be grown in certain regions), and the area and location of managed land, which differs considerably by the end of the century, especially in Africa (Fig. 2a). Sensitivity simulations in which N fertilizer rates, cropland area, atmospheric CO_2 mixing ratio, or the dynamic PHU calculation (i.e. adaption to climate change via selecting suitable crop varieties, see Sect. 2.1) were fixed at year 2009 levels indicate that around 62 and 39 % ($LPJG_{IMAGE}$ and $LPJG_{MAgPIE}$, respectively) of the crop production increase in the BASE simulations can be attributed to increases in N fertilizer rates, 22 and 74 % to cropland expansion, 26 and 10 % to increased atmospheric CO_2 levels, and 9 and 4 % to dynamic PHU calculation (Fig. S4a). The numbers do not add up to 100 % due to non-linear effects, interdependencies between variables (crop area/fertilization), and additional influences we did not analyse (e.g. climate, N deposition, crop types, and irrigation).

Crop production calculated with LPJ-GUESS is reduced in all mitigation simulations compared to BASE, by contrast to a set requirement in the LUMs to retain annual production at similar levels to BASE: in the LUMs this is achieved through further technology increases (for example through improved management, inputs, pest control, and better crop varieties) compared to BASE. The decline simulated in LPJ-GUESS, which is larger for $LPJG_{MAgPIE}$ than for $LPJG_{IMAGE}$, especially for ADAFF ($LPJG_{IMAGE}$ -3 % for the 2090–2099 period compared to 2090–2099 BASE; $LPJG_{MAgPIE}$ -35 %), occurs because LPJ-GUESS captures only yield increases achieved through higher N input, which only covers a part of the additional technological yield increase assumed by the LUMs for the mitigation scenarios (and which therefore allows for shrinking production area, see Table S2).

3.6 Nitrogen loss

Global N loss in the BASE simulations increases strongly over the 21st century by 82 % for $LPJG_{IMAGE}$ and 62 % for $LPJG_{MAgPIE}$ (Fig. 3a). Most of the increase is caused by fertilization but increasing N deposition contributes as well ($+19$ % over the century). N loss is higher for $LPJG_{MAgPIE}$ than for $LPJG_{IMAGE}$ at the beginning and end of the 21st century, but higher for $LPJG_{IMAGE}$ around mid-century (Table 2, Fig. S1j). As total fertilizer application is higher for $LPJG_{MAgPIE}$ throughout the entire century, these differences can be explained by spatial heterogeneity (e.g. in India, where fertilization has a large impact on N loss, fertilizer rates are generally higher for $LPJG_{IMAGE}$ than for $LPJG_{MAgPIE}$). Increases in N losses correspond roughly to increases in N application, and to crop production increases in the original LUMs. This indicates that crops in LPJ-GUESS approach N saturation, and cannot use the additional N for higher yields, and thus that N application rates, while consistent with LUM yield levels, are too high for LPJ-GUESS yields. Sensitivity simulations indicate that most of the N loss increase between 2000–2009 and 2090–2099 is in-

duced by increased fertilizer application and cropland expansions, while increasing atmospheric CO_2 and dynamic PHU calculation reduce N loss (Fig. S4b).

N loss in ADAFF decreases by 6.7 % for $LPJG_{IMAGE}$ and 13.2 % for $LPJG_{MAgPIE}$ compared to BASE 2090–2099 (Fig. 3b), but with large variability across regions (Fig. 4b). The decrease can be attributed to lower global fertilizer amounts in ADAFF than in BASE for both LUMs, as forests are not fertilized. In the BECCS simulations the decrease is larger for $LPJG_{IMAGE}$ (−10.3 %) than for $LPJG_{MAgPIE}$ (−7.6 %), including substantial regional variations, especially in South America (Fig. 4c). The fertilization of bioenergy crops (for which low fertilizer rates are assumed in the LUMs) adds N to the system; however, crop N uptake and subsequent removal during harvest are also enhanced, resulting in a net N removal in LPJ-GUESS (and thus less N available to leave the system via leaching or in gaseous form). N loss reductions in BECCS-ADAFF lie between ADAFF and BECCS for $LPJG_{MAgPIE}$ (−9.2 %) but are smallest amongst all mitigation simulations for $LPJG_{IMAGE}$ (−5.5 %).

3.7 BVOCs

Changes in BVOC emissions are dominated by isoprene emissions, which are, by weight, an order of magnitude higher than those of monoterpenes (Table 2, Fig. S1k–l). In the BASE simulations, total BVOC emissions from 2000–2009 to 2090–2099 decrease by 11 % for $LPJG_{IMAGE}$ but only by 2 % for $LPJG_{MAgPIE}$ (Fig. 3a). Spatially, BVOC emissions generally increase in high latitudes but decrease in the tropics (Fig. 4a), corresponding to northward forest shifts and deforestation or forest degradation concentrated in low latitudes (not shown). The tropics dominate the overall response due to much higher typical emission rates.

As expected from the generally high emission potential of woody vegetation (compared with herbaceous), BVOC emissions increase in the ADAFF simulations (24 and 16 % for $LPJG_{IMAGE}$ and $LPJG_{MAgPIE}$, respectively). Following the spatial change in forest cover, the increase mainly occurs in the tropics (Fig. 4b). In the BECCS simulations, BVOC emissions decrease by 8 % for $LPJG_{IMAGE}$ and by 2 % for $LPJG_{MAgPIE}$ (Fig. 3c) due to the low emissions of grassy bioenergy crops (corn in LPJ-GUESS). BECCS-ADAFF results in 11 and 7 % higher emissions for $LPJG_{IMAGE}$ and $LPJG_{MAgPIE}$, respectively (Fig. 3d).

4 Discussion

4.1 Modelling uncertainties under present-day and future climate

The ES indicators analysed in this study are subject to uncertainties arising from knowledge gaps, simplified modelling assumptions, and the need to use parameterizations suited for global simulations. LPJ-GUESS has been extensively evaluated against present-day C fluxes and stocks, both for natural and agricultural systems, at site scale and against global estimates (e.g. Fleischer et al., 2015; Piao et al., 2013; Pugh et al., 2015; Smith et al., 2014). The use of forcing climate data from only one climate model can be a major source of uncertainty as shown by the large variability in future terrestrial C stocks introduced by different climate change realizations even for the same emissions pathway (Ahlstrom et al., 2012). As we use the low-emission scenario RCP2.6 here, we expect this effect to be relatively small. The albedo calculation in this study was not used previously, but patterns simulated by LPJ-GUESS under present-day conditions (Fig. S5) broadly agree with Fig. 3 in Boisier et al. (2013). Evapotranspiration and runoff in LPJ were evaluated by Gerten et al. (2004). Global total runoff calculated in this study for the 1961–1990 period is 26 % higher than their results. Simulation biases against global estimates and observations from large river basins in the Gerten study were mainly attributed to uncertainties in climate input data and to human activities such as LUC (which is now accounted for) and human water withdrawal. Spatial runoff patterns as simulated by the current LPJ-GUESS version (Fig. S6.) seem to reveal some improvements compared to the biases reported in Gerten et al. (2004) in mid- and high latitudes, but the model still overestimates runoff in parts of the tropics. With respect to crop production, simulated crop yields in LPJ-GUESS are constrained by N and water limitation, but not by local management decisions, crop varieties or breeds, diseases, and weeds (Lindeskog et al., 2013; Olin et al., 2015b), and future improvement in plant breeding are ignored. While we accounted for the additional restrictions by scaling simulated present-day yields to observations, applying the unscaled LPJ-GUESS yield changes into the future might create substantial underestimation of future yields and crop production, as the only yield-augmenting factor for a given crop type in LPJ-GUESS is increased N input. Global N-leaching rates are highly uncertain but the annual rate simulated with LPJ-GUESS (if all N losses are assumed to be via leaching) is within the range of published studies (Olin et al., 2015a). Future modelled N leaching may also be affected by ignoring improvements in plant breeds, as the current representation of crops may not be able to absorb the N input computed in the LUMs for improved varieties and management. For BVOCs, global datasets for evaluation are not available (Arneth et al., 2007; Schurgers et al., 2009). Spatial emission patterns are in good agreement with other simulations (Hantson et al., 2017).

While LPJ-GUESS has thus been evaluated as comprehensively as possible, a further next step for multi-process evaluation would be adopting a formalized benchmarking system that also allows model performance to be scored (Kelley et al., 2013). Likewise, large uncertainties reside in the actual LUMs, which differ to a large degree in their estimates of main land-cover classes for the present day (Alexander et al., 2017; Prestele et al., 2016), and for which evaluation against

observations has been identified as a challenge (van Vliet et al., 2016).

4.2 Climate regulation via biogeochemical and biophysical effects

Our $LPJG_{IMAGE}$ simulations are slightly more effective than the $LPJG_{MAgPIE}$ simulations in terms of simulated C uptake, but all simulations diverge from the CDR target initially implemented in the LUMs (see Sect. 4.7). Land-based mitigation might also impact the emissions of other GHGs (e.g. N_2O; see Table 1), but future fertilizer application rates and emissions from bioenergy crops are highly uncertain (Davidson and Kanter, 2014). While N_2O contributes to global warming, the net effect of reactive N might be a cooling when accounting for short-lived pollutants and interactions with the C cycle (Erisman et al., 2011). In our LPJ-GUESS simulations, reductions in N losses suggest a decrease in gaseous N emissions for both ADAFF and BECCS; however, no quantifications are possible as LPJ-GUESS does not yet differentiate between different forms of N losses.

Climate effects of well-mixed GHG are global, whereas biophysical effects are primarily felt on the local scale (Alkama and Cescatti, 2016). Surface albedo in regions with seasonal snow cover is expected to decrease significantly for afforestation scenarios (Bala et al., 2007; Bathiany et al., 2010; Betts, 2000; Davies-Barnard et al., 2014), thereby opposing the biogeochemical cooling effect. Effects of enhanced forest cover are less pronounced in lower latitudes (Li et al., 2015) and for BECCS scenarios (Smith et al., 2016). A modelling study by Hallgren et al. (2013) found that while albedo effects and C emissions from deforestation for biofuel production might balance on the global scale, biophysical effects can be large locally. In our BECCS simulations, albedo changes are relatively small. However, we find noticeable albedo reductions in ADAFF despite the fact that for both LUMs afforestation was concentrated in snow-free regions where satellites rarely observe albedo differences between forests and open land exceeding 0.05 (Li et al., 2015).

High evapotranspiration rates, often observed in forests, cool the local surface. In tropical regions, this cooling effect exceeds the warming effect from lower albedo (Alkama and Cescatti, 2016; Li et al., 2015). Current anthropogenic land-cover changes have been estimated to reduce terrestrial evapotranspiration by $\sim 5\,\%$ (Sterling et al., 2013). In our simulations, impacts of land-based mitigation on global evapotranspiration range from $-0.4\,\%$ ($LPJG_{IMAGE}$ BECCS) to $+2.1\,\%$ ($LPJG_{IMAGE}$ ADAFF). On the regional scale this can translate to absolute changes of more than $100\,mm\,yr^{-1}$ in some tropical areas (e.g. central Africa). While these changes seem relatively small compared to the mean differences between forests and non-forests reported by Li et al. (2015) ($141\,mm\,yr^{-1}$ 20–50° N, $238\,mm\,yr^{-1}$ 20–50° S, $428\,mm\,yr^{-1}$ 20° S–20° N), our results still suggest that reducing emissions from deforestation and forest degradation (REDD) activities would not only help mitigate global climate change via avoided C losses but could provide additional local cooling, serving as a "payback" for tropical countries. The simulated evaporative water loss due to ADAFF at the end of the century ($\sim 1200\,km^3\,yr^{-1}$ for $LPJG_{IMAGE}$ and $750\,km^3\,yr^{-1}$ for $LPJG_{MAgPIE}$ for a C sequestration rate of ~ 0.8 and $1.4\,GtC\,yr^{-1}$, respectively) is higher than estimated by Smith et al. (2016) ($370\,km^3\,yr^{-1}$ for a C sequestration rate of $\sim 1.1\,GtC\,yr^{-1}$). Furthermore, Smith et al. (2016) assumed that dedicated rain-fed bioenergy crops consume more water than the replaced vegetation (with additional water required for CCS), while in our simulations bioenergy crops had little impact on evapotranspiration as they were represented as corn. LU-driven changes in evapotranspiration rates can also modify the amount of atmospheric water vapour and cloud cover, with consequences for direct radiative forcing, planetary albedo, and precipitation (e.g. Sampaio et al., 2007, see also Table 1); however, such interactions cannot be captured by our model setup.

BVOCs influence climate via their influence on tropospheric ozone, methane, and secondary organic aerosol formation (Arneth et al., 2010; Scott et al., 2014), which depend strongly on local conditions such as levels of nitrogen oxides (NO_X) or background aerosol (Carslaw et al., 2010; Rosenkranz et al., 2015). BVOC emissions also impact climate directly by reducing terrestrial C stocks, but the magnitude is small ($< 0.5\,\%$) compared to total GPP. While enhanced leaf-level BVOC emissions are driven by warmer temperatures, uncertainties arise from additional CO_2 effects (which suppress leaf emissions). On the canopy scale, isoprene emissions generally decrease for deforestation scenarios (Hantson et al., 2017) but increase for woody biofuel plantations, which tend to use high-emission tree species (Rosenkranz et al., 2015). In our simulations, we find increases in BVOC emissions for ADAFF but not so for BECCS as bioenergy crops were grown as low-emission corn. The high spatial and temporal variability of the BVOC emissions, complications of atmospheric transport, and gaps in our knowledge of the reactions involved make it difficult to judge whether an increase in BVOC emissions results in a warming or cooling. The global effect (assuming present-day air pollution in 1850 and excluding aerosol–cloud interactions) of historic (1850s–2000s) reductions in BVOC emissions (20–25 %) due to deforestation has been estimated to be a cooling of $-0.11 \pm 0.17\,W\,m^{-2}$ (Unger, 2014). Accordingly, the substantial increase in BVOC emissions in our ADAFF simulations (16 and 24 %) might induce a warming of similar magnitude.

4.3 Water availability

Forests generally reduce local river flow compared to grass- and croplands. Based on 26 catchment datasets including 504 observations worldwide, Farley et al. (2005) reported an average decrease of 44 and 31 % in annual stream flow caused

by woody plantations replacing grasslands and shrublands, respectively, with large variability across different plantation ages. Simulations by Sterling et al. (2013) suggest that historic land-cover changes were responsible for a 7 % increase in total runoff. The reduction in global annual runoff due to ADAFF (1200 and 600 $km^3\ yr^{-1}$ compared to BASE 2090–2099) corresponds to around 16–32 % of human runoff withdrawal (Oki and Kanae, 2006), which could be seen as a potential risk to freshwater supply. Regional changes range from −5.2 to +0.4 % across all scenarios, but in many cases impacts on irrigation (the largest consumer of freshwater) potential in fact might be small: modelling work suggests that renewable water supply will exceed the irrigation demand in most regions by the end of the century for RCP8.5 (Elliott et al., 2014). However, Elliott et al. (2014) also found that regions with the largest potential for yield increases from increased irrigation are also the regions most likely to suffer from water limitations. Patterns will be different in an RCP2.6 world as CO_2 fertilization significantly reduced global irrigation demand (8–15 % on presently irrigated area) in the Elliott et al. crop models and climate impacts are expected to be less severe in RCP2.6.

In uncoupled simulations, such as those carried out here, atmospheric feedbacks related to higher evapotranspiration cannot be captured. At regional or continental scale, there is evidence that afforestation might actually increase runoff as the larger evapotranspiration rates enhance precipitation (Ellison et al., 2012). However, based on regional climate modelling, Jackson et al. (2005) concluded that atmospheric feedbacks were not likely to offset water losses in temperate regions where the additional atmospheric moisture cannot be lifted high enough to form clouds.

Changing runoff affects water supply but can also contribute to changes in flood risks. Bradshaw et al. (2007), using a multi-model approach and data from 56 developing countries, calculated a 4–28 % increase in flood frequency and a 4–8 % increase in flood duration for a hypothetical reduction of 10 % natural forest cover, while van Dijk et al. (2009), for example, questioned forest potential to reduce large-scale flooding and argued that the frequency of reported floods can be mainly explained by population density. Ferreira and Ghimire (2012) extended the original Bradshaw sample to all countries (129) that reported at least one large flood between 1990 and 2009 and included socio-economic factors in their analyses. They did not find a statistically significant correlation between forest cover and reported floods. In our simulations, peak monthly runoff is generally reduced for ADAFF; however, given maximum regional changes of −3.6 % (Africa, $LPJG_{IMAGE}$ ADAFF) and presuming that floods are largely controlled by other factors than forest cover, we expect LU effects on flooding to be limited.

4.4 Food production

Increasing food production in a sustainable way to feed a growing population is a major challenge of the modern world (Tilman et al., 2002). Population and income growth (in SSP2 population peaks in 2070 at 9.4 billion people, and per capita GDP continues to increase until 2100; Dellink et al., 2017; Samir and Lutz, 2017) are projected to be accompanied by an increased need of total calories and shifts in diets (Popp et al., 2017). For SSP2, economic modelling suggests that global food crop demand will increase by 50–97 % between 2005 and 2050 (Valin et al., 2014). In the present study, the corresponding increase reported directly from the LUMs is 38 % for IMAGE and 52 % for MAgPIE in 2050 (78 and 96 % in year 2100). In our LPJ-GUESS BASE simulations we find crop production increases of 22 and 45 % ($LPJG_{IMAGE}$ and $LPJG_{MAgPIE}$, respectively) by 2050 and 24 and 64 % by the end of the century (corresponding to a per capita increase for MAgPIE but a decrease for IMAGE). However, the production increase is significantly reduced in the mitigation simulations, especially for $LPJG_{MAgPIE}$ ADAFF, due to production shifts and the abandonment of croplands for reforestation. Similar results have been reported by Reilly et al. (2012) who found that afforestation substantially increases prices for agricultural products, while the cultivation of biofuels has little impact on agricultural prices due to benefits of avoided environmental damage offsetting higher mitigation costs. Crop yields in LPJ-GUESS are a function of environmental conditions, fertilizers, irrigation, and adaption to climate change by selecting suitable varieties. In our BASE simulations, the combined effect is an average yield increase of ∼ 17 and ∼ 41 % ($LPJG_{IMAGE}$ and $LPJG_{MAgPIE}$) between 2000–2009 and 2090–2099. In the LUMs the mitigation scenarios are characterized by additional yield increases compared to BASE, triggered by increased land prices. This intensification is to some extent reflected in the fertilizer rates (derived from yields) provided by the LUMs; however, other management improvements and investments in research and development leading to higher-yielding varieties also impact future yield increases. Additional assumptions about yield increases driven by technological progress can thus not be captured by LPJ-GUESS. The simulated decline in productivity in response to shrinking cropland area in the mitigation scenarios suggests that, when adapting N fertilization, irrigation and cropland area, and location from the LUMs, additional yield increases of up to 6.6 and 35 % ($LPJG_{IMAGE}$ and $LPJG_{MAgPIE}$) would be required between the 2000s and the 2090s to produce the same amount of food crops as in the BASE scenario, equivalent to ∼ 0.07 and 0.33 % per year.

4.5 Water and air quality

Managed agricultural systems directly impact freshwater quality. Historically, approximately 20 % of reactive N

moved into aquatic ecosystems (Galloway et al., 2004), causing drinking water pollution and eutrophication. As N loss in LPJ-GUESS is largely driven by fertilization (Blanke et al., 2017), the much higher future fertilization rates compared to present-day (+78 % for $LPJG_{IMAGE}$; +95 % for $LPJG_{MAgPIE}$) lead to an increase in N loss of 82 and 62 % in BASE. Such a large increase would have severe impacts on waterways and coastal zones, where current levels of N pollution are already having substantial effects (Camargo and Alonso, 2006). However, as discussed above, the N application rates are derived from crop yields in the LUMs, and can only be partially utilized by LPJ-GUESS due to its lower yield levels. Increasing crop yields by increased N inputs leads to a strong decline in nutrient use efficiency and declining returns on yields (Cassman et al., 2002; Mueller et al., 2017). In contrast to the BASE simulations, the mitigation simulations result in somewhat lower N losses because less fertilizer is applied (ADAFF) or because bioenergy harvest removes more N than is added via bioenergy crop fertilization (BECCS). Simulated N losses in LPJ-GUESS are affected by different assumptions about N fertilizers and inconsistencies between the models: fertilizer rates in the LUMs were calculated to support the estimated crop yields (and hence the ensuing N demand). The resulting grid-cell averages available to LPJ-GUESS did not take into account differences in N application across crop types in a grid cell (Mueller et al., 2012). Additionally, IMAGE and MAgPIE simulate further increases in crop productivity and N use efficiency and therefore nutrient recovery in harvested biomass, which may only be partly captured by LPJ-GUESS (see Sect. 4.4).

Although we do not explicitly simulate emissions of N gases, increased N losses suggest an excess of soil N, which increases the likelihood of gaseous reactive N emissions such as NO_X and ammonia (NH_3) pollution, contributing to particulate matter formation, visibility degradation, and atmospheric N deposition (Behera et al., 2013). The chemical form and level of these emissions will strongly depend on soil water status (Liu et al., 2007). Improvements in air quality, e.g. via reductions in tropospheric ozone (O_3), are not only relevant for human health but can also enhance plant productivity and crop yields (Wilkinson et al., 2012). The response of O_3 to BVOC emissions changes depends on the local NO_X : BVOC ratio (Sillman, 1999). An increase in BVOC emissions slightly suppresses O_3 concentration in regions of low NO_X background but promotes it in polluted regions (Pyle et al., 2011). Ganzeveld et al. (2010) used a chemistry–climate model to study the effects of LUC in the SRES A2 scenario (tropical deforestation) on atmospheric chemistry. By year 2050, they found increases in boundary layer ozone mixing ratios of up to 9 ppb (20 %). Changes in the concentration of the hydroxyl radical resulting from deforestation (the primary atmospheric oxidant, and main determinant of atmospheric methane lifetime) are much less clear due to uncertainties in isoprene oxidation chemistry (Fuchs et al., 2013; Hansen et al., 2017; Lelieveld et al., 2008), but O_3 concentrations were not sensitive to this uncertainty (Pugh et al., 2010). ADAFF describes a reverse scenario, with forest expansion being largely concentrated in the tropics. The sign of changes in the ADAFF simulations is reverse to changes in Ganzeveld et al. (2010): by mid-century, global N loss in ADAFF decreases by ~ 8 and 4 % and isoprene emissions increase by ~ 14 and 4 % compared to BASE. Consequently, we would expect tropospheric O_3 burden in ADAFF to decrease in the tropics but to increase in large parts of the mid-latitudes. However, changes in overall air quality will likely be dominated by anthropogenic emissions rather than LUC (Val Martin et al., 2015). BVOC emissions might also increase in bioenergy scenarios (Rosenkranz et al., 2015) but this does not happen in our study as the LUMs assumed grasses to be the predominant bioenergy crop.

4.6 Potential impacts on biodiversity

Global-scale approaches that link changes in LU, climate, and other drivers to effects on biodiversity are scarce, and burdened with high uncertainty, though some approaches exist (Alkemade et al., 2009; Visconti et al., 2011). Biodiversity, whether it is being perceived as a requisite for the provision of ESs or an ES per se, with its own intrinsic value (Liang et al., 2016; Mace et al., 2012), has not been considered in our analysis. Nevertheless, it is evident that biodiversity can be in critical conflict with demands for land resources such as food or timber (Behrman et al., 2015; Murphy and Romanuk, 2014). LUC has been the most critical driver of recent species loss (Jantz et al., 2015; Newbold et al., 2014). This has led to substantial concerns that land requirements for bioenergy crops would be competing with conservation areas directly or by leakage. Santangeli et al. (2016) found around half of today's global bioenergy production potential to be located either in already protected areas or in land that has highest priority for protection, indicating a high risk for biodiversity in the absence of strong regulatory conservation efforts.

In principle, avoided deforestation and reforestation/afforestation should maintain and enhance habitat and species richness, since forests are amongst the most diverse ecosystems (Liang et al., 2016). Forestation could also support the restoration of degraded ecosystems. However, success of large-scale reforestation–afforestation programs under a C-uptake as well as a biodiversity perspective will depend critically on the types of forests promoted and so far show mixed results (Cunningham et al., 2015; Hua et al., 2016). Likewise, even under a globally implemented forest conservation scheme there may be cropland expansion into non-forested regions that could well be C-rich (implying reduced overall C mitigation) but also diverse such as savannas or natural grasslands.

4.7 Role of model assumptions on carbon uptake via land-based mitigation and implications for other ecosystem services

Our simulations show that trade-offs between C uptake and other ESs are to be expected. Consequently, the question of whether land-based mitigation projects should be realized depends not only on the effects on ESs, but also on the magnitude of C uptake that will be achieved. However, our study suggests that potential C uptake is highly model-dependent: C uptake in the three land-based mitigation options in LPJ-GUESS is lower than the target value used in the LUMs. When the underlying reasons for model–model discrepancies are explored, a number of reasons can be identified such as bioenergy yields, forest regrowth, legacy effects from past LUC, and recovery of soil carbon in response to reforestation. Additionally, in the BECCS scenarios, the CDR target was implemented as a CCS target which does not account for additional LUC emissions, partly explaining the lower CDR values.

For forest regrowth, the current model configuration of LPJ-GUESS simulates natural forest succession, including the representation of different age classes. Krause et al. (2016) showed that the recovery of C in ecosystems following different agricultural LU histories broadly agreed with site-based measurements. LPJ-GUESS also has N (and soil water availability) as an explicit constraint on forest growth and has been successfully tested against a broad range of observations (Fleischer et al., 2015; Smith et al., 2014). These studies indicate an overall realistic rate of forest growth under natural succession. However, much of the afforestation may occur with management facilitating fast built-up of C stocks (as assumed in MAgPIE), but LPJ-GUESS does not implement plantations and has thus not been evaluated against this type of regrowth. Forest (re)growth is simulated very differently in LPJ-GUESS (where different age classes and their competition are simulated), IMAGE (where in this study the dynamically coupled LPJmL DGVM simulates natural regrowth in one individual per PFT) and MAgPIE (where managed regrowth is prescribed towards potential C densities from LPJmL, see Sect. 2.2). LPJmL also does not yet consider N constraints on vegetation regrowth. C losses from deforestation and maximum C uptake following reforestation depend on potential C densities which are likely different in LPJmL and LPJ-GUESS. In the LUMs, the model's algorithm adopts C pools from LPJmL and can thus decide to reforest the most suitable areas, while in LPJ-GUESS other regions might have more reforestation potential. Finally, soil C sequestration rates are likely different between LPJ-GUESS and LPJmL, especially for MAgPIE-LPJmL where the assumption of soil C recovering within 20 years is likely overoptimistic (see Krause et al., 2016).

For BECCS, LPJ-GUESS simulates CCS rates of ~ 2.2 and $1.8\,\mathrm{GtC\,yr^{-1}}$ ($\mathrm{LPJG_{IMAGE}}$ and $\mathrm{LPJG_{MAgPIE}}$) by the end of the 21st century, compared to $\sim 2.8\,\mathrm{GtC\,yr^{-1}}$ reported from the LUMs directly. The number from the LUMs is close to the mean removal rate of $3.3\,\mathrm{GtC\,yr^{-1}}$ reported in Smith et al. (2016) for scenarios of similar production area (380–700, vs. 493 and 363 Mha in our IMAGE and MAgPIE BECCS scenarios, respectively) and slightly larger CO_2 concentrations (430–480 ppmv vs. 424 ppmv). Discrepancies between the models arise mainly from differences in assumptions about bioenergy crop yields. In our LPJ-GUESS simulations we grew bioenergy crops as corn (i.e. a crop functional type with parameters taken from corn). By the end of the century, simulated bioenergy yields are higher for $\mathrm{LPJG_{MAgPIE}}$ BECCS (on average $13.8\,\mathrm{t\,dry\,mass\,ha^{-1}\,yr^{-1}}$, 10 % of total above-ground biomass remaining on-site) than for $\mathrm{LPJG_{IMAGE}}$ BECCS ($12.2\,\mathrm{t\,dry\,mass\,ha^{-1}\,yr^{-1}}$) due to different fertilizer rates and production locations. Bioenergy crop yields in LPJ-GUESS might be influenced by inconsistencies between the models about fertilization of bioenergy crops: while the LUMs generally assume high N application, fertilizer rates are reduced in areas used for bioenergy production because bioenergy crops are less N-demanding. Consequently, the fertilizer rates from the LUMs might be insufficient to fulfil the N demand of the corn-based bioenergy crop in LPJ-GUESS, which responds strongly to fertilization (Blanke et al., 2017). In contrast, bioenergy crops in the LUMs are represented by dedicated lignocellulosic energy grasses. Reported yields of dedicated bioenergy crops under present-day conditions show large variability (*miscanthus* × *giganteus*: 5–44 $\mathrm{t\,dry\,mass\,ha^{-1}\,yr^{-1}}$; switchgrass: 1–35 $\mathrm{t\,ha^{-1}\,yr^{-1}}$; woody species: 0–51 $\mathrm{t\,ha^{-1}\,yr^{-1}}$), depending on location, plot size, and management (Searle and Malins, 2014). By the end of the century, the LUMs report average bioenergy yields of $\sim 15.0\,\mathrm{t\,ha^{-1}\,yr^{-1}}$ (IMAGE) and $\sim 20.3\,\mathrm{t\,ha^{-1}\,yr^{-1}}$ (MAgPIE), but how bioenergy yields will evolve in reality when averaged across regions (including more marginal land) is highly uncertain (Creutzig, 2016; Searle and Malins, 2014; Slade et al., 2014).

Legacy effects from historic LU might also impact future C uptake as the soil C balance continues to respond to LUC decades or even centuries after (Krause et al., 2016; Pugh et al., 2015). We assessed the contribution of legacy effects by comparing an LPJ-GUESS simulation in which LU (but not climate and CO_2) was held constant from year 1970 for IMAGE and 1995 for MAgPIE (consistent with the scenario starting years in each model) with a run with fixed LU from year 1901 on. The differences then seen over the 21st century between these two simulations would arise chiefly from legacy fluxes of 20th century LUC. These were found to be ~ 17–$18\,\mathrm{GtC}$ (not shown), accounting for part of the difference in uptake between LPJ-GUESS and the LUMs. In the LUMs, harmonization to history has been done with respect to land cover, but this was not possible with respect to changes in vegetation and soil C pools (prior to 1970/1995).

Our results show that assumptions about forest growth and C densities, bioenergy crop yields, and timescales of

soil processes can critically influence the C removal potential of land-based mitigation. Large uncertainties about forest regrowth trajectories in different DGVMs (Pongratz et al., in preparation) and BECCS potential to remove C from the atmosphere (Creutzig et al., 2015; Kemper, 2015) have been reported before, including the importance of second-generation bioenergy crops (Kato and Yamagata, 2014) and LU-driven C losses in vegetation and soils (Wiltshire and Davies-Barnard, 2015). This is clearly an important subject for future research. Additional analyses about the difference in C removal between the LUMs and LPJ-GUESS, including results from additional DGVMs, are ongoing and will be published in a separate paper (Krause et al., 2017).

5 Conclusions

Terrestrial ecosystems provide us with many valuable services like climate and air quality regulation, water and food provision, or flood protection. While substantial changes in ecosystem functions are likely to occur within the 21st century even in the absence of land-based climate change mitigation, additional impacts are to be expected from land management for negative emissions. In all mitigation simulations, what might generally be perceived as beneficial effects on some ecosystem functions and their services (e.g. decreased N loss improving water and air quality) were counteracted by negative effects on others (e.g. reduced crop production), including substantial temporal and regional variations. Environmental side effects in our ADAFF simulations were usually larger than in BECCS, presumably reflecting the larger area affected by land-cover transitions in ADAFF. Without a valuation exercise it is not possible to state whether one option would be "better" than the other. All mitigation approaches might reduce crop production (in the absence of assumptions about large technology-related yield increases) but potentially improve air and water quality via reduced N loss. Impacts on climate via biophysical effects and on water availability and flood risks via changes in runoff were found to be relatively small in terms of percentage changes when averaged over large areas, but this does not exclude the possibility of significant impacts, e.g. on the scale of large catchments.

Policy makers should be aware of manifold side effects – be they positive or negative – when discussing and evaluating the feasibility and effects of different climate mitigation options, possibly involving the prioritization of individual ESs at the costs of exacerbating other challenges. Our analysis makes some of these trade-offs explicit, but there are many other services offered by ecosystems much more difficult to quantify, particularly relating to cultural services, which also need to be considered. Any discussion about land-based climate mitigation efforts should take into account their effects on ESs beyond C storage in order to avoid unintended negative consequences, which would be intrinsically undesirable and may also affect the effective delivery of climate mitigation through societal feedbacks.

Data availability. Scientists interested in the LPJ-GUESS source code can contact the model developers (http://iis4.nateko.lu.se/lpj-guess/contact.html). Information about the land-use scenarios are available from the IMAGE and MAgPIE groups (jonathan.doelman@pbl.nl; florian.humpenoeder@pik-potsdam.de). The LPJ-GUESS simulation data are stored at the IMK-IFU computing facilities and can be obtained on request (andreas.krause@kit.edu).

The Supplement related to this article is available online at https://doi.org/10.5194/bg-14-4829-2017-supplement.

Competing interests. The authors declare that they have no conflict of interest.

Acknowledgements. This work was funded by the Helmholtz Association through the International Research Group CLUCIE and by the European Commission's Seventh Framework Programme, under grant agreement number 603542 (LUC4C). Andreas Krause, Anita D. Bayer, and Almut Arneth also acknowledge support by the European Commission's Seventh Framework Programme, under grant agreement number 308393 (OPERAs). This work was supported, in part, by the German Federal Ministry of Education and Research (BMBF), through the Helmholtz Association and its research program ATMO. It also represents paper number 22 of the Birmingham Institute of Forest Research.

The article processing charges for this open-access publication were covered by a Research Centre of the Helmholtz Association.

Edited by: Christopher A. Williams
Reviewed by: two anonymous referees

References

Ahlstrom, A., Schurgers, G., Arneth, A., and Smith, B.: Robustness and uncertainty in terrestrial ecosystem carbon response to CMIP5 climate change projections, Environ. Res. Lett., 7, 044008, https://doi.org/10.1088/1748-9326/7/4/044008, 2012.

Alexander, P., Prestele, R., Verburg, P. H., Arneth, A., Baranzelli, C., Silva, F. B. E., Brown, C., Butler, A., Calvin, K., Dendoncker, N., Doelman, J. C., Dunford, R., Engstrom, K., Eitelberg, D., Fujimori, S., Harrison, P. A., Hasegawa, T., Havlik, P., Holzhauer, S., Humpenoder, F., Jacobs-Crisioni, C., Jain, A. K., Krisztin, T., Kyle, P., Lavalle, C., Lenton, T., Liu, J. Y., Meiyappan, P., Popp, A., Powell, T., Sands, R. D., Schaldach, R., Stehfest, E., Steinbuks, J., Tabeau, A., van Meijl, H.,

Wise, M. A., and Rounsevell, M. D. A.: Assessing uncertainties in land cover projections, Glob. Change Biol., 23, 767–781, https://doi.org/10.1111/gcb.13447, 2017.

Alkama, R. and Cescatti, A.: Biophysical climate impacts of recent changes in global forest cover, Science, 351, 600–604, https://doi.org/10.1126/science.aac8083, 2016.

Alkemade, R., van Oorschot, M., Miles, L., Nellemann, C., Bakkenes, M., and ten Brink, B.: GLOBIO3: A framework to investigate options for reducing global terrestrial biodiversity loss, Ecosystems, 12, 374–390, https://doi.org/10.1007/s10021-009-9229-5, 2009.

Anderson, K. and Peters, G.: The trouble with negative emissions, Science, 354, 182–183, https://doi.org/10.1126/science.aah4567, 2016.

Arneth, A., Niinemets, Ü., Pressley, S., Bäck, J., Hari, P., Karl, T., Noe, S., Prentice, I. C., Serça, D., Hickler, T., Wolf, A., and Smith, B.: Process-based estimates of terrestrial ecosystem isoprene emissions: incorporating the effects of a direct CO_2-isoprene interaction, Atmos. Chem. Phys., 7, 31–53, https://doi.org/10.5194/acp-7-31-2007, 2007.

Arneth, A., Harrison, S. P., Zaehle, S., Tsigaridis, K., Menon, S., Bartlein, P. J., Feichter, J., Korhola, A., Kulmala, M., O'Donnell, D., Schurgers, G., Sorvari, S., and Vesala, T.: Terrestrial biogeochemical feedbacks in the climate system, Nat. Geosci., 3, 525–532, https://doi.org/10.1038/ngeo905, 2010.

Bala, G., Caldeira, K., Wickett, M., Phillips, T. J., Lobell, D. B., Delire, C., and Mirin, A.: Combined climate and carbon-cycle effects of large-scale deforestation, P. Natl. Acad. Sci. USA, 104, 6550–6555, https://doi.org/10.1073/pnas.0608998104, 2007.

Ban-Weiss, G. A., Bala, G., Cao, L., Pongratz, J., and Caldeira, K.: Climate forcing and response to idealized changes in surface latent and sensible heat, Environ. Res. Lett., 6, 034032, https://doi.org/10.1088/1748-9326/6/3/034032, 2011.

Bathiany, S., Claussen, M., Brovkin, V., Raddatz, T., and Gayler, V.: Combined biogeophysical and biogeochemical effects of large-scale forest cover changes in the MPI earth system model, Biogeosciences, 7, 1383–1399, https://doi.org/10.5194/bg-7-1383-2010, 2010.

Behera, S. N., Sharma, M., Aneja, V. P., and Balasubramanian, R.: Ammonia in the atmosphere: a review on emission sources, atmospheric chemistry and deposition on terrestrial bodies, Environ. Sci. Pollut. R., 20, 8092–8131, https://doi.org/10.1007/s11356-013-2051-9, 2013.

Behrman, K. D., Juenger, T. E., Kiniry, J. R., and Keitt, T. H.: Spatial land use trade-offs for maintenance of biodiversity, biofuel, and agriculture, Landscape Ecol., 30, 1987–1999, https://doi.org/10.1007/s10980-015-0225-1, 2015.

Bennett, E. M., Peterson, G. D., and Gordon, L. J.: Understanding relationships among multiple ecosystem services, Ecol. Lett., 12, 1394–1404, https://doi.org/10.1111/j.1461-0248.2009.01387.x, 2009.

Betts, R. A.: Offset of the potential carbon sink from boreal forestation by decreases in surface albedo, Nature, 408, 187–190, https://doi.org/10.1038/35041545, 2000.

Blanke, J. H., Olin, S., Stürck, J., Sahlin, U., Lindeskog, M., Helming, J., and Lehsten, V.: Assessing the impact of changes in land-use intensity and climate on simulated trade-offs between crop yield and nitrogen leaching, Agr. Ecosyst. Environ., 239, 385–398, https://doi.org/10.1016/j.agee.2017.01.038, 2017.

Boisier, J. P., de Noblet-Ducoudré, N., and Ciais, P.: Inferring past land use-induced changes in surface albedo from satellite observations: a useful tool to evaluate model simulations, Biogeosciences, 10, 1501–1516, https://doi.org/10.5194/bg-10-1501-2013, 2013.

Bondeau, A., Smith, P. C., Zaehle, S., Schaphoff, S., Lucht, W., Cramer, W., Gerten, D., Lotze-Campen, H., Muller, C., Reichstein, M., and Smith, B.: Modelling the role of agriculture for the 20th century global terrestrial carbon balance, Glob. Change Biol., 13, 679–706, https://doi.org/10.1111/j.1365-2486.2006.01305.x, 2007.

Boucher, O., Myhre, G., and Myhre, A.: Direct human influence of irrigation on atmospheric water vapour and climate, Clim. Dynam., 22, 597–603, https://doi.org/10.1007/s00382-004-0402-4, 2004.

Boysen, L. R., Lucht, W., and Gerten, D.: Trade-offs for food production, nature conservation and climate limit the terrestrial carbon dioxide removal potential, Glob. Change Biol., 23, 4303–4317, https://doi.org/10.1111/gcb.13745, 2017.

Bradshaw, C. J. A., Sodhi, N. S., Peh, K. S. H., and Brook, B. W.: Global evidence that deforestation amplifies flood risk and severity in the developing world, Glob. Change Biol., 13, 2379–2395, https://doi.org/10.1111/j.1365-2486.2007.01446.x, 2007.

Camargo, J. A. and Alonso, A.: Ecological and toxicological effects of inorganic nitrogen pollution in aquatic ecosystems: A global assessment, Environ. Int., 32, 831–849, https://doi.org/10.1016/j.envint.2006.05.002, 2006.

Carslaw, K. S., Boucher, O., Spracklen, D. V., Mann, G. W., Rae, J. G. L., Woodward, S., and Kulmala, M.: A review of natural aerosol interactions and feedbacks within the Earth system, Atmos. Chem. Phys., 10, 1701–1737, https://doi.org/10.5194/acp-10-1701-2010, 2010.

Cassman, K. G., Dobermann, A., and Walters, D. T.: Agroecosystems, nitrogen-use efficiency, and nitrogen management, Ambio, 31, 132–140, https://doi.org/10.1639/0044-7447(2002)031[0132:Anuean]2.0.Co;2, 2002.

Creutzig, F.: Economic and ecological views on climate change mitigation with bioenergy and negative emissions, Gcb Bioenergy, 8, 4–10, https://doi.org/10.1111/gcbb.12235, 2016.

Creutzig, F., Ravindranath, N. H., Berndes, G., Bolwig, S., Bright, R., Cherubini, F., Chum, H., Corbera, E., Delucchi, M., Faaij, A., Fargione, J., Haberl, H., Heath, G., Lucon, O., Plevin, R., Popp, A., Robledo-Abad, C., Rose, S., Smith, P., Stromman, A., Suh, S., and Masera, O.: Bioenergy and climate change mitigation: an assessment, Gcb Bioenergy, 7, 916–944, https://doi.org/10.1111/gcbb.12205, 2015.

Crutzen, P. J., Mosier, A. R., Smith, K. A., and Winiwarter, W.: N_2O release from agro-biofuel production negates global warming reduction by replacing fossil fuels, Atmos. Chem. Phys., 8, 389–395, https://doi.org/10.5194/acp-8-389-2008, 2008.

Cunningham, S. C., Mac Nally, R., Baker, P. J., Cavagnaro, T. R., Beringer, J., Thomson, J. R., and Thompson, R. M.: Balancing the environmental benefits of reforestation in agricultural regions, Perspect. Plant Ecol., 17, 301–317, https://doi.org/10.1016/j.ppees.2015.06.001, 2015.

Davidson, E. A. and Kanter, D.: Inventories and scenarios of nitrous oxide emissions, Environ. Res. Lett., 9, 105012, https://doi.org/10.1088/1748-9326/9/10/105012, 2014.

Davies-Barnard, T., Valdes, P. J., Singarayer, J. S., Pacifico, F. M., and Jones, C. D.: Full effects of land use change in the representative concentration pathways, Environ. Res. Lett., 9, 114014, https://doi.org/10.1088/1748-9326/9/11/114014, 2014.

DeFries, R. S., Foley, J. A., and Asner, G. P.: Land-use choices: balancing human needs and ecosystem function, Front. Ecol. Environ., 2, 249–257, https://doi.org/10.1890/1540-9295(2004)002[0249:Lcbhna]2.0.Co;2, 2004.

Dellink, R., Chateau, J., Lanzi, E., and Magne, B.: Long-term economic growth projections in the Shared Socioeconomic Pathways, Global Environ. Chang., 42, 200–214, https://doi.org/10.1016/j.gloenvcha.2015.06.004, 2017.

de Noblet-Ducoudre, N., Boisier, J. P., Pitman, A., Bonan, G. B., Brovkin, V., Cruz, F., Delire, C., Gayler, V., van den Hurk, B. J. J. M., Lawrence, P. J., van der Molen, M. K., Muller, C., Reick, C. H., Strengers, B. J., and Voldoire, A.: Determining Robust Impacts of Land-Use-Induced Land Cover Changes on Surface Climate over North America and Eurasia: Results from the First Set of LUCID Experiments, J Climate, 25, 3261–3281, https://doi.org/10.1175/Jcli-D-11-00338.1, 2012.

Doelman, J. C., Stehfest, E., Tabeau, A., van Meijl, H., Lassaletta, L., Gernaat, D. E. H. J., Neumann-Hermans, K., Harmsen, M., Daioglou, V., Biemans, H., van der Sluis, S., and van Vuuren, D. P.: Exploring SSP land-use dynamics using the IMAGE model: regional and gridded scenarios of land-use change and land-based climate change mitigation, submitted to Global Environ. Chang., 2017.

Elliott, J., Deryng, D., Mueller, C., Frieler, K., Konzmann, M., Gerten, D., Glotter, M., Florke, M., Wada, Y., Best, N., Eisner, S., Fekete, B. M., Folberth, C., Foster, I., Gosling, S. N., Haddeland, I., Khabarov, N., Ludwig, F., Masaki, Y., Olin, S., Rosenzweig, C., Ruane, A. C., Satoh, Y., Schmid, E., Stacke, T., Tang, Q. H., and Wisser, D.: Constraints and potentials of future irrigation water availability on agricultural production under climate change, P. Natl. Acad. Sci. USA, 111, 3239–3244, https://doi.org/10.1073/pnas.1222474110, 2014.

Ellison, D., Futter, M. N., and Bishop, K.: On the forest cover-water yield debate: from demand- to supply-side thinking, Glob. Change Biol., 18, 806–820, https://doi.org/10.1111/j.1365-2486.2011.02589.x, 2012.

Erisman, J. W., Galloway, J., Seitzinger, S., Bleeker, A., and Butterbach-Bahl, K.: Reactive nitrogen in the environment and its effect on climate change, Curr. Opin. Env. Sust., 3, 281–290, https://doi.org/10.1016/j.cosust.2011.08.012, 2011.

Farley, K. A., Jobbagy, E. G., and Jackson, R. B.: Effects of afforestation on water yield: a global synthesis with implications for policy, Glob. Change Biol., 11, 1565–1576, https://doi.org/10.1111/j.1365-2486.2005.01011.x, 2005.

Ferreira, S. and Ghimire, R.: Forest cover, socioeconomics, and reported flood frequency in developing countries, Water Resour. Res., 48, W08529, https://doi.org/10.1029/2011wr011701, 2012.

Fleischer, K., Warlind, D., van der Molen, M. K., Rebel, K. T., Arneth, A., Erisman, J. W., Wassen, M. J., Smith, B., Gough, C. M., Margolis, H. A., Cescatti, A., Montagnani, L., Arain, A., and Dolman, A. J.: Low historical nitrogen deposition effect on carbon sequestration in the boreal zone, J. Geophys. Res.-Biogeo., 120, 2542–2561, https://doi.org/10.1002/2015JG002988, 2015.

Foley, J. A., DeFries, R., Asner, G. P., Barford, C., Bonan, G., Carpenter, S. R., Chapin, F. S., Coe, M. T., Daily, G. C., Gibbs, H. K., Helkowski, J. H., Holloway, T., Howard, E. A., Kucharik, C. J., Monfreda, C., Patz, J. A., Prentice, I. C., Ramankutty, N., and Snyder, P. K.: Global consequences of land use, Science, 309, 570–574, https://doi.org/10.1126/science.1111772, 2005.

Friedlingstein, P., Meinshausen, M., Arora, V. K., Jones, C. D., Anav, A., Liddicoat, S. K., and Knutti, R.: Uncertainties in CMIP5 Climate Projections due to Carbon Cycle Feedbacks, J. Climate, 27, 511–526, https://doi.org/10.1175/Jcli-D-12-00579.1, 2014.

Fuchs, H., Hofzumahaus, A., Rohrer, F., Bohn, B., Brauers, T., Dorn, H. P., Haseler, R., Holland, F., Kaminski, M., Li, X., Lu, K., Nehr, S., Tillmann, R., Wegener, R., and Wahner, A.: Experimental evidence for efficient hydroxyl radical regeneration in isoprene oxidation, Nat. Geosci., 6, 1023–1026, https://doi.org/10.1038/NGEO1964, 2013.

Fuss, S., Canadell, J. G., Peters, G. P., Tavoni, M., Andrew, R. M., Ciais, P., Jackson, R. B., Jones, C. D., Kraxner, F., Nakicenovic, N., Le Quere, C., Raupach, M. R., Sharifi, A., Smith, P., and Yamagata, Y.: COMMENTARY: Betting on negative emissions, Nat. Clim. Change, 4, 850–853, https://doi.org/10.1038/nclimate2392, 2014.

Galloway, J. N., Dentener, F. J., Capone, D. G., Boyer, E. W., Howarth, R. W., Seitzinger, S. P., Asner, G. P., Cleveland, C. C., Green, P. A., Holland, E. A., Karl, D. M., Michaels, A. F., Porter, J. H., Townsend, A. R., and Vorosmarty, C. J.: Nitrogen cycles: past, present, and future, Biogeochemistry, 70, 153–226, https://doi.org/10.1007/s10533-004-0370-0, 2004.

Ganzeveld, L., Bouwman, L., Stehfest, E., van Vuuren, D. P., Eickhout, B., and Lelieveld, J.: Impact of future land use and land cover changes on atmospheric chemistry-climate interactions, J. Geophys. Res.-Atmos., 115, D23301, https://doi.org/10.1029/2010jd014041, 2010.

Gerten, D., Schaphoff, S., Haberlandt, U., Lucht, W., and Sitch, S.: Terrestrial vegetation and water balance – hydrological evaluation of a dynamic global vegetation model, J. Hydrol., 286, 249–270, https://doi.org/10.1016/j.jhydrol.2003.09.029, 2004.

Giglio, L., Randerson, J. T., van der Werf, G. R., Kasibhatla, P. S., Collatz, G. J., Morton, D. C., and DeFries, R. S.: Assessing variability and long-term trends in burned area by merging multiple satellite fire products, Biogeosciences, 7, 1171–1186, https://doi.org/10.5194/bg-7-1171-2010, 2010.

Hallgren, W., Schlosser, C. A., Monier, E., Kicklighter, D., Sokolov, A., and Melillo, J.: Climate impacts of a large-scale biofuels expansion, Geophys. Res. Lett., 40, 1624–1630, https://doi.org/10.1002/grl.50352, 2013.

Hansen, R. F., Lewis, T. R., Graham, L., Whalley, S. K., Seakins, P. W., Heard, D. E., and Blitz, M. A.: OH production from the photolysis of isoprene-derived peroxy radicals: cross-sections, quantum yields and atmospheric implications, Phys. Chem. Chem. Phys, 19, 2332–2345, https://doi.org/10.1039/c6cp06718b, 2017.

Hantson, S., Knorr, W., Schurgers, G., Pugh, T. A. M., and Arneth, A.: Global isoprene and monoterpene emissions under changing climate, vegetation, CO_2 and land use, Atmos. Environ., 155, 35–45, https://doi.org/10.1016/j.atmosenv.2017.02.010, 2017.

Hempel, S., Frieler, K., Warszawski, L., Schewe, J., and Piontek, F.: A trend-preserving bias correction –the ISI-MIP approach, Earth Syst. Dynam., 4, 219–236, https://doi.org/10.5194/esd-4-219-2013, 2013.

Hoogwijk, M., Faaija, A., van den Broek, R., Berndes, G., Gielen, D., and Turkenburg, W.: Exploration of the ranges of the global potential of biomass for energy, Biomass Bioenerg., 25, 119–133, https://doi.org/10.1016/S0961-9534(02)00191-5, 2003.

Hua, F. Y., Wang, X. Y., Zheng, X. L., Fisher, B., Wang, L., Zhu, J. G., Tang, Y., Yu, D. W., and Wilcove, D. S.: Opportunities for biodiversity gains under the world's largest reforestation programme, Nat. Commun., 7, 12717, https://doi.org/10.1038/Ncomms12717, 2016.

Humpenöder, F., Popp, A., Dietrich, J. P., Klein, D., Lotze-Campen, H., Bonsch, M., Bodirsky, B. L., Weindl, I., Stevanovic, M., and Muller, C.: Investigating afforestation and bioenergy CCS as climate change mitigation strategies, Environ. Res. Lett., 9, 064029, https://doi.org/10.1088/1748-9326/9/6/064029, 2014.

Jackson, R. B., Jobbagy, E. G., Avissar, R., Roy, S. B., Barrett, D. J., Cook, C. W., Farley, K. A., le Maitre, D. C., McCarl, B. A., and Murray, B. C.: Trading water for carbon with biological sequestration, Science, 310, 1944–1947, https://doi.org/10.1126/science.1119282, 2005.

Jantz, S. M., Barker, B., Brooks, T. M., Chini, L. P., Huang, Q. Y., Moore, R. M., Noel, J., and Hurtt, G. C.: Future habitat loss and extinctions driven by land-use change in biodiversity hotspots under four scenarios of climate-change mitigation, Conserv. Biol., 29, 1122–1131, https://doi.org/10.1111/cobi.12549, 2015.

Kato, E. and Yamagata, Y.: BECCS capability of dedicated bioenergy crops under a future land-use scenario targeting net negative carbon emissions, Earths Future, 2, 421–439, https://doi.org/10.1002/2014EF000249, 2014.

Keller, D. P., Feng, E. Y., and Oschlies, A.: Potential climate engineering effectiveness and side effects during a high carbon dioxide-emission scenario, Nat. Commun., 5, 3304, https://doi.org/10.1038/ncomms4304, 2014.

Kelley, D. I., Prentice, I. C., Harrison, S. P., Wang, H., Simard, M., Fisher, J. B., and Willis, K. O.: A comprehensive benchmarking system for evaluating global vegetation models, Biogeosciences, 10, 3313–3340, https://doi.org/10.5194/bg-10-3313-2013, 2013.

Kemper, J.: Biomass and carbon dioxide capture and storage: A review, Int. J. Greenh. Gas Con., 40, 401–430, https://doi.org/10.1016/j.ijggc.2015.06.012, 2015.

Klein Goldewijk, K., Beusen, A., van Drecht, G., and de Vos, M.: The HYDE 3.1 spatially explicit database of human-induced global land-use change over the past 12,000 years, Global Ecol. Biogeogr., 20, 73–86, https://doi.org/10.1111/j.1466-8238.2010.00587.x, 2011.

Krause, A., Pugh, T. A. M., Bayer, A. D., Lindeskog, M., and Arneth, A.: Impacts of land-use history on the recovery of ecosystems after agricultural abandonment, Earth Syst. Dynam., 7, 745–766, https://doi.org/10.5194/esd-7-745-2016, 2016.

Krause, A., Pugh, T. A. M., Bayer, A. D., Li, W., Leung, F., Bondeau, A., Doelman, J. C., Humpenöder, F., Anthoni, P., Bodirsky, B. L., Ciais, P., Müller, C., Murray-Tortarolo, G., Olin, S., Popp, A., Sitch, S., Stehfest, E., and Arneth, A.: Large uncertainty in carbon uptake potential of land-based climate change mitigation efforts, in preparation, 2017.

Lamarque, J.-F., Bond, T. C., Eyring, V., Granier, C., Heil, A., Klimont, Z., Lee, D., Liousse, C., Mieville, A., Owen, B., Schultz, M. G., Shindell, D., Smith, S. J., Stehfest, E., Van Aardenne, J., Cooper, O. R., Kainuma, M., Mahowald, N., McConnell, J. R., Naik, V., Riahi, K., and van Vuuren, D. P.: Historical (1850–2000) gridded anthropogenic and biomass burning emissions of reactive gases and aerosols: methodology and application, Atmos. Chem. Phys., 10, 7017–7039, https://doi.org/10.5194/acp-10-7017-2010, 2010.

Lamarque, J. F., Kyle, G. P., Meinshausen, M., Riahi, K., Smith, S. J., van Vuuren, D. P., Conley, A. J., and Vitt, F.: Global and regional evolution of short-lived radiatively-active gases and aerosols in the Representative Concentration Pathways, Climatic Change, 109, 191–212, https://doi.org/10.1007/s10584-011-0155-0, 2011.

Lelieveld, J., Butler, T. M., Crowley, J. N., Dillon, T. J., Fischer, H., Ganzeveld, L., Harder, H., Lawrence, M. G., Martinez, M., Taraborrelli, D., and Williams, J.: Atmospheric oxidation capacity sustained by a tropical forest, Nature, 452, 737–740, https://doi.org/10.1038/nature06870, 2008.

Le Quéré, C., Moriarty, R., Andrew, R. M., Canadell, J. G., Sitch, S., Korsbakken, J. I., Friedlingstein, P., Peters, G. P., Andres, R. J., Boden, T. A., Houghton, R. A., House, J. I., Keeling, R. F., Tans, P., Arneth, A., Bakker, D. C. E., Barbero, L., Bopp, L., Chang, J., Chevallier, F., Chini, L. P., Ciais, P., Fader, M., Feely, R. A., Gkritzalis, T., Harris, I., Hauck, J., Ilyina, T., Jain, A. K., Kato, E., Kitidis, V., Klein Goldewijk, K., Koven, C., Landschützer, P., Lauvset, S. K., Lefèvre, N., Lenton, A., Lima, I. D., Metzl, N., Millero, F., Munro, D. R., Murata, A., Nabel, J. E. M. S., Nakaoka, S., Nojiri, Y., O'Brien, K., Olsen, A., Ono, T., Pérez, F. F., Pfeil, B., Pierrot, D., Poulter, B., Rehder, G., Rödenbeck, C., Saito, S., Schuster, U., Schwinger, J., Séférian, R., Steinhoff, T., Stocker, B. D., Sutton, A. J., Takahashi, T., Tilbrook, B., van der Laan-Luijkx, I. T., van der Werf, G. R., van Heuven, S., Vandemark, D., Viovy, N., Wiltshire, A., Zaehle, S., and Zeng, N.: Global Carbon Budget 2015, Earth Syst. Sci. Data, 7, 349–396, https://doi.org/10.5194/essd-7-349-2015, 2015.

Li, Y., Zhao, M. S., Motesharrei, S., Mu, Q. Z., Kalnay, E., and Li, S. C.: Local cooling and warming effects of forests based on satellite observations, Nat. Commun., 6, 6603, https://doi.org/10.1038/Ncomms7603, 2015.

Liang, J. J., Crowther, T. W., Picard, N., Wiser, S., Zhou, M., Alberti, G., Schulze, E. D., McGuire, A. D., Bozzato, F., Pretzsch, H., de-Miguel, S., Paquette, A., Herault, B., Scherer-Lorenzen, M., Barrett, C. B., Glick, H. B., Hengeveld, G. M., Nabuurs, G. J., Pfautsch, S., Viana, H., Vibrans, A. C., Ammer, C., Schall, P., Verbyla, D., Tchebakova, N., Fischer, M., Watson, J. V., Chen, H. Y. H., Lei, X. D., Schelhaas, M. J., Lu, H. C., Gianelle, D., Parfenova, E. I., Salas, C., Lee, E., Lee, B., Kim, H. S., Bruelheide, H., Coomes, D. A., Piotto, D., Sunderland, T., Schmid, B., Gourlet-Fleury, S., Sonke, B., Tavani, R., Zhu, J., Brandl, S., Vayreda, J., Kitahara, F., Searle, E. B., Neldner, V. J., Ngugi, M. R., Baraloto, C., Frizzera, L., Balazy, R., Oleksyn, J., Zawila-Niedzwiecki, T., Bouriaud, O., Bussotti, F., Finer, L., Jaroszewicz, B., Jucker, T., Valladares, F., Jagodzinski, A. M., Peri, P. L., Gonmadje, C., Marthy, W., O'Brien, T., Martin, E. H., Marshall, A. R., Rovero, F., Bitariho, R., Niklaus, P. A., Alvarez-Loayza, P., Chamuya, N., Valencia, R., Mortier, F., Wortel, V., Engone-Obiang, N. L., Ferreira, L. V., Odeke, D. E., Vasquez, R. M., Lewis, S. L., and Reich, P. B.: Positive biodiversity-productivity relationship predominant in global forests, Science, 354, 6309, https://doi.org/10.1126/science.aaf8957, 2016.

Lindeskog, M., Arneth, A., Bondeau, A., Waha, K., Seaquist, J., Olin, S., and Smith, B.: Implications of accounting for land use in simulations of ecosystem carbon cycling in Africa, Earth Syst. Dynam., 4, 385–407, https://doi.org/10.5194/esd-4-385-2013, 2013.

Liu, G. D., Li, Y. C., and Alva, A. K.: Moisture quotients for ammonia volatilization from four soils in potato production regions, Water Air Soil Poll., 183, 115–127, https://doi.org/10.1007/s11270-007-9361-9, 2007.

Lotze-Campen, H., Muller, C., Bondeau, A., Rost, S., Popp, A., and Lucht, W.: Global food demand, productivity growth, and the scarcity of land and water resources: a spatially explicit mathematical programming approach, Agr. Econ.-Blackwell, 39, 325–338, https://doi.org/10.1111/j.1574-0862.2008.00336.x, 2008.

Mace, G. M., Norris, K., and Fitter, A. H.: Biodiversity and ecosystem services: a multilayered relationship, Trends Ecol. Evol., 27, 19–26, https://doi.org/10.1016/j.tree.2011.08.006, 2012.

Meinshausen, M., Smith, S. J., Calvin, K., Daniel, J. S., Kainuma, M. L. T., Lamarque, J. F., Matsumoto, K., Montzka, S. A., Raper, S. C. B., Riahi, K., Thomson, A., Velders, G. J. M., and van Vuuren, D. P. P.: The RCP greenhouse gas concentrations and their extensions from 1765 to 2300, Climatic Change, 109, 213–241, https://doi.org/10.1007/s10584-011-0156-z, 2011.

Millennium Ecosystem Assessment (MEA): Ecosystems and Human Well-being: Synthesis, Washington, DC, USA, 155 pp., 2005.

Mueller, N. D., Gerber, J. S., Johnston, M., Ray, D. K., Ramankutty, N., and Foley, J. A.: Closing yield gaps through nutrient and water management, Nature, 490, 254–257, https://doi.org/10.1038/nature11420, 2012.

Mueller, N. D., Lassaletta, L., Runck, B. C., Billen, G., Garnier, J., and Gerber, J. S.: Declining spatial efficiency of global cropland nitrogen allocation, Global Biogeochem. Cy., 31, 245–257, https://doi.org/10.1002/2016GB005515, 2017.

Murphy, G. E. P. and Romanuk, T. N.: A meta-analysis of declines in local species richness from human disturbances, Ecol. Evol., 4, 91–103, https://doi.org/10.1002/ece3.909, 2014.

Newbold, T., Hudson, L. N., Phillips, H. R. P., Hill, S. L. L., Contu, S., Lysenko, I., Blandon, A., Butchart, S. H. M., Booth, H. L., Day, J., De Palma, A., Harrison, M. L. K., Kirkpatrick, L., Pynegar, E., Robinson, A., Simpson, J., Mace, G. M., Scharlemann, J. P. W., and Purvis, A.: A global model of the response of tropical and sub-tropical forest biodiversity to anthropogenic pressures, P. Roy. Soc. B-Biol. Sci., 281, 1792, https://doi.org/10.1098/Rspb.2014.1371, 2014.

Oki, T. and Kanae, S.: Global hydrological cycles and world water resources, Science, 313, 1068–1072, https://doi.org/10.1126/science.1128845, 2006.

Olin, S., Lindeskog, M., Pugh, T. A. M., Schurgers, G., Wårlind, D., Mishurov, M., Zaehle, S., Stocker, B. D., Smith, B., and Arneth, A.: Soil carbon management in large-scale Earth system modelling: implications for crop yields and nitrogen leaching, Earth Syst. Dynam., 6, 745–768, https://doi.org/10.5194/esd-6-745-2015, 2015a.

Olin, S., Schurgers, G., Lindeskog, M., Wårlind, D., Smith, B., Bodin, P., Holmér, J., and Arneth, A.: Modelling the response of yields and tissue C : N to changes in atmospheric CO_2 and N management in the main wheat regions of western Europe, Biogeosciences, 12, 2489–2515, https://doi.org/10.5194/bg-12-2489-2015, 2015b.

O'Neill, B. C., Kriegler, E., Riahi, K., Ebi, K. L., Hallegatte, S., Carter, T. R., Mathur, R., and van Vuuren, D. P.: A new scenario framework for climate change research: the concept of shared socioeconomic pathways, Climatic Change, 122, 387–400, https://doi.org/10.1007/s10584-013-0905-2, 2014.

Peters, G. P., Andrew, R. M., Boden, T., Canadell, J. G., Ciais, P., Le Quere, C., Marland, G., Raupach, M. R., and Wilson, C.: COMMENTARY: The challenge to keep global warming below 2 °C, Nat. Clim. Change, 3, 4–6, https://doi.org/10.1038/nclimate1783, 2013.

Peters, G. P., Andrew, R. M., Canadell, J. G., Fuss, S., Jackson, R. B., Korsbakken, J. I., Le Quere, C., and Nakicenovic, N.: Key indicators to track current progress and future ambition of the Paris Agreement, Nat. Clim. Change, 7, 118–123, https://doi.org/10.1038/Nclimate3202, 2017.

Piao, S. L., Sitch, S., Ciais, P., Friedlingstein, P., Peylin, P., Wang, X. H., Ahlstrom, A., Anav, A., Canadell, J. G., Cong, N., Huntingford, C., Jung, M., Levis, S., Levy, P. E., Li, J. S., Lin, X., Lomas, M. R., Lu, M., Luo, Y. Q., Ma, Y. C., Myneni, R. B., Poulter, B., Sun, Z. Z., Wang, T., Viovy, N., Zaehle, S., and Zeng, N.: Evaluation of terrestrial carbon cycle models for their response to climate variability and to CO_2 trends, Glob. Change Biol., 19, 2117–2132, https://doi.org/10.1111/gcb.12187, 2013.

Popp, A., Humpenoder, F., Weindl, I., Bodirsky, B. L., Bonsch, M., Lotze-Campen, H., Muller, C., Biewald, A., Rolinski, S., Stevanovic, M., and Dietrich, J. P.: Land-use protection for climate change mitigation, Nat. Clim. Change, 4, 1095–1098, https://doi.org/10.1038/Nclimate2444, 2014.

Popp, A., Calvin, K., Fujimori, S., Havlik, P., Humpenoder, F., Stehfest, E., Bodirsky, B. L., Dietrich, J. P., Doelmann, J. C., Gusti, M., Hasegawa, T., Kyle, P., Obersteiner, M., Tabeau, A., Takahashi, K., Valin, H., Waldhoff, S., Weindl, I., Wise, M., Kriegler, E., Lotze-Campen, H., Fricko, O., Riahi, K., and van Vuuren, D. P.: Land-use futures in the shared socioeconomic pathways, Global Environ. Chang., 42, 331–345, https://doi.org/10.1016/j.gloenvcha.2016.10.002, 2017.

Posthumus, H., Morris, J., Hess, T. M., Neville, D., Phillips, E., and Baylis, A.: Impacts of the summer 2007 floods on agriculture in England, J. Flood Risk Manag., 2, 182–189, https://doi.org/10.1111/j.1753-318X.2009.01031.x, 2009.

Prestele, R., Alexander, P., Rounsevell, M. D. A., Arneth, A., Calvin, K., Doelman, J., Eitelberg, D. A., Engstrom, K., Fujimori, S., Hasegawa, T., Havlik, P., Humpenoder, F., Jain, A. K., Krisztin, T., Kyle, P., Meiyappan, P., Popp, A., Sands, R. D., Schaldach, R., Schungel, J., Stehfest, E., Tabeau, A., Van Meijl, H., Van Vliet, J., and Verburg, P. H.: Hotspots of uncertainty in land-use and land-cover change projections: a global-scale model comparison, Glob. Change Biol., 22, 3967–3983, https://doi.org/10.1111/gcb.13337, 2016.

Pugh, T. A. M., MacKenzie, A. R., Hewitt, C. N., Langford, B., Edwards, P. M., Furneaux, K. L., Heard, D. E., Hopkins, J. R., Jones, C. E., Karunaharan, A., Lee, J., Mills, G., Misztal, P., Moller, S., Monks, P. S., and Whalley, L. K.: Simulating atmospheric composition over a South-East Asian tropical rainforest: performance of a chemistry box model, Atmos. Chem. Phys., 10, 279–298, https://doi.org/10.5194/acp-10-279-2010, 2010.

Pugh, T. A. M., Arneth, A., Olin, S., Ahlström, A., Bayer, A. D., Klein Goldewijk, K., Lindeskog, M., and Schurgers, G.: Simulated carbon emissions from land use change are substantially enhanced by accounting for agricultural management, Environ. Res. Lett., 10, 124008, https://doi.org/10.1088/1748-9326/10/12/124008, 2015.

Pyle, J. A., Warwick, N. J., Harris, N. R. P., Abas, M. R., Archibald, A. T., Ashfold, M. J., Ashworth, K., Barkley, M. P., Carver, G. D., Chance, K., Dorsey, J. R., Fowler, D., Gonzi, S., Gostlow, B., Hewitt, C. N., Kurosu, T. P., Lee, J. D., Langford, S. B., Mills, G., Moller, S., MacKenzie, A. R., Manning, A. J., Misztal, P., Nadzir, M. S. M., Nemitz, E., Newton, H. M., O'Brien, L. M., Ong, S., Oram, D., Palmer, P. I., Peng, L. K., Phang, S. M., Pike, R., Pugh, T. A. M., Rahman, N. A., Robinson, A. D., Sentian, J., Abu Samah, A., Skiba, U., Ung, H. E., Yong, S. E., and Young, P. J.: The impact of local surface changes in Borneo on atmospheric composition at wider spatial scales: coastal processes, land-use change and air quality, Philos. T. R. Soc. B, 366, 3210–3224, https://doi.org/10.1098/rstb.2011.0060, 2011.

Reilly, J., Melillo, J., Cai, Y. X., Kicklighter, D., Gurgel, A., Paltsev, S., Cronin, T., Sokolov, A., and Schlosser, A.: Using Land To Mitigate Climate Change: Hitting the Target, Recognizing the Trade-offs, Environ. Sci. Technol., 46, 5672–5679, https://doi.org/10.1021/es2034729, 2012.

Reiner, D. M.: Learning through a portfolio of carbon capture and storage demonstration projects, Nat. Energy, 1, 15011, https://doi.org/10.1038/Nenergy.2015.11, 2016.

Rodriguez, J. P., Beard, T. D., Bennett, E. M., Cumming, G. S., Cork, S. J., Agard, J., Dobson, A. P., and Peterson, G. D.: Trade-offs across space, time, and ecosystem services, Ecol. Soc, 11, 28, https://doi.org/10.5751/ES-01667-110128, 2006.

Rogelj, J., Luderer, G., Pietzcker, R. C., Kriegler, E., Schaeffer, M., Krey, V., and Riahi, K.: Energy system transformations for limiting end-of-century warming to below 1.5 °C, Nat. Clim. Change, 5, 519–527, https://doi.org/10.1038/nclimate2572, 2015.

Rosenkranz, M., Pugh, T. A. M., Schnitzler, J. P., and Arneth, A.: Effect of land-use change and management on biogenic volatile organic compound emissions – selecting climate-smart cultivars, Plant Cell Environ., 38, 1896–1912, https://doi.org/10.1111/pce.12453, 2015.

Samir, K. C. and Lutz, W.: The human core of the shared socioeconomic pathways: Population scenarios by age, sex and level of education for all countries to 2100, Global Environ. Chang., 42, 181–192, https://doi.org/10.1016/j.gloenvcha.2014.06.004, 2017.

Sampaio, G., Nobre, C., Costa, M. H., Satyamurty, P., Soares, B. S., and Cardoso, M.: Regional climate change over eastern Amazonia caused by pasture and soybean cropland expansion, Geophys. Res. Lett., 34, L17709, https://doi.org/10.1029/2007gl030612, 2007.

Santangeli, A., Toivonen, T., Pouzols, F. M., Pogson, M., Hastings, A., Smith, P., and Moilanen, A.: Global change synergies and trade-offs between renewable energy and biodiversity, Gcb Bioenergy, 8, 941–951, https://doi.org/10.1111/gcbb.12299, 2016.

Schurgers, G., Arneth, A., Holzinger, R., and Goldstein, A. H.: Process-based modelling of biogenic monoterpene emissions combining production and release from storage, Atmos. Chem. Phys., 9, 3409–3423, https://doi.org/10.5194/acp-9-3409-2009, 2009.

Scott, C. E., Rap, A., Spracklen, D. V., Forster, P. M., Carslaw, K. S., Mann, G. W., Pringle, K. J., Kivekäs, N., Kulmala, M., Lihavainen, H., and Tunved, P.: The direct and indirect radiative effects of biogenic secondary organic aerosol, Atmos. Chem. Phys., 14, 447–470, https://doi.org/10.5194/acp-14-447-2014, 2014.

Scott, V., Haszeldine, R. S., Tett, S. F. B., and Oschlies, A.: Fossil fuels in a trillion tonne world, Nat. Clim. Change, 5, 419–423, https://doi.org/10.1038/Nclimate2578, 2015.

Searle, S. Y. and Malins, C. J.: Will energy crop yields meet expectations?, Biomass Bioenerg., 65, 3–12, https://doi.org/10.1016/j.biombioe.2014.01.001, 2014.

Sillman, S.: The relation between ozone, NO_x and hydrocarbons in urban and polluted rural environments, Atmos. Environ., 33, 1821–1845, https://doi.org/10.1016/S1352-2310(98)00345-8, 1999.

Slade, R., Bauen, A., and Gross, R.: Global bioenergy resources, Nat. Clim. Change, 4, 99–105, https://doi.org/10.1038/Nclimate2097, 2014.

Smith, B., Wårlind, D., Arneth, A., Hickler, T., Leadley, P., Siltberg, J., and Zaehle, S.: Implications of incorporating N cycling and N limitations on primary production in an individual-based dynamic vegetation model, Biogeosciences, 11, 2027–2054, https://doi.org/10.5194/bg-11-2027-2014, 2014.

Smith, L. J. and Torn, M. S.: Ecological limits to terrestrial biological carbon dioxide removal, Climatic Change, 118, 89–103, https://doi.org/10.1007/s10584-012-0682-3, 2013.

Smith, P., Ashmore, M. R., Black, H. I. J., Burgess, P. J., Evans, C. D., Quine, T. A., Thomson, A. M., Hicks, K., and Orr, H. G.: The role of ecosystems and their management in regulating climate, and soil, water and air quality, J. Appl. Ecol., 50, 812–829, https://doi.org/10.1111/1365-2664.12016, 2013.

Smith, P., Davis, S. J., Creutzig, F., Fuss, S., Minx, J., Gabrielle, B., Kato, E., Jackson, R. B., Cowie, A., Kriegler, E., van Vuuren, D. P., Rogelj, J., Ciais, P., Milne, J., Canadell, J. G., McCollum, D., Peters, G., Andrew, R., Krey, V., Shrestha, G., Friedlingstein, P., Gasser, T., Grubler, A., Heidug, W. K., Jonas, M., Jones, C. D., Kraxner, F., Littleton, E., Lowe, J., Moreira, J. R., Nakicenovic, N., Obersteiner, M., Patwardhan, A., Rogner, M., Rubin, E., Sharifi, A., Torvanger, A., Yamagata, Y., Edmonds, J., and Cho, Y.: Biophysical and economic limits to negative CO_2 emissions, Nat. Clim. Change, 6, 42–50, https://doi.org/10.1038/Nclimate2870, 2016.

Stehfest, E., van Vuuren, D., Kram, T., Bouwman, L., Alkemade, R., Bakkenes, M., Biemans, H., Bouwman, A., den Elzen, M., Janse, J., Lucas, P., van Minnen, J., Müller, C., and Prins, A.: Integrated Assessment of Global Environmental Change with IMAGE 3.0: Model description and policy applications, The Hague, PBL Netherlands Environmental Assessment Agency, The Hague, the Netherlands, 2014.

Sterling, S. M., Ducharne, A., and Polcher, J.: The impact of global land-cover change on the terrestrial water cycle, Nat. Clim. Change, 3, 385–390, https://doi.org/10.1038/Nclimate1690, 2013.

Tilman, D., Cassman, K. G., Matson, P. A., Naylor, R., and Polasky, S.: Agricultural sustainability and intensive production practices,

Nature, 418, 671–677, https://doi.org/10.1038/nature01014, 2002.

Unger, N.: Human land-use-driven reduction of forest volatiles cools global climate, Nat. Clim. Change, 4, 907–910, https://doi.org/10.1038/nclimate2347, 2014.

Valin, H., Sands, R. D., van der Mensbrugghe, D., Nelson, G. C., Ahammad, H., Blanc, E., Bodirsky, B., Fujimori, S., Hasegawa, T., Havlik, P., Heyhoe, E., Kyle, P., Mason-D'Croz, D., Paltsev, S., Rolinski, S., Tabeau, A., van Meijl, H., von Lampe, M., and Willenbockel, D.: The future of food demand: understanding differences in global economic models, Agr. Econ.-Blackwell, 45, 51–67, https://doi.org/10.1111/agec.12089, 2014.

Val Martin, M., Heald, C. L., Lamarque, J.-F., Tilmes, S., Emmons, L. K., and Schichtel, B. A.: How emissions, climate, and land use change will impact mid-century air quality over the United States: a focus on effects at national parks, Atmos. Chem. Phys., 15, 2805–2823, https://doi.org/10.5194/acp-15-2805-2015, 2015.

van Dijk, A. I. J. M., van Noordwijk, M., CaldeR, I. R., Bruijnzeel, S. L. A., Schellekens, J., and Chappell, N. A.: Forest-flood relation still tenuous – comment on "Global evidence that deforestation amplifies flood risk and severity in the developing world" by Bradshaw et al., Glob. Change Biol., 15, 110–115, https://doi.org/10.1111/j.1365-2486.2008.01708.x, 2009.

van Vliet, J., Bregt, A. K., Brown, D. G., van Delden, H., Heckbert, S., and Verburg, P. H.: A review of current calibration and validation practices in land-change modeling, Environ. Modell. Softw., 82, 174–182, https://doi.org/10.1016/j.envsoft.2016.04.017, 2016.

van Vuuren, D. P., Edmonds, J., Kainuma, M., Riahi, K., Thomson, A., Hibbard, K., Hurtt, G. C., Kram, T., Krey, V., Lamarque, J. F., Masui, T., Meinshausen, M., Nakicenovic, N., Smith, S. J., and Rose, S. K.: The representative concentration pathways: an overview, Climatic Change, 109, 5–31, https://doi.org/10.1007/s10584-011-0148-z, 2011.

van Vuuren, D. P., Deetman, S., van Vliet, J., van den Berg, M., van Ruijven, B. J., and Koelbl, B.: The role of negative CO_2 emissions for reaching 2 °C-insights from integrated assessment modelling, Climatic Change, 118, 15–27, https://doi.org/10.1007/s10584-012-0680-5, 2013.

Viglizzo, E. F., Paruelo, J. M., Laterra, P., and Jobbagy, E. G.: Ecosystem service evaluation to support land-use policy, Agr. Ecosyst. Environ., 154, 78–84, https://doi.org/10.1016/j.agee.2011.07.007, 2012.

Visconti, P., Pressey, R. L., Giorgini, D., Maiorano, L., Bakkenes, M., Boitani, L., Alkemade, R., Falcucci, A., Chiozza, F., and Rondinini, C.: Future hotspots of terrestrial mammal loss, Philos. T. Roy. Soc. B, 366, 2693–2702, https://doi.org/10.1098/rstb.2011.0105, 2011.

Warszawski, L., Frieler, K., Huber, V., Piontek, F., Serdeczny, O., and Schewe, J.: The Inter-Sectoral Impact Model Intercomparison Project (ISI-MIP): Project framework, P. Natl. Acad. Sci. USA, 111, 3228–3232, https://doi.org/10.1073/pnas.1312330110, 2014.

Whitehead, P. G., Wilby, R. L., Battarbee, R. W., Kernan, M., and Wade, A. J.: A review of the potential impacts of climate change on surface water quality, Hydrolog. Sci. J., 54, 101–123, https://doi.org/10.1623/hysj.54.1.101, 2009.

Wilkinson, S., Mills, G., Illidge, R., and Davies, W. J.: How is ozone pollution reducing our food supply?, J. Exp. Bot., 63, 527–536, https://doi.org/10.1093/jxb/err317, 2012.

Williamson, P.: Scrutinize CO_2 removal methods, Nature, 530, 153–155, https://doi.org/10.1038/530153a, 2016.

Wiltshire, A. and Davies-Barnard, T.: Planetary limits to BECCS negative emissions, AVOID2 WPD.2a Report 1, available at: http://www.avoid.uk.net/2015/07/planetary-limits-to-beccs-negative-emissions-d2a/ (last access: 27 October 2017), 2015.